Technische Universität München

Institut für Entwicklungsgenetik
GSF-Forschungszentrum für Umwelt und Gesundheit, Neuherberg

Molecular analysis of the βB2-crystallin gene (*Crybb2*) in mouse eye and brain of the wild-type and *O377* mutant.

Koustav Ganguly

Vollständiger Abdruck der von der Fakultät

Wissenschaftszentrum Weihenstephan für Ernährung, Landnutzung und Umwelt

der Technischen Universität München zur Erlangung des akademischen Grades

eines

Doktors der Naturwissenschaften

(Dr. rer. nat.)

genehmigten Dissertation.

<u>**Vorsitzender:**</u>   **Univ.-Prof. Dr.rer.nat. Alfons Gierl**

<u>**Prüfer der Disseration:**</u>

1. apl. Prof. Dr.rer.nat., Dr.rer.nat. habil. Joachim Graw

2. Univ.-Prof. Dr.rer.nat. Hans-Joachim Leppelsack

Die Disseration wurde am **14.04.2005** bei der Technischen Universität München eingereicht
und durch die Fakulät Wissenschaftszentrum Weihenstephan für Ernährung, Landnutzung und
Umwelt am **11.06.2005** angenommen.

I dedicate this work to my parents.

Lebenslauf

Koustav Ganguly

Geburtsdatum: 27.05.1977

Geburtsort: Kalkutta (Calcutta), Indien

Nationalität: Inder

Familienstand: Verheiratet

Schulbildung

1983-1993: Gesamtschule (1. bis 10. Schuljahr), "West Bengal Board of Secondary Education", Indien

1993-1995: Höhere Schule bis zur Hochschulreife, "West Bengal Board of Higher Secondary Education", Indien

Studium

1995-1998: Bachelor of Sciences (**B.Sc**) in Botanik (Hauptfach), Zoologie & Chemie (Nebenfach) an der Universität von Kalkutta, Indien

1998-2000: Master of Sciences (**M.Sc**) in Botanik mit Schwerpunkt **Zellbiologie, Molecularer Genetik & Pflanzengewebekultur** an der Universität von Kalkutta, Indien

2000-2002: Aufbaustudium mit Diplomabschluß in **Informationstechnologie-Management** am "Asia Pacific Institute of Management", Neu Delhi, Indien (Abschluß im April 2002)

2002$_{Mai}$-2005$_{April}$: Doktorarbeit am **GSF**- Forschungszentrum für Umwelt und Gesundheit, Neuherberg, am Institut für **Entwicklungsgenetik** in der Gruppe für **Molekulare Augenentwicklung.**

Curriculum Vitae

Koustav Ganguly

Date of Birth: 27.05.1977.

Place of Birth: Kolkata (Calcutta), India

Nationality: Indian

Marital status: Married

Educational and Professional Qualification:

1983-1993:   10 years of schooling (1-10th Standard); 'West Bengal Board of Secondary Education'; India.

1993-1995:   (10+2) Standard; 'West Bengal Board of Higher Secondary Education'; India.

1995-1998:   Bachelor of Sciences (**B.Sc.**) in **Botany** (major), Zoology and Chemistry (minor); University of Calcutta, India.

1998-2000:   Master of Sciences (**M.Sc.**) in Botany with specialization in **Cell Biology, Molecular Genetics and Plant Tissue Culture**; University of Calcutta, India.

2000-2002:   Post Graduate Diploma in **Management of Information Technology** (PGDMIT); Asia Pacific Institute of Management, New Delhi, India (Course completed on April, 2002).

2002$_{May}$-2005$_{April}$:   Pursuing **Ph.D.** at **GSF**-National Research Center for Environment and Health, Neuherberg, Germany; in the research group of **Molecular Eye Development**; Institute of **Developmental Genetics**.

Zusammenfassung (Abstract):

Die Mutante *O377* besitzt eine 57 Basenpaar-Insertion am Anfang des Exon 6 des *Crybb2* Gens, die zu einer 19 Aminosäure-Insertion im Protein führt. Die betroffenen Tiere entwickeln eine dominante, fortschreitende, erbliche Katarakt als Folge des fehlerhaft gefalteten Proteins. Beta-B2-Kristallin wird, außer in der Linse, auch in der Retina und im Gehirn, insbesondere in den glomerulären und Mitralzellen des Riechkolbens, den Pyramidalzellen des Kortex, den Zellen der CAI, CAII und CAIII (CA= *Cornu ammonis*) Bereiche und des *Gyrus dentatus* im Hippocampus sowie in den Purkinje-und Sternzellen des Cerebellums exprimiert. Die Anzahl der Purkinje Zellen ist im Gehirn der homozygoten Mutanten höher (11%). Die Expression außerhalb der Linse sowie die histologischen und molekularen Ergebnisse (z.B. die differentiell exprimierten Gene im *O377* Mutanten-Gehirn deuten auf eine Zusätzliche Funktion des beta-B2-Kristallins in der Phosphat- und Calcium-Homeostase hin.

Abstract:

Mutant *O377* contain a 57 bp insertion at the beginning of exon 6 of *Crybb2* that leads to a 19aa insertion in the protein. The animals develop dominant progressive hereditary cataract as a result of the misfolded protein. βB2-crystallin is also expressed in the retina and in the brain, particularly in the glomerular and mitral cells of the olfactory bulb; pyramidal cells of the cortex; CAI, CAII, CAIII (CA= *Cornu ammonis*) region cells and dentate gyrus of the hippocampus; and Purkinje and stellate cells of the cerebellum apart from lens. The numbers of Purkinje cells are higher (11%) in the homozygous mutant brain. Most of the differentially expressed genes in homozygous and heterozygous mutant brains are involved in phosphate and calcium pathways. Non-lenticular expression coupled with the findings at histological and molecular levels in the *O377* mutant brain suggest the non-refractive function of βB2-crystallin to be in phosphate and calcium homeostasis.

Zusammenfassung (Abstract) Submitted at:

Contents:

Chapter 3: Results

Chapter 1

Introduction:

βB2-crystallin is one of the most important structural proteins of the vertebrate eye lens responsible for creating its high refractive index and in maintaining the clarity of the lens by its spatial distribution and high stability, together with other crystallins. It constitutes a major part of the water soluble proteins of the eye lens along with other β and γ-crystallins. It is mainly expressed in the lens cortex and its expression has been reported in retina, brain and testis (Magabo *et al.,* 2000; Xi *et al.,* 2003). βB2-crystallin is basic in nature and the protein consists of four Greek key motifs; a characteristic of all the members of β- and γ-crystallins. It is encoded by the gene *Crybb2* located on chromosome 5 (60cM) [Kerscher *et al.,* 1995] in mouse and in case of humans the gene *CRYBB2* is located on chromosome 22 (22q11.2-12). In this chapter a brief introduction to the crystallins is given with a detailed discussion of βB2-crystallin at its molecular level along with the different known human and mouse hereditary cataracts caused due to mutation in the βB2-crystallin gene.

[Reviews: Bhat, 2004; Graw, 2004; Bhat, 2003; Graw, 2003; Graw and Loster 2003, Graw, 1997]

1.1: <u>The crystallins:</u>

Crystallins are the structural proteins of vertebrate eye lens, synthesized in the fiber cells, that provides transparency by dint of their high concentration (constitutes up to 90% of the total soluble proteins which account for about 38% of the wet weight of the lens) thereby making the ocular lens as perfect physical system of immaculate optics. Since lens fiber cells lack nuclei, there remains no chance of the self renewal of crystallins. Hence, the proteins which appear during early embryogenesis have to survive the life of the organism. Crystallins are thus presumed to be inherently stable (Bhat, 2003).

Mörner (1893), described three chromatographic fractions of water soluble lens proteins and named them as α-, β- and γ-crystallins. A brief outline of the different crystallins is depicted in figure 1.1. α–crystallins (αA and αB) share 55% sequence identity and immunoreactivity. The β-crystallins are composed of acidic βA (63% homologous), and basic βB (56% homologous) polypeptides. The γ-crystallins are 70-80% homologous. The β- and γ–crystallins have a common evolutionary origin, share sequence and structural similarities and immunogenicity. Thus, on the basis of sequence and structural affinities alone, there are only two groups of proteins, the α–crystallins and β/γ-crystallins that characterize the mammalian lens (Bhat, 2003). Some crystallins are also known to be expressed outside the eye, βB2-crystallin being one of them.

Mutations of α-, β- and γ-crystallins are linked with the phenotype of loss of lens transparency. Evolutionary analysis has also linked the relationship of crystallins to the proteins involved in stress response.
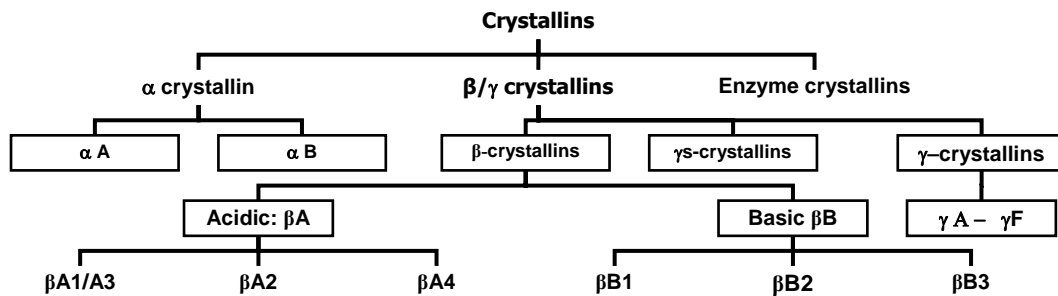
Figure 1.1: The different crystallins constituting the vertebrate lens.

1.1.1: <u>The α-crystallins:</u>

The α-crystallins are considered to be molecular chaperones (Horwitz, 1992) and members of the small heat shock protein family exhibiting autokinase activity (Kantorow, 1994) and are involved in γ-crystallin gene activation. The α-crystallins are associated with a broad variety of neurological disorders. Chaperon activity is essential in the lens, as degradation and extrusion of defective proteins is not possible as it is in other tissues. Moreover, lens is exposed to a variety of damaging agents, particularly lights of various wave lengths that lead to peroxidative effects on a number of lens proteins (Das *et al.*, 1995).

The α-crystallin complexes are mainly composed of two related proteins, αA- and αB-crystallin. They are encoded by the genes *Cryaa* and *Cryab* respectively in mouse (*CRYAA* and *CRYAB* in human). Both these genes contain three exons of similar size. In rodents an alternative splice product can be observed in 10-20% of the αA-crystallins, referred as αA^ins-crystallin, where from intron A an additional 69 bp are included in the mature mRNA leading to a protein, 23 amino acids longer than the usual αA-crystallin. It is still unknown if this particular splice product has some specific function or is only a transient product of evolution in rodents (Graw, 1997).

During embryogenesis, *Cryaa* expression is observed in the rat lens pit (van Leen *et al.*, 1987) and in the mouse lens cup at E10 to E10.5 (Robinson and Overbeek, 1996). It is present on the posterior half of the mouse lens vesicle (Tréton *et al.*, 1991) and later on αA-crystallin becomes very abundant in lens fiber cells (Robinson and Overbeek., 1996). *Cryab* is expressed ubiquitously in rat lenses. αB-crystallin can be first detected at the end of the

embryonic development in rat (Aarts *et al*., 1989). In mouse, it is present at E9.5 and later on, it is found preferentially in the epithelial cells (Robinson and Overbeek, 1996).

Mutations in *CRYAA* lead to recessive and dominant cataracts. On the basis of only a few cases in humans and mice (Pras *et al*., 2000; Chang *et al*., 1999; Litt *et al*., 1998., Graw *et al*., 2001) it can be concluded that mutations affecting the N-terminus of the protein lead to recessive phenotypes whereas those affecting the C-terminus are dominant. Only the homozygous *Cryaa*-knockout mice develops cataract (Brady *et al*., 1997) but the *Cryab* develops normal lenses (Brady *et al*., 2001), which shows that at least in mouse, *Cryab* is not essential for transparent lens formation. In human, mutation in *CRYAB* causes dominant congenital cataract at the posterior pole of the lens (Berry *et al*., 2001). In this case, the cataract was mapped close to the *CRYAB* locus and a deletion was found in exon 3 of *CRYAB* that resulted in a frameshift and an aberrant protein of 184 residues was detected among four-generations of a family of English descent. The phenotype is therefore attributed to the dominant negative function of this mutated protein. (Graw, 2003)

1.1.1A: <u>Non-lenticular and non-ocular expression of α-crystallins and its association with neurological disorders:</u>

Xi *et al*. (2003) showed the expression and distribution of αB-crystallins in the ganglionic cell layer, inner photoreceptor layer and outer nuclear layer of 10-20 days old mouse retina following microarray, qRT-PCR, immunoblotting and immunofluorescence studies.

αB-crystallin is reported to be expressed in heart, lung, thymus, brain, muscle and kidney (Gopal-Srivastava *et al*; 1995; Krausz *et al*., 1996). Infact, a tissue specific promoter (αBE-4 element) activity of the αB-crystallin gene has been shown by Gopal-Srivastava *et al.* (1995) in cardiac muscle. It has been also found to be associated with a broad variety of neurological disorders; like-Scrapie infected hamster brain cells (Duguid, 1988); brains of human having Creutzfeld-Jacob disease (CJD) where αB-crystallin is reported to be expressed in the spongiotic tissue (representing progressively altered astrocytes in CJD) instead of its normal occurrence in oligodendroglia cells (Renkawek *et al*., 1992); brains of patients suffering from Alexander's disease (Iwaki *et al*., 1989). In addition to this, a large number of αB-crystallin positive ballooned neurons are frequently observed in the deep cortical pyramidal cell layers of the limbic and paralimbic system among patients with progressive supranuclear palsy (Higuchi *et al*., 1995). Significant increase in the expression of αB-crystallin has been observed in some different categories of human brain tumors: schwannomas, astrocytic tumors, meningoblastomas and chordomas. αB-crystallin over-expression in tumors coincides

with the over expression of hsp27 and also with the presesence of oestrogen receptors (Hitotsumatsu *et al.*, 1996). It is also associated with diffused Lewy body disease, indicating its transient role in the biogenesis of cortical Lewy bodies (Lowe *et al.*, 1990). Under non-pathological conditions αB-crystallin can also be recovered from the insoluble cell components of the heart (Chiesi *et al.*, 1992; Barbato *et al.*, 1996).

Table 1.1: The α-crystallins

Gene	Chromosome		Protein	Organs of expression	Function
	Mouse*	Human			
Cryaa	17 (17.4)	21	αA-crystallin; 20 kDa αA^{ins}-crystallin; 25 kDa	lens, spleen	Structural protein Chaperone Autokinase Gene activator
Cryab	9 (29.0)	11q12-q23	αB-crystallin; 22kDa	lens, heart, brain, muscle, kidney	Structural protein Heat shock protein

*cM position according to the mouse genome database (2005)

1.1.2: <u>The β/γ- crystallin superfamily:</u>

The β- and γ-crystallin polypeptides are recognized as the β/γ- crystallin superfamily encoded by the *Cryb* and *Cryg* genes (Table 1.2). The β/γ- crystallin superfamily is characterized by the presence of four Greek key motifs in the protein, which allows the dense packing of the proteins in the lens. Greek key motifs are anti-parallel β-sheets linked with random coils. They are named so because of their resemblance with ancient Greek pottery. In the β-crystallins, individual Greek key motifs are encoded by separate exons (Inana *et al.*, 1983), whereas in the γ-crystallin genes two motifs are encoded by one exon reflecting the modular nature of the proteins during evolution. A typical γ-crystallin gene consists of three exons; the first contains only 9 bp (codes for 3 amino acids) and is followed by a short intron of about 100 bp. The second exon (243 bp) and the third exon (273-276 bp) are separated by a large intron (1-2 kb). The second and third exons are responsible for two Greek key motifs each. The non-translated 3'-end is short (about 40 bp). The *Cryge* and *Crygf* genes are strongly expressed in rodents during late phase of gestation and in the juvenile phase but are not expressd in humans and therefore referred to as pseudogenes (Brakenhoff *et al.*, 1990). Structure of a typical *Cryb* gene (the *Crybb2*) is discussed in section 1.2.1.

 The various N- and C- terminal extensions of the β/γ- crystallins are mainly responsible for their distinct biophysical and biochemical properties. Modifications in the β/γ- crystallins or

5

mutations in their genes lead to opafication of the eye lens (cataract) [Table 1.3]. Crystallographic studies have shown that each of the β- and γ-crystallins is composed of two domains built up by two Greek key motifs and it is widely accepted that β/γ-crystallins evolved in two duplication steps from an ancestral protein folded like a Greek key (Wistow, 1995; Lubsen *et al.*, 1988).

The β-crystallins are characterized as oligomers (the molecular mass of the monomers is between 22 and 28 kDa) with native molecular masses ranging up to 200 kDa for octameric forms. All the β-crystallin subunits are highly homologous but contain different N-terminal extensions. The basic (βB) members of this group contain C-terminal extensions while the acidic members (βA) do not have this extension (Zarina *et al.*, 1994). Biochemically, the β-crystallins are characterized by blocked N-termini (by acetylation; Wistow, 1995; Lampi *et al.*, 1997). In contrast the native γ-crystallin proteins are characterized as monomers with molecular weights of 20 kDa and a free N-terminus. β-crystallin sequences differ from γ-crystallins mainly in having extensions at the N- and C- termini and in the conformation of the connecting peptide. In β-crystallins, this connecting peptide is extended, whereas in γ-crystallins it takes a sharp turn. As a result, pairs of domains associate intra-molecularly to form monomeric proteins in γ-crystallins, whereas in the β-crystallins the interaction is inter-molecular, leading to oligomeric association (Zarina *et al.*, 1994; Wistow, 1995).

There is one protein that was earlier designated as βS-crystallin because of its slow chromatographic migration among the β-crystallin fraction and it's blocked N-terminus. However, since it can be only found as a monomer, it is referred as γS-crystallin (van Rens *et al.*, 1989).

β-crystallins are expressed from early developmental stages in the eye lens and their expression continues and rises after birth so that the highest concentrations are found in the lens cortex. However, the expression pattern varies among individual β-crystallins. Aarts *et al.* (1989) showed the expression of *Cryba1*, *Crybb2* and *Crybb3* genes in the rat (by an quantitative Northern blot analysis) where all the three genes were found to be expressed from E13 onward; the *Crybb3* reaches its maximal expression around birth and drops down to background level after 6 months; *Cryba1* transcripts are maximally present 2 months after birth and reach background level at the age of 8 months. The expression pattern of the other members of acidic *Cryb* genes (*Cryba2* and *Cryba4*) investigated in calf lens suggested they have similar expression pattern as the *Cryba1* gene (van Leen *et al.*, 1987). In contrast, *Crybb2* expression increases until 6 months after birth and the corresponding transcripts are present in remarkable amounts even after one year. The *Crybb1* is present only in the

terminally differentiated fiber cells (van Leen *et al.*, 1987). Data in our laboratory showed the expression of *Crybb2* in mouse lens is detectable from E17.5 onward and that in Dr. Jack Favor's laboratory (Institute of Human Genetics, GSF) shows the onset of *Crybb2* expression in mouse lens from E17 onward.

Table 1.2: The β/γ- crystallins

Gene	Chromosome		Protein
	Mouse[*]	Human	
Cryba1	11(46)	17	βA1/A3- crystallin; 23/25kDa
Cryba2	1(41)	2	βA2-crystallin; 22kDa
Cryba4	5(59)	22q11.2-13.1	βA4-crystallin; 22kDa
Crybb1	5(59)	22q11.2-12.1	βB1-crystallin; 28kDa
Crybb2	5(60)	22q11.2-12	βB2-crystallin; 23kDa
Crybb3	5(60)	22q11.2-12.1	βB3-crystallin; 24kDa
CRYBψB2(Pseudogene)	-	22	-
Crygs	16	3	γS-crystallin; 20kDa
Cryga - Crygf	1(32)	2q33-35	γA-γF-crystallin; 20kDa

*cM position according to the mouse genome database (2005)

Several mutations in the β-crystallin genes (*Cryb* in mouse and *CRYB* in human) resulting in hereditary cataracts have been reported (Table 1.3). Among the *Cryb* genes *Crybb2* coding for the βB2-crystallins is the most affected due to cataract causing mutations both in human and mouse and are discussed in section 1.3.

Among the other β-crystallin related mutations (Table 1.3) resulting in congenital cataract, *Cryba1* is the second most affected gene to *Crybb2*. *Cryba1* codes for two acidic β-crystallins- βA1- and βA3-crystallins which differ by the length of their N-terminal extension (Peterson *et al.*, 1986). In mouse, just one *Cryba1* mutation (*progressive opacity, op*) which has a similar phenotype to the murine *Crybb2* mutations (i.e. *Philly* mouse and *Aey2*) is reported (Graw *et al.*, 1999). Interestingly, in human, two independent mutations affecting the same 5' (donor) splice site of intron 3 are affected. In the first case, it is a G→A transition (Kannabiran *et al.*, 1998), and in the second case it is a G→C transversion (Bateman *et al.*, 2000). The authors could not characterize the novel splice product due to unavailability of the human lens cDNA but the phenotype was described as zonular cataract with sutural opacity (Kannabiran *et al.*, 1998) or pulverulent, star-shaped or radial opacity (Bateman *et al.*, 2000). Reddy *et al.* (2004) reported the third mutation as a G91 deletion causing a lamellar cataract with variable severity in a five-generation family. The other *CRYB* related mutation concerns

CRYBB1, where a non-sense mutation (G220X) is associated with a fine, dust like opacity affecting mainly the central zone of the lens (Mackay *et al*., 2002) (Graw, 2004).

The *Cryg* genes are expressed in the mouse lenses from E13.5 onwards in the primary fibers and later in the secondary fiber cells but not in the epithelial cells (van Leen *et al*., 1987; Santhiya *et al*., 1995). The expression of *Cryg* genes reaches its maximum in mice at the first weeks after birth (Goring *et al*., 1992). In human, the *Cryg* expression is restricted to the prenatal development, because of the different time scale of mouse and human intra-uterine life. In contrast to mammals, γ-crystallins appear in amphibians first, even before the α-crystallins (Shastry, 1989)

20 mouse mutants (Table: 1.3) affecting the *Cryg* gene cluster (*Cryga→Crygf*), affecting all the six genes have been reported (Cartier *et al*., 1992; Klopp *et al*., 1998, 2001; Smith *et al*., 2000; Graw *et al*., 2001; Graw *et al*., 2002; Graw *et al*., 2004)

Table 1.3: Mutant alleles coding for crystallin proteins involved in congenital cataracts (Reproduced from Graw, 2004)

Name	Allele Symbol	Phenotype	Molecular Lesion	Consequence for Protein
Cryaa	*Cryaa⁻/⁻*	Recessive progressive opacity	Targeted deletion	Loss of function
	lop18	Recessive nuclear and cortical cataract	R54H	Not determined
	Aey7	Nuclear cataract	V124E	Not determined
CRYAA		Recessive cataract	W9X	Loss of function
CRYAA		Dominant nuclear cataract	R49C	Abnormal nuclear localization
CRYAA		Dominant nuclear cataract	R116C	Increased membrane binding capacity
Cryab	*Cryaa⁻/⁻*	No ocular phenotype	Targeted deletion	Loss of function
CRYAB		Myopathy with cataract	R120G	Irregular structure
		Posterior polar cataract	450delA	Aberrant protein
Cryba1	*Po*	Progressive cataract	Splicing intron 6	4th Greek key motif
			W168R; ΔW168	
CRYBA1		Zonular cataract	Splicing intron 3	Not determined
CRYBA1		Pulverulent cataract	Splicing intron 3	Not determined
CRYBA1		Lamellar cataract	G91del	Reduced solubility
CRYBA1		Cataract	Splicing intron	Not determined
CRYBB1		Pulverulent cataract	G220X	Reduced solubility
Crybb2	*Philly*	Progressive cataract	12-bp deletion in exon 6	4th Greek key motif
	Aey2	Progressive cataract	V187E	4th Greek key motif
CRYBB2		Cerulean cataract	Q155X	Not determined
CRYBB2		Coppock-like cataract	Q155X	Not determined
CRYBB2		Suture cataract and cerulean opacity	Q155X	Not determined
CRYBB2		Central nuclear cataract	W151C	Loss of solubility?
Cryga-f **Refer table 1.4**	*Several alleles in mouse*	Various types of cataract	Missense, non.sense, deletion/insertion	Mainly Greek key motifs affected

Table 1.4: List of characterized mutations at the *Cryg* gene cluster on mouse chromosome 1 (Reproduced from Graw *et al*., 2004)

Name	Previous Symbol	Phenotype (Graded Severity)	Paternal Treatment	Molecular Lesion	Consequence for Protein		
					aa Alterations	pI	Greek Key Motif
Cryga^{ENU369}	ENU369; Cat2^{tol}	Total cataract with vacuoles (severe)	ENU	*Cryga*: T127C	Trp43→Arg	pH 7.5–8.5	2nd not formed
Cryga^{1Neu}	ENU-436	Diffuse nuclear opacity (medium)	ENU	*Cryga*: A222G	Asp74→Gly	pH 7.5–8.0	No effect
Crygb^{Nop}	Nop	Nuclear opacity (medium)	Spontaneous	*Crygb*: Δ417-427/Ins4	Ser139: 6 new aa; stop	pH 7.6–5.5	4th not formed
Crygc^{Cbl3}	Cbl3	Total and lamellar opacity (medium)	Chlorambucil	*Crygc*: Δ420-425	ΔG141, R142	pH 7.6–6.9	4th not formed
Crygc^{MNUS}	MNU-8	Total opacity with vacuoles (medium)	MNU	*Crygc*: G471A	Trp157→stop 15 aa missing	pH 7.6–6.9	No effect
Crygd^{ENU4011}	ENU4011	Cloudy nuclear opacity (medium)	ENU	*Crygd*: T134C	Leu45→Pro	pH 6.6–7.0	2nd not formed
Crygd^{Aey4}	Aey4	Nuclear and cortical cataract (medium)	ENU	*Crygd*: T227A	Val76→Asp	pH 6.6–6.6	No effect
Crygd^{ENU910}	ENU910	Diffuse total cataract (mild)	ENU	*Crygd*: A275T	Ile90→Phe	pH 6.6–7.0	No effect
Crygd^{K10}	K-10	Total cataract (medium)	Spontaneous	*Crygd*: C432G	Tyr144→stop 28 aa missing	pH 6.6–5.9	4th not formed
Crygd^{Lop12}	Lop12	Irregular nuclear lens opacity (medium)	Spontaneous	*Crygd*: G470A	Trp157→stop 18 aa missing	pH 6.6–6.2	No effect
Cryge^{Aey1}	Aey1	Nuclear cataract (medium)	ENU	*Cryge*: A1T	new protein (13 kDa)	pH 7.7–9.5	No motif
Cryge^{ENU418}	ENU418	Nuclear and lamellar cataract (medium)	ENU	*Cryge*: Intron A, A66G, lariat formation and splicing inhibited	Ile4: 153 new aa	pH 7.7–10.1	No motif
Cryge^{Z2}	Z2	Total lamellar cataract (medium)	Spontaneous	*Cryge*: Δ12-21	Ile4: 119 new aa	pH 7.7–9.8	No motif
Cryge^{Nz}	Nzc; 116	Nuclear and zonular cataract (medium)	γ-ray	*Cryge*: Δ89T	Phe30: 96 new aa	pH 7.7–8.4	Motifs 2-4 not formed
Cryge^{ADD15306}	ADD15306	Zonular cataract (medium)	ENU	*Cryge*: T134C;	Leu45→Pro	pH 7.7–7.1	2nd not formed
Cryge^{ENU449}	ENU449	Capsular opacity (mild)	ENU	*Cryge*: G376A	Val126→Met	pH 7.7–7.1	No effect
Cryge^{Elo}	Elo	Eye lens obsolescence (medium)	Spontaneous	*Cryge*: Δ403	Glu135: 11 new aa and stop	pH 7.7–6.4	4th not formed
Cryge^t	R324; Cat2^t	Total opacity (severe)	X-ray	*Cryge*: C432G	Tyr144→stop	pH 7.7–6.4	4th not formed
Cryge^{Ns}	K134; Scat	Suture cataract (mild)	Spontaneous	*Cryge*: Del >2kb	Hybrid protein?	?	4th motif affected?
Crygf^{Rop}	Rop	Radial opacity (medium)	Procarbazine	*Crygf*: T113A	Val38→Glu	pH 7.1–6.7	4th not formed

A of the ATG start codon is counted as nt 1; Met encoded by the start codon is counted as amino acid 1.

1.1.2A: <u>Non-lenticular and non-ocular expression of β/γ-crystallins:</u>

Xi *et al* (2003) reported the occurrence of β-crystallin in the ganglionic cell layer, inner photoreceptor layer and outer nuclear layer of the retina. Magabo *et al*. (2000) showed the expression of βB2-crystallin protein and mRNA in the retina, brain and testis in multiple species.

B2-crystallin mRNA was detected in human retina, rat brain (RNA prepared from the cerebellum and brain stem) and rat testis by RT-PCR. The βB2-crystallin protein from bovine retina, rat brain and rat testis was FPLC purified and its identity was confirmed by immunoblotting. The identity of bovine retinal βB2-crystallin protein was confirmed by microsequencing (Magabo *et al*., 2000). Head *et al*. (1995) had earlier reported the expression of βB2-crystallin in mouse and cat neural and pigmented retinas and in cat iris. Dirks *et al*. (1998) had reported the expression of βB2-crystallin transcript in the retina, spleen, liver, kidney and heart. Graw *et al*. (2001) showed the occurrence of only the 3'-half of the *Crybb2* transcripts in the brain of *Aey2* mutant mice and suggested it as an alternative splice product in the brain tissue.

In mammals, the γ-crystallin genes (*Cryg*) were also discovered in the retina (Jones *et al*., 1999). Xi *et al*., (2003) reported the expression of γ-crystallin in adult mouse retinas (10-20 days old) following qRT-PCR, immunoblotting and immunofluorescence studies. Distribution of γ-crystallin has been detected in the ganglionic cell layer, inner photoreceptor layer and the outer nuclear layer of the retina by them. They also reported variability of retinal γ-crystallin expression among different animals.

1.1.3: <u>γS-Crystallin:</u>

An intermediate member of the βγ-superfamily is the γS-crystallin, previously also referred to as βS-crystallin. The corresponding gene is mapped to mouse chromosome 16 (Sinha *et al*., 1998). The *Crygs* gene is composed of three exons and two introns. The first exon consists of 9 bp (carp) or 21 bp (bovine) and is followed by an intron of 4.25 kb. The exon 2 codes for 81 amino acids and exon 3 for 90 amino acids; the intermediate intron is only 400 bp long (van Rens *et al*., 1989) The human *Crygs* gene was mapped using hamster-human hybrid cells to chromosome 3, and is obviously independent from other *Cryb* or *Cryg* genes. The bovine γS-crystallin is monomeric without the tendency to form assemblies up to the milli molar range. The expression pattern of the *Crygs* is unique among the *Cry* families because its transcripts cannot be detected during embryogenesis. During the first month after birth it starts to accumulate in the lens and reaches its maximal concentration after 2-3 months. It is expressed

at very low level (20% of the maximum at 3 months) eight months after birth and remains stable at this level in rat lens (Aarts *et al*., 1989).

The cataract mutation *opj (opacity due to poor junctions)* [Everett *et al*., 1994; Kerscher *et al*., 1996] was mapped close to *Crygs*. Sequence analysis of *Opj* mice revealed a mutation coding for a key residue of the core of the N-terminal domain of the protein (Wistow *et al*., 1998). The first recessive mutation in mouse *Cryg* is characterized by a stop codon leading to a truncated protein that has a missing 16 aa at the C-terminus in the mouse *Crygs* gene (Bu *et al*., 2002).

1.1.4: Taxon-specific crystallins / Enzyme crystallins:

Other proteins found to be expressed at relatively high levels in the lens are characterized by their strong relationship to well known enzymes. They are referred to as enzyme-crystallins. For example, the ξ-crystallins, which evolved from a quinone oxidoreductase using a lens specific promoter, and a mutation in ξ-crystallin leads to cataract formation. The chicken δ-crystallin has close similarity to argininosuccinate lyase and the duck ε-crystallin to lactate dehydrogenase (Graw, 1997). Analysis of a broad variety of animals revealed a long list of species specific crystallins, which were obviously recruited from enzymes and are expressed in the lens up to 10-20% of the water-soluble proteins. The concept of recruitment of lens crystallins by gene sharing from enzymes, which are active outside the lens has been described by Wistow *et al*. (1987) and Wistow (1993). μ-crystallin is another such taxon specific crystallin considered to be the mammalian homologue of *Agrobacterium* ornithine cyclodeaminase and is expressed in human retina (Kim *et al*., 1992).

ξ-crystallin detected in guinea pig (Huang *et al*., 1987), in camels (Garland *et al*., 1991) and in cattle (Rao *et al*., 1997) are interesting in particular to human diseases. This enzyme crystallin is structurally similar to alcohol dehydrogenase (Borras *et al*., 1989) and has quinine oxidoreductase activity (Rao *et al*., 1992). The use of lens-specific alternative promoter that does not require host specific factor explains the recruitment of this enzyme as crystallin (Richarson *et al*., 1995). ξ-crystallins belong to a superfamily of medium chain dehydrogenases/reductases (MDR) including the quinine reductase, glucose dehydrogenase and alcohol dehydrogenase. The ξ-crystallin itself has an oxidoreductase activity and requires NADPH as a cofactor, but lacks a Zn binding site. The amino acid sequence shows that the guineapig ξ-crystallin contains 5 thiol groups/subunits like the γ-crystallins (Borras *et al*., 1989; Rao *et al*., 1992). Bovine ξ-crystallin (Rao *et al*., 1997) has distinct functional characteristics. Besides sharing 83% sequence identity and similar physical and chemical

properties to that of guineapig ξ-crystallin, it exhibits minimal quinine oxidoreductase activity, but a strong binding affinity to single stranded DNA. This difference in property has been attributed to the exchange of Tyr[59] (guinea pig) to a His in the corresponding bovine form. An autosomal dominant cataract line in guinea pig (13/N) is due to a di-nucleotide deletion at the acceptor splice site of intron 6 of *Cryz*, which results in the elimination of exon 7 during mRNA processing and the corresponding ξ-crystallin protein is truncated by 34 amino acids (Rodriguez *et al*., 1992). This information helps to explain the altered structural and enzymatic properties of ξ-crystallin in guinea-pig hereditary caracats (Rao *et al*., 1992). ξ-crystallin is also expressed in human lens (Gonzalez *et al*., 1995) and the encoding *CRYZ* is located at human chromosome 1p22-31 (Heinzmann *et al*., 1994).

1.2: <u>The βB2-crystallin:</u>

1.2.1: The *Crybb2* gene

The *Crybb2* gene is considered as a typical β-crystallin encoding gene, consisting of six exons of which the first exon is not translated, the second one encodes the N-terminal extension and each of the subsequent four exons are responsible for one Greek key motif each of the βB2-crystallin protein (Chambers *et al* 1995). *Crybb2* is highly conserved *Cryb* gene along with *Cryba1* (Duncan *et al*., 1995). Figure 1.2 explains the structure of the *Crybb2* gene at the genomic and mRNA levels. Expression of *Crybb2* starts from E17.5 (laboratory data) and increases until six months after birth and the corresponding transcripts are present in remarkable amounts even after one year (van Leen *et al*., 1987).
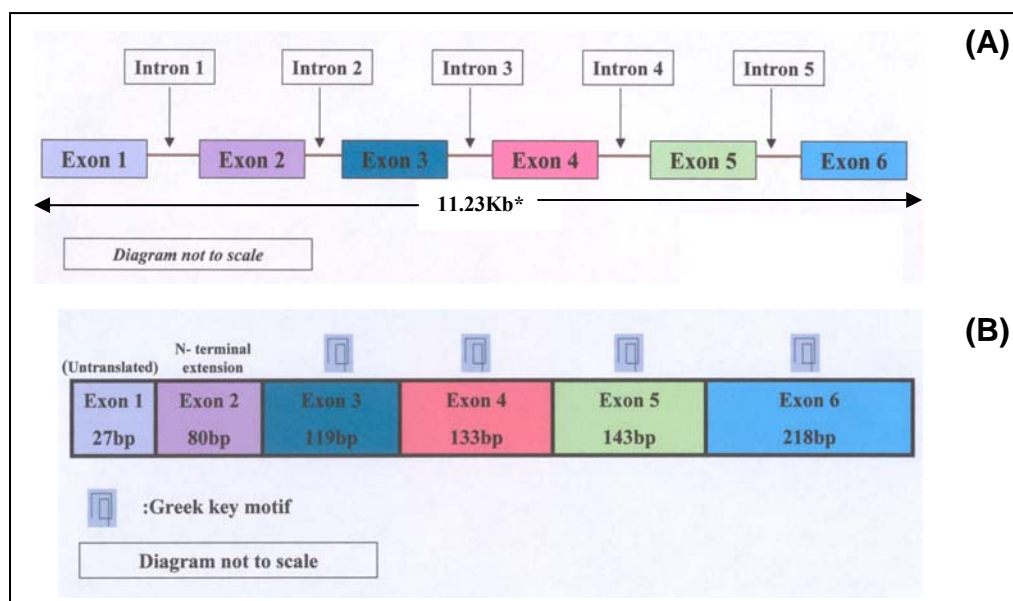
Figure 1.2: The schematic structure of the *Crybb2* at the genomic level is shown in figure 1.2A and the transcript information is presented in figure 1.2B. *The information on the size of exons and transcript structure is according to ENSEMBL data base (March, 2005).

1.2.2: The *CRYBψB2* pseudogene in human:

In human a second *Crybb2* has been found; it is an incomplete gene (coding only the exons one to three); the fourth exon sequence of the gene contains a one triplet deletion and a mutated splice acceptor site and since no transcripts from the βB2-crystallin gene could be detected in the human lens it is called as a pseudogene. This missing triplet should encode the serine residue which is involved in maintaining the characteristic 'Greek key' protein fold. The effect of this one amino acid deletion is unclear; but the mutation at the acceptor splice site has been predicted to shift the splice site by two nucleotides upstream resulting in a shift of the reading frame and premature termination at the third triplet (TGA) after the splice site. Apparent relaxation of the selective pressure on this sequence coupled with the extent of change of the coding sequence of the *CRYBψB2* gene (relative to the calf or rat sequence it is almost twice as high as that of the *CRYBB2*) have lead to refer it as a pseudogene (Brakenhoff *et al.*, 1992).

Interestingly, a sequence-specific gene conversion between *CRYBB2* and its closely linked pseudogene [Q155X] (Vanita *et al.*, 2001; Gill *et al.*, 2000) has been described as the underlying genetic mechanism behind three phenotypically distinct autosomal dominant congenital cataracts (ADCC) among three genetically unrelated families (Sections 1.3.1A-C).

1.2.3: The murine *Crybb2* promoter region:

In mouse the promoter fragments of -275/+30 or -110/+30 are able to activate a reporter gene in a lens-derived cell line but not in the cells of non lens in origin. The **TATA** box is at the correct place, approximately 25 bp upstream from the transcriptional start point. The regulatory elements which determine the activity of this gene in the rat are located in a large distal region (-750/-123) and in the first intron. These regions together constitute an enhancer only during specific stages of differentiation. Otherwise, they act individually as silencers; another silencer element is located between -123/-77. A Pax6 binding site, which is found *in-vitro*, is obviously not used *in-vivo* (Figure 1.3) [Dirks *et al.*, 1996].
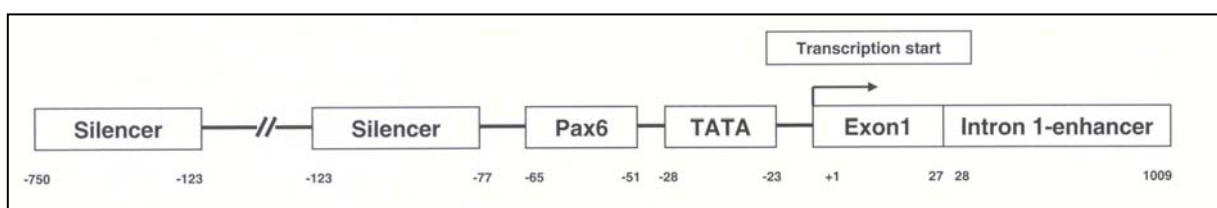
Figure 1.3: Promoter of the murine *Crybb2* gene.

Maf responsive elements (MARE) have been detected in the promoter of rat βB2-crystallin gene. c-Maf has been reported to be present in rat lens only up to 3 months of age whereas *Crybb2* mRNA reaches its maximum level at 6 weeks of age. This discrepancy has been explained by the fact that although βB2-crystallin promoter activity is enhanced by c-Maf both in *in-vitro* differentiating rat lens fiber cells and CHO cells but it does not play a major role in regulating the βB2-crystallin promoter activity. This statement is supported by the experimental results where deletion of the βB2-crystallin MARE (mapped to-143/-123) does not decrease βB2-crystallin promoter activity in lens fiber cells and furthermore a dominant c-Maf construct does not inhibit the activity of βB2-crystallin promoter in lens fiber cells. Thus the putative Sox binding site at (-164/-159) and a positive element at (-14/-7) are the primary regulatory elements (Doerwald *et al.*, 2001).

1.2.3. The βB2-crystallin protein:

The crystallographic structure of βB2-crystallin has been determined, however the terminal 8 and 10 residues of the amino- and carboxy- terminal arms respectively cannot be resolved on electron density maps, suggesting they do not occupy a fixed position. NMR study of βB2-crystallin in solution shows the terminal extensions possess little ordered structure, are accessible to solvent, and flex freely from the main body of the protein. However, the question of the terminal extension's structure and their possible role in βB2-crystallin function remains still largely unresolved. The protein statistics are as follows according to the ENSEMBL database:

Table 1.5: Protein statistics of βB2-crystallin protein (ENSEMBL database; March,.2005)

Isoelectic point	=	7.0234
Charge	=	2.5
Molecular weight	=	23380.92 Da
Number of residues	=	205
Average residue weight	=	114.053 Da

The protein consists of two domains, an N-terminal domain and a C-terminal domain as the core. Each domain consists of two Greek key motifs; each Greek key motif consisting of four anti-parallel β-strands. The two domains are connected by a distinct connecting peptide (Figure 1.4).
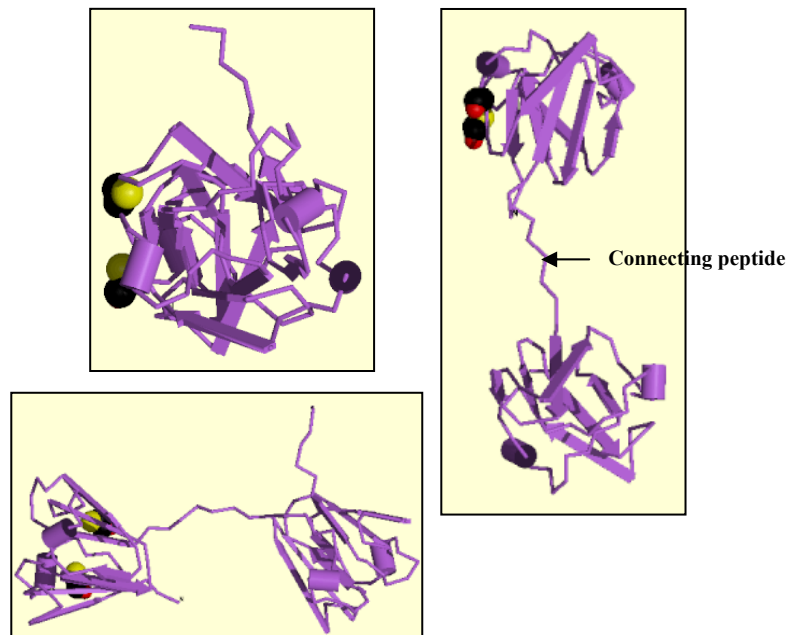
Figure 1.4: Secondary structure and ligands of βB2-crystallin; Source: Bovine (*Bos taurus*) lens; 3 orthogonal views; Protein: 181 residues - (4 helices, 14 strands); Resolution: 2.10A°. R-factor: 0.186.
http://srv2.lycoming.edu/~newman/courses/bio44499/ghani/right-a.htm

1.2.4A: <u>Post-translational modifications of βB2-crystallin:</u>

It has been reported that βB2-crystallin undergoes extensive truncation during aging in human lenses producing fragments with M_r between 4 and 19 kDa isolated from lenses of 20-87 year old donors (Srivastava *et al.,* 2003). Zhang *et al.* (2003) reported that βB2-crystallin is the least modified β-crystallin in adult lenses with around three sites of partial deamidations. They also reported the tendency of the modified β-crystallins to form non-covalent complexes. The presence of βB2-crystallin (the least modified and most soluble of β-crystallin) in these complexes has been attributed to a possible role of βB2-crystallin in solubilizing the more heavily modified β-crystallins. Loss of C-terminal serine residue in case of bovine βB2-crystallin has been reported by Kilby *et al.* (1995) as an age related phenomenon.

1.2.4B: <u>Structural similarities of β/γ-crystallin with other proteins:</u>

Proteins with Greek key motifs have also been known in some lower organisms like the yeast killer toxin from *Williopsis mrakii* (WmKt; one Greek key motif) [Antuch *et al*., 1996], sperulin 3a from *Physarum polycephalon* (two Greek key motifs) [Wistow, 1990; Rosinke *et al*., 1997], *Streptomyces* killer toxin-like protein (SKLP; 2 Greek key motifs) [Ohki *et al*., 2001], protein S from *Myxococcus xanthus* (four Greek key motifs) [Wistow *et al*., 1985; Teintze *et al*., 1988; Bagby *et al*., 1994], the epidermis- specific protein from *Cynops pyrrhogaster* (EDSP or ED37; four Greek key motifs) [Wistow *et al*., 1995], calmodulin-

binding membrane protein family (PCM) from *Paramecium tetraurelia* (Chan *et al*., 1999), and the putative human tumor suppressor protein AIM1 (twelve Greek key motifs) [Ray *et al*., 1997] . These proteins are among the most long lived globular proteins, known generally to be expressed under stress, adverse conditions or in differentiating tissues (Rajini *et al*., 2001).

It is noteworthy to mention that the protein S (from the gram-negative soil bacterium *Myxococcus xanthus*) is a 173 residue Ca^{+2} binding protein mostly found on the dehydrated coat of the myxospores where it oligomerizes to form a multilayer protective coat in a process that specifically requires Ca^{+2} (Bagby *et al.,* 1994). It is also thought that this may act as a cell to cell adhesive. It has also been reported that Ca^{+2} binding influences significantly the conformational stability of protein S (Wenk *et al.,* 1998). Protein S (Figure 1.5) is a heat stable acidic protein that can bind 2 calcium ions. The N-terminal calcium binding site has a higher affinity than the C-terminal calcium binding site. It contains two domains and the overall folds of the two domains are essentially identical. Within each domain there are two Greek key motifs. One motif contains an alpha helix while the other does not. The presence of alpha helix differentiates it from the βγ-crystallin. Sperulin 3a (from *Physarum polycephalon*) shares the typical two Greek key motif and is stabilized by dimerization and Ca^{+2} binding (Kretschmar *et al.,* 1999). Calcium binding properties of AIM1 (absent in melanoma) have been shown by Rajini *et al*. (2001). A single crystallin domain of AIM1 comprising of two Greek key motifs, binds calcium with an affinity comparable to that of the γ-crystallins (Rajani *et al*., 2001).
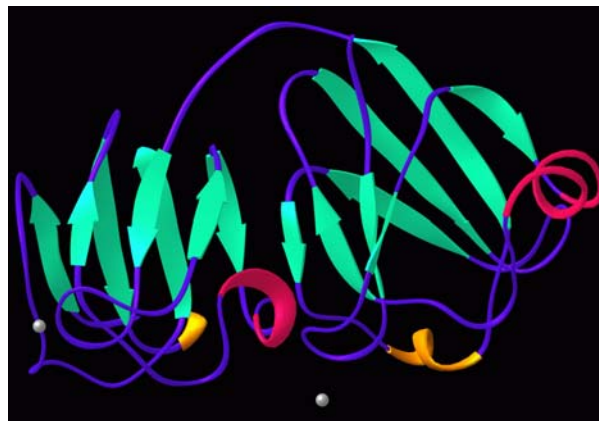
Figure 1.5: Protein S from *Myxococcus xanthus*. Protein S is made up of 4 internally homologous motifs which form 2 domains. Each domain consists of 2 Greek keys. Overall, the protein looks like a triangular prism. Protein S is 173 amino acid residues long. It consists of 15 beta strands, 2 alpha helices (magenta), and two 3_{10}-helices (gold) [The 3_{10}-helix, suggested to be the intermediate between a nascent helix and an alpha-helix (Millhauser, 1995)]. It is a calcium (Ca^{2+})-binding protein that binds 2 calcium ions (shown in silver). [http://www-nmr.cabm.rutgers.edu/photogallery/structures/html/page42.html]

1.2.4C: <u>Calcium binding properties of β-crystallins:</u>

β-crystallins are low affinity and moderate capacity calcium binding proteins that have no well defined structural motifs such as EF-hand or helix-loop-helix like the calmodulins and troponin C. 3-4 calcium binding sites have been in detected in $β_H$-crystallin* based on Scatchard plot by Sharma *et al.* (1996). Terbium binding (a frequently used approach to detect the binding of calcium ion), yielded positive results suggesting $β_H$-crystallin binds Ca^{+2}. J bands [620-630nm; J bands are induced when the dye binds to a globular domain of the macromolecule] were detected in case of $β_H$-crystallin following Stains-all- binding (using the cationic carbocyanine dye-Stains-all); a procedure specific to detect calcium binding. Parvalbumins (well known calcium binding protein) also induces the J band of the dye (Sharma *et al.*, 1996). β-crystallins have also been reported to undergo conformational changes (both in secondary and tertiary structures) in presence of calcium ions in low ionic strength buffers (Sharma *et al.*, 1996). Rajini *et al.* (2001) proposed the Greek key crystallin fold (The four stranded Greek key β-sheet peptide) as a novel calcium binding motif.

*[β-crystallins can be isolated in several aggregation states, spanning a molecular weight range from about 46 kDa to > 200 kDa. These include octameric $β_H$, the tetrameric $β_{L1}$ and the dimeric $β_{L2}$. The βB2-crystallin polypeptide predominates in both the $β_H$ and $β_L$ -crystallin fractions accounting for about 50% of the total in the prenatal bovine lenses.]

1.2.4D: <u>βB2-crystallin and phosphorylation:</u>

Zarbalis *et al.* (1996) identified a putative protein-kinase C phosphorylation site immediately in front of the fourth Greek key motif among all basic β-crystallins (βB2-crystallin is basic) but not among the acidic ones following sequencing of all available vertebrate *Crybb* sequences. Kleiman *et al.* (1988) had earlier reported the *in-vivo* phosphorylation of only the Ser^{230} in the βB2-crystallin protein (only in $β_L$ fraction). βB2-crystallin has also been reported to be involved in cAMP dependent (Kleiman *et al.*, 1988) and cAMP independent phosphorylation pathways (Kantorow *et al.*, 1997; ARVO abstract).

1.3: βB2-crystallin related diseases:

Cataracts as opacities of the ocular lens are frequent diseases in man and often observed in animal models. It can be both congenital and/ age related. In particular age related cataracts are a major cause of lens extraction. Moreover, environmental influences like UV radiation and nutritional effects are thought to initiate or accelerate cataract formation. Congenital cataracts in man occur with an incidence of about 1-2 among 10.000; in about 1/3rd of the cases a positive family history was found (Krumpasky *et al.*, 1996). Inherited cataracts due to mutations in the βB2-crystallin gene are known in case of both humans (4 cases, Litt *et al.*, 1997; Gill *et al.*, 2000; Vanita *et al.*, 2001; Santhiya *et al.*, 2004) and mouse [2 cases, *Philly* mouse (Kador *et al.*, 1980; Chambers *et al.*, 1991) and *Aey2* (Graw *et al.*, 2001)]. They are discussed in the following section.

1.3.1: Inherited cataracts as a result of mutation in *CRYBB2* in human:

1.3.1A. Cerulean blue cataract: [Litt *et al.,* 1997].

Autosomal dominant congenital cataracts (ADCC) are the most common familial form in the Western world. In an American family, such an autosomal dominant cerulean cataract (CCA$_2$; congenital cataract of cerulean type 2) was mapped to a region of human chromosome 22 containing the three genes coding for different β-crystallins and has been found to be associated with a chain termination mutation in the *CRYBB2* following sequence analysis (C$_{475}$T; Glu$_{155}$X). In this case, the βB2-crystallin polypeptide lacks 51 of the 55 amino acid residues normally encoded by exon VI. Cerulean cataracts have peripheral bluish and white opafications with occasional central lesions arranged radially. The lens opacity is observable during foetal development and in childhood; usually visual acuity is reduced in adulthood when lens extraction is generally necessary.

1.3.1B. Coppock-like cataract (CCL) [Gill *et al.,* 2000]:

The genetic defect for the Coppock-like cataract (CCL) [different from that affecting the *CRYGC* gene; Héon *et al.*, 1999] affecting a Swiss family, was linked to the chromosome 2q33-35 CCL locus, and has been reported to be due to a mutation in the exon VI of the *CRYBB2* gene. This sequence change is identical with that of previously described [Section 1.3.1A] (Litt *et al.,* 1997) cerulean blue cataract, a clinically distinct entity. Thus, the CCL phenotype (Figure 1.6) is considered to be genetically heterogeneous with a second gene on chromosome 22q11.2, *CRYBB2*. The CCL and the cerulean cataract are two distinct clinical

entities associated with the same gene defect. Thus, the role of an unidentified modifier factor influencing cataract formation has been suggested (Gill *et al.,* 2000).
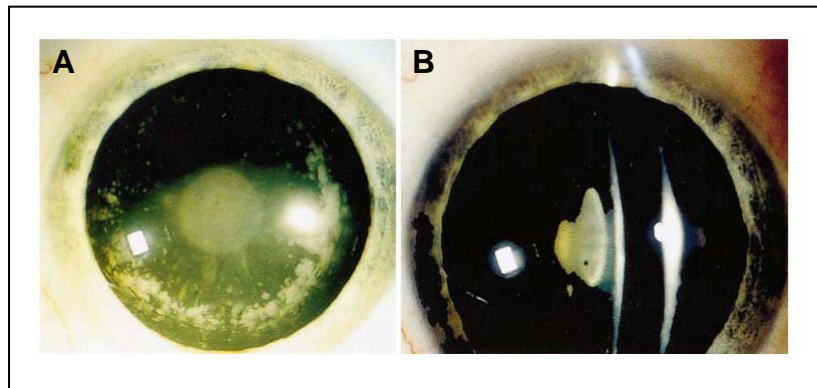
Figure 1.6: Slit lamp photographs of an individual affected with CCL. Figure 1.6A is the front view and Figure 1.6B slit view of the lens and cornea. [Gill *et a*l., 2000]

1.3.1C. <u>**Unique form of autosomal dominant cataract explained by gene conversion between βB2-crystallin and its pseudogene**</u> [Vanita *et al.,* 2001]**:**

The cause of an autosomal dominant sutural cataract with punctuate and cerulean opacities (Figure 1.7) affecting a large Indian family has been mapped to chromosome 22 following linkage analysis. Two cosegregating sequence changes (475C→T and 483C→T) were identified in the *CRYBB2* gene. The first finding was earlier reported in two genetically unrelated families with other inherited forms of cataract (Litt *et al*., 1997; Gill *et al*., 2000). The later, with the two sequence alterations are identical to the sequence of the *CRYBψB2* pseudogene that is 228 kb apart. Furthermore, the pseudogene-like fragment within the *CRYBB2* gene is flanked by chromosomal junction sequences. Gene conversion has been described as the mechanism leading to this mutation. Alternatively, dual point mutation can also explain these findings.

The phenotype of this Indian family, sutural cataract with punctuate and cerulean opacities, differs from all other reported forms of cataract. The American family has pure cerulean cataract (Litt *et al*., 1997) and the Swiss family shows Coppock-like cataract (Gill *et al*., 2000). Moreover the prominent pulverulent central disc-like opacity involving the embryonal and foetal nucleus observed in the Swiss family is not observed among the American or the Indian family. Thus there is not even an overlap between the phenotype of the Swiss family and the other two families.

 In addition, since all of these three families with the Q155X mutations showed different types of cataract, role of other modifying factors in determining the type of cataract is speculated with the main cause being mutation in the *CRYBB2*. The different cataract phenotype is

thought to depend on modifying genetic and epistatic factors. *Cis* acting major modifiers could explain the considerable phenotypic variability between families. Minor modifying factors acting in *trans* could also cause the phenotypic differences among families but not in case of the Indian family, as the minor modifier in this family is not linked to the Q155X mutation (since there is considerable clinical variability within these patients who share identical haplotype). Interestingly this excludes three further crystallin genes (*CRYBA4, CRYBB1* and *CRYBB3*), from being the minor modifier. On the other hand, exactly these three crystallin genes are candidates to be the major modifier (Vanita *et al.*, 2001)
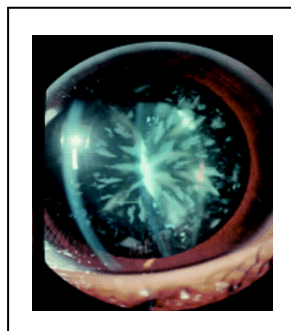
Figure 1.7: 3-D photograph of the eye of a 9 year old patient through slit lamp microscope. At the centre of the lens there is a dense, white, sharply defined sutural opacity with two of its branches showing fish tail-like division towards the periphery. A large number of sharply defined, elongated, spindle shaped, and oval punctate opacities are directed radially. Similar presence and distribution of opacities are seen posteriorly which are much larger and denser than the anterior ones (Vanita *et al.*, 2001).

Thus, all the three above mention (1.3.1A-C) different types of ADCC (autosomal dominant congenital cataracts) found among three independent families are caused due to the same mutation (Q155X). The genetic mechanism involved in all these cases is attributed to a sequence-specific gene conversion between *CRYBB2* and its closely linked pseudogene (Vanita *et al.*, 2001; Gill *et al.*, 2000).

1.3.1D: <u>A new congenital cataract causing allele in *CRYBB2* gene</u> [Santhiya *et al.,* 2004]**:**
A substitution (W151C) in exon VI of *CRYBB2* has been identified as the causative mutation underlying the phenotype of central nuclear cataract in all affected members of an Indian family with congenital cataracts. Protein structural interpretations demonstrated no major structural alterations and that even the hydrogen bonds to the neighboring Leu166 were unchanged. Hydropathy analysis of the mutant βB2-crystallin featuring the amino acids at position 147 to 155, further increased the hydrophobicity, which can potenially impair the solubility of the mutant protein. The Cys residue at position 151 can possibly be involved in

intramolecular disulphide bridges with other cysteines during translation, thereby possibly leading to dramatic structural changes and the resulting cataract phenotype. Exon VI of *CRYBB2* thus appears to be a critical region susceptible for mutations leading to lens opacity

1.3.2. Inherited cataracts as a result of mutation in *Crybb2* in mouse:

Philly mouse cataract and *Aey2* are the well known mouse cataract models due to mutation in the *Crybb2* gene.

1.3.2A: *Philly* mouse cataract:

This is one of the earliest and well studied mouse cataract models characterized by anterior and posterior subcapsular opacity that is inherited as an autosomal dominant trait (Kador *et al.*, 1980). The Philly lens lacks a functional mRNA responsible for *Crybb2*. The corresponding cDNA from the *Philly* lenses contains an in-frame deletion of 12 bp resulting in a loss of 4 amino acids. The region in which the deletion of the 4 amino acids occur is close to the carboxy-terminus which is essential for the formation of the tertiary structure of the βB2-crystallin protein (Chambers *et al.*, 1991). The formation of cataract begins after birth and continues progressively. The lenses develop normally until the first postnatal week; during this time particles appear in the anterior cortex that extend by the 10th day to the anterior subcapsular area. The loss of normal lens denuleation process and swelling of the lens fibers follows. The characteristic bow configuration of the nuclei is replaced by fan shaped configuration (Uga *et al.*, 1980). The following changes are observed with time (table 1.4).

Table 1.6: Changes during cataractogenesis in Philly eye with age. (Kador *et al.*, 1980)

Age	Changes
Day 15	Faint anterior opacities
Day 25	Sutural cataracts
Day 30	Nuclear cataract
Day 35	Lamellar perinuclear opacities
Day 45	Total nuclear cataracts with anterior and posterior polar involvements

Cataractogenesis parallels with a variety of osmotic changes like intralenticular increase in water, sodium and calcium and a decrease in potassium, reduced glutathione and ATP. An altered membrane permeability is the cause of the increased outward leak of potassium (Kador, 1980). Associated with this altered membrane permeability in the *Philly* mouse lens,

a changed pattern of membrane glyoproteins (Garadi *et al.*, 1983) and membrane lipids (Andrews *et al.*, 1984) have been reported. The increasing severity of the disease is temporally correlated to the expression of *Crybb2* gene (Graw, 1997).

The cause of these biochemical changes may be due to the different biophysical properties of the altered βB2-crystallin (like the absence of heat stable characteristics as reported by Nakamura *et al.*, 1998). Moreover, the altered form of βB2-crystallin in *Philly* mouse lens is present primarily in the heavy-molecular weight fraction, indicating its probable interaction with other β-crystallins in the lens (Russel., 1990). It is a matter of speculation whether the interactions of the altered βB2-crystallin with other lens proteins cause rapid aggregation of the cellular proteins, leading to the formation of the heavy weight material resulting in cataract.

1.3.2B. *Aey2*, another mutation in the *Crybb2* gene of mouse (Graw *et al.*, 2001):

This mutation was found during an ethylnitrosourea (ENU) screening, where the mice were tested for the occurrence of dominant cataracts. The cortical opafication, visible at the eye opening, progresses to an anterior suture cataract (Figure 1.8) and reaches its final phenotype as total opacity at 8 weeks of age. There is no obvious difference between the heterozygous and the homozygous mutants. This mutation has been found to be due to a **T → A** exchange at position 553 in the *Crybb2* gene, leading to an exchange of Val for Glu. It therefore affects the same region as the *Philly* allele. Correspondingly, the loss of the fourth Greek key motif probably takes place. This region is considered essential for the correct formation of the tertiary structure of the βB2-crystallin, even though previous structural examination of the C-terminal region focussed on the amino acids from 173 to 185, but did not include Val187 (Sergeev *et al.*, 1998). Therefore it is likely that the mechanisms involved in both (*Philly* mouse and *Aey2*) cataractogenic processes are very similar. However, the lenses of the *Aey2* mutant showed a slower progression of the opafication which terminates between 8 and 11 weeks of age. The dust like particles present in the anterior cortex of the *Philly* mouse, which are most likely to be breakdown products of cell nuclei which do not undergo the regular degradation process that occurs in the normal lens fiber cells. The slower progression in cataractogenesis may be due to a smaller molecular lesion in the *Aey2* (Graw *et al.*, 2001) mice than in the *Philly* mouse.
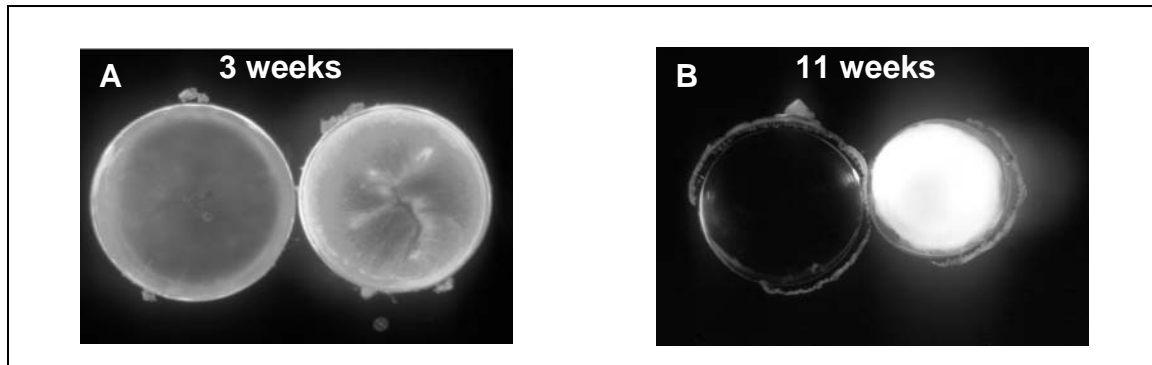
Figure 1.8: Gross appearance of lenses of the *Aey2* mutant mouse. (**A**) Lenses of wild-type (*left*) and homozygous *Aey2* mutant (*right*) mice at the age of 3 weeks. Both genotypes showed the same cortical and anterior suture opacity. The anterior suture was abnormally branched. Original size of the lenses was approximately 2 mm. (**B**) The lens of a heterozygous *Aey2* mutant at the age of 11 weeks was completely opaque (*right*). For comparison, an age-matched wild-type (*left*) is shown. Original size of the wild-type lens is approximately 3 mm. [Graw *et al*., 2001]

1.4. **Mutation *O377*** [Favor, J.; unpublished]

This is the latest inclusion (third allele following *Philly* and *Aey2*) of the *Crybb2* related inherited cataracts in mouse. It is a dominant progressive cataract mutation discovered in the offsprings of paterntally irradiated (3 Gy X-irradiation)) mice. The mutation has been mapped to chromosome 5, between the markers *D5Mit239* and *D5Mit138*, which is the region containing the *Crybb1, Crybb2, Crybb3* and *Cryba4* gene cluster. Sequencing of cDNAs of all four genes revealed a 57 bp insertion at the beginning of exon VI in *Crybb2*. The remaining three genes were not affected. Analysis of genomic DNA indicated the mutation to be due to an **A → T** bp substitution at the first position of the intron 5 acceptor splice site leading to the inclusion of 57 bp from intron V into the cDNA.

 A detailed analysis at the phenotypic and molecular level of this mutant (*O377*) was carried out in this project in comparison to the wild-type (C3H) to reveal more about the molecular mechanisms involved during cataract progression and to detect the expression of βB2-crystallin in the brain and retina and also to find out consequences of the mutated βB2-crystallin in the brain.
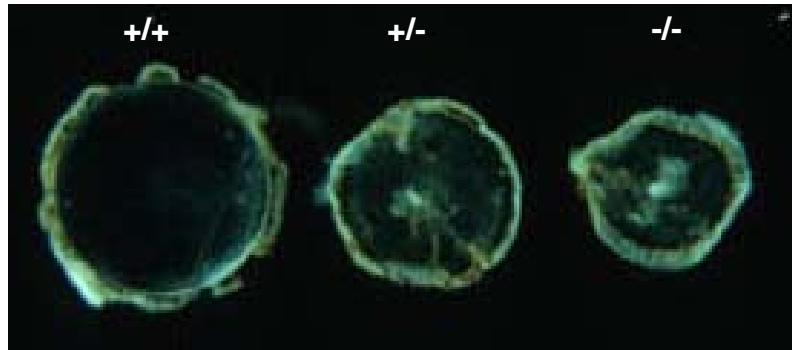
Figure 1.9:. Gross appearance of lenses (dark field photograph) of the *O377* mutant mouse at the age of 6 months (Favor, unpublished).

Dr. Neuhäuser-Klaus, A. (unpublished) has already shown the histological features in transverse sections of the eyes of the *O377* mutants at various ages. Figure 1.10 shows such a study in the eyes of 3 weeks old animals following Methylene blue and basic fuchsin staining in both heterozygous and homozygous *O377* mutants. The two lateral cortical regions and the posterior region of the lens develop patchy appearances and high vacuolation which can be observed in almost the entire lens tissue in the hetereozygote. Severe form of the same phenotype can be observed in the homozygous lens with almost a crumbling appearance.
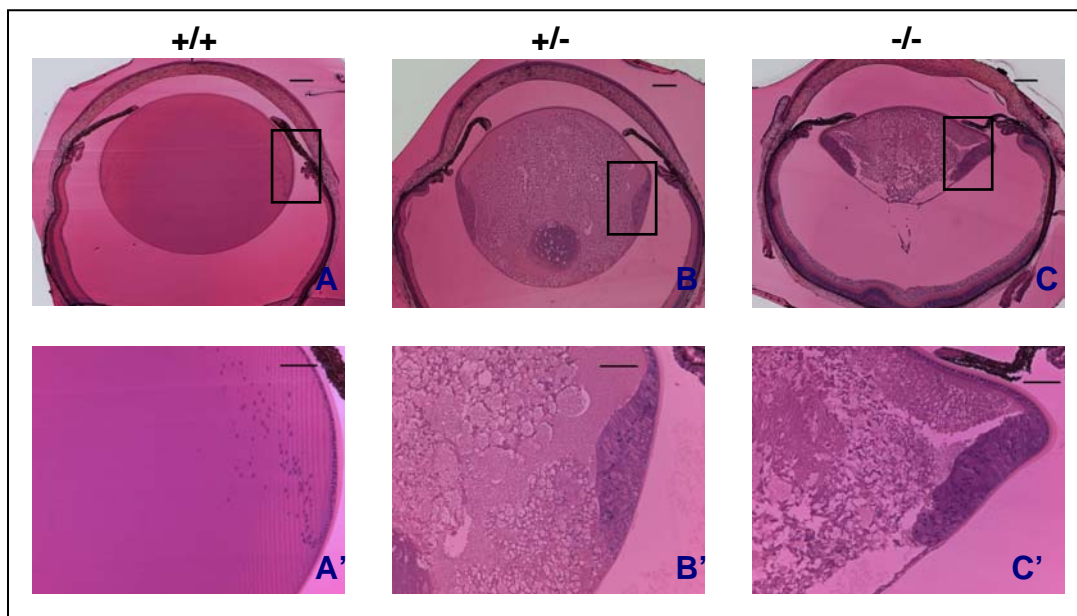
Figure 1.10: Transverse section of eyes (3μm) from 3 week old animals followed by Methylene blue and basic fuchsin staining shows the heterozygous mutant lens (Figure B, B') to be highly vacuolated and with patchy appearances on the two lateral sides in the region of lens fiber cells and posterior region of the lens, and the homozygote lens (C, C') apart from showing severe forms of similar histological features as in the heterozygous lens; has a crumbling appearance and is on the verge of collapse. It is only at the age of 3 weeks that all the mutant animals start developing well defined cataractous phenotype. Figures A and A' are of wild-type animals as control sets **[Neuhäuser-Klaus, A.; unpublished]**

24

1.5: <u>Aim of the study:</u>

Identification of the mutant *O377* in the group of Dr. J. Favor at the Institute of Human Genetics, GSF-National Research Center for Environment and Health, lead to the establishment of this new cataract mouse model due to the mutation in the *Crybb2* gene. Characterization of this new mouse model of cataract at the molecular and phenotypic level is considered to be valuable for better understanding of the causes and mechanism of congenital ocular opacities affecting huge percentage of human population. This knowledge would have significant inputs in learning how to prevent the formation of protein aggregates in the lens that impede light transmission which would not only ameliorate cataracts but will also help to understand other pathologies precipitated by protein denaturation and misfolding (Bhat, 2004; Bhat, 2003). The other interesting prospect was the detailed study on the expression of *Crybb2* in the non-ocular (brain) and non-lenticular (retina) tissues where it has been reported to be expressed in the wild-type (Magabo *et al.*, 2000). Thus, this study attempts to throw light on the non-structural role/s played by βB2-crystallin. It is well known that crystallins bring about lens transparency but its mechanism is still unknown. Therefore it is important to know how this phenotype is maintained and how to protect it from genetic predisposition, age and environment. We have only known of lens protein as inanimate building blocks but not as active catalytic kingpins that sustain transparency. Knowledge on the non-structural function of crystallins will potentially reveal the bio-molecular processes that sustain the physical phenotype of transparency (Bhat, 2004; Bhat, 2003) and also its un-elucidated role in brain.

Materials and methods:

2.1. Equipments:

All the equipments that were used in this study along with its respective manufacturer are listed in the following table 2.1.

Table: 2.1. List of different equipments and its manufacturers.

Equipment	Manufacturer
Agarose-Gel electrophoresis:	GIBCO BRL, Karlsruhe, Germany
Analysis balance:	Chyo balance Corp, Japan
Analysis balance (Mettler PL 1200):	Utting, Germany
Bacterial incubator WT-Binder:	Bottmingen, Switzerland
Bacterial shaker :	Infors, München, Germany
Bio photometer:	Eppendorf, Hamburg, Germany
Cell culture incubator :	Heraeus, Hanau, Germany
Refrigerated centrifuge (Universal 16R) :	Hettich, Tuttlingen, Germany
Refrigerated centrifuge (Sorvall RC-5B) :	Sorvall, Bad Homburg, Germany
Centrifuge 5810R	Eppendorf, Germany
Electrophoresis power supply (ST 304) :	Gibco, BRL, France
Hybridisation oven Hybaid:	United Kingdom
Incubator (WTE Binder) :	Tuttingen, Germany
Light microscope (Axiolab):	Zeiss , Oberkochen, Germany
Light microscope (Axiovert 35):	Zeiss, Oberkochen, Germany
Light microscope (Axioplan 2):	Zeiss, Oberkochen, Germany
Light microscope (Orthoplan):	Leitz, Wetzlar, Germany
Microtome (Jung RM 2055) :	Leica, Nussloch, Germany
PCR- thermal cycler (PTC-225):	Biozym, Germany
Shaker-incubator (CH-4103):	Bottmingen, Germany

[Table: 2.1. Continued]

Equipment	Manufacturer
Spectrophotometer (UltrospecIII®):	Amersham, Germany
Stereo microscope (Stemi SVII):	Zeiss, Oberkochen, Germany
Stereo microscope (Stemi SVII):	Leica, Beinsheim, Germany
Stereo microscope (MZ APO):	Leica, Beinsheim, Germany
Thermo mixer (5436):	Eppendorf, Hamburg, Germany
Thermostat 5320:	Eppendorf, Hamburg, Germany
Vortex-2genie:	Scientific Industries USA
15 mm Tissue Culture Plate (24 wells)	Nunc, Wiesbaden, Germany
15 ml Tubes	Nunc, Wiesbaden, Germany
50 ml Tubes	Nunc, Wiesbaden, Germany
2 ml Collection tube	Eppendorf, Hamburg, Germany
1.5 ml Collection tube	Eppendorf, Hamburg, Germany
Cryosectioning machine	Mikrom, Germany
Cell strainers	BD Falcon, Germany
Perfusion pump	Neolab, Germany
Syringe & needle	BRAUN, Germany
Glass cubettes	Neolab, Germany
Superfrost®, Plus Slides	Menzel GmbH & Co KG, Braunschweig, Germany
Microwave	Samsung, Germany
Histowax	Cambridge Instruments, Nussloch
Coverslips	Marienfeld, Germany
Heidolph DIAX 900	John Morris Scientific

2.2. <u>Commonly used buffers/solutions:</u>

- **PBS**

  30 ml NaCl (5M)

  15 ml Sodium Phosphate Buffer (1M), pH 7.3

  volume adjusted to 1litre with DEPC water

- **4% PFA**

  4 g PFA (Para formaldehyde)

  100 ml DEPC/PBS

  A few drops NaOH (10N); pH adjusted between 6.0-
  7.0 with HCl, indicator paper was used for adjusting
  pH.

- **10X SDS**

  10g SDS in 100ml water

- **TBE**

  5 X TBE (Tris/Broat)

  0.45 M Tris

  0.45 M Boric acid

  10 mM EDTA

2.3: <u>Softwares and databases :</u>

<u>Vector NTI:</u>	Sequence analysis, primer designing
<u>Relquant:</u>	(Version 1.0); Roche; Analysis of the lightCycler data
<u>Microarray:</u>	http://www.gsf.de/ieg/groups/exppro_cpt.html#PAM
<u>Stereoinvestigator:</u>	Used for stereological counting of cells
<u>Databases:</u>	Ensembl; http://www.ensembl.org/
	NCBI: http://www.ncbi.nlm.nih.gov/entrez/query.fcgi
<u>WebTools:</u>	http://www.expasy.org/ [Proteomics server]
	www.mdl.com
	http://swissmodel.expasy.org//SWISS-MODEL.html
	http://bioinf.cs.ucl.ac.uk/psipred/

2.4: <u>Methods:</u>

In this section a detailed description of the different methods used during this work along with the list of necessary reagents, kits etc. are given.

2.4.1. <u>Tissue preparation, fixation and dissection:</u>

This was the first step of all the experiments that were carried out. The tissue preparation methodology varied according to the experimental objective. The mice were sacrificed*, trans-cardially perfused (when necessary) and then the desired tissue/s were dissected out, processed (when necessary) and stored as stated in table 2.2.

Mice were sacrificed either by CO_2 asphyxiation or by cervical dislocation; however mice were never sacrificed by cervical dislocation if intact brain structure was necessary.

Tissue fixation: The tissue was fixed quickly in 4% PFA in PBS. An ideal fixative prevents the tissues from autodigestion (autolysis); inhibits bacterial or fungal growth (preservation); is isotonic with the tissue and therefore does not alter tissue volume; preserves the tissue structure; does not dissolve tissue components, makes the tissue resistant to damage during subsequent processing, embedding and sectioning stages; and finally is not detrimental to the tissue component of interest. A fixative for ISH (*In-situ* hybridization) and/ immunohistochemistry ideally retains mRNA and/ protein within the tissue while preserving tissue morphology but does not significantly raise background; and simultaneously allow probes to penetrate the tissue and hybridise with the maximum number of target molecules.

Before dissecting out the brain for histological and immunohistochemical studies, the sacrificed animal was **transcardially perfused** i.e. blood was drained out from the body and a fixative (4% PFA in PBS) solution was pumped into the vascular system. Removing the blood improves the results of staining and the fixative preserves and hardens the brain so that it could be sectioned without tearing.

<u>Chemicals/Kits</u>

- 4% Paraformaldehyde (PFA)
- PBS buffer
- Carnoy's solution
   - 60ml 100% Ethanol
   - 30ml Chloroform
   - 10ml Acetic acid

Table 2.2 outlines the procedure of tissue preparation, fixation and storage for different experiments.

Purpose	Tissue	Dissection and preparation	Storage
RNA and protein isolation	**Brain, Lens, Retina**	i)**Brain**: The skull was opened and carefully the intact brain was taken out and transferred in to a 1.5ml tube and immediately snap frozen in dry ice. ii)**Lens:** At-first the eye/s were dissected out, placed on a Petriplate with little PBS buffer to prevent it from drying. Each eye was then taken on a dry Petriplate and the lens was dissected out by giving a small incision at the back of the eye in the region from where the optic nerve emerges. 2 lenses were placed in one 1.5 ml tube and immediately snap frozen in dry ice iii)**Retina:** After taking out the lens, rest of the eye is mostly the retina and cornea, which were collected, 2 per 1.5ml tube and immediately snap frozen in dry ice.	**-80°C**
Histology	**Eye**	The eyes were dissected out and placed immediately in a 2ml tube containing freshly prepared Carnoy's solution and incubated overnight at 4°C for fixation. On the following day they were transferred into 70% ethanol and were subjected to graded dehydration in series of alcohol following which they were embedded in JB-4® Embedding kit according to manufacturer's instructions.	**RT**
***In-situ* hybridisation experiments, Immunohistochemical studies**	**Eye**	The eyes were dissected out and placed immediately in a 2ml tube with 4%PFA in PBS and incubated overnight at room temperature. The following day they were transferred into 70% ethanol and were subjected to graded dehydration in series of alcohol following which they were embedded in paraffin blocks for sectioning.	**-20°C**
Histology, *In-situ* hybridisation experiments, Immunohistochemical studies and stereological studies	**Brain**	The perfused animal was decapitated and absolute care was taken to dissect out the intact brain after opening the skull. Then the tissue was transferred into a 50ml tube containing 4%PFA in PBS and incubated overnight at room temperature. The following day the dissected brains were transferred into 70% ethanol and were subjected to graded dehydration in series of alcohol following which they were embedded in paraffin blocks for sectioning. For **stereological studies**, after dissecting out the brain as described above, the brains were transferred into a 50ml tube containing 4%PFA in PBS for 2 hours and then into 20% sucrose solution and incubated over night. On the following day; the brains were frozen in dry ice for 10 minutes and stored. Before freezing, sucrose solutions were carefully wiped off from the tissue.	**4°C** **-20°C** **(Samples for Stereology)**

2.4.2. Tissue Sectioning:

Tissue sectioning is a very crucial step for carrying out **histological, immunohistochemical and *in-situ* hybridisation studies on eye and brain** and on any other tissues because intact tissue structure is a neccessity for such procedures. For soft tissues like brain, it is important to make the tissue a little hard before dissecting out from the animal, hence transcardial perfusions were carried out in sacrificed mouse with 4% PFA in PBS. The dissected tissues (eyes and brains) were then dehydrated in gradient alcohol series and embedded in paraffin blocks. Brains were sectioned (8μm thick) in a microtome through sagittal plane in series of eight and mounted on precleaned grease free slides. This arrangement of sections is vital for colocalization studies and to utilize the huge number of sections in a optimum way. Thus a set of slides (A^1-X^1 or A^2-X^2 and so on as in figure 2.1.) containing sagittal brain sections represents the whole brain in specific interval. The eyes were transversely sectioned (5μm) and mounted on precleaned grease free slides.
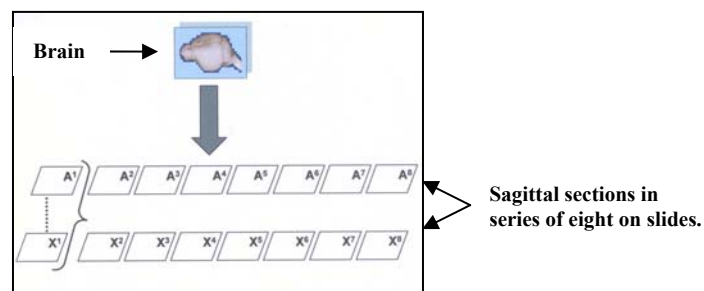
Figure 2.1.: The paraffin embeded brain was sectioned in sagittal plane and the sections were arranged in series of eight on grease free slides. A set of slides numbered as A^1-X^1 or A^2-X^2 or A^3-X^3 to A^8-X^8 represents the entire brain in a specific interval.

Stereological studies were carried out with free floating sections. Frozen brain samples were taken out from -20°C, kept inside the cryo-microtome for 20 minutes and then mounted on the metallic block in the quick fix mounting solution over the quick freeze block and left inside the cryo-microtome for 20-30 minutes. Following this, cryosections (50μm) were made in sagittal plane in series of twelve and the sections were placed in cryoprotection solution contained in two 6 well cell culture plates (with cell strainer in each well) as explained in the figure 2.2. Thus, all the samples of each well together represents the whole brain at a specific interval. In the cryoprotection solution [125ml glycerine (MERCK) ; 125ml ethylene glycol (Fluka) ; 250ml PBS] the samples can be stored for long time at -20°C without being frozen. After all the samples were sectioned, prior to mounting them on the slides, the cell strainers containing the desired samples were washed O.N. (over night) in PBS with atleast 4 changes

of the buffer. All the free floating sections in the wells numbered. **2, 6 and 10 (Figure 2.2)** were mounted on precleaned grease free slides, the sections were arranged sequentially on every slide.
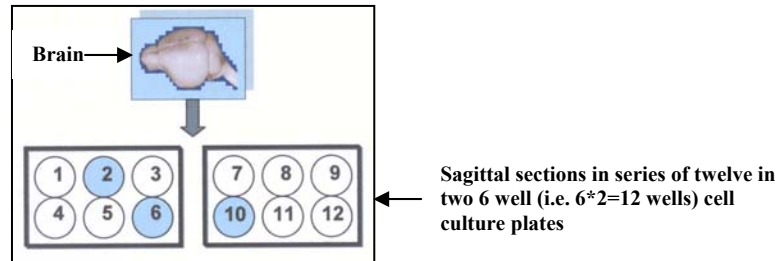
Figure 2.2: The fixed brain was cryo-sectioned (50µm) in sagittal plane and the sections were arranged in series of twelve in two 6 well cell culture plates (with cell strainers in each well) containing cryoprotection solution. All the sections of each well represents the entire brain at a specific interval. Section from wells 2, 6 and 10 were mounted sequentially on clean grease free slides

2.4.3. <u>RNA isolation:</u>

<u>Kits/Chemicals</u>

- RNeasy® Midi kit, Qiagen; Germany
- RNeasy® Mini kit, Qiagen; Germany
- RNAzol™ B, Campro Scientific B.V., Amsterdam, Netherlands
- β-mercaptoethanol (β-ME)
- Chloroform, MERCK
- Isopropanol, MERCK
- 70% Ethanol (MERCK)
- DEPC (Diethylpyrocarbonate) water, to make the water RNase free

2.4.3A. <u>Tissue type: Brain</u>

RNeasy® Midi kit was used for the isolation of total RNA from brains of animals of the ages P1, P7, P14, P21, 4 weeks, 6weeks and 8 months .

Normally, an adult mouse brain of either sex weighs between 400-500 mg but a maximum of 250mg tissue can be processed with one RNeasy® Midi kit column. Therefore, the homogenized sample of each brain was processed over **2 columns** and combined after elution.

10μl β-mercaptoethanol (β-ME) was added per 1ml buffer RLT (supplied in kit; contains guanidine isothiocyanate) just before use. β-ME is toxic; hence, it was dispensed in a fume hood and appropriate protective clothings were worn. RNA was isolated in the following way according to the manufacturer's instructions.

Buffers RLT and RW1 (both contains guanidine isothiocyanate); RPE and RNase-free water were supplied in the kit.

I. The frozen samples were quickly transferred into tubes containing 4ml Buffer RLT+ β-ME. Then the tissue was homogenized for 1 minute with Heidolph DIAX 900 homogeniser at its highest speed (26,000 rpm).

II. 4ml Buffer RLT+ β-ME was added again to the tissue lysate, mixed and centrifuged for 10 minutes at 4000 rpm[*] at RT.

[*Centrifugations performed with Centrifuge 5810R, Eppendorf; Rotor: A-4-62]

III. The supernatant was then carefully transferred to a new 50ml tube by pipeting.

IV. 1 volume (8ml) of 70% ethanol was then added to the homogenized lysate and mixed immediately by vigorous shaking. The sample was applied to **two RNeasy[®] Midi spin columns**, centrifuged for 5 minutes at 4000 rpm[*].

V. The flow-through was discarded and the rest of the homogenized lysate was applied to the column, centrifuged for 5 minutes at 4000 rpm[*]. Again the flow through was discarded.

VI. 4ml buffer RW1 was added to the RNeasy[®] Midi spin column. Centrifuged for 5 minutes at 4000 rpm[*]. Flow through was discarded.

VII. 2.5ml buffer RPE (ethanol added) was added to the RNeasy[®] Midi spin column. Centrifuged for 2 minutes at 4000 rpm[*]. Flow through was discarded.

VIII. 2.5ml buffer RPE (ethanol added) was added to the RNeasy[®] Midi spin column. Centrifuged for 5 minutes at 4000 rpm[*]. The flow through was discarded.

IX. The RNeasy[®] Midi spin column was centrifuged for 10 minutes at 4000 rpm[*] to dry the spin column membrane.

X. To elute, the RNeasy[®] Midi spin column was transferred to a new 15ml collection tube. 100μl of RNase-free water was added into the spin column membrane, incubated at RT for 1 minute and then centrifuged for 7 minutes at 4000 rpm[*].

XI. The elution step was again repeated with the eluate from step X.

XII. Eluates from both columns were then combined, concentration measured and simultaneously stored at -80°C.

[*Centrifugations performed with Centrifuge 5810R, Eppendorf; Rotor: A-4-62]

2.4.3B. Tissue type: Lens

Total RNA from lens was isolated using both **RNeasy**® **Mini kit and RNAzol**™ **B.**

2.4.3B.1. Isolation of total RNA by RNeasy® **Mini kit:**

4-6 lenses were taken in each 1.5ml Eppendorf tube and RNA was extracted from them. **10μl** β-mercaptoethanol (β-ME) was added per 1ml buffer RLT just before use. β-ME is toxic; hence, it was dispensed in a fume hood and appropriate protective clothings were worn. RNA was isolated in the following way according to the manufacturer's instructions.

Buffers RLT and RW1 (both contains guanidine isothiocyanate); RPE and RNase-free water are supplied in the kit.

I. 350μl Buffer RLT was added to each eppendorf tube and the tissue was crushed using a plastic pestle (atleast 20 times). Then the tissue was homogenized by passing it through a 20-gauge needle fitted with a RNase free syringe for at least 5 times.

II. The tissue lysate was then centrifuged for 3 minutes at 13,000 rpm* at RT. The supernatant was then carefully transferred to a new 1.5ml Eppendorf tube by pipetting, the tube containing the pellet was discarded.

[* Centrifugations performed with Biofuge, Hereaus Instruments; Rotor: PP1/97 #3324]

III. 350μl of 70% ethanol (1 volume; adjusted accordingly if some tissue lysate was lost in previous steps) was added to the cleared lysate and mixed immediately by pipetting.

IV. The whole sample (~700μl) was then added to the RNeasy® mini column placed on a 2ml collection tube. The tube was closed gently and centrifuged at 13,000 rpm* at RT for 15 seconds. The flow-through was discarded.

V. 700μl buffer RW1 was then added to the RNeasy® column, tube closed gently and centrifuged at 13,000 rpm* at RT for 15 seconds.

VI. The RNeasy® column was then transferred to a new 2ml collection tube. 500μl of Buffer RPE (ethanol added) was then added to the RNeasy® column, tube closed gently and centrifuged for 15 seconds at 13,000 rpm* at RT to wash the column. Flow-through was discarded.

VII. Again 500μl buffer RPE was added to the RNeasy® column, tube closed gently and centrifuged for 2 minutes at 13000 rpm* at RT to dry the RNeasy® silica-gel membrane. Flow-through was discarded.

VIII. To eliminate any possible buffer RPE carryover, the RNeasy® column was placed on a new 2 ml collection tube and centrifuged for 1 minute at 13,000 rpm* at RT. Any flow-through was discarded.

IX. The RNeasy® column was then transferred to a new 1.5ml collection tube for elution. 30-50µl RNase-free water was pipetted directly onto the RNeasy® silica-gel membrane; tube closed gently and centrifuged at 13.000 rpm* for 1 minute at RT.

X. A second elution step was performed with the first eluate into the same elution tube to achieve higher RNA concentration.

XI. The concentrations were measured and the RNA samples were stored at -80°C.

The concentration and purity of RNA was determined by measuring the absorbency (optical density) at 260 nm (A260) and 280 nm (A280). An absorbency of 1 unit at 260 nm corresponds to 40 µg of RNA per ml (A260 = 1 = 40 µg/ml). The measurements were in water diluted 2:198, and purity was estimated through the ratio between the absorbency values at 260 and 280 nm. RNA was checked at 1% agarose gel for 10 min at 200V.

Calculations involved in RNA quantitation were:

Volume of RNA sample =100 µl

Dilution = 10 µl of RNA sample + 490 µl water (1:50)

A260 = 0.23; measured in water A260 value of 1 was equal to 40 µg/ml of RNA.

The ratio between the readings taken at 260 nm and 280 nm (A260/ A280) provided an estimate of the purity of RNA, ranging from 1.5-1.9 is for different types of water, ratio of 1.8-2.1 for 10 mM Tris/HCl, and pH 7.5.

[* All centrifugations performed with Biofuge, Hereaus Instruments; Rotor: PP1/97 #3324]

2.4.3B.2. Isolation of total RNA by RNAzol™ B:

During this method all preparations were made on ice and under hood.

I. 100µl of RNAzol™ B was added to the 1.5ml eppendorf tube containing **two** lenses. The tissues were homogenized very well with the help of plastic stems.

II. Chloroform was added in the proportion of 1:10 to the volume of RNAzol™ B added i.e. 10µl in this case. Then the mixture was vortexed for 15 seconds and kept on ice for 15 minutes.

III. Following to that, it was centrifuged for 15 minutes at 13,000 rpm* at 4°C.

[* Centrifugations performed with Centrifuge Sigma 3K18; Rotor: #12154-H]

IV. The supernatant i.e. RNA was collected and its volume was measured.

V. Equal volume of isopropanol was added to the supernatant to precipitate RNA, and the mixture was vortexed and again incubated for 15 minutes on ice.

VI. It was then subjected to centrifugation for 30 minutes at 13,000 rpm* at 4°C.

VII. The supernatant was discarded and the precipitate was washed with 300µl of 70% ethanol and vortexed.

VIII. Again the mixture was centrifuged for 15 minutes at 13,000 rpm* at 4°C.

IX. The supernatant was discarded and the sample was dried in vacuum for 5 minutes. Care was taken for not over-drying them.

X. 50µl DEPC added water was then added to eluate.

XI. The RNA was dissolved at 60°C for 10-15 minutes and then stored at -80°C. Concentration of the sample was also measured.

[* All centrifugations performed with Centrifuge Sigma 3K18; Rotor: #12154-H]

2.4.3C. <u>Tissue type: Retina</u>

Total RNA from retina was isolated using **RNAzol^{TM} B.** The extraction process is exactly the same as in case of lens except that the retinal tissue was cut into several pieces before homogenisation and retinal tissue from two eyes was taken during each extraction process. At the elution step 100µl DEPC water was used.

2.4.4: <u>Generation of full length first-strand cDNA from mRNA:</u>

Full length first-strand cDNA from mRNA was generated by using **Ready To Go^{TM} T-Primed First Strand kit (RTG);** Amersham pharmacia biotech**.** This kit contains all the necessary reagents required for the generation of full length first strand cDNA from mRNA template using an oligo (dT) primer containing *Not*I restriction site. The procedure for the production of full length first-strand cDNA from mRNA using RTG kit is as follows**:**

i. DEPC treated water was added to 5µg of undegraded (gel checked) total RNA in a RNase free microcentrifuge tube so as to make the final volume to 33µl.

ii. Both the RTG mix and the RNA sample were incubated at 65°C for 5 minutes simultaneously.

iii. Following that, both were incubated at 37°C for 5 minutes.

iv. RNA solution was then transferred to the tube containing RTG mix but was not mixed.

v. It was then incubated at 37°C for 5 minutes and mixed gently.

vi. The mixture was centrifuged for 1 minute at 13,000 rpm* at RT.

vii. Then the mixture was incubated at 37°C for 1 hour. After this incubation cDNA was ready to use and stored at -20°C for future use.

[* All centrifugations performed with Biofuge, Hereaus Instruments; Rotor: PP1/97 #3324]

Components of the RTG mix:

- dATP, dCTP, dGTP, dTTP- all FPLC pure
- Murine Reverse Transcriptase
- RNA guard (porcine)
- RNase/DNase free BSA
- *Not*I-d (T)$_{18}$ primer
  (5'-d[ACTGGAAGAATTCGCGGCCGCAGGAAT$_{18}$]-3')

2.4.5: Preparation of primers:

i.   The DNA fragment to be amplified is determined by selecting primers. Primers are short, artificial strands of oligonucleotides (ideally around 20-22 bases) that exactly match the beginning and end of the DNA fragment to be amplified. They anneal to the DNA template at these starting and ending points, where the DNA polymerase binds and begins the synthesis of the new DNA strand.

The primers which were availed from AG BIO DV (Mr. Utz Linzner) were prepared as follows:

i.   200µl of milliQ H$_2$O was added to the lyophilized oligoneucleotides.

ii. Incubated at 60°C for 15 minutes on a thermoshaker.

iii. Following that, it was incubated on ice for 5 minutes and then centrifuged for 5 minutes at 13,000 rpm[*]. The stock solution was ready.

iv. The concentration of the working solution was 10 Picomol/100µl. To prepare the working solution, the concentration was calculated in picomol. Let the value be X.

v.   Working solution: **Stock:**   1000/X µl

                    MilliQ H$_2$O: 100µl-(1000/X)µl

   The working solution was then mixed well and stored at -20°C for future use.

[* Centrifugations performed with Biofuge, Hereaus Instruments; Rotor: PP1/97 #3324]

2.4.6: Reverse Transcription Polymerase Chain Reaction (RT-PCR):

RT-PCR is one of the most sensitive techniques for mRNA detection and quantitation. Compared to the two other commonly used techniques for quantifying mRNA levels, Northern blot analysis and RNase protection assay, RT-PCR can be used to quantify mRNA levels from much smaller samples. In fact, this technique is sensitive enough to enable quantitation of RNA from a single cell [http://www.ambion.com/techlib/basics/rtpcr/]. This technique basically comprises of two steps:

1. Production of cDNA from mRNA by reverse transcription and
2. Amplification of a particular sequence by polymerase chain reaction (PCR).

2.4.6A. Production of cDNA from mRNA by reverse transcription:

The methodology for the production of cDNA from mRNA by reverse transcription has been already described in the previous section 2.2.4. **Ready To Go^{TM} T-Primed First Strand kit (RTG)** was used for this purpose.

2.4.6B. Polymerase Chain Reaction (PCR):

The PCR technique was invented in early 1980s by Kary B Mullis**.** The purpose of a PCR (**P**olymerase **C**hain **R**eaction) is to make a huge number of copies (amplification) of a particular sequence of a gene or the whole gene itself driven by the enzyme DNA polymerase obtained from thermophilic bacteria (*Thermus aqaticus*). This is necessary to have enough starting template for further procedures like sequencing, cloning, restriction digestion studies etc. There are three major steps; **Denaturation, Annealing and Extension**; in a PCR (Table: 2.3) which are repeated for 30 or 40 cycles, in an automated cycler, which can heat and cool the tubes with the reaction mixture in a very short time.
[http://allserv.rug.ac.be/~avierstr/principles/pcr.html; http://en.wikipedia.org/wiki/PCR]

1. **Denaturation:** This step is performed at a temperature of **94-95°C**. During the denaturation step, the double strand of DNA melts open to single stranded DNA, all enzymatic reactions stop (for example : the extension from a previous cycle).

2. **Annealing:** This step is performed between a temperature range of **54°C-60°C,** according to the optimal annealing temperature of the primer pair of a given fragment of interest. It is important to determine the optimum annealing temperature for a sample by performing a PCR with gradients of annealing temperatures. The primers jiggles around, caused by the Brownian motion. Ionic bonds are constantly formed and broken between the single stranded primer and the single stranded template. The more stable bonds last a little bit longer (primers that fit exactly) and on that little piece of double stranded DNA (template and primer), the polymerase can attach and starts copying the template. Once there are a few bases built in, the ionic bond is so strong between the template and the primer, that it does not break anymore.

3. **Extension:** This step is performed at a temperature of **72°C** which is the ideal working temperature of the polymerase. The primers, where there are a few bases built in, already have a stronger ionic attraction to the template than the forces breaking these attractions. Primers that are on positions with no exact match, get loose again (because of the higher temperature) and don't give an extension of the fragment. The bases (complementary to the template) are coupled to the primer on the 3' side (the polymerase adds dNTP's from 5' to 3', reading the template from 3' to 5' side; bases are added complementary to the template).

Table 2.3: Different steps of PCR.

Step	Reaction	Time	Temperature	Cycles
1	Denaturation	1-2 minutes	95°C	1X
	Denaturation	30 seconds-1 minute	95°C	
2	Annealing	30 seconds-1 minute	54-60°C	30-40X
	Extension	30 seconds-2 minutes	72°C	
3	Extension	10-15 minutes	72°C	1X

RT-PCR reaction was performed with cDNA produced from RNA isolated from lens, brain and retina for the genes *Crybb2* and *β-actin*. The PCR mix and PCR programme

varied a little bit according to the sample and/ gene of interest (2.4.6C). They were as follows:

Enzymes/buffers/chemicals

- **Taq DNA polymerase;** GlBCO BRL, Karlsruhe
- dNTP- Set Pharmacia, Freiburg, Germany
- **PCR buffer:**
    100 mM Tris/HCl pH 8.3
    15, 17.5 or 20 mM MgCl2
    500 mM KCl
    0.1 % Glycerine
- **DMSO** (Dimethyl sulphoxide)
- **Primers;** *AG BIODIV* (Table:2.4)

Table 2.4: List of primers used for RT-PCR amplification of *Crybb2*.

Name	Lab no.	Sequence (5'-3')	Tm (°C)	Primer Pair	Product length (bp)	
					C3H	*O377*
*Crybb2*_L3	41335	ATG GCC TCA GAC CAC CAG ACA C	57.5	*Crybb2*_L3/R1	707	764
*Crybb2*_L4	37633	GGA GAA GGC GGG CTC CG	57.8	*Crybb2*_L4/R1	570	627
*Crybb2*_L5	37634	GGG CGA GTA CCC ACG GTT GG	60.9	*Crybb2*_L5/R1	480	537
*Crybb2*_L6	41792	ATG AGA ACC CCA ACT TTA CTG GCA	57.8	*Crybb2*_L6/R1	373	430
*Crybb2*_L7	41793	TTG ATA CCA GGA AAA GGT GTC TTC C	58.4	*Crybb2*_L7/R1	303	360
*Crybb2*_R1	36073	GGC ACG AGC CAC ACT TTA TTC TTC	58.0			

2.4.6C. <u>**PCR mix and PCR programmes :**</u>

- <u>**Lens cDNA**</u>

    Gene of interest: *Crybb2*

    Primer pairs: *Crybb2*_L3-L6/ R1

PCR mix	
PCR buffer (15µm):	2µl
dNTP:	2µl
Taq Polymerase:	0.2µl
H₂O:	13µl
cDNA	1µl
Right primer:	1µl
Left primer:	1µl

PCR programme		
Denaturation:	94°C for 2minutes	
Denaturation:	94°C for 45 seconds	
Annealing:	56°C for 45 seconds	40X
Extension:	72°C for 45 seconds	
Extension:	72°C for 10 minutes	
8°C forever		

- <u>**Brain cDNA**</u>

    Gene of interest: *Crybb2*

    Primer pairs: *Crybb2*_L3/ R1

PCR mix	
PCR buffer (15µm):	2µl
dNTP:	2µl
DMSO (fresh):	**1µl**
Taq Polymerase:	0.2µl
H₂O:	13µl
cDNA	**3µl**
Right primer:	1µl
Left primer:	1µl

PCR programme		
Denaturation:	94°C for 2minutes	
Denaturation:	94°C for 45 seconds	
Annealing:	53°C for 45 seconds	40X
Extension:	72°C for 45 seconds	
Extension:	72°C for 10 minutes	
8°C forever		

- <u>**Lens and brain cDNA**</u>

    Gene of interest: *β-actin*

PCR mix	
PCR buffer (15µm):	2µl
dNTP:	2µl
Taq Polymerase:	0.2µl
H₂O:	13µl
cDNA	1µl
Right primer:	1µl
Left primer:	1µl

PCR programme		
Denaturation:	94°C for 2minutes	
Denaturation:	94°C for 45 seconds	
Annealing:	58°C for 45 second	40X
Extension:	72°C for 45 seconds	
Extension:	72°C for 10 minutes	
8°C forever		

After the PCR reaction was over, the products were assessed by 1% Agarose gel electrophoresis against a known DNA ladder to check if the product of desired size and quality is obtained. Some of these products were extracted from the gel and used as template for probes of RNA *in-situ* hybridisations or for cloning in special vector for cDNA. Sometimes the PCR product was directly used for cloning into a special vector for cDNA or for sequencing.

2.4.7: Gel Electrophoresis:

It is necessary to analyze the PCR product, extracted RNA, extracted protein etc. by gel electrophoresis to check if the product is of correct size and/ desired quality. There are always possibilities of excess starting template, poor amplification, excess and/mismatched primer for a PCR reaction, which can be detected only after analyzing the products in a gel electrophoresis. These conditions for a PCR reaction need to be optimized by trial and error. Once done, then the PCR product can be used for further studies like cloning, sequencing etc. The PCR products and proteins were always compared to a known ladder for gel analysis.

2.4.7A: Principle of gel electrophoresis:

Gel electrophoresis is a method that separates macromolecules; either nucleic acids or proteins; on the basis of size, electric charge, and other physical properties. Separation of large (macro) molecules depends upon two forces: charge and mass. When a biological sample, such as proteins or DNA, is mixed in a buffer solution and applied to a gel, these two forces act together. The electrical current from one electrode repels the molecules while the other electrode simultaneously attracts the molecules. The frictional force of the gel material acts as a "molecular sieve," separating the molecules by size. After staining, the separated macromolecules in each lane can be seen in a series of bands spread from one end of the gel to the other. [http://www.bergen.org/AAST/Projects/Gel/]

There are two basic types of materials used to make gels: agarose and polyacrylamide. **Agarose** is a natural colloid extracted from sea weed. Agarose gels have very large "pore" size and are used primarily to separate very large molecules with a molecular mass greater than 200 kDa. Agarose gels can be processed faster than polyacrylamide gels, but their resolution is inferior. Agarose is usually used at concentrations between 1% and 3%. Agarose gels were prepared by suspending dry agarose in aqueous buffer, then boiling the mixture

until a clear solution forms. This was poured and allowed to cool to room temperature to form a rigid gel.

The **polyacrylamide** gel electrophoresis (PAGE) technique was introduced by Raymond and Weintraub (1959). The pore size for these gels may be varied to produce different molecular seiving effects for separating proteins or DNA fragments of different sizes. By controlling the percentage (from 3% to 30%), precise pore sizes can be obtained, usually from 5 to 2,000 kDa. This is the ideal range for gene sequencing, protein, polypeptide, and enzyme analysis. Polyacrylamide gels can be cast in a single percentage or with varying gradients. Gradient gels provide continuous decrease in pore size from the top to the bottom of the gel, resulting in thin bands. Because of this banding effect, detailed genetic and molecular analysis can be performed on gradient polyacrylamide gels. Polyacrylamide gels offer greater flexibility and more sharply defined banding than agarose gels but they have a smaller range

.

2.4.7B: <u>Agarose gel electrophoresis:</u>

<u>**Reagents/chemicals/buffers etc.**</u>

- **Agarose (high and low melt)**
  Biozym, Oldendorf, Germany

- **TBE buffer**
  5 X TBE (Tris/Broat)
  0.45 M Tris
  0.45 M Boric acid
  10 mM EDTA

- **Agarose gel staining:**
  Ethidium bromide (Stock solution)
  10 mg/ml Ethidiumbromide in water
  Light protected stored at 4 °C

- **Loading dye**
  6 X DNA Loading buffer
  30% Glycerol
  0.2% Bromphenolblue
  0.2% Xylencyanol
  Diluted in Tris/HCl (pH 7.5)

- DNA Molecular weight standard III and VIII MBI Ferments, St.Leon-Rot, Germany

Agarose gels (1% agarose in TBE buffer) were prepared for analysis of PCR and restriction enzyme digested products. 1% agaorse gel wasprepared at room temperature for about 20 minutes on a gel casting block (the two open sides of the casting block were sealed by adhesive tape). Wells were prepared using well forming teflon combs. For PCR product extraction small DNA Low Melt Agarose was used. Agarose gel (1% agarose in TBE buffer)

was also used to test the quality of isolated RNA and preparation of *in-situ* hybridisation probes. In case of later, ethidiumbromide was added while preparing the gel (2 µl in 100 ml gel-pool); the gel was run at a voltage of 200V for 15-25 minutes.

2.4.7C: <u>Poly-acrylamide gel electrophoresis (PAGE):</u>

Sodium dodecyl (lauryl) sulphate -polyacrylamide gel electrophoresis (SDS-PAGE) separates the proteins by size. SDS PAGE is used to establish protein size, to identify proteins, to determine sample purity, to quantify proteins, for blotting applications etc. The SDS [Sodium dodecyl (lauryl) sulphate] portion acts as a detergent. SDS is an anionic detergent that binds quantitatively to proteins, giving them linearity and uniform charge, so that they can be separated solely on the basis if their size. The SDS has a high negative charge (two in each molecule) that overwhelms any charge the protein may have, imparting all proteins with a relatively equal negative charge. The SDS has a hydrophobic tail that interacts strongly with protein (polypeptide) chains. The number of SDS molecules that bind to a protein is proportional to the number of amino acids that make up the protein. SDS also disrupts the forces that contribute to protein folding (tertiary structure), ensuring that the protein is not only uniformly negatively charged, but linear as well.

[http://lsvl.la.asu.edu/resources/mamajis/western/western.html]

12-16% SDS PAGE were used to separate the proteins for Western blotting. Different samples were loaded in wells or depressions at the top of the polyacrylamide gel. The proteins moved into the gel when an electric field is applied. The gel minimizes convection currents caused by small temperature gradients, and it minimizes protein movements other than those induced by the electric field. Proteins were visualized after electrophoresis by treating the gel with a stain called Coomassie blue, which binds to the proteins but not to the gel itself. Each band on the gel represented a different protein (or a protein subunit); smaller proteins were found near the bottom of the gel.

2.2.8: <u>Sequencing:</u>

This is the ultimate step in order to confirm the identity of a particular sequence, which was done commercially from Sequiserve, Vaterstetten, Germany **[State of the art technique: ABI Prism 3730 capillary sequencer]**. However, prior to sending the samples for sequencing, PCR was performed; the PCR product was further amplified by cloning it into a vector, so as

to provide optimum template for sequencing. The entire process of cloning is summarized in the following flowchart (Figure 2.3) and discussed in details later.
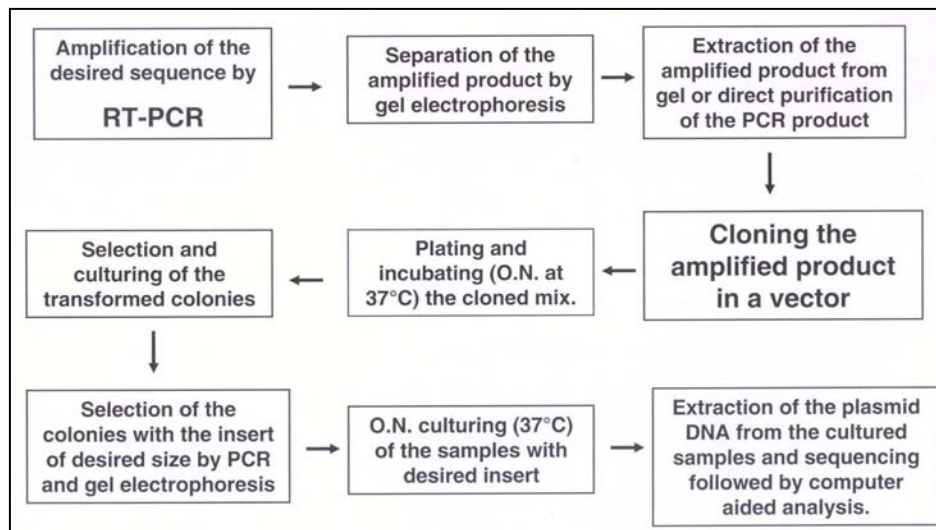
Figure 2.3: Flowchart outlining the procedure to clone a PCR amplified product into a vector which was subsequently sequenced.

2.4.9: <u>Cloning of the amplified sequence in a vector:</u>

<u>Kits/reagents/media/Plasmid etc.:</u>

DNA extraction from gel and plasmid:

- NucleoSpin® Extract 2 in 1 kit; Macherey-Nagel, Düren
- NucleoSpin® Plasmid kit; Marcherey-Nagel, Düren

- PCR-TOPO Cloning® Kit Invitrogen, Karlsruhe, Germany
- **Plasmid:** pCR®.2.1-TOPO® Invitrogen, Karlsruhe
- X-gal Peqlab Biotechnologie, Erlangen
- **LB-Medium**
  1% Bacto-Tryton
  0.5% Bacto-Yeast extracts
  1% NaCl
  pH adjusted to 7.0 with NaOH and autoclaved

- **LB Agar**
  15 g/l Difco-Agar, Autoclaved
- **SOC-Medium**
  2% Bacto-Trypton
  0.5% Bacto-Yeast extracts
  10 mM NaCl
  2.5 mM KCl
- X-Gal 20 mM Glucose (sterile filtrated)
  20 mg/ml X-Gal in Dimethylformamide

Light protected and stored at –20°C

- IPTG 200mg/ml in water, (sterile filtrated), Stored at –20°C

46

- **Antibiotic:**

    Ampicilin 10 mg/ml in water; Kanamycin 10 mg/ml in water

For selection with antibiotics, "Selections medium" with 100 μg/ml Ampicilin or Kanamycin was used. For blue-white selection 40 μl X-Gal and 4 μl IPTG was added.

These experiments were carried out with TOPO TA Cloning® Kit, Invitrogen™ Life Technologies and according to the manufacturer's instructions.

The working protocol was as follows:

i. 2-4μl of the extracted DNA and 3-1μl of salt solution was mixed in 0.5ml PCR tube so that the end volume is 5μl.

ii. 1μl of vector was added to the above mix and mixed well by rotating the tip inside the tube.

iii. The mixture was then incubated at room temperature for 5 minutes. Then the mixture placed on ice for transformation (This mixture can also be freezed at -20°C for future use till 1 week).

iv. The cells for transformation was then taken out from -80°C and to it (2.0-2.5)μl of the prepared mix (DNA + salt solution + vector) was added, mixed well by rotating the tip inside the tube.

v. This was then incubated on ice for 30 minutes.

vi. Heat shock at 42°C for 45 seconds was then applied to the mix and again placed back to ice.

vii. 250μl of SOC medium was then added to the mix and incubated on a shaker at 37°C for 1 hour.

viii. The culture plates with media were then placed at 37°C for pre-warming for 30 minutes.

ix. After the culturing in SOC medium was over, each sample were spread on two plates (100μl in one and the rest in the other) with the help of metallic loops and maintaining aseptic conditions.

x. The plates were incubated O.N. at 37°C.

xi. On the following day; colonies with inserts were selected. White colonies were with inserts and blue colonies without inserts. Only big white colonies were picked by 10μl sterile tips and the tips were inserted in 1.5 ml tubes containing

100μl LB medium. The tips were left inside the tube, vortexed well and incubated at 37°C for 1 hour. From each plate atleast 12 colonies were picked.

xii. Then a PCR was performed with these samples. The PCR mix and programme was as follows:

PCR Mix	PCR programme
2μl culture (The tip left inside respective eppendorf tube were used to pipette from the culture).	1 minute 95°C ----------1X
2μl 17,5mm $MgCl_2$ buffer	
2μl dNTP	30 seconds 95°C
1μl M13 forward primer	30 seconds 46°C } 40X
1μl M13 reverse primer	45 seconds 72°C
0.2μl Taq polymerase	
12μl H_2O	10 minutes 72°C -------1X
	(5 minutes if fragment size < 500bp)

xiii. The desired band size was 200 bp more than the actual insert. The PCR products were analyzed by1% agarose gel electrophoresis followed by Ethidium bromide staining and the samples containing the desired insert (based on band size in gel) were selected; cultured O.N. at 37°C on a shaker on LB medium with amplicillin (500 μl of 50μg/ml ampicillin in 500ml LB medium). 10-20μl of the culture in SOC medium was used for this sub-culturing procedure.

xiv. On the following day plasmid extraction was performed with Nucleospin[®] plasmid extraction kit only from the samples that had turned turbid as a result of O.N. culturing, according to manufacturer's instruction.

xv. O.D of the extracted DNA was measured.

The concentration and quality of a DNA sample was measured with a UV spectrophotometer. A solution containing 50 μg/ml of double strand DNA have an absorbency (optical destiny) of 1.0 at 260 nm. DNA quality measurement is based on the fact that OD at 260 nm is twice to that of at 280 nm if the solution contains pure DNA. Clean DNA has an $OD_{260/280}$ between 1.8 and 2.0.

xvi.   Following to that an *Eco*RI restriction digestion and 1% agarose gel analysis was carried out to select the samples suitable for sequencing.

Restriction digestion Mix

0.5µg DNA
0.5µl *Eco*RI
1.0µl *Eco*RI buffer
H_2O to make up the total
volume to 10µl

xvii.   The samples showing two distinct band of which one should be of the size of insert were send for sequencing commercially.

2.4.10: Isolation of water soluble proteins:

- **Lens extraction (LE) buffer:**

  50mM Tris-HCl, pH 7.8   606mg/100ml

  3mM DTT   46.3mg/100ml

  0.1mM PMSF   17.42mg/100ml (Methanol pa = 10mM)

Only water soluble proteins were isolated from lens and brain tissues because βB2-crystallin, the protein of interest is water soluble and therefore it can be detected in the water soluble fraction.

2.4.10A: Tissue type: Lens

50µl lens extraction (LE) buffer was added to the tube containing the 2 lenses. It was taken care of that the tissue does not thaw before adding the buffer. The lens tissues were then crushed and homogenized using a clean plastic pestle. The lysate was then centrifuged at 10,000 rpm* for 10 minutes at 2°C. The supernatant was collected and stored at -80°C. The concentration of the sample was measured.

[* Centrifugations performed with Centrifuge Sigma 3K18; Rotor: #12154-H]

2.4.10B: <u>Tissue type: Brain</u>

The frozen brain was first cut into two pieces and placed in two separate 1.5 ml eppendorf tubes. To each, 200μl LE buffer was added and then crushed and homogenized using a plastic pestle. The lysate was then centrifuged at 10,000 rpm* for 10 minutes at 2°C. the supernatants from each were collected and stored in one tube and stored at -80°C. The concentration of the sample was measured.

[* All centrifugations performed with Centrifuge Sigma 3K18; Rotor: #12154-H]

2.4.11: <u>Measurement protein concentration:</u>

RC DC™ Protein assay kit from BIO RAD was used for this purpose and the proceedre was carried out according to manufacturer's instruction. This is a colorimetric assay for determining protein concentration in the presence of both reducing agents and detergents. This assay is based on the modification of the Lowry protocol (Lowry *et al.,* 1951). The Lowry procedure is one of the most widely used protein assays. The principle behind this method is; under alkaline conditions, copper complexes with protein. When folin phenol reagent (phospho-molybdic-phosphotungstic reagent) is added, the Folin-phenol reagent binds to the protein. Bound reagent is slowly reduced and changes colour from yellow to blue. Bovine serum albumin (BSA) was used as the standard.

<u>Working protocol:</u>

i.   20μl **reagent S** was added to 1ml **reagent A**. This mixture is stable for 1 week.

ii. 25μl of **reagent (A+S)** was then added to the standard and/ samples.

iii. To this 200μl of **reagent B** was added.

iv. The entire mixture was then incubated in dark for 15 minutes, following which the O.D at 680 nm of each sample was measured and standard curve prepared (Annexure 1) to calculate the protein concentrations.

2.4.12: <u>Western Blotting:</u>

The entire procedure of Western blotting to detect a protein in a mixture of any number of proteins can be divided in the following steps. However, this method is dependent on the use of a specific antibody directed against a desired protein.

i.   Separation of proteins by SDS-PAGE

ii. Transferring the proteins to the nitrocellulose membrane from the gel. Another gel with the same samples is fixed, stained and dried for reference [Calculation of relative mobilities (Rf)].

iii. Blocking the nitrocellulose membrane by incubating it in a fat free milk solution.

iv. Incubating the nitrocellulose membrane with a primary antibody.

v.   Incubating the nitrocellulose membrane with a secondary antibody (antibody-enzyme conjugate).

vi. Staining the membrane following DAB (Diaminobenzidine) staining method.

vii. Documentation of the result immediately as the intensity of staining reduces fast with time.

[http://lsvl.la.asu.edu/resources/mamajis/western/western.html]

2.4.12A. <u>Preparation of the SDS-PAGE gel:</u>

- **<u>SDS PAGE gel casting:</u>**

  1.5M Tris-HCl (pH8.8)

  0.5M Tris-HCl (pH7.0)

  10% SDS:

  30% Acrylamide-Bis:

  10% Ammonium per sulphate (APS):

  TEMED

  (N,N,N',N'-tetramethylethylenediamine)

- **<u>Lämmlli's sample buffer:</u>**

  16mM Tris

  2% SDS

  0.001% Bromophenol blue

  10% β-mercaptoethanol

  pH: 6.8

i.   The gel casting glass plate pair/s were cleaned with 70% ethanol, rubber strips were applied between them and then locked on the two lateral sides and the lower side by the clips, leaving the upper side open for pouring the gel mixture. The system was then set at an upright position.

ii. The resolving gel mixture was then added in the casting block till 3/4th of the block is filled. Few drops of butanol (MERCK) was then added over the resolving gel to make the surface of the gel uniform. Care was taken to make the entire surface of the gel at the same plane.

iii.   The resolving gel was then allowed to polymerize for 45 minutes.

iv.   After polymerization, the butanol was decanted, the gel was carefully washed with water, and the excess water was soaked with tissue paper.

v.   The stacking gel mixture was then loaded over the resolving gel to fill up the rest 1/4th of the casting block which was again set in an upright position as before.

vi.   The teflon comb was then placed over the stacking gel to make the loading wells for the samples.

vii.   This was then allowed to polymerize for 30 minutes.

viii.   Then the SDS PAGE gel was ready for use, the clips and rubber strips were then carefully removed from the casting block. This gel is also usable when stored at 4°C in a moist covering (usually wrapped in wet tissue paper and inside a plastic cover) till 7 days after preparation.

Composition of the resolving gel:	
H$_2$O:	4.2ml
1.5M Tris-HCl: (pH:8.8)	3.2ml
10% SDS:	125.0μl
30% Acrylamide-Bis:	5.0ml
10% APS:	63.0μl
TEMED:	6.3μl
*This composition is to cast 2 resolving gels.	

Composition of the stacking gel:	
H$_2$O:	1.6ml
0.5M Tris-HCl: (pH:7.0)	0.7ml
10% SDS:	25.0μl
30% Acrylamide-Bis:	325.0μl
10% APS:	25.0μl
TEMED:	5.0μl
*This composition is to cast 1 stacking gel.	

2.4.12B: Preparation of protein samples and the marker:

Both the sample proteins and the marker were dissolved in protein extraction buffer. Usually 10μg of lens protein and 70-80μg of brain protein were used to detect βB2-crystallin by Western blot technique. The quantity of protein taken in case of brain samples was so high because of the very low expression of βB2-crystallin in brain (Figure 3.8B). The lens protein samples were usually diluted 10 fold.

Preparation of protein samples and the marker:

Probe protein samples:	**Marker Protein sample:**

- Lens: 10μg   ~ 2μl
  Brain: 70-80μg   ~ 1μl

10μl sample dissolved in
 protein extraction buffer
 2μl sample loading bufer

- 3-4μl protein extraction buffer to
  make the volume 5μl.
- 2μl sample loading buffer
- Final volume: 7μl

Final volume:12μl

- ➢ Both the probe protein samples and the marker protein samples were incubated at 100°C for 5 minutes to denaturate the disulphide bonds.

2.4.12C: Electrophoresis:

The vertical electrophoresis chamber was prepared by this time, with the casted gel/s placed properly (inner side of the casting block facing inwards), running buffer (1X SDS) loaded in the electrophoresis chamber, carefully the teflon comb was taken out of the gel (no air bubble should accumulate in the wells or in the chamber), samples were loaded, the chamber was closed and power was switched on. The electrophoresis was carried out at an electricity of 272V and 30 mA supplied from a power block specially designed (GIBCO BRL) for this purpose. The gel was run till the loading buffer (visible by its blue colour) reached the bottom of the gel but should not run out of the gel. With fresh running buffer the time is usually around 60 minutes. The samples were loaded in the gel in such a way that one half of the gel was used for blotting and another half with exactly the same orientation of the samples plus the marker be used for staining and drying.

After the gel run was finished, the casting block was carefully taken out of the chamber , the inner lid of the casting block removed, the gel was cut according to the sample orientation for staining and blotting, and the respective parts were transferred to the cubette containing Coomasie blue dye R250 and Solution C for Western blotting.

The part which was stained in Coomasie blue dye R250 for about 60 minutes was then destained till the protein bands were distinctly visible (usually the destaining solution was changed twice in an interval of 60 minutes each). The acetic acid (in water) content of the stain keeps the proteins denatured in the gel thereby acting as a fixative. The gel was then dried and documented for reference [to calculate relative mobility (Rf) of the bands of interest etc.].

2.4.12D: <u>Transferring the proteins to the nitrocellulose membrane:</u>

- **<u>Washing solutions :</u>**

  <u>Western Blot Solution A:</u>

  0.3 M Tris-HCl + 20% Methanol; pH 10.4

  <u>Western Blot Solution B:</u>

  0.25 M Tris-HCl + 20% Methanol; pH 10.4

  <u>Western Blot Solution C:</u>

  0.25 M Tris-HCl + 20% Methanol; pH 9.0

  <u>60% ethanol</u>

i.   The gel was pre-treated in Western Blot solution C for 15 minutes and the pure nitrocellulose membrane (0.2µm; Trans-Blot® Transfer medium; *BIORAD*) was pre-soaked in 60% ethanol for 10-15 minutes and then in Western Blot solution B for 10 minutes.

ii. Whatmann's filter papers soaked in Western Blot solution A were placed on the lower positive (+) plate of the blotting machine. This was followed by placing Whatmann's filter papers soaked in Western Blot solution B above these.

iii. Then the pre-soaked nitrocellulose membrane was placed.

iv. The gel was then placed over the nitrocellulose membrane; size of the gel was marked on the membrane by a pencil.

v.   Whatmann's filter papers soaked in Western Blot solution C was then placed over the gel.

vi. The upper negative (-) lid of the blotting machine was the applied and power was switched on at 200 mA.

vii. Blotting was continued for 1.5-2 hours.

viii. After this the nitrocellulose membrane with the transferred proteins was taken out and placed in the blocking solution, the gel and filter papers were disposed off.

2.4.12E: <u>Blocking the nitrocellulose membrane:</u>

The nitrocellulose membrane was incubated for 1.5 hours in the blocking solution [5% fat free milk powder (ROTH) in PBS] at RT on a shaker. This step is important because of the fact that antibodies are also proteins and proteins always have the tendency to bind to the nitrocellulose membrane, thus it is necessary to mask the nitrocellulose membrane by

incubating it in a blocking solution. The membrane was washed 3 times in PBS at an interval of 20 minutes each. [http://lsvl.la.asu.edu/resources/mamajis/western/western.html]

2.4.12F: <u>Incubating the nitrocellulose membrane with a primary antibody:</u>

The nitrocellulose membrane was incubated overnight in the primary antibody solution (Anti βB2-crystallin antibody developed in rabbit) O.N. at 4°C on a shaker.

<div style="border:1px solid black; padding:10px">

<u>Concentration of primary antibody:</u>

1:1000 for both lens and brain protein

[for example : 5µl in 5 ml (1:1000)]

Primary Antibody was dissolved in blocking solution
Primary antibody against βB2-crystallin, was kindly provided by Dr. Horwitz, University of California, LosAngeles, USA.

</div>

2.4.12G: <u>Incubating the nitrocellulose membrane with the secondary antibody (antibody-enzyme conjugate):</u>

On the following day the nitrocellulose membrane was taken out of the primary antibody solution, washed 3 times in PBS at an interval of 20 minutes each and then incubated in the secondary antibody solution for 1 hour. Anti rabbit IgG (whole molecule) with peroxidase conjugate; developed in goat (Sigma); was used as the secondary antibody.

<div style="border:1px solid black; padding:10px">

<u>Concentration of secondary antibody:</u>

1:1000

[for example: 1:1000)]

Secondary antibody was dissolved in PBS
Peroxidase conjugated secondary antibody against rabbit IgG (whole molecule), Sigma, Taufkirchen, Germany

</div>

2.4.12H: <u>Staining the membrane:</u>

The nitrocellulose membrane was washed 3 times in PBS buffer at an interval of 20 minutes each, after taking it out of the secondary antibody solution. The staining solution was prepared atleast 30 minutes prior to use, as DAB takes time to dissolve. The solution was stored in dark as DAB is photo sensitive. Just before use 10-20µl Hydrogen peroxide (H_2O_2) was added to the staining solution. The staining solution was then added to the membrane taken in a cubette and gently shaked. Dark brown bands indicate the proteins of interest. Dark brown colour is the result of precipitation of DBA after the peroxidase of secondary antibody reacts with H_2O_2 of the staining solution. The exact position of the protein in the membrane was determined by calculating the relative mobilities (Rf*); which is the distance migrated by a particular band to that of bromophenol blue (the loading dye) and then comparing it with the same in the dried reference gel.

[*Rf = Distance migrated by the protein band / Distance migrated by the tracking dye]

<u>**Staining solution:**</u>
(Photo sensitive)

		<u>**5X Buffer**</u>		
5X Buffer:	5ml	Tris base	45g	(15g/l)
H₂O:	20ml	Glycine	216g	(72g/l)
DAB:	1 spatula	SDS	15g	(5g/l)
(3, 3'-Diaminobenzidine**)**		Diluted to 3 litres by distilled		
Cobalt chloride solution:	100µl	water, stored at 4°C,		
(CoCl₂)		warmed to 37°C before use.		
Hydrogen peroxide:	10-20µl			
(H₂O₂), added just before use				

Staining solution for SDS PAGE gel

0.1% Coomasie blue powder

40% Methanol

10% Aecetic acid

Volume made up by distilled water

Destaining solution for SDS PAGE gel

40% Methanol

10% Aecetic acid

Volume made up by distilled water

2.4.12I: <u>Documentation:</u>

The wet nitrocellulose membrane was then dried in dark and the data was electronically documented.

2.4.13: <u>Immunohistochemical studies:</u>

The purpose of this study is localisation and visualisation of tissue cell antigens by the binding of specific primary antibodies to tissue antigens. These antigen bound primary antibodies are then linked to secondary biotinylated antibodies followed with streptavidin enzyme conjugates. The colour reaction is developed when DAB reacts with the enzyme peroxidase, producing the brown coloured product. A positive tissue control and a negative control are to be included in every test run and for every antisera. The tissue control is known to contain the antigen being tested. The negative control is the tissue section which has the primary antibody omitted and substituted by normal serum (i.e. normal horse or goat serum depending on which was used to dilute the primary antibody) to check the specificity of the antibody. Further in-depth specificity studies of the primary antibodies used for the first time in immunohistochemical studies can be done by immunoblotting or immuno-precipitation and preabsorption experiments. [http://home.primus.com.au/royellis/immuno.html]

The ABC method (VECTASTAIN®; Vector Laboratories) employs biotinylated antibody and a preformed A**vidin** : B**iotinylated** enzyme C**omplex**. Because avidin has such an extraordinarily high affinity for biotin (over one million times higher than antibody for most antigens), the binding of avidin to biotin is essentially irreversible. In addition, avidin has four binding sites for biotin, and most proteins including enzymes can be conjugated with several molecules of biotin. These properties allow macromolecular complexes (ABC's) to be formed between avidin and biotinylated enzymes. The VECTASTAIN® ABC kits contain Avidin and biotinylated enzyme, which are matched reagents and have been specially prepared to form ideal complexes for immunohistochemical staining and other applications. Although the structure of the Avidin : biotinylated enzyme complex is still not completely understood but evidence suggests that it consists of many biotinylated enzyme molecules crosslinked by avidin into a three-dimensional array. The complex apparently has few exposed biotin residues but has at least one remaining biotin binding site. Formation of the complex is achieved by merely mixing Avidin and biotinylated enzyme in dilute solution and in defined amounts prior to use. After the initial incubation, there appears to be little change in the complex, as judged by only a marginal in-crease in immunohistochemical staining sensitivity. The complex remains stable for many hours after formation and, in general, can be used for several days after preparation (http://www.vectorlabs.com). The procedure followed is according to Vogt Weisenhorn *et al*. (1998).

<u>Reagents/Chemicals/antibodies/ Kits etc.</u>

- <u>Deparaffinization of sections:</u>   Xylol and Rotihistol (ROTH).

- <u>Dehydration and rehydration:</u>   70%. 96%, 100% Ethanol, distilled water

- <u>Washing buffers/ blocking solution</u>
  <u>/antibody dilution:</u>

      Sodium citrate

      PBS

      PBS+H_2O_2

      0.05M Tris HCl; pH 7.4

      Foetal calf serum (FCS)

- **<u>Antibodies</u>**

  - <u>Primary antibodies against:</u>

    βB2-crystallin;

    calbindin , calretinin (Swant, Bellinzona Switzerland)

  - <u>Secondary antibody against:</u>

  Biotin conjugated affinipure goat anti rabbit IgG (H+L), Jackson Immunoresearch laboratories Inc., Dianova.

- Pure $β_H$-crystallin protein (StressGen Biotechnologies group) for preabsorption studies

- ABC kit Vectastain: Vector Laboratories

- <u>Staining solution:</u>   DAB (3, 3'-Diaminobenzidine), 0.05M Tris-HCl (pH 7.4), H_2O_2

- <u>Rotihistokit</u> (ROTH)
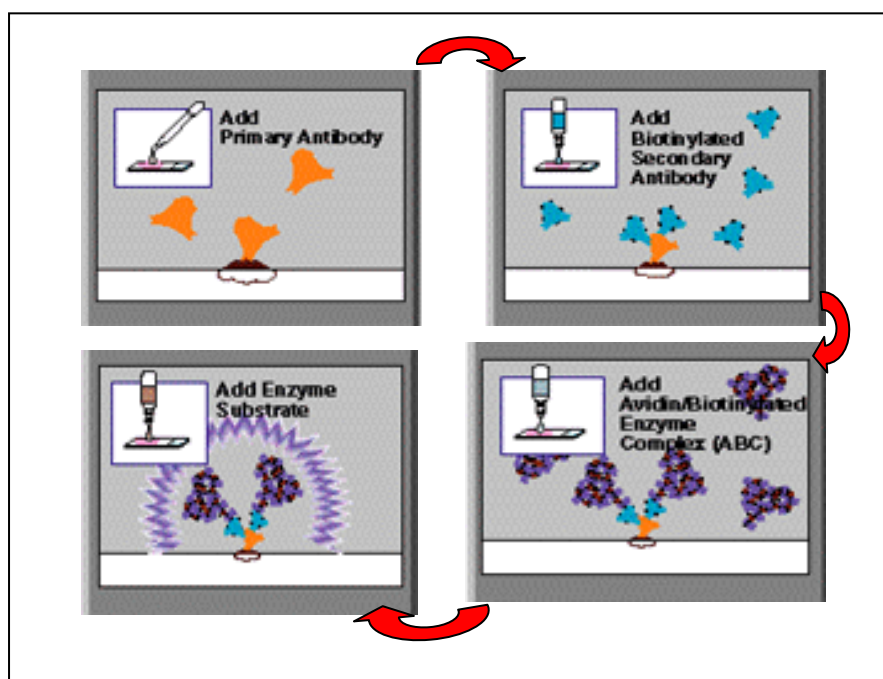
Figure 2.4: Explains the principle of immunohistochemical method using ABC kit.

Reference: http://www.vectorlabs.com/ABC/ABCmet.html

2.4.13A: <u>Working Procedure:</u>

The entire immunohistochemical protocol was performed according to Vogt Weisenhorn *et al*. (1998) as summarized in table 2.5 in a step wise manner with the paraffin sections already mounted on dry grease free slides. Cleaned and autoclaved glass cubettes and slide racks were used during this experiment.

Table 2.5: Working protocol for immunhistochemistry

<u>Reagent</u>	<u>Duration</u>	<u>Repeats</u>	<u>Purpose</u>
Xylol	Atleast 45min	1X	Adequate deparaffinization, working under hood
100% Ethanol	5 min	2X	Rehydration in graded alcohol series
96% Ethanol	5 min	2X	
70% Ethanol	5 min	2X	
Rinsing in distilled H$_2$O	Atleast 10 min	1X	Washing
0.01M Sodium citrate (pH 6.0)	3 min	1X	Washing
Microwave	5 min (for adult brain) 1' min (P1 eye)	1X	Antigen retrival
Cooling	20 -30 min	-	
PBS	5 min	2X	Washing
0.1% H$_2$O$_2$ in PBS	5 min	1X	Blocking of endogenous peroxidase
PBS	5 min	2X	Washing
Blocking reagent	1 hour	1X	To minimize unspecific binding
PBS	5 min	2X	Washing
Primary antibody	O.N.	1X	Specific binding
PBS	5 min	3X	Washing
Secondary antibody	1 hour	1X	Binding to primary antibody
PBS	5 min	2X	Washing
ABC-solution	30 min	1X	Binding to secondary antibody
PBS	5 min	2X	Washing
0.05M Tris-HCl	5 min	1X	
DAB reagent	15 min	1X	Staining
PBS	5 min	2X	Washing
70% Ethanol	2 min	2X	Graded dehydration
96% Ethanol	2 min	2X	
100% Ethanol	2 min	2X	
Xylol	5 min	2X	Xylol acts as a clearing agent; working under hood

**Each cubette was filled with 200-250 ml of the respective solution; 1ml solution added per slide.*

The sections were then mounted with **DPX** (contains Di-n-butyl phthalate; Polystyrene; and Xylene) as the mounting medium and coverslips placed properly over them, let to dry over night under the hood and studied under light microscope on the following day and documented.

2.4.13B: <u>Composition of blocking solution:</u>

 The blocking solution was composed by dissolving 10% FCS, 0.05% Triton X in PBS buffer.

<u>Composition of working solution
for 20 slides</u>

PBS: **18ml**

 FCS: **2ml**

10% Triton X in PBS: 200μl

2.4.13C: <u>Primary antibody solution:</u>

Primary antibody was dissolved in 10% FCS in PBS.
The concentration used for anti βB2-crystallin antibody was 1:1000 and for antibodies against calcium binding (calbindin, calretinin) proteins was 1:5000.

<u>Composition of working solution for 20 slides</u>

PBS: **18ml**

FCS: **2ml**

Primary antibody: **20μl**
                              (anti-βB2 crystallin)
                                      4μl
              (anti-calbindin, anti-calretinin,)

2.4.13D: <u>Secondary antibody solution:</u>

Biotinylated anti rabbit IgG was used as the secondary antibody as all the above mentioned primary antibody used were developed in rabbit. The secondary antibody was diluted at an concentration of **1:300** in 10% FCS in PBS.

<u>Composition of working solution for 20 slides</u>

PBS: **18ml**

FCS: **2ml**

Secondary antibody: **66.5μl**

2.4.13E: <u>ABC-solution:</u>

This solution was always prepared at least 30 minutes before use as reagents in solutions A and B of the ABC kit (Vectastain) takes time to dissolve. Both solutions A and B were diluted at a concentration of 1:300 in 10% FCS in PBS.

Composition of working solution for 20 slides	
PBS:	18ml
FCS:	2ml
Solution A:	66.5µl
Solution B:	66.5µl

2.4.13F: <u>Staining solution:</u>

Composition of working solution for 20 slides	
DAB (stock solution):	1ml
0.05M Tris-HCl:	19ml
Hydrogen peroxide (35%): (H_2O_2)	15µl

2.4.14: <u>Preabsorption studies:</u>

Specificity control studies of antibodies are very important for the correct interpretation of its localisation in cells and tissues. One of such important studies is the so called absorption or pre-absorption studies where the antibody is mixed with the peptide or protein of its origin so as to eliminate the binding of the antibody to the protein in the tissue. Theoretically, incubating the peptide with the antibody at appropriate concentrations will result in occupancy of all binding sites. However, a small but significant dissociation occurs during the incubation, which can lead to dissociation of some of the antibody from the peptide and results in antibody binding to the protein in the tissue. Thus, the absorption control can actually be positive (i.e., the antibody still produces staining) even though the antibody is specific for the peptide or protein in the tissue which can be explained by binding of the antibody : protein complex via. the proteins in tissue sections; protein-protein interaction cannot be over-ruled either. In reality; a significant reduction in the staining intensity is a good sign instead of complete inhibition of staining. (Burry, 2000)

To undertake such a pre-absorption study, the anti βB2-crystallin antibody (dilution: 1:1000) was incubated over night with pure Bovine β_H-crystallin [0.9mg/ml stock] (StressGen Biotechnolgies Corp.) in PBS at 4°C on a shaker; and this solution was used on the following day as the primary antibody solution for immunohistochemical staining.

2.2.14A: <u>Working protocol:</u>

A gradient series of protein concentrations [150μg, 500μg, 1mg, 1.5mg, 2mg and 2.5mg] were first incubated with the antibody solution (Conc. 1:1000) in PBS and each of these solutions were tried in the immunohistochemical method as the primary antibody solution (50μl FCS added to each tube just before use) to detect the optimum concentration that reduces the intensity of staining against a control set and a negative control. The sample containing 2mg β_H-crystallin was found to be the optimum one. The experiment was repeated with 2mg β_H-crystallin protein to confirm the results against a control set and a negative control.

<u>**Determination of the optimum concentration:**</u>

- 6μl anti βB2-crystallin antibody was added to 6ml PBS and mixed.
- This was divided into 6 equal aliquots in six different eppendorf tubes (i.e. each containing 1ml).
- To these stocks, 150μg, 500μg, 1mg, 1.5mg, 2mg and 2.5mg pure β_H-crystallin protein was added in a series.
- The solutions were incubated O.N. on a shaker.
- On the following day these solutions were used as the primary antibody solution for the immunohistochemical studies (as described in the previous section) against a positive and negative control set.
- Just before use 50μl FCS was added to each tube.

<u>**Confirming the pre-absorption study results**</u>

- 3μl anti βB2-crystallin antibody was added to 3ml PBS and mixed.
- This was divided into 3 equal aliquots in three different eppendorf tubes (i.e. each containing 1ml).
- To each of these stocks, 2000μg pure β_H-crystallin protein was added.
- The solutions were incubated O.N. on a shaker.
- On the following day these solutions were used as the primary antibody solution for the immunohistochemical studies (as described in the previous section) against a positive and negative control set.

2.4.15: <u>Histology:</u>

Histology refers to the microscopic study of tissue. The visualisation of the eye and brain's cytoarchitecture is an integral part of ophthalmic and neuroscience research. Histology also refers to the techniques used to prepare tissue for microscopic study. This includes not only staining tissue for light and electron microscopy, but also more advanced techniques such as tracing fiber tracts, identifying receptor types present in a given brain region, and mapping the distribution of the expression of a particular gene. These latter techniques are more properly described as histochemistry, which is the art and science of localizing the various chemical constituents of cells. This is an interesting approach that makes use of methods from areas as diverse as biochemistry, molecular genetics and image processing.

2.4.15A: <u>Histology Eye:</u>

-JB4®embedding kit; Polysciences Inc., Eppelhein, Germany.

- **Fixation:** The eyes were fixed in Carnoy's solution (60ml 100% Etanol; 30ml Chloroform; 10ml Acetic acid) O.N at 4°C.
- The JB4® Catalyzed Infiltration Resin was then prepared by adding 0.90g of dry catalyst C to 100ml JB4® Solution A. Mixed until dissolved.
- 1ml of JB4® Solution B was then added to 25ml of fresh catalyzed solution A.
- The eyes were embedded in this solution in a plastic mould and allowed to polymerized O.N. at RT.
- Tissue was sectioned with a microtome designed for plastic sectioning at a thickness of 3μm with a dry glass knife.
- Methylene blue-basic fuchsin staining:

Stock solution Methylene blue (Polysciences Inc.): 0.13% in distlled water

Stock solution: Basic fuchsin (Polysciences Inc.): 0.13% in distilled water

- Stainng solution: (For 1 small cubette)

Methylene blue solution: 12ml

Basic fuchsin: 16ml

PBS (0.2M) pH 7.6   20ml

Ethanol (95%)   12ml

- Incubated RT for 30-60 seconds; washed by distilled water, and made ready for microscopy.

2.4.15B: <u>Histology Brain:</u>

<u>**Reagents/chemicals etc.**</u>

<u>**Cresyl violet staining:**</u>

- <u>Deparaffinization of sections:</u>   Xylol and Rotihistol (ROTH).

- <u>Dehydration and rehydration:</u>   70%. 96%, 100% Ethanol, distilled water.

- <u>Cresyl violet stain:</u>   Cresyl violet, Sodium acetate, Acetic acid:

<u>**Myelin staining:**</u>

- Solutions for dehydration and rehydration:

- Pyridine solution: Pyridine solution and Acetic anhydrite

- Incubation solution: $AgNO_3$ and NH_4NO_3

- Physical developer: Na_2CO_3, $AgNO_3$, NH_4NO_3, Tungstosillic acid, 37% Formalin.

<u>**Cryoprotection solution:**</u>

- PBS: 250ml

- Ethylene glycol (Fluka): 125ml

- Glycerine (MERCK):   125ml

2.4.15B.1: <u>Cresyl violet staining</u> (Nissl, 1894):

[Used mainly to study neurons]

Cresyl violet, a Nissl stain colours cell bodies a brilliant violet. Nissl is the term used by classical cytologists for endoplasmic reticulum. Exposing the tissue to a stain which attaches to the ER allows us to differentiate cell bodies from fiber paths and from surrounding extracellular matrix. Since all cells contains Endoplasmic Reticulum (ER), *cresyl violet* stains both neurons and glia. But somewhat surprisingly, Nissl staining also allows us to differentiate neurons from glia; as neurons and glia contains different amounts of ER, So when viewed under microscope, anything with a cell body (or 'perikaryon'), especially if any processes are visible, are neurons. Glial cells do not have much ER, so only their nuclei stains. Here cresyl violet staining is used to study the neurons specifically.

[http://psych.colorado.edu/~dbarth/PDFs/4052/4052%20Manual%20Chapters/Histology%20I.pdf]

Working protocol for paraffin sections:

The staining solution was prepared a day before use and the subsequent steps were performed as mentioned:

- **Staining Solution:**

Cresyl violet:	**2.5g**
Sodium acetate:	**0.102g**
Acetic acid:	**1.55ml**
Distilled H$_2$O:	**500ml**

pH adjusted to 3.5 with 1N HCl
Filtered before use

➢ **Rehydration of sections in graded alcohol series:**

Table: 2.6: Rehydration procedure prior to Cresyl violet staining

Reagent	Duration	Repeats
Xylol	1 hour	1X
100% ethanol	5 min	2X
96% Ethanol	5 min	2X
70% Ethanol	5 min	2X
Distilled H$_2$O	Atleast 10 min	1X

➢ **Staining:**

The slides were stained for atleast 15-20 minutes in the cresyl violet stain.

➢ **Destaining:**

Table: 2.7: Destaining procedure following cresyl violet staining

Reagent	Duration	Repeats
Distilled H$_2$O	2 min	2X
70% Ethanol	2 min if slides have lost their intensity significantly next step can be skipped	2X
96% ethanol + 1ml Acetic acid	15-30 seconds (slides loose intensity very quickly, checked in every minute, slides get final appearance)	1X
96% Ethanol	2min	2X
100% Ethanol	2 min (till this step slides can be brought back)	2X
Xylol	5 min (slides gain some intensity, slides should preferentially not be brought back) longer in xylol is not a problem but slides should be exposed to air for as short as possible.)	2X

In the case when intensity of staining is not sufficient slides can bet rehydrated and again put back to Cresyl violet staining solution.

In each cubette 200-250ml of solution was taken, so that slide racks with slides immerse completely.

The sections were then mounted with **DPX** as the mounting medium and coverslips placed properly over them: let to dry O.N. under the hood and studied under light microscope on the following day and documented.

Working protocol for free floating cryosections
(used for sterological studies):

➢ **Washing :**

The cell strainers (BD Falcon) containing free floating cryosections in cryoprotection solution were transferred to new 6 well plates containing PBS and washed on a shaker to remove any cryoprotection solution from the sections; the solution was changed atleast thrice at an interval of 1 hour during washing and then washed O.N. on a shaker at 4°C. On the following day, the tissue sections were carefully mounted on grease free slides, dried O.N. in dust free conditions preferably under the hood and stored in slide boxes at RT for future use. The staining procedure was as follows:

• The slides were rinsed in distilled water for 2-3 minutes.
• They were transferred to the cubette containing Cresyl violet staining solution and stained for 30 minutes; two times.

Table 2.8: Working protocol for cresyl violet staining of free floating sections

Reagent	Duration	Repeats
70% Ethanol	5 min	2X
96%Ethanol + 1ml Acetic acid	5-15 min **(slides loose intensity very quickly, checked in every minute for the staining in the cell/s of interest, slides get final appearance)**	1X
96% Ethanol	5 min	2X
100% Ethanol	5 min	2X
Rotihistol	5 min longer in Rotihistol is not a problem but slides should be exposed to air for as short as possible.)	2X

The sections were then mounted with **Roti histo kit (ROTH)** as the mounting medium and coverslips placed properly over them: let to dry O.N. under the hood and studied under light microscope on the following day and documented.

2.4.15B.2: <u>Myelin staining (Silver staining according to Gallyas) on free floating cryosections:</u>

Gallyas (1979) had developed a physical development technique for staining myelin with silver that renders visibility even for the thinnest fibers in various animal species, including fishes and reptiles. This technique is useful even for tissues in early phase of myelination and is applicable to both frozen and embedded materials. The principle behind this method is that myelin can form and bind colloidal silver particles in 0.1% ammoniacal silver nitrate solution of pH 7.5. The production of metallic silver by other tissue elements is suppressed by the sections pre-treated with a 2:1 mixture of pyridine and acetic anhydride for 30 minutes. The colloidal silver particles bound in the myelin are enlarged to the microscopic dimensions by a special physical developer. The fibers appear as brownish black with a slight red tinge.

Very clean and absolutely dust free working is an absolute necessity for this procedure. If required, all glassware should be incubated O.N. in 1% HCl. Only distilled water should be used to prepare the solutions.

<u>Preparation of the solutions:</u>

A) Pyridine solution:

200ml pyridine (99.9_+%)
100 ml acetic anhydride (99%)

Total: 300 ml

* The solution gets hot while mixing because of the anhydride; hence appropriate precautions were taken.

This solution should be prepared at least 4 hours (better one day) before use; the solution must be clear not dark orange.

B) Incubation solution:

1g NH_4NO_3 (Ammonium nitrate)
1g $AgNO_3$ (Silver nitrate)

Volume adjusted to 1000 ml by distilled water

pH was adjusted to 7.5 with NaOH (Sodium hydroxide); solution must be clear.

* The solution was let to mature one day in light and 2 days in dark. It is stable for maximum 1 week at RT.

C) Physical developer:

This solution was prepared fresh by mixing three solutions- A, B and C (Tables 2.9 and 2.10).

Table 2.9: Composition of the physical developer solution

Solution A:	Solution B:	Solution C:
5g Na_2CO_3 (sodium carbonate) in 100 ml distilled water.	0.2g $AgNO_3$ 0.2g NH_4NO_3 dissolved in 100 ml distilled water. They were mixed after dissolving the two substances separately	0.2g $AgNO_3$ 0.2g NH_4NO_3 1g Silico tungstenic acid 7ml Formalin (37%) dissolved in 100ml distilled water

Table 2.10: Preparation of the physical developer solution.

Temperature	Solution A	Solution B	Solution C	Total Volume
20°C	10ml	3ml	7ml	20ml
25°C	10ml	5ml	5ml	20ml
RT	10ml	7ml	3ml	20ml

Working protocol:

Table 2.11: Working protocol for myelin staining

Purpose	Reagent	Duration	Repeats
Rinsing	Distilled water	10 min	2X
Pyridine pre-tratment	Pyridine solution	30 min	1X
Washing	Distilled water	5 min	2X
Incubation (slides get slightly brown in colour)	Incubation solution	1 hour at 20°C/RT or 50 min at 30°C/15 min at 25°C	1X
Washing	Distilled water	10 min	3X
Development	Fresh physical developer solution	3-5 min (has to be determined on spot)	1X
Stopping	1% Acetic acid	10 min	3X
Dehydration	70% Ethanol	5 min	2X
	96% Ethanol	5 min	2X
	100% Ethanol	5 min	2X
Clearing agent	Rotihistol	5 min	2X

The sections were then mounted with **Rotihisto kit** as the mounting medium and coverslips placed properly over them: let to dry O.N. under the hood and studied under light microscope on the following day and documented.

2.4.16: *In-situ* hybridisation:

In situ hybridization techniques allow specific nucleic acid sequences to be detected in morphologically preserved chromosomes, cells or tissue sections. In combination with immunocytochemistry, *in-situ* hybridization relates microscopic topological information to gene activity at the mRNA level. Possibility of preparation of nucleic acid probes with a stable nonradioactive label has opened new opportunities interms of wide scale applications and also for combining different labels in one experiment. The many sensitive antibody detection systems available for such probes further enhanced the flexibility of this method. [http://www.roche-applied-science.com/PROD_INF/MANUALS/InSitu/InSi_toc.htm; http://www.genedetect.com]

There are two types of nonradioactive hybridization methods: **direct and indirect**.
Direct method: In this method the detectable molecule (reporter) is bound directly to the nucleic acid probe so that probe-target hybrids can be visualized under a microscope immediately after the hybridization reaction.

Indirect method: This procedure requires the probe to contain a reporter molecule, introduced chemically or enzymatically, that can be detected by affinity cytochemistry. The reporter molecule should, however, be accessible to antibodies.

In this work, indirect labelling method using digoxigenin (detected by specific antibody) was performed according to Grimm *et al,* (1999).

The DIG (Digoxigenin) **labeling method** is based on a steroid isolated from digitalis plants (*Digitalis purpurea* and *Digitalis lanata*, Figure 2.5). Since only the blossoms and the leaves of these plants are the natural source of digoxigenin, the anti-DIG antibody does not bind to other biological material. Digoxigenin is linked to the C-5 position of uridine nucleotides via a spacer arm containing eleven carbon atoms and two nitrogen atoms (Figure 2.6). The DIG labelled nucleotides may be incorporated, at a defined density, into nucleic acid probes by DNA polymerases (such as *E. coli* DNA Polymerase I, T4 DNA Polymerase, T7 DNA

Polymerase, Reverse Transcriptase, and Taq DNA Polymerase) as well as RNA Polymerases (SP6, T3, or T7 RNA Polymerase), and Terminal Transferase. DIG label may be added by random primed labeling, nick translation, PCR, 3'-end labeling/tailing, or *in vitro* transcription. Nucleic acids can also be labeled chemically with DIG-NHS ester or with DIG Chem-Link. Hybridized DIG-labeled probes may be detected with high affinity anti-digoxigenin (anti-DIG) antibodies that are conjugated to alkaline phosphatase, peroxidase, fluorescein, rhodamine, or colloidal gold. Alternatively, unconjugated anti-digoxigenin antibodies and conjugated secondary antibodies may be used. Detection sensitivity depends upon the method used to visualize the anti-DIG antibody conjugate.
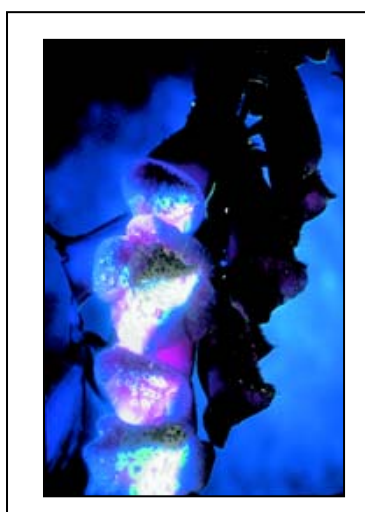
Figure 2.5: *Digitalis purpurea*
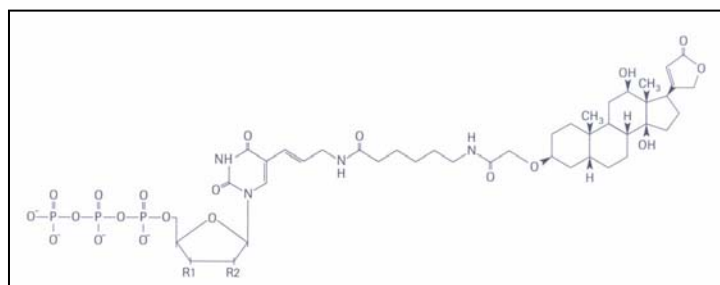
Figure 2.6: Structure of Digoxigenin-UTP/dUTP/ddUTP, alkali-stable.
Digoxigenin-UTP (R1 = OH, R2 = OH)
Digoxigenin-dUTP (R1 = OH, R2 = H)
Digoxigenin-ddUTP (R1 = H, R2 = H)

▪ *Kits/Soltions/Buffers/Chemicals/ antibodies etc.*

- **RNA probes**

   DEPC (Diethyl Pyrocarbonate) Sigma, St. Louis, USA

   DIG RNA Labelling Mix Roche, Mannheim, Germany

   DNAse RNase free Roche, Mannheim, Germany

   RNAse Inhibitor MBI fermentas, St. Leon Rot, Germany

   RNA polymerase SP6 Roche, Mannheim, Germany

   RNA polymerase T3 Roche, Mannheim, Germany

   RNA polymerase T7 Roche, Mannheim, Germany

   t RNA, (10 μg/μl) Roche, Mannheim, Germany

All the solutions were prepared using DEPC-H2O to make them of RNase free; autoclaved for 1 hour.

Table 2.12: Solutions and buffers for *In-situ* hybridisation

Citric acid	1 M in DEPC water
Deionised formamide	ROTH
DEPC-H2O	0.01% DEPC (50 µl/500 ml)
Heparin (Sigma)	100 mg/ml in 4 x SSC DEPC
Hybridisation buffer	5 ml Deionised formamide 2.5 ml 20 x SSC 5 µl heparin 10 µl Tween20 2.5 ml DEPC water Adjusted to pH 6.0 with 1 M citric acid
MAB (Maleic acid buffer)	11.6 g maleic acid 0.1 M; 8.8 g NaCl 0.15 M 800 ml water added; pH adjusted to 7.5 with solid NaOH; Volume made upto 1L.
MABT	MAB + 0.1%Tween20
PBS (Phosphate-Buffered Saline)	30 ml NaCl (5M) 15 ml Sodium Phosphate Buffer (1M), pH 7.3 volume adjusted to 1litre with DEPC water
PBT	PBS, 0.1% Tween 20
PBT/Glycine	PBS Glycine 2 mg/ml
4% PFA/PBS	4 g PFA (Para formaldehyde) 100 ml DEPC/PBS A few drops NaOH (10N); pH adjusted between 6.0-7.0 with HCl, indicator paper was used.

4%PFA/0.2% glutaraldehyde/ PBT	4%PFA/PBT pH 6-7 400 µl glutaraldehyde 25% pH adjusted to 6-7 with HCl dissolved in 50 ml PBT
Proteinase K	1.5 µg/ml in Proteinase K Buffer
Proteinase K Buffer	Proteinase K Buffer 10ml 1M Tris/HCl (pH 7.0), 1ml (0.5 M) EDTA Volume adjusted to 500ml with water
RIPA buffer **(Radio-Immunoprecipitation Assay)**	2.5 ml 10%SDS 15 ml NaCl (5M) 5 ml NP40 25 ml 10% Deoxycholate 1 ml EDTA (0.5M) 25 ml (1M) Tris/HCl pH 8.0 Added to 500 ml DEPC water
RNase A Buffer	1ml NaCl 5 M 100 µl Tris HCl 1 M, pH 7.5 10 µl Tween20 8.89 ml water
RNase A (Sigma)	Dissolve RNase A at a conc. of 10 µg /µl in 0.01 M NaAc pH 5.2 Heated to 100°C for 15 min.; Cooled slowly at RT pH adjusted by adding 0.1 volumes of 1 M Tris/HCl pH 7.4; Stored as aliquots at –20°C
20 X SSC	17.53 g NaCl 8.82 g sodium citrate Dissolved in 80 ml DEPC water pH adjusted to 7.0 with HCl Volume made up to 100 ml and autoclaved

SSC/Formamide/Tween20	5 ml 20 x SSC
	25 ml FA
	50 µl Tween20
	Added to 50 ml with water
10 x TBS (Tris buffered saline)	8 g NaCl
	0.2 g KCl
	25 ml Tris 1 M, pH 7.5
	Added to 100 ml with water
TBST	added 0.1% Tween20 to aliquot before use
tRNA	10 µg/µl in DEPC water
	Phenolized 2X and stored as aliquots at –20°C

Blocking stock solution:

Blocking reagent (Roche) was dissolved in MAB to a final concentration of 10% with shaking and heating either on a heating block or in a microwave oven. This stock solution was autoclaved and stored as aliquots at –20°C subsequently or at 4°C; 0.1% Tween 20 added on the day of usage.

Dig Antibodies coupled to AP (Roche)

TBST*/Levamisol TBST

2 mM Levamisol

*Tris buffered saline-Tween20

Alkaline Phosphatase Buffer 1 ml NaCl 5M

2.5 ml MgCl 1M

50 µl Tween20

5 ml Tris 1M, pH 9.5

To 50 ml with water

Staining solution

BM purple AP substrate Added 2 mM Levamisole

0.5-1% Tween20 added

Centrifuged, pellet was not used

The tissues were embedded on Histowax embedding block (Cambridge Instruments, Nussloch) was used. BM Purple was used to stain paraffin sections. After staining, the slides were embedded with Kaiser's Glycerol gelatine (Merck) and covered with Cover slips from Marienfeld, Germany.

An *in-situ* hybridisation protocol follows this general outline:

- Fixation of material and preparation of slides.
- Preparation of probe
- Pretreatments of material on slides, *e.g.* permeabilization of cells and tissues
- *In situ* hybridization
- Posthybridization washes
- Immunocytochemistry
- Microscopy

2.4.16A: Preparation of material:

Tissue samples were fixed in paraformaldehyde, dehydrated in graded alcohol series, embedded in paraffin blocks and tissue sections were prepared as described earlier in section 2.4.1 and 2.4.2.However, from a chemical point of view, there is little limitation in the type of fixation used because RNA is fairly unreactive to crosslinking agents.

2.4.16B: Probe selection:

Probes are complimentary sequences of nucleotide bases to the specific mRNA sequence of interest. These probes can be as small as 20-40 base pairs or be up to 1000 bp. The strength of the bonds between the probe and the target plays an important role. The strength decreases in the order RNA-RNA to DNA-RNA. This stability is in turn influenced by the various hybridization conditions such as concentration of formamide, salt concentration, hybridization temperature, and pH.

There are essentially four types of probe that can be used in performing *in- situ* hybridization.

- **Oligonucleotide probes**

These are produced synthetically by an automated chemical synthesis. The method utilizes readily available deoxynucleotides which are economical, but requires the specific nucleotide sequence wished to prepare. These probes have the advantages of being resistant to RNases and are small, generally around 40-50 base-pairs. These are good for *in situ* hybridization because of their small size which allows easy penetration into the cells or tissue of interest.

- **Single stranded DNA probes.**

These have similar advantages to the oligonucleotide probes except they are much larger, probably in the 200-500 bp size range. They can be produced by reverse transcription of RNA or by amplified primer extension of a PCR-generated fragment in the presence of a single antisense primer. This should be followed by another round of PCR using the first PCR product as template, but only using the anti-sense primers, thus producing single stranded DNA.

- **Double stranded DNA probes**

These can be produced by the inclusion of the sequence of interest in a bacteria which is replicated, lysed and the DNA extracted, purified and the sequence of interest is excised with restriction enzymes. Because the probe is double stranded, it has to be denatured prior to hybridization in order for one strand to hybridize with the mRNA of interest. These probes are generally less sensitive because of the tendency of the DNA strands to rehybridize to each other.

- **RNA probes (cRNA probes or riboprobes)**

RNA probes have the advantage that RNA-RNA hybrids are very thermostable and are resistant to digestion by RNases. This allows the possibility of post-hybridization digestion with RNase to remove non-hybridized RNA and therefore reduces the possibility of background staining.

There are two methods of preparing RNA probes:

1. Complimentary RNA's are prepared by an RNA polymerase-catalyzed transcription of mRNA in the 3' to 5' prime direction.
2. Alternatively, *in vitro* transcription of linearized plasmid DNA with RNA polymerase can be used to produce the RNA probes. Here plasmid vectors containing polymerase from bacteriophages T3, T7 (from *E. coli* Bacteriophages) or SP6 (from *Salmonella* bacteriophage) are used. These three polymerases all have similar biochemical properties and consist of a single polypeptide chain. Each is highly specific for its own promoter and does not use other bacteriophage, plasmid, bacterial or eukaryotic promoters at a significant rate. For ISH, subclone with an insert in the range 500 - 1000 bp is enough to be sensitive, but small enough to penetrate tissue after proteinase K treatment.

For this study RNA probes were used as this is the most widely used and well established technique in our laboratory. The probe for *Crybb2* was selected from the region coding the N'terminal extension of the protein.

2.4.16C: Probe preparation:

2.4.16C.1: Probe Generation

RNA probes were generated utilizing *in vitro* transcription. In this method, the selected sequence was amplified by PCR and then cloned into pCR®II vector (Invitrogen Life Technologies) containing phage transcription promoters (Sp6 and T7 promoters) that can initiate transcription in the presence of the corresponding RNA polymerase. Since, two different phage transcription promoters are placed on both sides of the polylinker cloning sites of the vector in opposite orientations, it was possible to selectively transcribe sense and antisense RNA probes. For the *Crybb2* probe strands transcribed by polymerase Sp6 was the antisense and by polymerase T7 was the sense.

2.4.16C.2: Probe Labelling:
In-situ hybridisation RNA probes were labelled with Dioxigenin-rUTP (Boehringer Mannheim) and were synthesized from linearized cDNA templates according to the manufacturer's instructions. *Crybb2* probes were linearized with restriction enzymes *BamHI* and *XbaI*, and synthesized with T7 and Sp6 RNA polymerase.

Working protocol for probe preparation:
- A loop full of the extracted vector with DNA insert (probe) was taken and spread on a culturing plate.
- The plate was incubated O.N at 37°C
- One large colony was selected, picked up with a 10µl tip and was inserted it in a culture tube containing 5ml of LB ampicillin medium
- This was then cultured O.N. at 37°C on a shaker
- On the following day plasmid DNA was extracted following plasmid extraction kit protocol and O.D of the DNA was measured.

Preparation of linearized template:

- 6μl DNA
- 1μl restriction enzyme
  *Bam*HI and *Xba*I (but in separate samples)
- 1.5μl restriction buffer
  (specific for *Bam*HI or *Xba*I
- 5.5μl H_2O
- End Volume=15μl
- Incubated O.N. at 37°C
- **5μl of the digest was analyzed in 1% agarose gel with ethidium bromide.**
  (0.5-1μl ethidium bromide was added in 50ml Agarose)

Labelling of probe:

- 8μl linerarized template DNA
  (1.5μg approximately)
- 2μl DIG NTP Labelling mix
- 2μl 10X Transcription Buffer
- 2μl Polymerase(20μg/μl)
  Sp6 polymerase in *Xba*I digest,
  T7 polymerase in *Bam*HI digest
- 1μl RNase inhibitor(20μg/μl)
- 5μl DEPC H_2O

Total volume= 20μl

- The labelling mix was then centrifuged* (13,000rpm/15 seconds/RT).

  [*Centrifugations performed with Biofuge, Hereaus Instruments; Rotor: PP1/97 #3324]

- It was then incubated for 3 hours at 37°C

- 1μl RNase free DNase was then added.

- Following to that it was incubated for 15 minutes at 37°C

2.4.16C.3: Filling of the labelling mix:

The labelled mix was then filled by adding the following:
- 1μl t-RNA(10μg/μl)
- 100μl DEPC
- 33μl Ammonium acetate (7.5M)
- 300μl 100% Ethanol(-20°C)

- The mix was then incubated at –80°C for 30 minutes

- Following that it was centrifuged at 14,000rpm*/4°C/30mins

  [*Centrifugations performed with Centrifuge Sigma 3K18; Rotor: #12154-H]

- The pellet was then washed with 70% ethanol.

- Again centrifuged at 14,000rpm*/4°C/ 30 minutes

- The sample was then dried in a speed vacuum.

- 100μl DEPC H_2O and 1μl Rnase inhibitor was then added to the dried sample.

- 5μl of the sample was then analysed in 1% agarose gel (ethidium bromide added) at 200V for 15-20 minutes.

- The probe was then ready to use.

2.4.16D: <u>Pre-treatment of materials on the slide:</u>

DNA and RNA target sequences are surrounded by proteins and that extensive crosslinking of these proteins masks the target nucleic acid. Therefore, permeabilization (viz. Proteinase K treatment) procedures are required. This includes the procedures for deparaffinization, graded dehydration, post fixation of tissue sections, endogenous enzyme inactivation, RNase treatment, HCl treatment, detergent treatment and protease treatment. The fixation and pretreatment protocols have to be optimized for different applications.

- **<u>Deparaffinization:</u>** This procedure was carried out by treating the slides in xylol for 10 minutes to 1 hour.
- **<u>Graded dehydration:</u>** This procedure was carried out by treating the slides in different grades of ethanol (100%, 95%, 90%, 80%, 70%, 50% and 30%).
- **<u>Post fixation:</u>** This procedure was carried out by treating the slides 4%PFA in PBS.
- **<u>Endogenous enzyme activation:</u>** When an enzyme is used as the label, the endogenous enzyme activity may have to be inactivated. For peroxidase, this is done by treating the sections with 1% H_2O_2 in methanol for 30 minutes. For alkaline phosphatase, levamisole may be added to the substrate solution, but this may be unnecessary since residual alkaline phosphatase activity is usually lost during hybridization, as in this case.
- **<u>RNase treatment:</u>** RNase treatment serves to remove endogenous RNA and may improve the signal-to noise ratio in DNA-DNA hybridizations. This treatment can also be used as a control in hybridizations with (m)RNA as target. It is done by incubating the preparations in DNase-free RNase (100 µg/ml) in 2x SSC at 37°C for 60 min. (SSC = 150 mM NaCl, 15 mM sodium citrate, pH 7.4).
- **<u>HCl treatment:</u>** In several protocols a 20 - 30 min treatment with 200 mM HCl is included. The precise action of the acid is not known, but extraction of proteins and partial hydrolysis of the target sequences may contribute to an improvement in the signal-to-noise ratio.
- **<u>Deteregent treatment:</u>** Preparations may be pretreated with Triton X-100, sodium dodecyl sulphate (SDS), or other detergents if lipid membrane components have not been extracted by other procedures such as fixation, dehydration, embedding, and endogenous enzyme inactivation procedures.
- **<u>Protease treatment:</u>** Protease treatment serves to increase target accessibility by digesting the protein that surrounds the target nucleic acid. To digest the sample, the preparations were incubated in 1.5 µg/ml Proteinase K in 20 mM Tris-HCl, 1 mM EDTA, pH 7.2, for 3 minutes at RT.

Table 2.13: Working protocol for pre-treatment of material on slide:

Solution	Repeats	Duration
Xylol	1X	15 min
Xylol	2X	10 min
100%Ethyl Alcohol	1X	2min
95%Ethyl Alcohol	1X	2min
90%Ethyl Alcohol	1X	2min
80%Ethyl Alcohol	1X	2min
70%Ethyl Alcohol	1X	2min
50%Ethyl Alcohol	1X	2min
30%Ethyl Alcohol	1X	2min
PBS	2X	5min
4%PFA in PBS	1X	20-30 min
ProteinaseK (1.5µg/ml – 2.0µgin20mM Tris /HCL, 1mM EDTA,pH /.2 Fresh	1X	3min
PBS	1X	5min
4%PFA in PBS	1X	30min
PBS	2X	5min
2X SSC	2X	2min
Tris Glycine Buffer	1X	2 hours

2.4.16E: Pre-hybridisation:

A prehybridization incubation is sometimes better to prevent background staining. The prehybridization mixture contains all components of a hybridization mixture except for probe and dextran sulfate.

2.4.16F: <u>Hybridization</u>

Hybridization here depends on the ability of mRNA to reanneal with complementary strands. Parameters influencing optimal hybridization conditions are the probe length, probe concentration, pore size, the inclusion of dextran sulphate and target, the washing conditions and whether the probes will be single- or double stranded. The last parameter was excluded from consideration as single stranded probe were chosen over double stranded probes because a number of competing reactions occur during *in- situ* hybridization with double-stranded probes like:

- Probe renaturation in solution
- *In-situ* hybridization
- *In-situ* renaturation (possibly, for double stranded targets)

Consequently, the use of single-stranded probes is more advantageous for *in situ* hybridization over double stranded probes.

<u>Probe length:</u> The rate of the renaturation of DNA in solution is proportional to the square root of the (single-stranded) fragment length. Consequently, maximal hybridization rates are obtained with long probes. The fragment length also influences thermal stability.

<u>Probe concentration:</u> The probe concentration affects the rate at which the first few base pairs are formed (nucleation reaction). The higher the concentration of the probe, the higher the reannealing rate.

<u>Pore size:</u> The size of the pore made by proteinase K on the cell membrane is also an important factor influencing hybridisation. Too small pore size results in poor documentation because the tissue cannot be recognized and larger pore size results in unspecific bindings. It is important to optimize the proteinase K concentration for each tissue type.

<u>Dextran sulphate</u>

In aqueous solutions dextran sulfate is strongly hydrated. Thus, macromolecules have no access to the hydrating water, which causes an apparent increase in probe concentration and consequently higher hybridization rates.

<u>Stringency washes:</u>

During hybridization, duplexes form between perfectly matched sequences and between imperfectly matched sequences. To remove the background associated with non-specific hybridization, the samples were washed with a dilute solution of salt. The lower the salt concentration and the higher the wash temperature, the more stringent is the wash. In general, greater specificity is obtained when hybridization is performed at a high stringency and washing at similar or lower stringency, rather than hybridizing at low stringency and washing at high stringency.

Working protocol for hybridization :

- A mixture of probe (1:50), hybridization buffer, heparin (100μg/ml) stock and tRNase was prepared.

- The mixture was denatured at 80°C for 3 minutes.

- 120μl of this hybridisation mixture was added per slide and cover slip was applied on the slides. Care was taken to eliminate any air bubble in between slide and coverslip.

- The slides were placed in a hybridisation chambers and incubated O.N. at 65-68°C in a moist chamber.

2.4.16G. Post-hybridization washing:

Labelled probe can hybridize non-specifically to sequences which are partially but not entirely

homologous to the probe sequence. Such hybrids are less stable than perfectly matched hybrids. They can be dissociated by performing washes of various stringencies. Stringency of the washing can be manipulated by varying the formamide concentration, salt concentration, and temperature. Often a wash in 2X SSC containing 50% formamide suffices. For some applications the stringency of the washes should be higher. However, stringent hybridization should be preferred rather than stringent washing.

- Coverslips were detached from the slides by placing the slides in **5X SSC** solution in a beaker, Gentle pressure was applied if the slides did not detach automatically after 3-5 minutes.

Table 2.14: Working protocol for post hybridisation washing

Solution	Repeats	Duration	Temperature
5X SSC	3X	20mins	
0.5X SSC, 20% foramide (Prewarmed. at 68°C)	2X	30min	65°C
0.5X SSC, 20% Foramide	1X	1hour	37°C
NTE	1X	15min	37°C
NTE + 10μg/ml RNaseA	1X	30min	37°C
NTE	1X	15min	37°C
0.5X SSC,20% Foramid	2X	30min	65°C
2X SSC	1X	30min	RT

2.4.16H. Immunocytochemistry:

Blocking reaction:

Performing a blocking step by treating the slides in 1% blocking solution in MAB-T for 30 minutes at room temperature prior to the immunological procedure removes high background.

Antibody reaction:

Blocked target tissue was then incubated it with the anti-digoxigenin antibody conjugated with alkaline Phosphatase solution O.N. at 4°C in a moist chamber.

- The anti body solution was pre-cooled at 4°C on a shaker.
- Concentration of Antibody solution was 1:5000 in 1% blocking solution in MAB-T.
- 200µl of this antibody solution was applied per slide, coverslip placed properly
- Incubated in a moist chamber O.N. at 4°C.

Removal of unbound antibody

The coverslips were detached in TBS-T (gentle pressure applied when necessary) and the sections were then washed in TBS-T for 1 hr and in NTMT (2-3 times) for 10 minutes each at room temperature. This removed unbound antibodies and blocking agents.

Detection:

Staining was performed with BM purple AP substrate. This is a chromogenic substrate for alkaline Phosphatase (AP) designed for precipitating enzyme immunoassay. It gives a permanent, dark purple band or spot at the AP binding site (Montgomery, 2002). Before use BM purple AP was centrifuged at 2500 rpm[*] for 7 minutes; and 2 mM Levamisol and 0.1% Tween 20 was added to it.

[* Centrifugations performed with Biofuge, Hereaus Instruments; Rotor: PP1/97 #3324]

Staining Solution:

120µl BM purple + 2mMlevamasol + 0.1% Tween 20……………for 1 slide

This stain is photosensitive, hence was never exposed to bright light and all procedures for staining were carried out under yellow light. After applying the staining solution on the slides and placing the coverslips properly, they were incubated in dark in a moist chamber at RT

during day time and at 4°C O.N. This is called as controlled staining and the intensity of the staining was observed daily to decide the timing to stop the reaction. The staining reaction for *Crybb2* was carried on for a maximum of 3 days; in any case the staining reaction should not be carried out for more than 7 days as this will result in background staining or unspecific staining. The slides hybridized with anti-sense probe should show bluish violet staining and the one's hybridized with sense probe should exhibit no staining; this actually serves as a control for the probe apart from the known positive control to determine the quality of the entire procedure as a whole.

2.4.16I: Stopping the Reaction

The staining reaction was stopped by detaching the coverslips from the slides in Fresh NTMT solution (gentle pressure applied when necessary), followed by washing the slides in these solutions:

- Fresh NTMT: 2X   15 minutes
- 4% PFA in PBS   1X   3-5 minutes
- Millipore H_2O 2X   2 minutes

2.4.16J: Preparation of slides for microscopy:

Kaiser's Glycerol gelatine was warmed up in a water bath at 50-55°C until it was liquid. Slides were air-dried and then on each slide 500 µl Kaiser's Glycerol gelatine were applied and covered with a cover slip. The slides were dried in a dust free condition, O.N. in dark and were then ready for microscopic analysis. The permanent slides were stored at 4°C.

2.4.17: <u>DNA microarray technique:</u>

It is known that thousands of genes and their products (i.e., RNA and proteins) in a given living organism function in a complicated and orchestrated way that creates the mystery of life. However, traditional methods in molecular biology generally work on a **"one gene in one experiment"** basis, which means that the throughput is limited and the "whole picture" of gene function is difficult to obtain. DNA microarray helps to overcome this drawback by monitoring the whole genome on a single chip so that researchers can have a better picture of the interactions among thousands of genes simultaneously (Brown *et al*., 1999; Sterrenberg *et al.,* 2002; Wride *et al.,* 2003)

Base-pairing (i.e., A-T and G-C for DNA; A-U and G-C for RNA) is the underlining principle of DNA microarray. An array is an orderly arrangement of samples. It provides a medium for matching known and unknown DNA samples based on base-pairing rules and automating the process of identifying the unknowns. An array experiment can make use of common assay systems such as microplates or standard blotting membranes, and can be created by hand or make use of robotics to deposit the sample. In general, arrays are described as *macroarrays* or *microarrays*, the difference being the size of the sample spots. Macroarrays contain sample spot sizes of about 300 microns or larger and can be easily imaged by existing gel and blot scanners. The sample spot sizes in microarray are typically less than 200 microns in diameter and these arrays usually contains thousands of spots. Microarrays require specialized robotics and imaging equipments. DNA microarray or DNA chips are fabricated by high-speed robotics, generally on glass but sometimes on nylon substrates, for which probes with known identity are used to determine complementary binding, thus allowing massively parallel **gene expression and gene discovery studies**. An experiment with a single DNA chip can provide researchers information on thousands of genes simultaneously. (Brown *et al.,* 1999). [http://www.gene-chips.com/]

The microarray (DNA chip) technology is having a significant impact on genomics study. Many fields, including drug discovery and toxicological research, are benefiting from the use of DNA microarray technology.

Microarray:

<div align="center">

Kits/reagents/chemicals etc.

</div>

- (3-aminoallyl)-2'deoxyuridine-5'-triphosphate (AA-dUTP) [Sigma]

- 100 mM dNTP Set PCR grade (Fermentas)

- Random Hexamer primers (3mg/ml) (Fermentas)

- SuperScript II RT (200 µg/µl) (Invitrogen)

- Cy-3 ester (AmershamPharmacia)

- Cy-5 ester (AmershamPharmacia)

- QIAquick PCR Purification Kit (Qiagen)

- RNeasy® Midi and Mini Kit (Qiagen)

Reagent preparation:

Phosphate Buffers

- 1M K_2HPO_4 and 1M KH_2PO_4

- 1M **Phosphate buffer** (K PO_4, pH 8.5-8.7)

1M K_2HPO_4……..9.5 ml

1M KH_2PO_4……..0.5 ml was combined

- For 100 ml **Phosphate wash buffer** (5 mM KPO_4, pH 8.0, 80% Ethanol):

1 M KPO_4 pH 8.5	0.5 ml
MilliQ water	15.25 ml
95% Ethanol	84.25 ml was mixed

Note: Wash buffer was slightly cloudy in appearance.

- **Phosphate elution buffer** was prepared by diluting 1 M KPO_4, pH 8.5 to 4 mM with MilliQ water.

Aminoallyl dUTP

- For a final concentration of 100mM;

19.1 µl of 0.1 M KPO_4 buffer (pH 7.5) was added to a stock vial containing 1 mg of aa-dUTP. Gently vortexed to mix and transfer the aa-dUTP solution into a new microfuge tube. Stored at –20°C.

- The concentration of the aa-dUTP solution was measured by diluting an aliquot 1:5000 in 0.1 M KPO_4 (pH 7.5) and measuring the OD289. (Stock concentration in mM = OD289 x 704).

Labeling Mix (50X) with aa-dUTP and dTTP in the ratio of (2:3):

The following reagents were mixed:

<div align="center">

Final concentration

dATP (100 mM)………5µl…... (25 mM) $\rightarrow$ 47.5 µl

dCTP (100 mM)………5µl…... (25 mM) $\rightarrow$ 47.5 µl

dGTP (100 mM)………5µl…... (25 mM) $\rightarrow$ 47.5 µl

dTTP (100 mM)………3µl…(15 mM) $\rightarrow$ 28.4 µl

aa-dUTP (100 mM)…...2µl……(10 mM) $\rightarrow$ 19.1 µl

</div>

Total: 20µl $\rightarrow$ 190 µl

The unused solution was stored at –20°C.

- **Sodium Carbonate Buffer** (Na_2CO_3): 1M, pH 9.0

    - 10.8 g Na_2CO_3 was dissolved in 80 ml of MilliQ water and pH adjusted to 9.0 with 12N HCl; volume was made up to 100 ml with MilliQ water.

- To prepare a 0.1 M solution for the dye coupling reaction it was diluted with 1:10 water.

Note: Carbonate buffer changes composition over time; it was prepared fresh every couple of weeks to a month.

Cy-dye esters

- Cy3-ester and Cy5-ester were provided as dry products in 5 tubes by the manufacturer (Amersham). Each tube of dye ester was resuspended in 73 µl of DMSO before use.

- All reaction tubes were wrapped with aluminium, foil and protected from light as much as possible to prevent photobleaching of the dyes.

Note: Dye esters were either be used immediately or aliquoted and stored at –80°C. Any introduced water to the dye esters results in a lower coupling efficiency due to the hydrolysis of the dye esters. Since DMSO is highly hygroscopic it was stored in a well sealed desiccant.

Working procedure:

(Drobyshev *et al.,* 2003a; Drobyshev *et al*., 2003b; Seltmann *et al*., 2005; Greenwood, Horsch *et al*., in press).

DNA microarray experiments were performed in collabolaration with Dr. Johannes Beckers; the Expression Profiling group at the Institute of Experimental Genetics, GSF.

2.4.17A: <u>Isolation of total RNA</u>

Total RNA was isolated just before processing for expression profiling. For preparation of total RNA, brain and lens tissues were thawed in buffer containing chaotropic salt [RLT buffer (supplied), Qiagen] and homogenised using a Polytron homogeniser. Total RNA from individual samples was obtained according to manufacturer's protocols (described in section 2.4.3) using RNeasy® Midi/Mini kit (Qiagen). 2µg RNA aliquots were run on a formaldehyde agarose gel to check for RNA integrity and the concentration was calculated from $OD_{260/280}$ measurement. The RNA was stored at –80°C in RNase free water (Qiagen).

2.4.17B: <u>Chip design</u>

A glass-surface DNA-chip containing ≈ 21000 probes was used. About 20200 of these probes are from the commercial Lion mouse array-TAG clone set, which is mostly derived from 3'UTRs. Chips were kindly availed by the collaborator (Dr. J. Beckers; Expression profiling group, Inst. of Experimental Genetics, GSF). **[**All Lion probes were already sequenced. The remaining probes were isolated in a subtractive screen for differentially expressed genes in the mesoderm of Delta/Notch pathway deficient mouse embryos. Mouse array-TAG clones have the general ID [MG-VW-XYZ**)** and the Delta/Notch specific probes are named as [rda-X]. (Drobyshev *et al.,* 2001; Seltmann *et al.,* 2005; Greenwood, Horsch *et al*., in press**]**

2.2.17C: <u>DNA Microarrays</u>

Prepared aldehyde coated microarray slides were availed which were pre-hybridised for 1 hour in pre-hybridisation buffer (6X-SSC, 1%BSA, 0,5 %SDS) rinsed in water, dried and hybridised the same day.

2.4.17D: <u>Reverse Transcription and Fluorescent Labelling</u>

For labelling, 20µg of total RNA was used for reverse transcription and indirectly labelled with **Cy3** or **Cy5** fluorescent dye according the TIGR protocol (http://pga.tigr.org/sop/M004_1a.pdf). Labelled cDNA was dissolved in 30µl hybridisation buffer (6X SSC, 0,5% SDS 5X-Denhardt's solution and 50% formamide) and mixed with 30µl of reference cDNA solution (pool from wild type animals) labelled with the second dye. This hybridisation mixture was placed on a pre-hybridised microarray, under a cover slip, placed into a hybridisation chamber (Genetix, Munich-Domach, Germany) and immersed in a

thermostatic bath at 42°C for at least 16 hours. After hybridisation slides were washed in 40ml of 3X SSC, 40ml of 1X SSC and 40ml of 0,25X SSC at room temperature. For drying slides were placed in an empty 50ml Falcon tube (Becton Dickinson, USA) and centrifuged at 4000 rpm[*]. Dried slides were scanned with a GenePix 4000A microarray scanner and the images were analysed using the GenePix Pro3.0 image processing software (Axon Instruments, USA). All data were normalised by adjusting the median of log-ratios of Cy5 to Cy3 intensities to 0. For data analysis in-house produced LabView based software was used (http://www.gsf.de/ieg/groups/exppro_cpt.html#PAM).

[* All centrifugations performed with Centrifuge 5810R, Eppendorf; Rotor: A-4-62]

2.4.17E: <u>Aminoallyl (aa) labelling of microarrays:</u>

This protocol describes the labeling of eukaryotic RNA with aminoallyl labeled nucleotides via first strand cDNA synthesis followed by a coupling of the aminoallyl groups to either Cyanine 3 or 5 (Cy3/Cy5) fluorescent molecules.

<u>Working procedure for Aminoallyl Labelling</u>

    i.   To 20 µg of total RNA (or 2 µg poly (A+) RNA) which has been DNase I-treated and Qiagen RNeasy® purified, 2 µl $T_{xx}VN$-Mix (3mg/ml) was added and the final volume was made up to 39 µl with RNase-free water.

    ii.   Mixed well and incubated at 70°C for 10 minutes.

Following that the mix was snap-frozen in dry ice/ethanol bath for 30 seconds, centrifuged briefly at >10,000 rpm* and the rest of the procedure was continued at room temperature. [*Centrifugations performed with Biofuge, Hereaus Instruments; Rotor: PP1/97 #3324]

    iii.   The following mix was then prepared:

5X First Strand buffer	12 µl
0.1 M DTT	6 µl
50X aminoallyl-dNTP mix	1.2 µl
SuperScript II RT (200µg/µl)	2 µl
Total: 21.2 µl - 20.5 µl added	

    v.   Mixed and incubated at 42°C for at least 3 hours to O.N.

    vi.   To hydrolyze RNA, 1 M NaOH 20 µL and 0.5 M EDTA 20 µL was added and then mixed and incubated at 65°C for 15 minutes.

vii.   20 µL of 1 M HCl was added to neutralize pH.

2.4.17F: Reaction Purification I: Removal of unincorporated aa-dUTP and free amines (Qiagen PCR Purification Kit)

This purification protocol is modified from the Qiagen QIAquick PCR purification kit protocol. The phosphate wash and elution buffers are substituted for the Qiagen supplied buffers because the Qiagen buffers contain free amines which compete with the Cy dye coupling reaction.

i.   cDNA reaction mixture was mixed with 600 µl (5X reaction volume) buffer PB (Qiagen supplied) and transferred to QIAquick column.

ii.   The column was then placed in a 2 ml collection tube (Qiagen supplied) and centrifuged at ~13,000 rpm* for 1 minute. Flow through was discarded.

iii.   To wash, 750 µl phosphate wash buffer was added to the column and centrifuged at ~13,000 rpm* for 1 minute.

iv.   The flow through was discarded and the washing and centrifugation in step (iii) was repeated.

v.   The flow through was again discarded and the column was centrifuged for an additional 1 minute at maximum speed.

vi.   The column was then transferred to a new 1.5 ml microfuge tube and carefully 30µl phosphate elution buffer was added to the centre of the column membrane.

vii.   This was then incubated for 1 minute at room temperature.

viii.   Elution was done by centrifugation at ~13,000 rpm* for 1 minute.

ix.   A second elution was carried out into the same tube by repeating steps (vi-viii).

x.   The final elution volume was ~60 µl.

xi.   The samples were dried in a speed vac.

[*Centrifugations performed with Biofuge, Hereaus Instruments; Rotor: PP1/97 #3324]

2.4.17G: Coupling aa-cDNA to Cy Dye Ester:

i.   Aminoallyl-labeled cDNA was resuspended in 4.5 µl of 0.1 M sodium carbonate buffer (Na$_2$CO$_3$), pH 9.0.

Note: Carbonate buffer changes composition over time, so fresh (not older than 2 weeks) carbonate buffer was used.

ii.   4.5 µl of the appropriate NHS-ester Cy dye (prepared in DMSO) was added.

Note: To prevent photobleaching of the Cy dyes all reaction tubes were wrapped in aluminium foil and were kept sequestered from light as much as possible.

iii.   The reaction mixture was incubated for 1 hour in the dark at room temperature.

2.4.17H: <u>Reaction Purification II: Removal of uncoupled dye (Qiagen PCR Purification Kit)</u>

i.   To the reaction mixture 35 µl 100 mM NaOAc (pH 5.2) was added.

ii.   250 µl (5X reaction volume) Buffer PB (Qiagen supplied) was then added to it.

iii. A QIAquick spin column was placed in a 2ml collection tube (Qiagen supplied); the sample was applied to the column, and centrifuged at ~13,000 rpm[*] for 1 minute. Flow through was discarded.

iv.   To wash, 0.75 ml buffer PE (Qiagen supplied) was added to the column and centrifuged at ~13,000 rpm[*] for 1 minute.
      Note: Buffer PE was ethanol added before use according to manufacturer's instruction.

v.   The flow through was discarded and the column was centrifuged for an additional 1 minute at maximum speed.

vi.   The column was placed in a clean 1.5 ml microfuge tube and 30 µl of buffer EB (Qiagen supplied) was carefully added to the centre of the column membrane.

vii. This was then incubated for 1 minute at room temperature.

viii. This was then eluted by centrifugation at ~13,000 rpm[*] for 1 minute.

ix.   Elution was performed for a second time into the same tube by repeating steps (vi-viii).

x.   The final elution volume was ~60 µl.

Note: This protocol is modified from the Qiagen QIAquick Spin Handbook (04/2000, page. 18).

[*Centrifugations performed with Biofuge, Hereaus Instruments; Rotor: PP1/97 #3324]

2.4.17I: <u>Pre-hybridisation</u>

For aldehyde coated slides, pre-hybridisation is necessary to minimize background. The slides and cover slips were immersed into the pre-hybridisation buffer at 42 °C for 45 min**, then they were** immersed in ddH$_2$O, once in ethanol and dried in oven briefly.

```
Pre-hybridisation buffer

    6X SSC:              15 ml   (Stock: 20xSSC)


    0.5% SDS:            2.5 ml  (Stock: 10%SDS)


    1% BSA:              5 ml    (Stock: 10% BSA)
                         27.5 ml  ddH₂O
    ─────────────────────────────────────────────
                    Total   50 ml

    Pre-hybridisation buffer warmed to 42°C before use
```

2.4.17J: <u>Hybridisation</u>

  i.   Cy3 and Cy5 labeled cDNAs were combined in one 1.5 ml tube

  ii. 2ul salmon sperm DNA (10 µg/µl, Sigma D7656) and 15 µl of polydA (1 µg/µl, Sigma P-0887) was added to that.

  iii. The tubes were then placed into speedvac at 45 °C for 1.5 hours.

  iv. Each sample was then dissolved in 65 µl of pre-warmed Hybridization Buffer

  v.   The samples were then into 0.2 ml PCR tubes, denatured at 95°C 5-10 min, cooled in ice-water.

  vi. The samples were spinned down.

1ml of hybridisation buffer on each slide, coverslips placed and then 15 µl DEPC-Water was applied in the hybridisation chamber and incubated at 42°C overnight (>16 hours),

```
Hybridisation buffer/slide
    50% formamide:       500µl   formamide
    6xSSC:               300µl   20X SSC
    0.5%SDS:             50µl    10% SDS
    5X Denhardt's :      100µl   50X Denhardt's
                         50µl    dd H₂O
    ─────────────────────────────────────────────
                         1000µl   Total
```

2.4.17K: <u>Washing:</u>

Following O.N. hybridization, washing of the slides were carried out sequentially in the following buffers:

    3X SSC; 1X SSC; 0.5X SSC; 0.25X SSC; and **0.1X SSC**

    Slides were dried by spinning at 4000 rpm*/1minute and scanned following washing, the slides were protected from light during this procedure. [* All centrifugations performed with Centrifuge 5810R, Eppendorf; Rotor: A-4-62]

2.4.18: <u>Real Time- qPCR:</u>

Real–time or quantitative PCR (qPCR) allows quantification of starting amounts of DNA, cDNA, or RNA templates. qPCR is based on the detection of a fluorescent reporter molecule that increases as PCR product accumulates with each cycle of amplification. Fluorescent reporter molecules include dyes that bind double-stranded DNA (i.e. SYBR Green I) or sequence–specific probes (i.e. Molecular Beacons or TaqMan® Probes). qPCR exceeds the limitations of traditional end–point PCR methods by allowing either absolute or relative quantification of PCR product at the end of each cycle. This ability has greatly enhanced several areas of research including gene expression analysis and genotyping assays. SYBR Green I, a commonly used fluorescent DNA binding dye, binds all double–stranded DNA and detection is monitored by measuring the increase in fluorescence throughout the cycle. SYBR Green I has an excitation and emission maxima of 494 nm and 521 nm, respectively. The fluorescent dye SYBR Green I binds to the minor groove of the DNA double helix. In solution, the unbound dye exhibits very little fluorescence, however, fluorescence is greatly enhanced upon DNA-binding. Since SYBR Green I dye is very stable (only 6% of the activity is lost during 30 amplification cycles) and the LightCycler instrument's optical filter set matches the wavelengths of excitation and emission, it is the reagent of choice when measuring total DNA. After annealing of the primers, a few dye molecules can bind to the double strand. DNA binding results in a dramatic increase of the SYBR Green I molecules to emit light upon excitation. During elongation, more and more dye molecules bind to the newly synthesized DNA. If the reaction is monitored continuously, an increase in fluorescence is viewed in real-time. Upon denaturation of the DNA for the next heating cycle, the dye molecules are released and the fluorescence signal falls. Fluorescence measurement at the end of the elongation step of every PCR cycle is performed to monitor the increasing amount of amplified DNA. Together with a melting curve analysis performed subsequently to

the PCR, the SYBR Green I format provides an excellent tool for specific product identification and quantification.

Differential expression of selected genes was verified by real-time qPCR using the LightCycler (Roche). 1µg of total RNA was reverse transcribed at 42°C for 1 hour using random nonamers according to the manufacturer's protocol (Invitrogen). The enzyme was heat inactivated and the cDNA diluted 1:5 with water. PCR reactions were done with the FastStart SYBRGreen I kit (Roche). Primers were designed to be 20-22bp in length with 55% GC to amplify PCR products of a maximum of 200bp spanning at least 1 intron or exon/exon boundaries. Primers from the mouse *Hprt* genes were used as internal controls. Cycling conditions were 10 minutes at 95°C to activate the enzyme followed by 45 cycles of 20 seconds at 95°C, 20 seconds at 55°C and 10 seconds at 72°C each. Analysis of PCR reactions was done with the RelQuant 1.0 software (Roche). [Seltmann *et al.,* 2005]

- 5X First strand buffer (Life Technologies):
- 10X DTT, 0.1M (Life Technologies):
- RNase inhibitor, 40µg/µl (Roche)
- 20X 4dNTmix, 10mM each (AP Biotech)
- Superscript II MMLV RT200µg/µl (Life Technologies)
- RNase free ddH$_2$O without DEPC.
- LC_FastStart DNA master SYBR Green I kit (Roche)

Table 2.15: List of the primers used in Real Time-qPCR

Name	Sequence (5'-3')	Tm (°C)
Ank_For1	CCC TGA TAG CCT ACA GTG AC	59.4
Ank_Rev1	GGC TAC GAA AAC AAC CTG AG	57.3
Camk_For1	CAC CAG GAA CTT CTC CGG AG	61.4
Camk_Rev1	ATG AAA GTC CAG GCC CTC CAC	61.8
Hlp_For1	GTG AAG TTC TTC CCC TAT GG	57.3
Hlp_Rev1	CCC ACC ATT TTG TAG ATA GCC TCG	62.7
Nrgn_For1	GCA GAG AGA AGG GTC GCA AG	61.4
Nrgn_Rev1	GCT GCT CTT CCC ACA GCT TC	61.4
TB4_For	CCT TCC AGC AAC CAT GTC TG	59.4
TB4_Rev	GCT CGT GGA ATG TAC AGT GC	59.4
Lpl_For	CCG TGT GAT TGC AGA GAG AG	59.4
Lpl_Rev	GTT GCT TGC CAT CCT CAG TC	59.4
Atpv0_For	CGT GGC TAT CCT GCT GAT CA	59.4
Atpv0_Rev	AGG CAA GAG AGA CAC AGC TG	59.4

2.4.18A: <u>Working procedure:</u>

(According to Seltmann *et al.,* 2005)

First strand cDNA synthesis:

A combination of Life Tech and Clontech protocols was used for First strand cDNA synthesis for qPCR.

    i.   Atfirst the master mix was prepared for all the samples according to the following formulation.

<table>
<tr><td colspan="2" align="center"><u>Preparation of master mix:</u></td></tr>
<tr><td>5X First strand buffer (Life Tech):</td><td>4µl</td></tr>
<tr><td>10X DTT, 0.1M (Life Tech):</td><td>2µl</td></tr>
<tr><td>RNase inhibitor, 40µg/µl (Roche)</td><td>1µl</td></tr>
<tr><td>20X 4dNTmix, 10mM each (AP Biotech)</td><td>1µl</td></tr>
<tr><td>Superscript II MMLV RT200µg/µl (Life Tech)</td><td>1µl</td></tr>
<tr><td align="right">Total:</td><td>9µl</td></tr>
<tr><td colspan="2" align="center">Stored at RT and continued.</td></tr>
</table>

    ii.   RNA samples were then thawed on ice and 1µg of total RNA was transferred to each 0.2ml PCR tubes. The total volume was adjusted to 10µl by RNase free ddH$_2$O without DEPC.

    iii.   1µl of random monomers, 0.1mM stock were then added.

    iv.   The mix was then incubated at 70°C for 5 minutes. Following that, it was chilled in ice water.

    v.   The mix was then let to stand for 5 minutes for primer annealing at RT.

    vi.   9µl of the master mix was then added to each tube and incubated at 42°C for 1 hour; then at 70°C for 15 minutes to inactivate superscript II; and finally at 20°C for ever.

    vii.   The 20µl of sample was then diluted by five fold (100µl) with MilliQ H$_2$O and 2µl of this was then used for LightCycler runs.

2.4.18B: <u>Oligonucleotides:</u>

High quality oligos were ordered from MWG Biotech. The general criteria followed while selecting these primers were as follows:

- 18-22 nucleotides (ideally 20) long
- 55-60% GC content.
- Spanning a 135-225 bp gene specific PCR product
- Primers were selected from exon-exon boundary or different exons.
- Three or more G/C was avoided at the 3'end as this stabilizes non-specific primer annealing.
- Self complementary 3' ends were avoided.

Working solutions were prepared at a concentration of 100pmol/µl as instructed by the manufacturer and stored at -20°C for future use.

2.4.18C: <u>Running the LightCycler experiment:</u>

LC_FastStart DNA master SYBR Green I kit (Roche) was used to perform the light cycler experiment.

    i.   Preparation of master mix:

<u>Master mix:</u>	
H_2O:	11.6 µl
$MgCl_2$, 25mM stock (Blue):	2.4 µl
Primer mix , 5µg each	2.0 µl
LC_FastStart DNA master SYBR Green I:	2.0 µl
[10µl from vial (**1a**) added to vial (**1b**)]	
Total:	18 µl

    ii.   18µl of the master mix was then pipetted into glass capillaries (32 slot caroussel).

    iii.   Then to each capillary 2µl of cDNA was added.

    iv.   Stopper was applied to each glass capillary and the caroussel was spinned.

    v.   The light cycler was switched on.

vi.   Cycling conditions using FastStartkit, Roche:

> - 5-10 minutes at 95°C hot start activation
> - 55°C annealing temperature
> - 25 bases per second (+ 5 seconds for detection) amplification time.
> - 45 cycles.

2.4.18D: <u>Analysis using RelQuant 1.0 (Roche) software:</u>

i.   File was exported using LightCycler3 program/quantification/standard curve.

ii.   Using Relquant software my own user folder/export/file was opened.

iii.   Wildtype_cDNA (calibrator) positions were defined for all the samples in the 32 slot caroussel. **Number of replicates taken:** Duplicate

iv.   Analysis module: fine for SYBR Green experiments, slope 3.1-3.6.

v.   Coefficient file module, correcting efficiency differences for Hyb probes etc.; slope 4-5.

vi.   Master cDNA_target and master cDNA_reference reactions were always included in each run since they are being used for calculating normalised ratios for comparing different runs.

Chapter 3

Results:

3.1: Detection of *Crybb2* and *Crybb2^{O377}* transcripts in lens and brain:

RT-PCR analysis was carried out to detect the *Crybb2* and *Crybb2^{O377}* transcripts in different tissues of eye (lens and retina) and brain of the wild-type and mutant *O377* animals respectively. Primers (Table: 2.4) for RT-PCR reaction to amplify *Crybb2* transcript was designed from the mRNA sequence available in GenBank. A schematic presentation of the location of primers in exons is given in figure 3.1. The sequence of *Crybb2* mRNA as obtained from NCBI database along with the position of primers is provided in annexure 2.
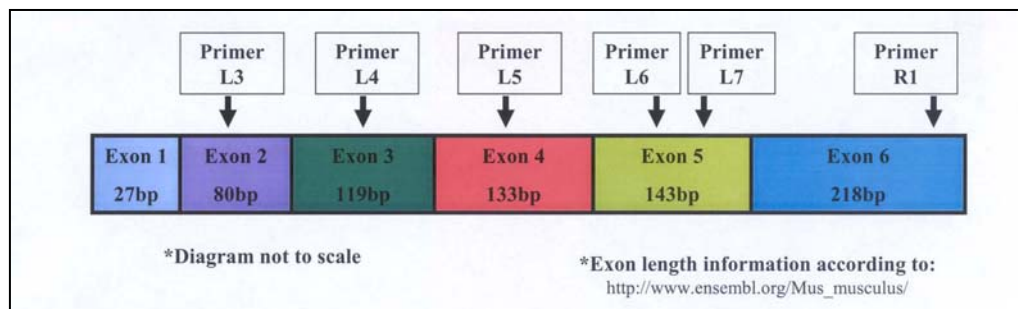
Figure 3.1: A schematic representation of the location of different primers in different exons of *Crybb2* used for RT-PCR experiments to amplify the *Crybb2* transcript..

The lengths of amplified products for primer pairs *Crybb2*_L3/R1, *Crybb2*_L4/R1, *Crybb2*_L5/R1, *Crybb2*_L6/R1 and *Crybb2*_L7/R1 are listed in table 2.4. All these primers were used to amplify the *Crybb2* transcript from lens tissue and only the primer pair *Crybb2*_L3/R1 worked optimally for amplification in the brain tissue. The *Crybb2* transcript in retina could not be detected by RT-PCR analysis. The results of RT-PCR analysis in lens and brain samples are described in detail in the following sections 3.1.1 and 3.1.2 respectively.

3.1.1: RT-PCR analysis; Lens:

Analysis of *Crybb2* transcript following RT-PCR amplification with *Crybb2*_L3-L7/R1 primer pairs revealed, in each case the *Crybb2* transcript in the *O377* lens to be 57 bp longer (Figure 3.2) than the wild-type (C3H) as mentioned in table 2.4. This is the expected result as can be observed from figure 3.1 that all the forward primers (*Crybb2*_L3-L7) were chosen from the region before the 57 bp insertion at the beginning of exon VI and the reverse primer (*Crybb2*_R1) chosen from the region after the 57 bp insertion in the exon VI of the *Crybb2* gene.
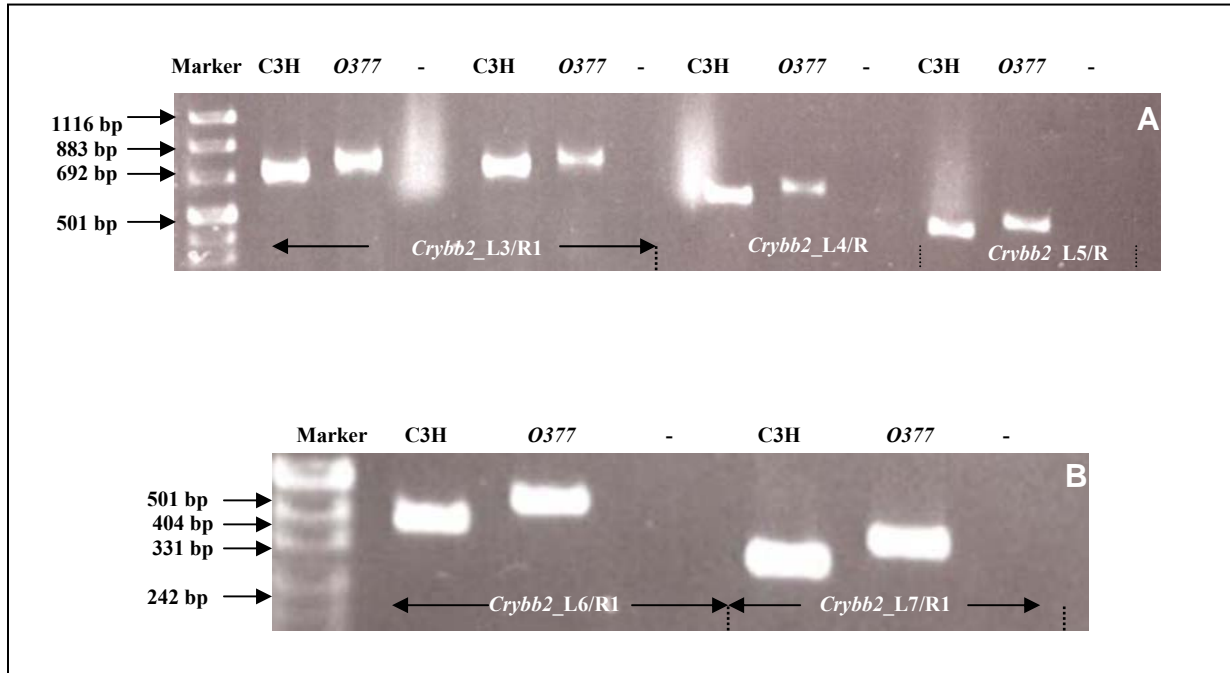
Figures 3.2 A and B shows the 57 bp insertion in the *Crybb2* gene in *O377* mutant lens following RT-PCR experiments with primers pairs listed in table 2.4.

3.1.2: RT-PCR analysis; Brain:

Both *Crybb2* and *Crybb2^O377^* transcripts were also detected in the wild-type and mutant brain respectively. However, it is important to mention that the expression level of the *Crybb2* transcript in the brain is very low compared to that in the lens in both wild-type and mutant animals. This can be inferred from the fact that higher amounts of cDNA (3μl) was always necessary to perform the PCR reactions in case of the brain samples as mentioned in section (2.4.6C), to achieve reproducible bands of the *Crybb2* transcript. The quality of cDNA used was good for both lens and brain samples as verified by PCR for standard *β-actin* amplification, so the question of poor cDNA quality can be ruled out. Moreover, DMSO (Dimethyl sulfoxide) was used in the PCR mix specifically for the brain cDNA samples to amplify *Crybb2* in order to get reproducible bands; as PCR without DMSO yielded feeble bands. In case of the lens sample PCR reactions worked excellent without DMSO because of the high expression of *Crybb2* transcript in lens but it also worked with DMSO (Figure: 3.3). To maintain identical PCR conditions, PCR mix was always prepared with DMSO in case of both brain and lens samples while detecting *Crybb2* transcript in the brain (lens being the positive control). DMSO is an often used additive to optimize PCR amplifications, as it is known to increase the yield and/ specificity of a reaction (Frackman *et al*., 1998). As DMSO

acts as an adjuvant and higher amounts of cDNA being used for brain samples for PCR amplification (i.e. amplified product can form a complex with DMSO resulting in higher molecular weight or changed charged ration), coupled with factors like moderately fresh electrophoresis buffer etc., sometimes the amplified band was observed a little higher than the expected level in the gel. In such situation, it was necessary to isolate and clean the PCR product and to run the gel again or to clone the PCR product in the plasmid pCR®.2.1-TOPO® (Invitrogen, Karlsruhe) following procedures described in section 2.4.9, followed by restriction digestion to separate the cloned PCR product from the plasmid. The restriction digested product always showed the band of the desired size. These complicated situations can be avoided by using fresh DMSO, cleaning the product immediately following PCR amplification and by using absolutely fresh electrophoresis buffer.
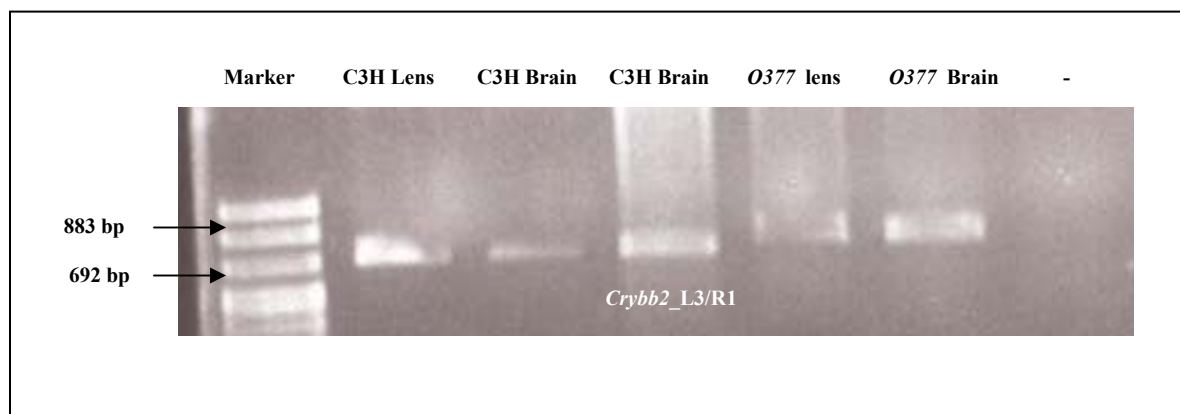
Figure 3.3: Both the wild-type (*Crybb2*) and mutant transcripts (*Crybb2^{O377}*) of the βB2-crystallin gene have been detected in the wild-type and *O377* mutant brain respectively following RT-PCR studies. The identities of the products have been confirmed by sequencing (Sequiserve).

The identities of the PCR products amplified by primer pair L3/R1 (as it covers almost the entire sequence) were confirmed by sequencing (Sequiserve, Vaterstetten, Germany). Sequencing revealed an inclusion of the 57 bp (indicated in red in table 3.4) at the beginning of exon VI of *Crybb2* in the *O377* mutant lens and brain. This inclusion of 57 bp has lead to the inclusion of 19 amino acids in the protein (Figure 3.7). The results of sequencing of the lens sample reconfirmed the findings at the labortarory of Dr. J. Favor at the Institute of Human Genetics, GSF. Detection and sequencing of the *Crybb2* and *Crybb2^{O377}* in the wild-type (C3H) and mutant brains respectively were novel findings. The sequences of *Crybb2* in brain were exactly the same to that in the lens i.e. no alternative splice product was observed in the brain as mentioned in case of *Aey2* (Graw *et al.*, 2001).

(A)*

```
  1 ctcgacgcca gagagtccac catggcctca gaccaccaga cacaggcggg caagccccag
 61 cccccttaacc ccaagatcat catcttcgaa caggagaact tccagggcca ttcccacgag
121 ctcagcgggc cctgccccaa cctgaaggag actggtatgg agaaggcggg ctccgtcctg
181 gtgcaggctg gaccctgggt gggctacgag caggctaatt gcaagggcga gcagtttgtg
241 tttgaaaagg gcgagtaccc acgttgggac tcctggacca gcagccggag gacagactcc
301 ctcagctctc tgaggcccat caaagtggac agccaagagc acaagatcat cttatatgag
361 aaccccaact ttactggcaa gaagatggag attgtagacg acgatgtgcc cagcttccat
421 gcccatggat accaggaaaa ggtgtcttcc gtgcgtgtgc agagcggcac gacactccag
481 ctggcttctt ttgacctcac catgtcttcc cgtacctctg cctgctggtg ggtggggtac
541 cagtaccctg ctaccgtgg gctgcagtac ctgctggaga aggggggatta caaggacaac
601 agcgacttcg ggcccctca cccccaggtg cagtctgtgc gtcgcatccg tgacatgcag
661 tggcaccagc gaggtgcctt ccacccctcc agctagagcc ctgaccctcc ccttccccag
721 ggtccaggcc cgccacctcg gagcctcctg acacccagag tgaagaataa agtgtggctc
781 gtgcc
```

*Corresponding amino acid sequence in figure 3.4B

O377: L D A R E S T **Met** A S D H Q T Q A G K P Q P L N P K I I I F E Q E N F Q G H S H
C3H: L D A R E S T **Met** A S D H Q T Q A G K P Q P L N P K I I I F E Q E N F Q G H S H

O377: E L S G P C P N L K E T G **Met** E K A G S V L V Q A G P W V G Y E Q A N C KGE
C3H: E L S G P C P N L K E T G **Met** E K A G S V L V Q A G P W V G Y E Q A N C KGE

O377: Q F V F E K G E Y P R W D S W T S S R R T D S L S S L R P I K V D S Q E H K I IL
C3H: Q F V F E K G E Y P R W D S W T S S R R T D S L S S L R P I K V D S Q E H K I IL

O377: Y E N P N F T G K K **Met** E I V D D D V P S F H A H G Y Q E K V S S V R V Q S G
C3H: Y E N P N F T G K K **Met** E I V D D D V P S F H A H G Y Q E K V S S V R V Q S G

O377: T **T L Q L A S F D L T Met S S R T S A C W** W V G Y Q Y P G Y R G L Q Y L LE
C3H: T - W V G Y Q Y P G Y R G L Q Y L LE

O377: KG D Y K D N S D F G A P H P Q V Q S V R R I R D **Met** Q W H Q R G A F HP SS
C3H: KG D Y K D N S D F G A P H P Q V Q S V R R I R D **Met** Q W H Q R G A F H PSS

O377: **Stop** S P D P P L P Q G P G P P P R S L L T P R V K N K V W L V
C3H: **Stop** S P D P P L P Q G P G P P P R S L L T P R V K N K V W L V

Figure 3.4: (A) The *Crybb2^O377* sequence shows the inclusion of 57 bp (indicated in red colour), as revealed from sequencing (Sequiserve) of the *Crybb2*_L3/R1 primer pair amplified products in both the lens and brain. **(B)** Comparison of the amino acid sequences of βB2-crystallin*^O377* and βB2-crystallin^C3H as obtained from ExPASy Proteomics tools (http://www.expasy.org/tools/dna.html) following translation of the *Crybb2*^O377 and *Crybb2* nucleotide sequences respectively. The 19 amino acid insertion in the βB2-crystallin*^O377* is indicated by red colour.

In order to get an idea about the region of expression of *Crybb2* transcript in the wild-type and mutant brain, RT-PCR analysis was performed with mRNA isolated from 5 regions of the brain (Figure: 3.5A). *Crybb2* transcript has been found to be expressed in all these five brain regions in both wild-type (Figure: 3.5B) and mutant brain (Figure: 3.5C).
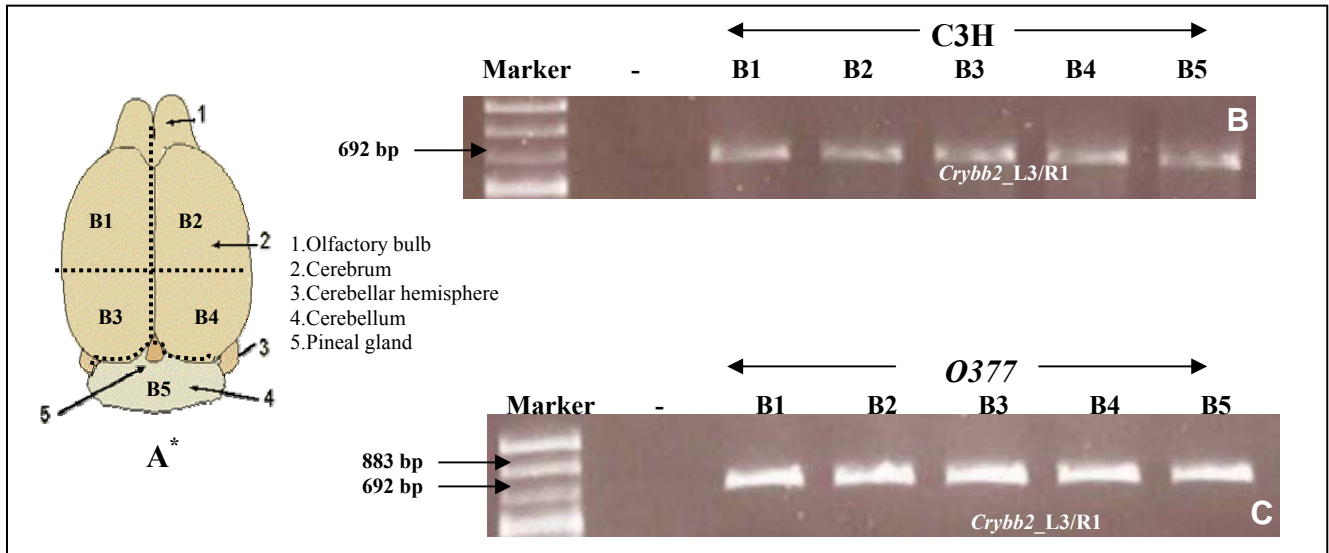
Figure 3.5: *Crybb2* transcripts were detectable in all the five regions (B1-B5, Figure 3.5A) of the brain from which RNA was extracted in both C3H and *O377* mice (Figures 3.5 B and 3.5C).

[*]http://www.niaid.nih.gov/dir/services/animalcare/MouseNecropsy/brain.html

Expression of *Crybb2* transcript in the brain was also studied in an age gradient (Figure 3.6) and it was observed that the expression of *Crybb2* transcript in brain reaches it's optimum level during the age 3-4 weeks and diminishes thereafter and was not detectable at the age of 8 months both in *C3H* and *O377* mice. However, it must be mentioned here that at the protein level βB2-crystallin is detectable only between the ages 3-4 weeks (Figure 3.7). Hence for all further studies, brains from animals of age between 3-4 weeks were used.
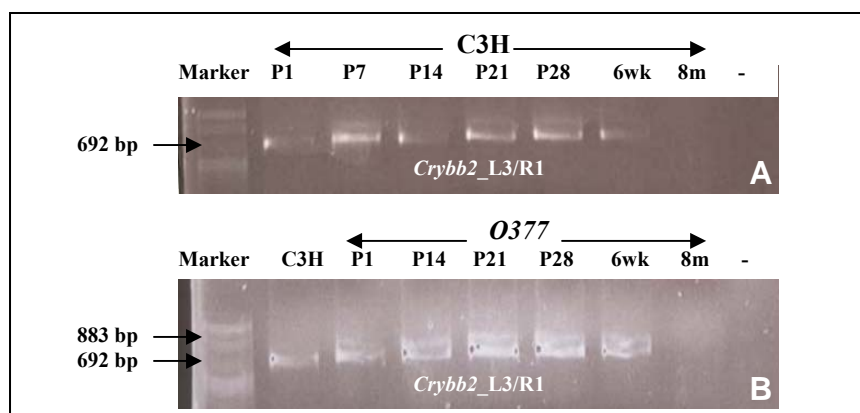
Figure 3.6: The expression of *Crybb2* transcript in brain reaches it's optimum level during the age 3-4 weeks (wk) and diminishes thereafter and was not detectable at the age of 8 months (m) both in *C3H* (Figure A) and *O377* strains (Figure B).

3.2: Protein analysis:

Three different approaches were taken to analyse the effect of mutation at the protein level. First, using the online translation tool, the amino acid sequence of the βB2-crystallin^{O377} was deduced and compared with the wild-type; second, the verification of the predicted change in molecular weight of the mutated protein [i.e. 19 amino acids insertion should result in approximately **1.9 kDa** (19×100Da) higher molecular weight] and simultaneously detection of the wild-type and mutated proteins in wild type and mutant brains respectively with the respective lens protein as the control through Western blot analysis; and the third is to analyse the secondary structure of the mutated protein through predictive modelling using freely available softwares (Section 2.3) in the world wide web (www).

3.2.1: Deduced protein sequence:

The predicted mutated protein (http://www.expasy.org/tools/dna.html) contains an insertion of 19 amino acids (indicated by red colour) near the carboxy terminus of the βB2-crystallin^{O377} protein due to the 57 bp insertion in the mRNA as shown in the figure 3.4B.

3.2.2: Detection of the βB2-crystallin protein in the C3H and *O377* lens and brain (Western blot analysis).

The Western blot analysis revealed the mutant βB2-crystallin protein (24.9 kDa) to be 1.9 kDa heavier than the wild-type protein (23 kDa) in the lens (Figure 3.7A), as predicted. This 1.9 kDa heavier weight of the βB2-crystallin^{O377} protein is due to the inclusion of 19 amino acids at the C-terminal end of the protein. Degradation products of the βB2-crystallin protein in lens are also visible in the Western blot analysis (Figures 3.7A, B and C) [Srivastava *et al.*, 2002]. The bands of βB2-crystallin protein in the SDS-PAGEs were detected following comparison with the marker protein. The same Rf values (0.59 for βB2-crystallin^{C3H} and 0.55 for βB2-crystallin^{O377} in lens; Figure 3.7A) of the βB2-crystallin and βB2-crystallin^{O377} proteins in each of SDS PAGE and Western blot along with the use of highly specific polyclonal primary antibody against βB2-crystallin confirmed their identity. Both the wild-type and mutant form of βB2-crystallin protein (Figure 3.7C) has also been detected in the wild-type and mutant brain respectively.

In an attempt to quantify the expression level of βB2-crystallin protein in the brain (Figure 3.7B), a gradient of protein amounts from wild-type brain were used along with 5μg protein

from the wild-type lens in a Western blot analysis. A distinct visible and reproducible protein band of βB2-crystallin in brain was achieved only for the sample containing 80μg of protein, samples containing 16μg and 40μg protein showed faint bands in ascending order of intensities and no band was visible in the sample containing 8μg of the brain protein; whereas a distinct visible band with degradation products was observed in the lens protein sample containing only 5μg of protein. Hence, all Western blot experiments with brain protein were carried out with 70-80μg of fresh samples (not more than 2 months old stored at -80°C) to detect βB2-crystallin. It was important to use fresh samples as the level of expression of βB2-crystallin in brain is very low; in samples older than 2 months even if stored at -80°C, βB2-crystallin was sometimes undetectable in Western blot analysis. The same Rf values (0.67 for βB2-crystallin[C3H] in Figure 3.7B) of the bands of βB2-crystallin protein in the SDS-PAGE gel and the Western blot for each of C3H lens and C3H brain again confirms the identity of the bands apart from the use of highly specific polyclonal primary antibody against βB2-crystallin.

In case of Western blotting of the brain protein samples, apart from using higher amount of protein, higher amounts of substrate (H_2O_2) was also used in the staining solution, because one can expect the amount of peroxidase conjugated secondary antibodies bound to the low expressed βB2-crystallin protein in the brain samples to be also low. By doing this, the maximum possible DAB (Diaminobenzidine) could be precipitated from secondary antibody bound to the βB2-crystallin of brain samples in order to develop clearly visible and reproducible bands Expression of βB2-crystallin protein is best detectable between the age 3-4 weeks (similar to the *Crybb2* transcript) in brains of both the mutant and wild-type animals. The same Rf values (0.69 for βB2-crystallin[C3H] and 0.65 for βB2-crystallin[O377] in Figure 3.7C) of the bands of βB2-crystallin protein in the SDS-PAGE gel and the Western blot for each of C3H lens, C3H brain, *O377* lens and *O377* brain again confirms the identity of the bands apart from the use of highly specific polyclonal primary antibody against βB2-crystallin. It is worthy to mention here that from different Western blot analysis, the level of expression of βB2-crystallin in the brains of both wild-type and mutants appeared to vary even among animals of the same litter. This observation was made from the intensities of the βB2-crystallin band developed during Western blot analysis using approximately the same amounts of protein in all cases. The level of expression of βB2-crystallin was found to be lower in the mutants at the age of 3 weeks (all Western blots shown in figure 3.7).

A) Detection of βB2-crystallin in wild-type and mutant lens
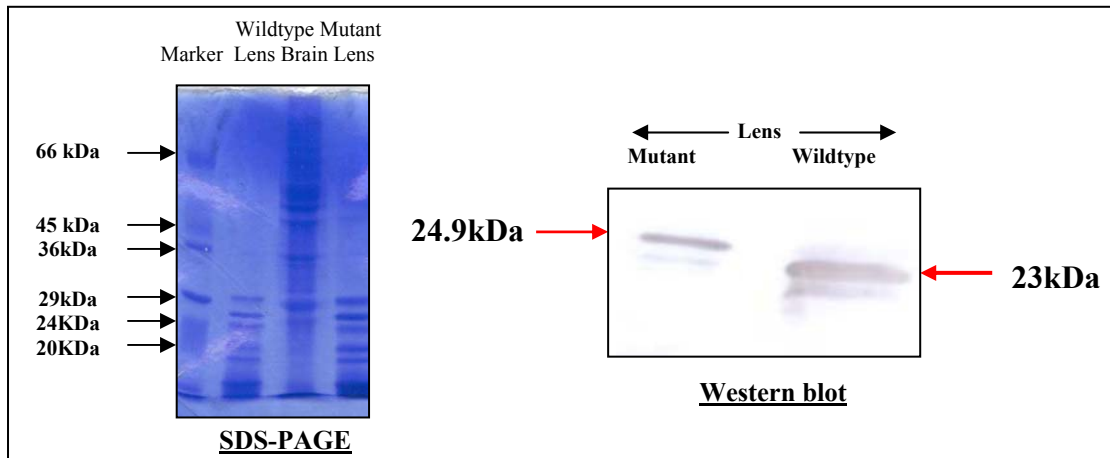
B) Estimation of the expression levels of βB2-crystallin in brain compared to that wild-type lens
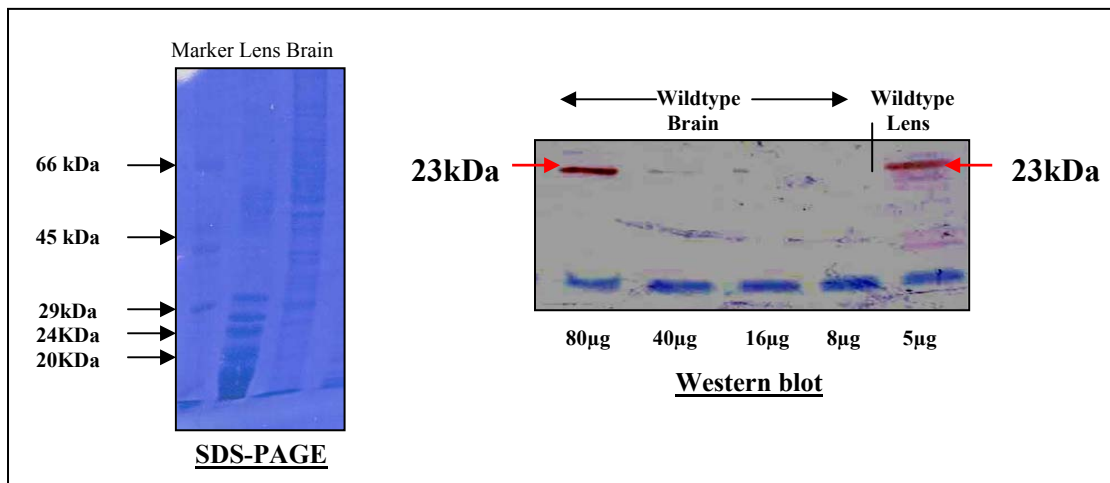
C) Detection of βB2-crystallin in C3H and *0377* Brain:
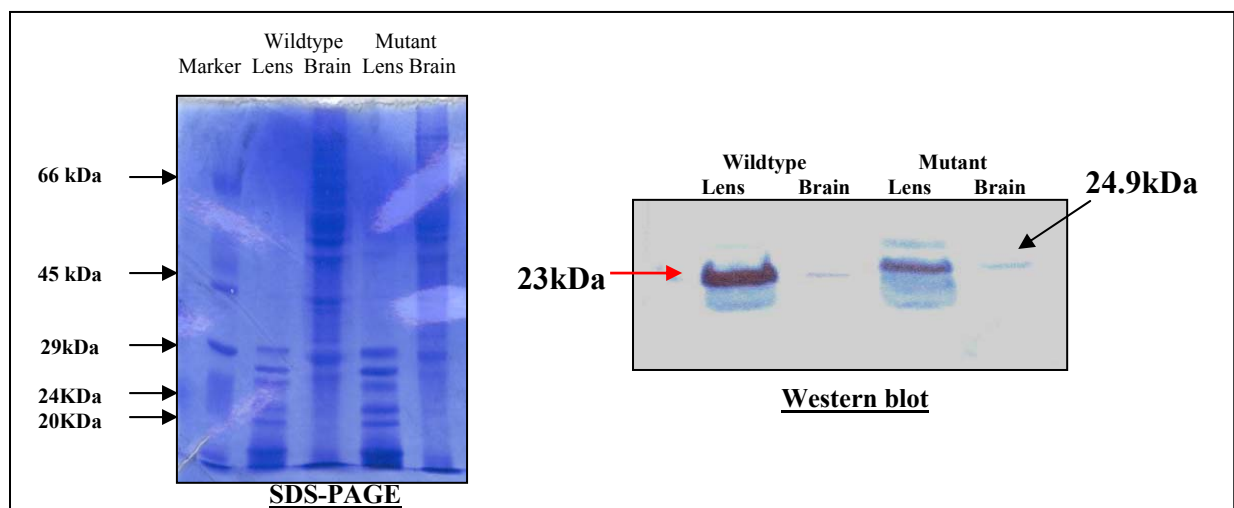
Figure 3.7: Western blot analysis of the βB2-crystallin protein in both the wild-type and mutant lens and brain. **(A)** The βB2-crystallin^{O377} protein in lens is 1.9 kDa heavier than that of βB2-crystallin^{C3H} protein. **(B)** 80µg of brain protein is required for Western blot analysis to yield a reproducible band of βB2-crystallin whereas 5µg of lens protein yields a reproducible band of βB2-crystallin along with its degradation products. **(C)** The SDS-PAGE and its corresponding Western Blot to detect βB2-crystallin^{O377} in the mutant brain. In all cases (A, B and C) the SDS-PAGE shows the clear separation of proteins during electrophoresis which also indicates the good quality of the protein used.

3.2.3: Prediction of the βB2-crystallin^{O377} protein structure:

The predicted mutated protein is misfolded near the carboxy terminus due the inclusion of 19 amino acids in motif IV (According to Motif scanning option of PROSITE, http://myhits.isb-sib.ch/cgi-bin/motif_scan) of the βB2-crystallin protein. The misfolding is indicated by red arrows in figure 3.8. This misfolded βB2-crystallin protein in the *O377* mutant lens is deposited around the entire peripheral region of the lens cortex (shown in figure 3.13), thereby causing severe form of lens opacity (cataract) and disturbing the entire lens structure as early as by the third week of age.
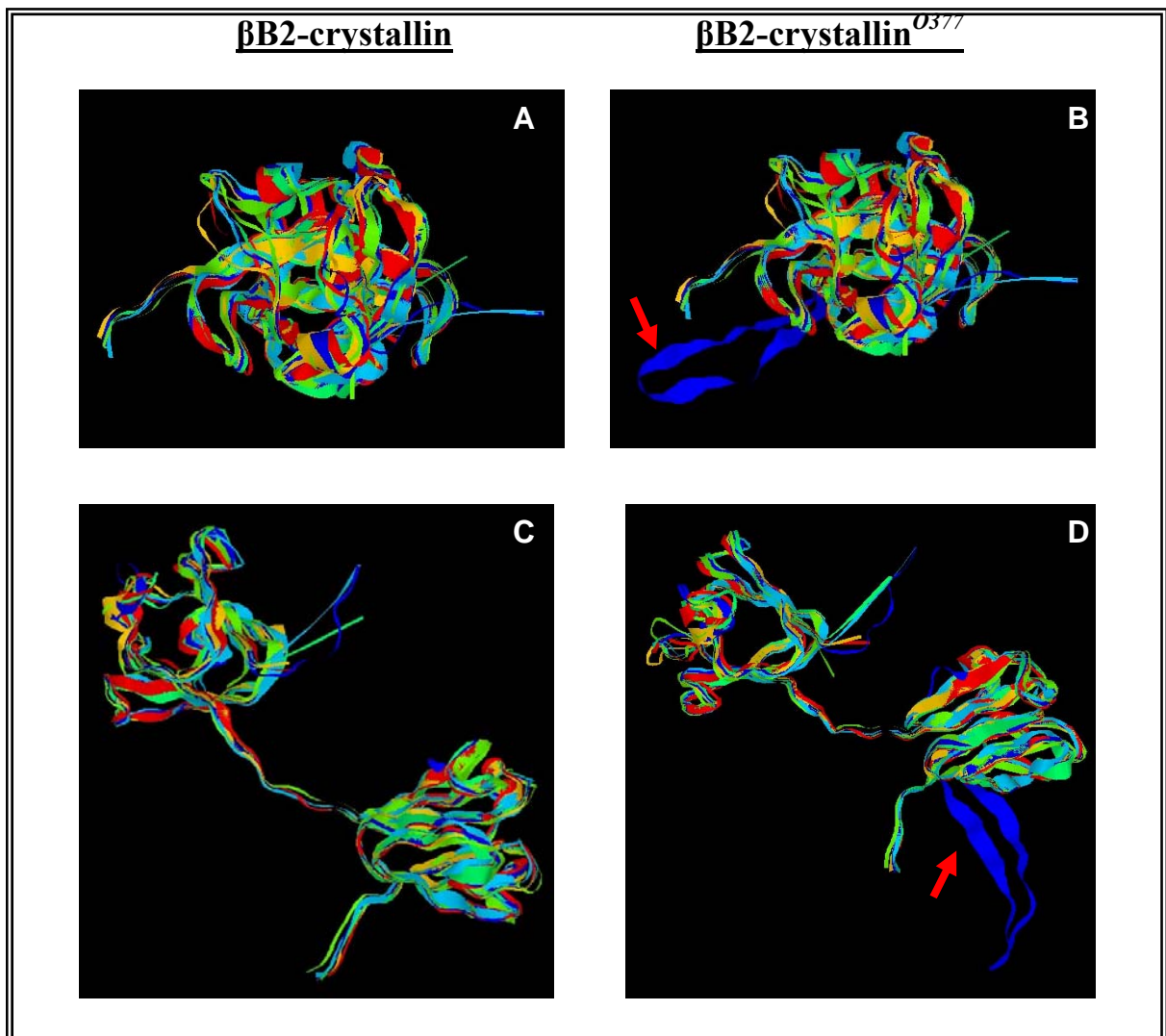
Figure 3.8 showing the misfolding of the βB2-crystallin^{O377} protein near the carboxy terminus (indicated by red arrows). This model has been developed using the MDL Chime software (http//www.mdl.com). The PDB file used to model the proteins was generretaed from The SwissModel First Approach Mode [http://swissmodel.expasy.org//SWISS-MODEL.html]. Figures 3.8A and B are under identical rotational angles whereas figures 3.8 C and D are not under identical rotational angles (option not available in the software) but the misfolding in the βB2-crystallin^{O377} protein in clearly visible in each case.

The figure 3.9 explains exactly how the βB2-crystallin[O377] protein is misfolded due changes in the helix, strands and coils near the C-terminus in the IVth motif following detailed structural analysis of the predicted βB2-crystallin[O377] protein:
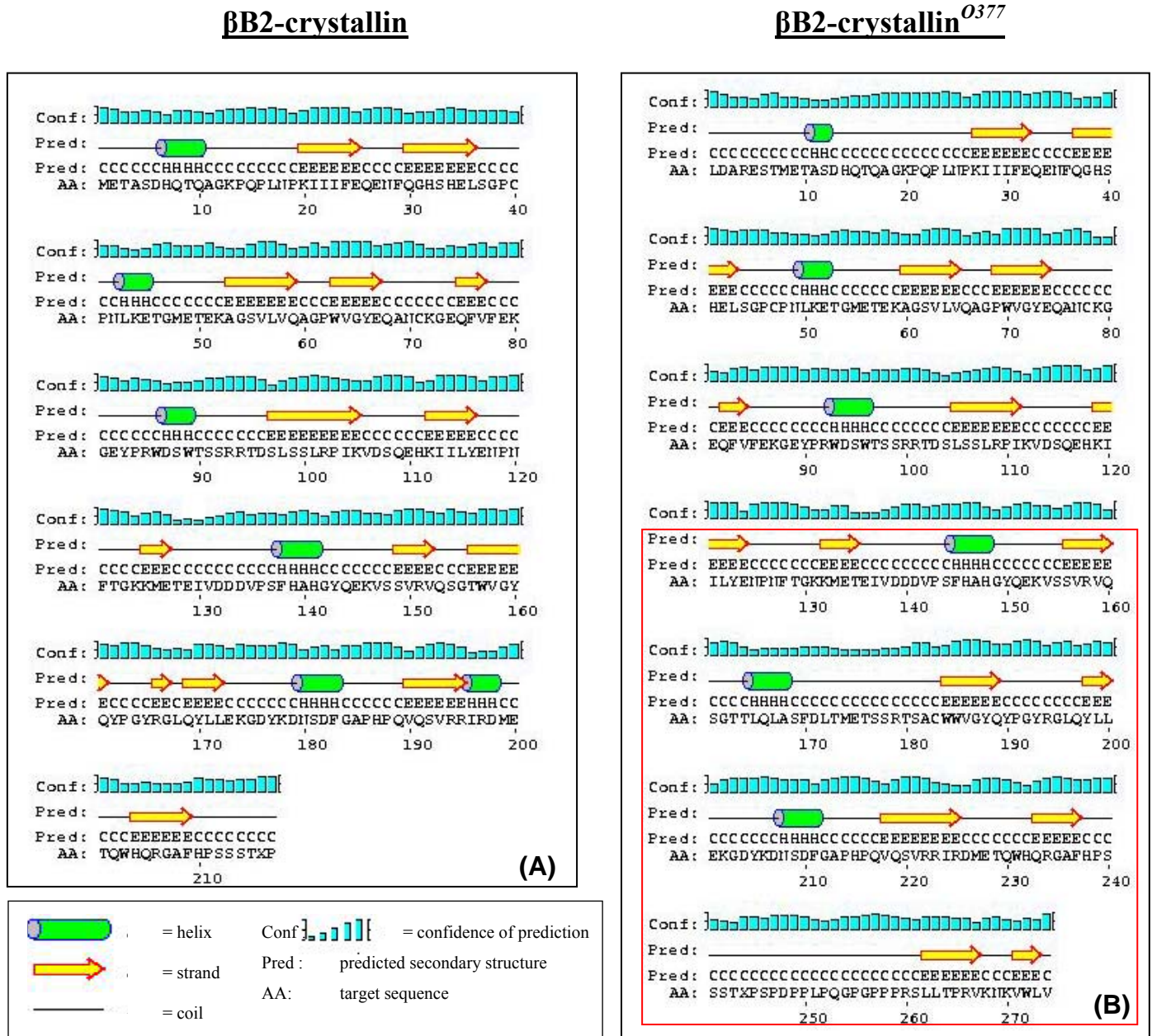
βB2-crystallin   **βB2-crystallin[O377]**

Figure 3.9 explains exactly how the βB2-crystallin[O377] protein is misfolded due changes in the helix, strands and coils near the carboxy terminus (indicated by the red box in 3.9B) in motif IV. Figure 3.9A shows the detailed structure of wild-type βB2-crystallin protein. This model was generated from the PSIPRED Protein Structure Prediction Server [http://bioinf.cs.ucl.ac.uk/psipred/psiform.html].

3.3: <u>Histological analysis of the eye:</u>

Transverse section of eyes from 2 week old animals followed by Methylene blue and basic fuchsin staining shows the homozygous lens (Figure 3.10C, C') to be highly vacuolated and with patchy appearances on the two lateral sides of cortex in the region of lens fiber cells and posterior region of the lens; and the heterozygote lens (Figure 3.10B, B') has started to show a crumbling appearance and initial signs of cataractous phenotype. Figures 3.10A and 3.10A' are of wild-type animals as control sets. *However it must be mentioned here that other studies (Neuhäuser-Klaus, A.; unpublished) with O377 mutant eye revealed that the onset of cataractous phenotype to be slightly variable with age (as can be expected in a biological system).* It is only at the age of 3 weeks that all the mutant animals (heterozygous and homozygous) develop well defined cataractous phenotype. As the effect is also severe even in the heterozygous lens, it is difficult to generalize the histological features of the homozygous and heterozygous mutant eyes on a time curve basis.
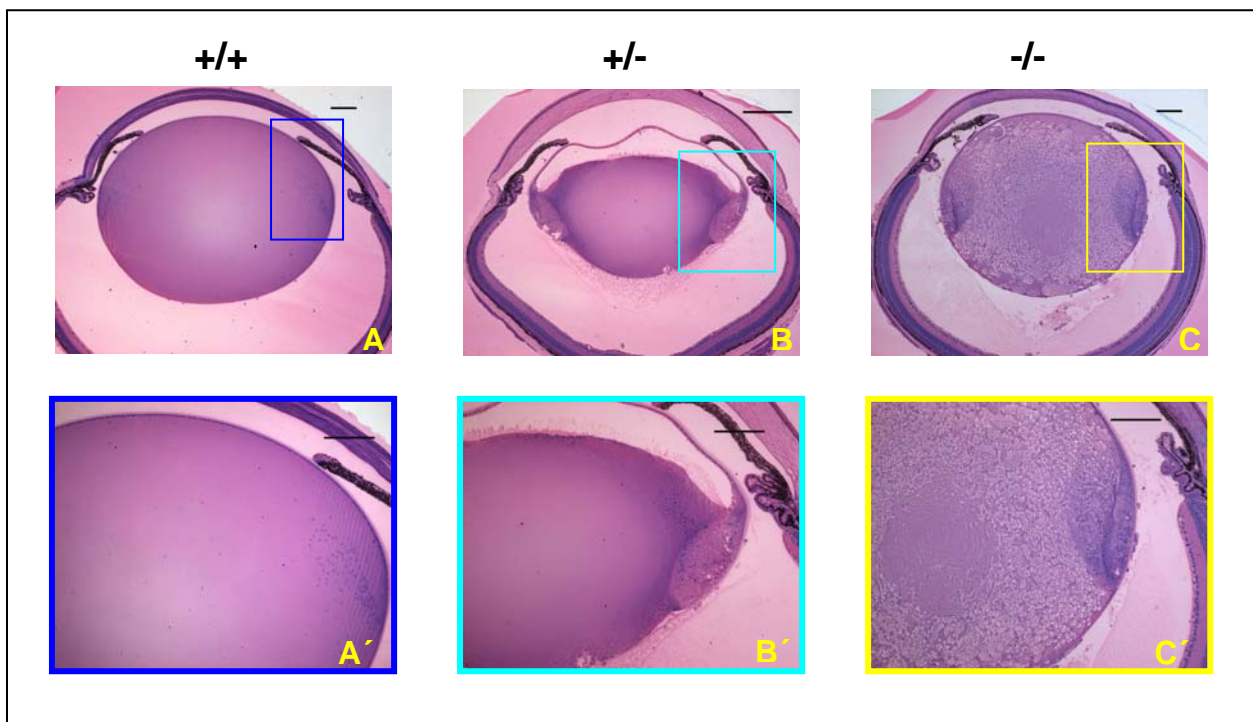
Figure 3.10: Histological analysis in transverse sections of the mutant (*O377*) eyes at the age of 2 weeks. Figures A and A´ are transverse sections of C3H (Age: P14) eyes as control sets. The homozygous lens (C, C´) is highly vacuolated and have patchy appearances on the two lateral sides of the lens cortex (in the region of lens fiber cells) and posterior region of the lens; and the heterozygote lens (B, B´) has started to show a crumbling appearance and looks disorganized at this age. Follow the colour codes to view the respective enlarged images. Scale bars= 50μm in all and 100μm in B.

3.4: Expression domains of βB2-crystallin in eye and brain:

Expression domains of βB2-crystallin at the mRNA and protein level in lens, retina and brain have been detected by *in-situ* hybridization and immunohistochemical studies. βB2-crystallin has been found to be expressed in the lens cortex, internal limiting membrane of retina and in some specific neuronal cell types of the olfactory bulb, cortex, hippocampus and the cerebellum. The detection of the expression domains of βB2-crystallin in the specific regions and neuronal cell types in the brain is absolutely a novel information and will definitely enhance research on the non-structural role of βB2-crystallin and crystallins in general in non-lenticular and non-ocular tissues. To focus more light on the role of βB2-crystallin in brain, immunohistological studies were followed by histological analysis to detect any change in the tissue structure, specifically in the regions where βB2-crystallin has been found to be expressed.

3.4.1: Tissue type: Lens:

In-situ **hybridization** experiments at the mRNA level (Digoxigenin labelling method) in transverse sections of eyes of 1 day old animals revealed the expression of *Crybb2* transcript to be localized in the two lateral regions of lens cortex in the region of fiber cells in wild-type animals (Figure 3.11 A, B); in the homozygous mutant animals (Figure 3.11 D-G) *Crybb2* is present in the entire peripheral region of the lens cortex (i.e. also in the anterior and posterior regions apart from the normal lateral region of expression) and the expression level of *Crybb2* is up-regulated to a good extent at this age (P1). Figures 3.11 C and H are the sense controls of the experiment for C3H and *O377* respectively. The up-regulation of *Crybb2* in lens [approximately 3 fold; obtained from scanning of the picture] at this age is an interesting observation and probably can reveal more about the mechanism of *Crybb2* regulation especially in the situation when early signals of developing lens opacity has been realized in the lens tissue.

Wildtype (C3H)

A

B

C

Sense

Mutant _O377_

D

E

H

F

G
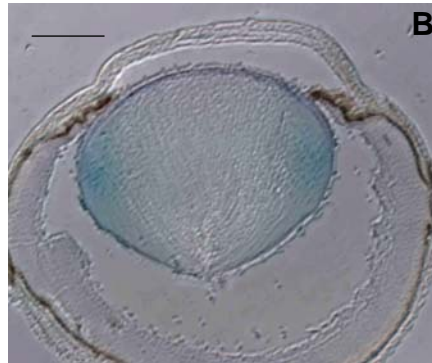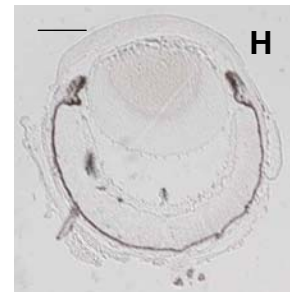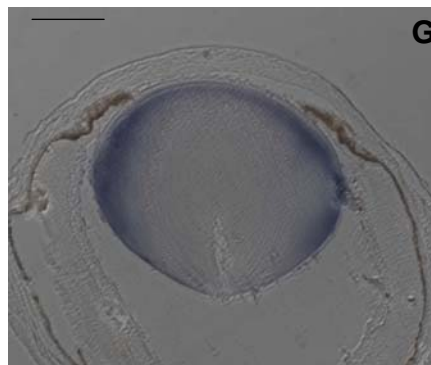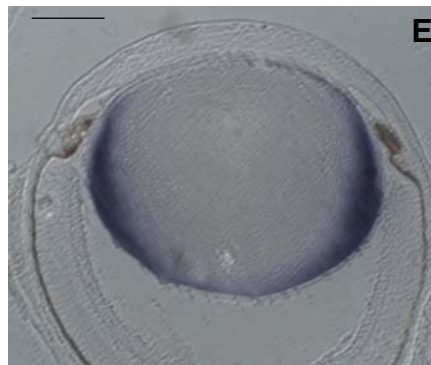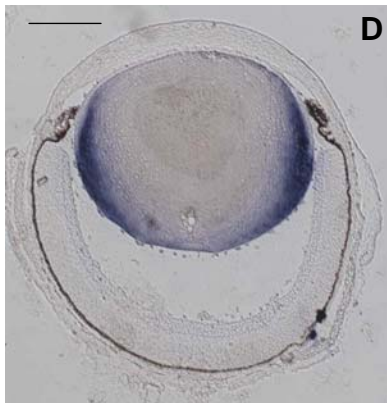
Sense

Figure 3.11: _In-situ_ hybridization studies at the mRNA level by digoxigenin labelling method in transverse sections of eyes from 1 day old animals revealed the expression of _Crybb2_ transcript to be localized in the two lateral regions of lens cortex in wild-type animals (Figure A, B) whereas in the homozygous mutant animals (Figures D-G) it is up-regulated and also present in the anterior and posterior regions of the lens cortex apart from its natural occurrence as in the wild-type. Figures C and H are the sense controls for wild-type and mutant respectively. Scale bars = 0.2mm (A, D, F, C, H) and 100µm (B, E, H).

Immunohistochemical studies performed to detect the expression domains of βB2-crystallin at the protein level in the lens following the avidin-biotin-peroxidase method (Vector laboratories) [Vogt Weisenhorn *et al.*, 1998] on transverse sections of P1 eyes revealed that βB2-crystallin protein is expressed exactly in the same way as its mRNA (Figure 3.11) at this age both in case of the wild-type and the homozygous mutant. In the wild-type lens (3.12A), the expression of the protein is in the two lateral regions of the lens cortex in the region of lens fiber cells. The expression of βB2-crystallin protein is higher in the homozygous mutant (3.12 B and 3.12C) and is also present in the posterior and anterior regions of the lens cortex apart from its normal occurrence in the two lateral cortical regions. It must also be mentioned here that βB2-crystallin^{O377} probably form aggregates as in the case of mutated γB-crystallins (Sandilands *et al.*, 2002).

Figure 3.12: Immunohistochemical studies by ABC staining method (Vector laboratories) in transverse sections of eyes from 1 day old animals revealed the expression of βB2-crystallin protein to be localized in the two lateral regions of lens cortex in wild-type animals (Figure A) whereas in the homozygous mutant animals (Figures B and C) it is up-regulated and also present in the anterior and posterior regions of the lens cortex apart from its natural occurrence as in the wild-type. Scale bars = 0.2mm

The immediate cause behind development of opacity in the mutant lens in this case is the disorganization of the fiber cell anatomy as shown in Figures 3.10 and 1.10). In figures 3.13A-C, deposition of βB2-crystallin protein in uniform manner can be observed in the wild-type lens. Deposition of βB2-crystallin ^{O377} protein in higher amounts in one of the lateral sides of lens cortex (Figure 3.13D and E) and in a highly vacuolated region at the posterior (Figure 3.13 D and F) lens cortex can be observed in the homozygous mutant eye. Both these regions have been shown to develop patchy appearances in histological studies (Figure 3.10, 1.10) in the homozygous mutants at later stages.
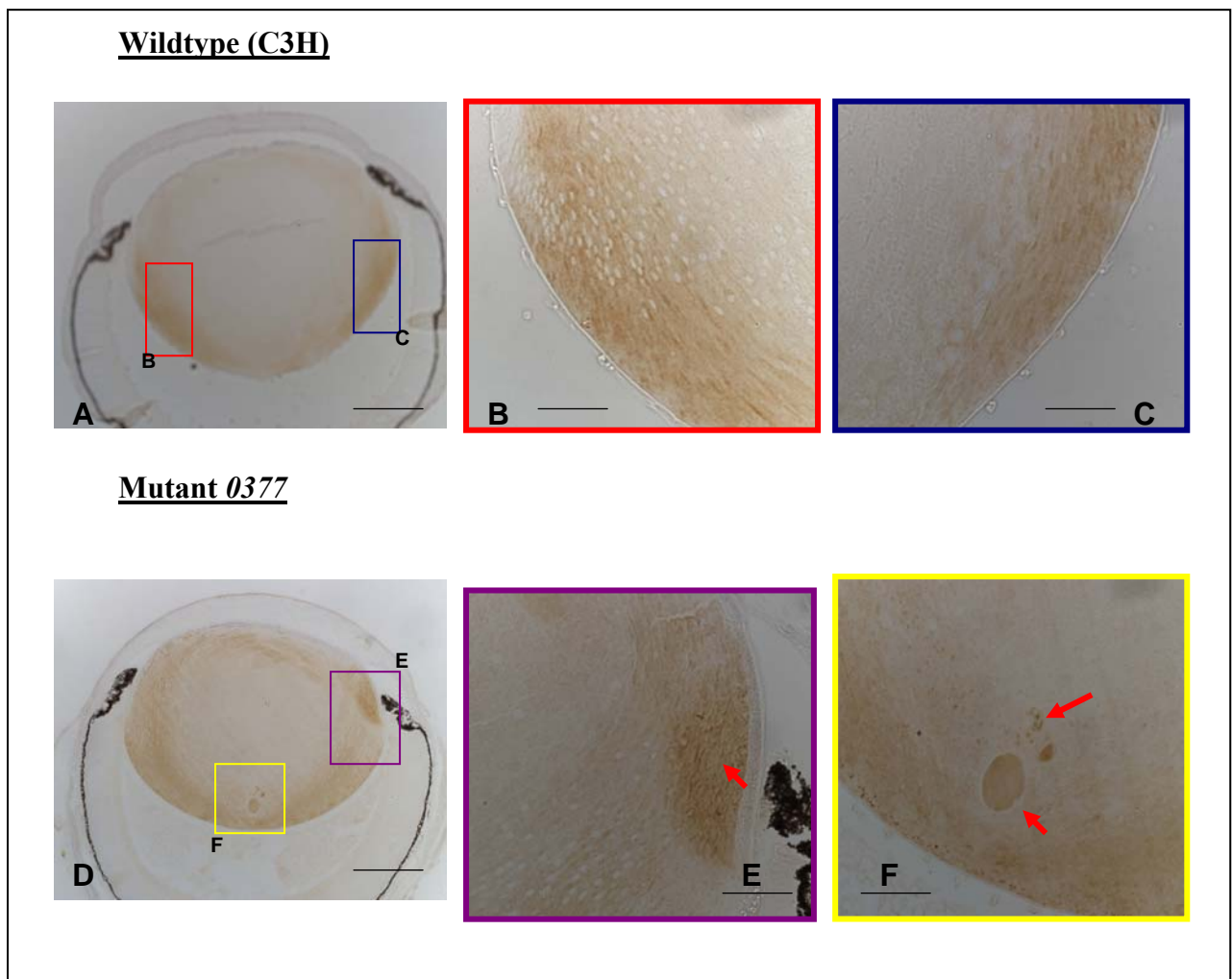
Figure 3.13: Immunohistochemical studies by ABC staining method (Vector laboratories) in transverse sections of eyes from 1 day old animals revealed the deposition of βB2-crystallin protein (Figure 3.13 D-F) in the lateral and posterior region of the mutant lens cortex. Figures 3.13 A-C shows the uniform deposition of βB2-crystallin protein in the wild-type lens. Follow the colour codes to view the respective enlarged image. Scale bars= 100μm (A, D) and 50μm (B, C, E, F).

3.4.2: Tissue type: Retina

Transcripts of *Crybb2* has also been detected in the internal limiting membrane of the retina (Figure 3.14) by *in-situ* hybridisation experiments but interestingly its expression is found to be restricted to the region near the iris both in C3H (Figure 3.14A) and *C57BL6/J* (Figure 3.14B) mice; however in the retina of *O377* (Figure 3.14C) mice, *Crybb2* expression could not be detected. *Crybb2* in retina could not be detected by RT-PCR experiments among *C3H, C57BL6/J* or *O377* mice. The point to be noted is that C3H mouse develops retinal degeneration (Pittler *et al*; 1991) (caused due to a mutation in the rod photoreceptor cGMP phosphodiesterase beta subunit gene) by the age of 3 weeks. Thus *C57BL6/J* mice were used as control sets for retinal studies. However the *in-situ* hybridisation experiments were also carried out with eyes of 1 day old C3H animals when no retinal degenerations have been reported.
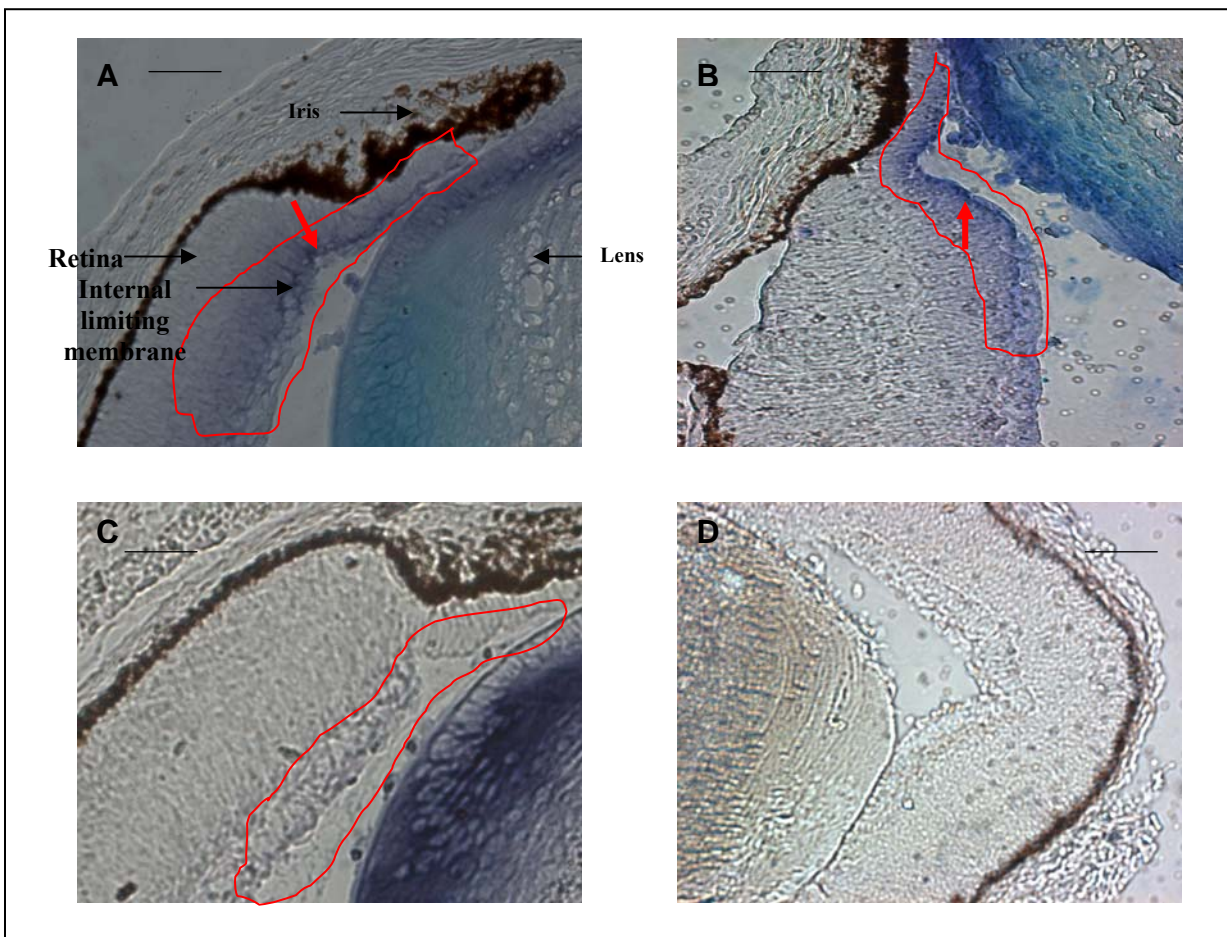
Figure 3.14: *In-situ* hybridization experiments in transverse sections of eyes of 1 day old *C3H* (3.14A) and *C57 Bl6/J* (3.14B) mice shows the presence of *Crybb2* transcript in the inner limiting membrane of the retina but restricted to the region near iris only other than its normal occurrence in the lens as already explained for C3H mice. Expression of *Crybb2* was not detected in the retina of *O377* mice (Figure 3.14C). Figure 3.14D shows the sense control with no staining. Expressions indicated by red arrows and red border. Scale bars= 20μm.

Immunohistochemical studies by ABC staining method (Vectastain; Vector laboratories) [Vogt Weisenhorn et al.,, 1998] on sagittal sections of brain from 3 weeks old animals revealed the expression domains of βB2-crystallin protein to be in some specific neuronal cell types in the olfactory bulb, cerebellum, hippocampus and cortex in both the C3H and mutant animals. Detailed microscopic analysis revealed the expression of βB2-crystallin to be in the **glomerular and mitral cell layer** of the olfactory bulb; **Purkinje cells** and **stellate cells** (Molecular layer) of the cerebellum; **pyramidal cells** of the cortex and in the **CAI, CAII, CAIII region** [CA= *Cornu ammonis*] and **dentate gyrus** of the hippocampus in both the wild-type and homozygous mutant. Histological analysis of the brain was also performed to detect any histological changes that may have resulted due to the mutation. In this section the expression domains of βB2-crystallin are discussed in detail along with the histological analysis of the corresponding brain regions in sagittal plane of 3 weeks old wild-type and mutant animals.

3.4.3: <u>Tissue type: Olfactory bulb (Brain):</u>

Expressions of βB2-crystallin have been detected in the glomerular and mitral cells (Figures 3.15B, C) of the olfactory bulb in both the wild-type and mutant animals. The glomerular cells receives the impulses of olfaction from the ciliated olfacatory epithelium through the cribriform plate, which is then transmitted to granular cells through the mitral cells and ultimately reaches the olfactory cortex of brain through the lateral olfactory tract.
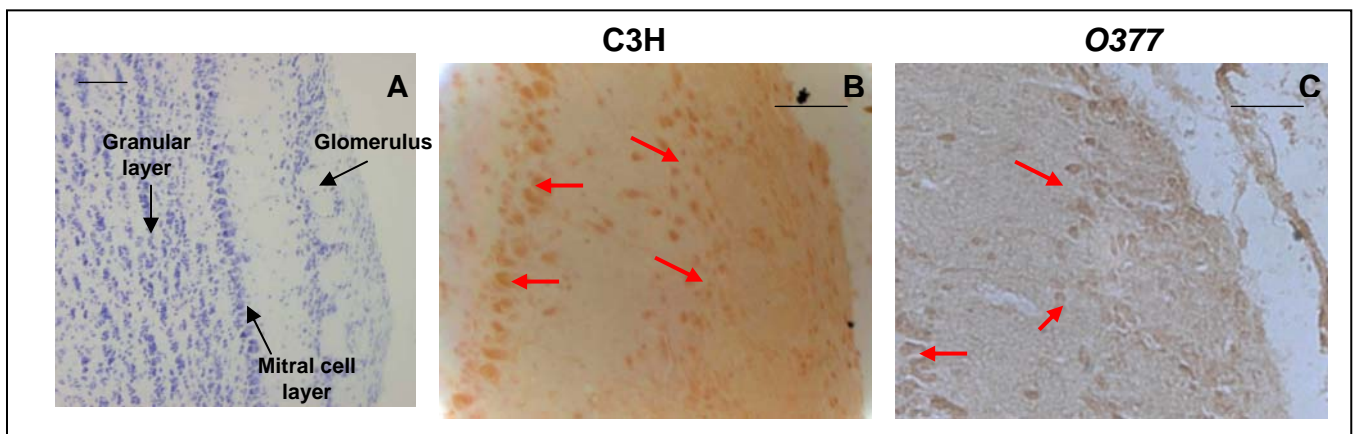
Figure 3.15: Immunohistochemical studies by ABC staining method (Vectastain; Vector laboratories) in sagittal sections of brain from 3 weeks old animals revealed the expression domains of βB2-crystallin protein to be in the glomerulus and mitral cell layer of the olfactory bulb (Figures: B, C) in both the wild-type and mutant respectively; Figure A is a Cresyl violet staining of the olfactory bulb of wild-type animal in sagittal plane. Scale bars= 50µm (A) and 20µm (B, C)

The structure of the olfactory bulb in sagittal section in the mutant does not show any histological changes in comparison to the wild-type. Clearly differentiated glomerulus, mitral cell layer and subsequent granular layers are observed in sagittal sections of the olfactory bulbs (Figure 3.16) of P21 brain both in C3H and *O377* homozygous mutants with no visible difference among them.
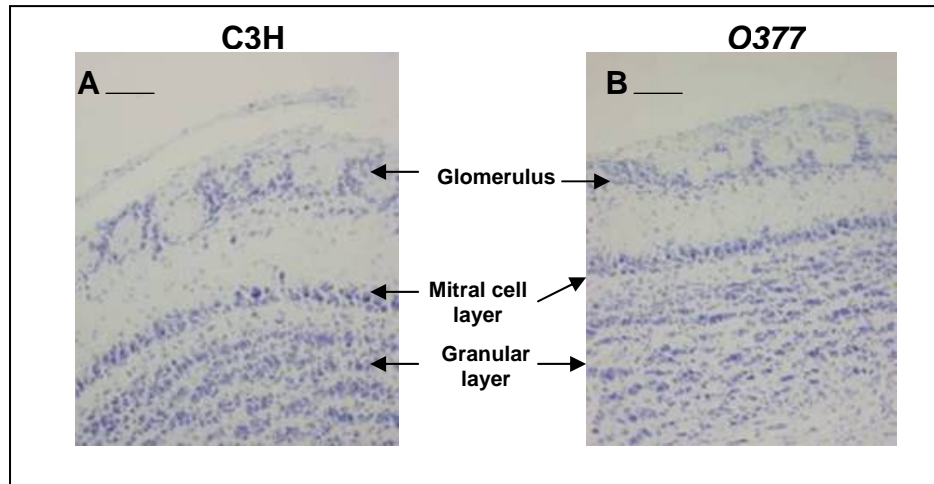
Figure 3.16 shows the histological structure of olfactory bulb of C3H (3.16A) and *O377* (3.16B) brains of 3 weeks old animals in sagittal plane; no difference in histological structure was observed in the olfactory bulb between them. Scale bars= 50µm.

3.4.4: Tissue type: Brain cortex

Expressions of βB2-crystallin have been detected in the pyramidal cells of third and fifth layers (Figure 3.17) of the cortex in both the wild-type and mutant animals.
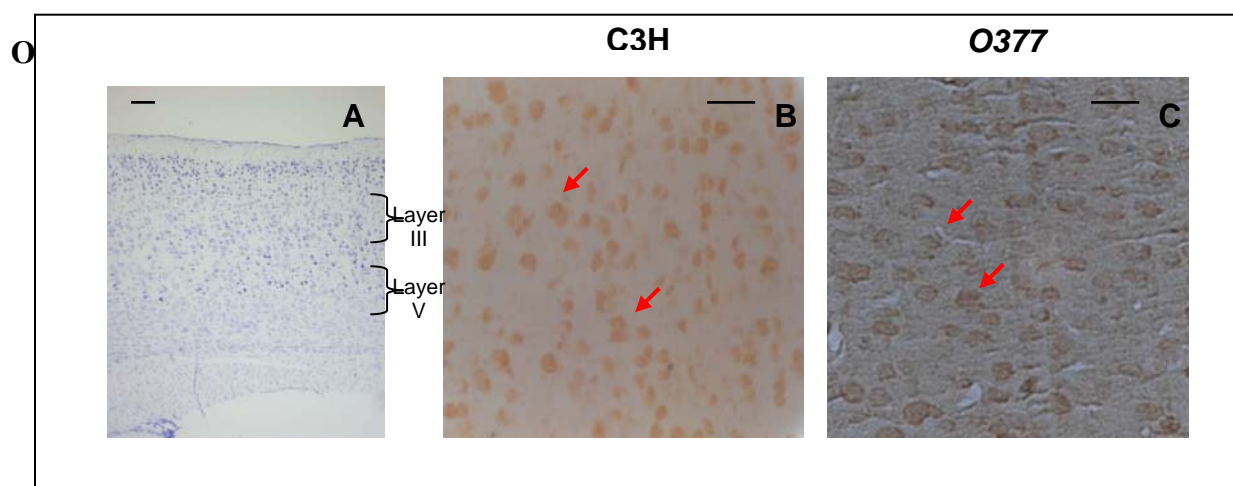
Figure 3.17: Immunohistochemical studies by ABC staining method (Vectastain; Vector laboratories) in sagittal sections of brain from 3 weeks old animals revealed the expression domains of βB2-crystallin protein to be in the pyramidal cells of the cortex (Figures: B, C). Expressions indicated by red arrows. Scale bars= 50µm (A) and 20µm (B, C)

115

The brain cortex both in wild-type and the mutants show the typical six layered structure, with pyriamidal cells as the major cell type in the third and fifth layers; granular cells present in high numbers in the third and fourth layers; and fusiform cells in the sixth layer. Pyramidal cells (small, medium, large and giant) of varying sizes and granular cells are also present more or less in all the layers in both wild-type and mutant.
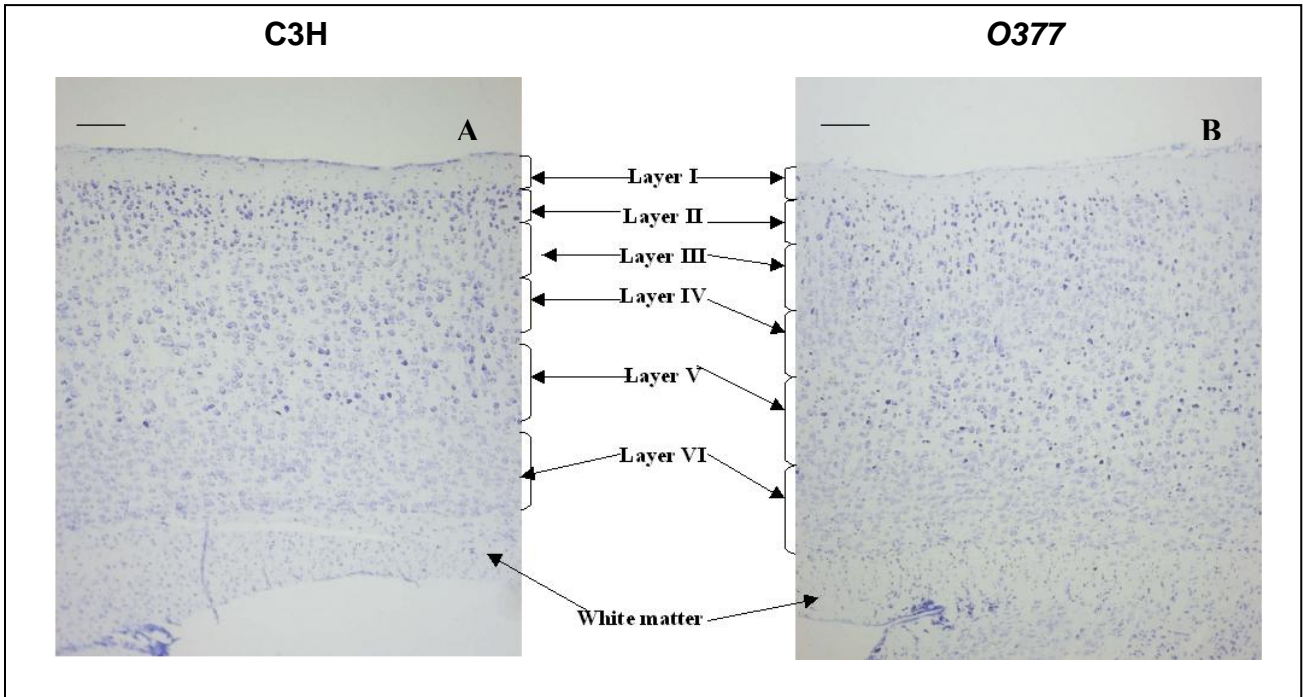
Figure 3.18 shows the histological structure of brain cortex C3H (3.18A) and *0377* (3.18B) brains of 3 weeks old animals in sagittal plane; no difference in histological structure was observed in the cortex between them with both showing the characteristic six layered cortex. Scale bars= 50μm.

3.4.5: Tissue type: Hippocampus (Brain)

Expressions of βB2-crystallin have also been detected in the CAI, CAII and CAIII region (Figure 3.19 B, C) cells of the hippocampus proper (*Cornu ammonis*) and in the dentate gyrus of the hippocampus both in the wild-type and mutant animals. The divisions of CA regions are based on cell morphology, pattern of termination and distribution of fibre pathways and electrophysiological properties of the cell types. The major cell type in the hippocampus is the pyramidal cells and in the dentate gyrus it is dentate granular cells.
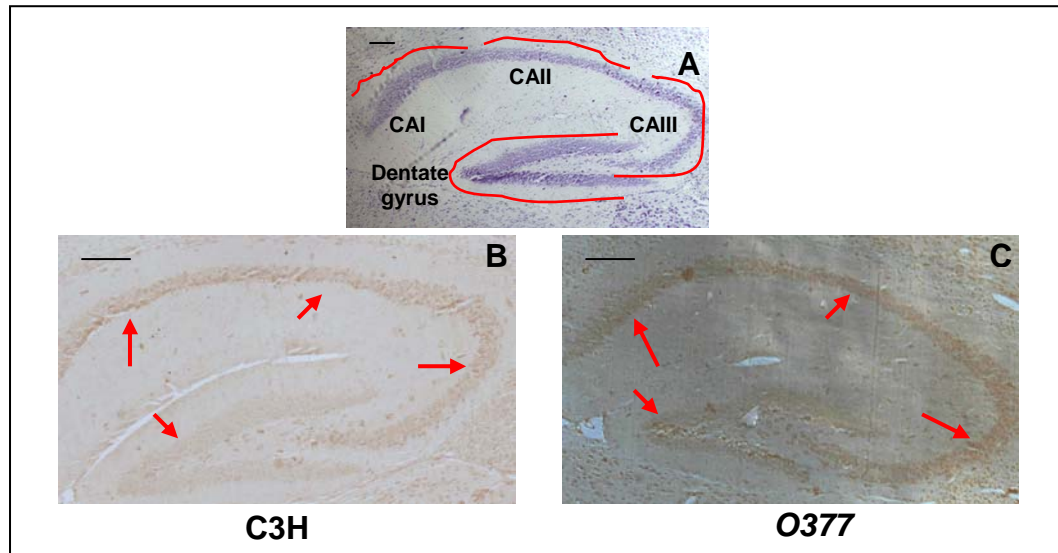
Figure 3.19: Immunohistochemical studies by ABC staining method (Vectastain; Vector laboratories) in sagittal sections of brain from 3 weeks old animals revealed the expression domains of βB2-crystallin protein to be in the CAI, CAII, CAIII and dentate gyrus of the hippocampus (Figures: B, C) in both the wild-type and homozygous mutant. Figure A shows the histology of hippocampus in sagittal plane of a 3 week old wild-type animal following Cresyl violet staining. Expressions indicated by red arrows. Scale bars= 0.1mm.

The hippocampus also looked normal in the mutant when compared to the wild-type with distinct CAI, CAII and CAIII regions in the hippocampus proper; dentate gyrus and hilus. Under higher magnification the neuronal structures in these regions appeared same in the mutant as in the wild-type.
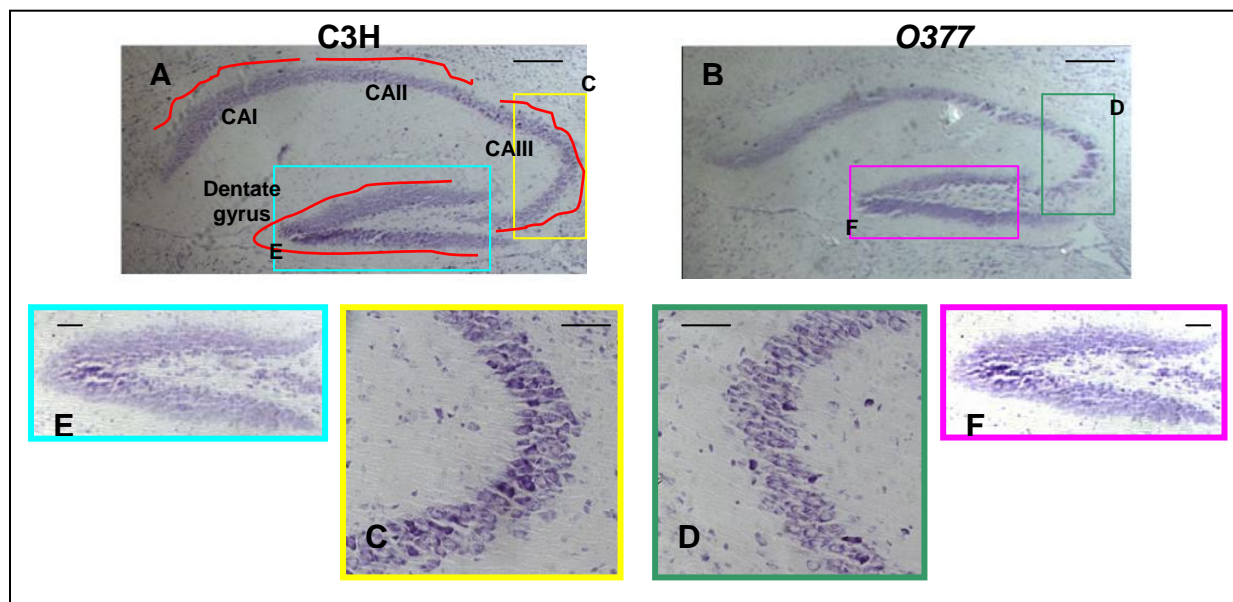
Figure 3.20 shows the histological structure of the hippocampus C3H (3.20A) and *O377* (3.21B) brains of 3 weeks old animals in sagittal plane; no difference in histological structure was observed in the hippocampus between them; figures 3.20C and E represents the magnified views of CAII/CAII region and dentate gyrus of the C3H animals and figures 3.20D and F represents the same for *O377* animals. Follow the colour codes to view the respective magnified pictures of CA II/CAIII regions and dentate gyrus of C3H and *O377* mutants. Scale bars= 0.1mm (A, B) and 20μm (C, D, E, F).

3.4.6: Tissue type: Cerebellum (Brain):

In the cerebellum, expressions of βB2-crystallin have been detected in the Purkinje cells and stellate cells (molecular layer) of both the wild-type and mutant animals (Figure 3.21).
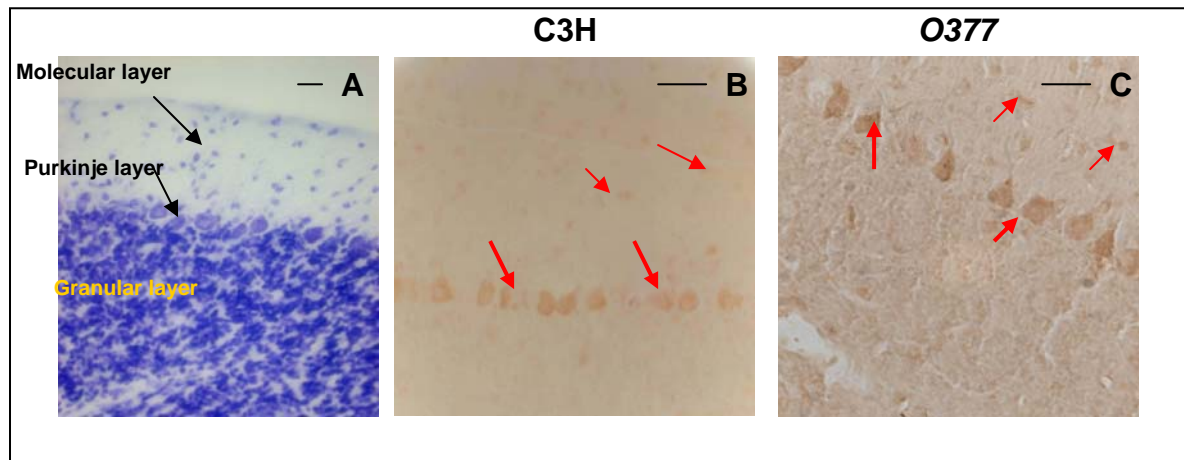
Figure 3.21: Immunohistochemical studies by ABC staining method (Vectastain; Vector laboratories) in sagittal sections of brain from 3 weeks old animals revealed the expression domains of βB2-crystallin protein to be in Purkinje cells and stellate cells (Molecular layer) of the cerebellum in both the wild-type (Figure B) and homozygous mutant (Figure C). Figure A shows the cytoarchitecture of the cerebellum following Cresyl violet staining in sagittal plane of a 3 week old wild-type animal. Expressions indicated by red arrows. Scale bars= 20μm (A) and 10 μm (B, C)

In some animals (1 for each genotype) expression of βB2-crystallin was also detected in the axons (Figure 3.22) of Purkinje cells in both the wild-type and mutant. Since, the expression in this region could not be detected in majority/all of the 5 animals of each type tested; it can be considered as an good example of variation.
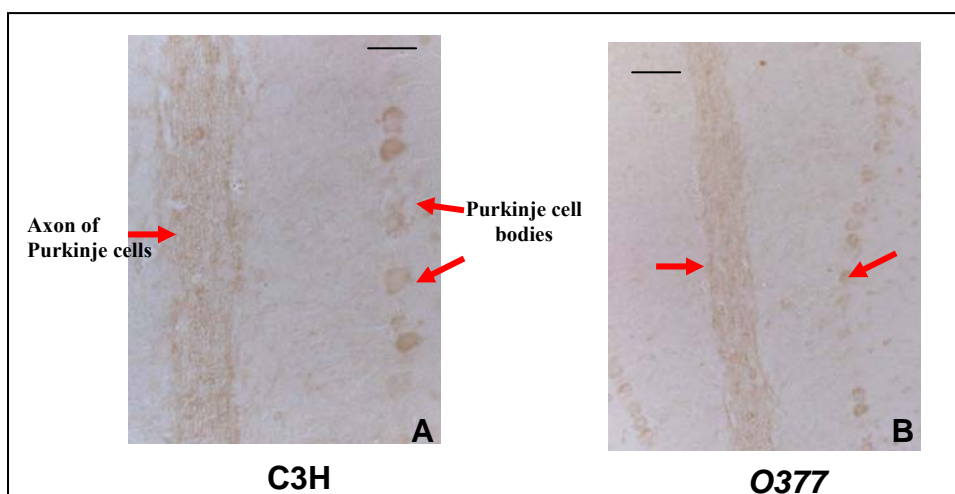
Figure 3.22: A and B shows the expression of βB2-crystallin also in the axons of Purkinje cells apart from the Purkinje cell bodies both in the C3H and *O377* mutants respectively. However this observation was true for only 1 animal out of 5 animals of each genotype studied. Expressions indicated by red arrows. Scale bars= 10μm.

The cerebellum typically consists of foliae composed of cortex and white matter. The three layered cortex contains the inner granular layer, the middle Purkinje cell layer and the outer molecular layer on a core of white matter. The molecular layer in the animals of both genotypes typically consists of stellate cells and basket cells. All these three layers are distinctly visible in the mutant with no major change when compared to C3H following Cresyl violet staining (Figure 3.23). However, when observed carefully a subtle change can be observed in the Purkinje cell layer of the homozygous mutants when compared to the wild-type. The number of Purkinje cells is slightly higher (Table 3.1) and in size they are slightly smaller (at vermis*) in the homozygous mutant animals (P21). In identical portions of the sections, under the same microscopic magnification a difference of 2-3/4 cells were persistently observed between the wild-type and the mutant. Since the difference is so subtle, it had to be stereologically evaluated to be established. The difference was most prominent in the Vth lobe of the cerebellum, because it is the best observable cerebellar lobe in sagittal plane.* *Part of the cerebellum lying in the midline between the two cerebellar hemispheres*.
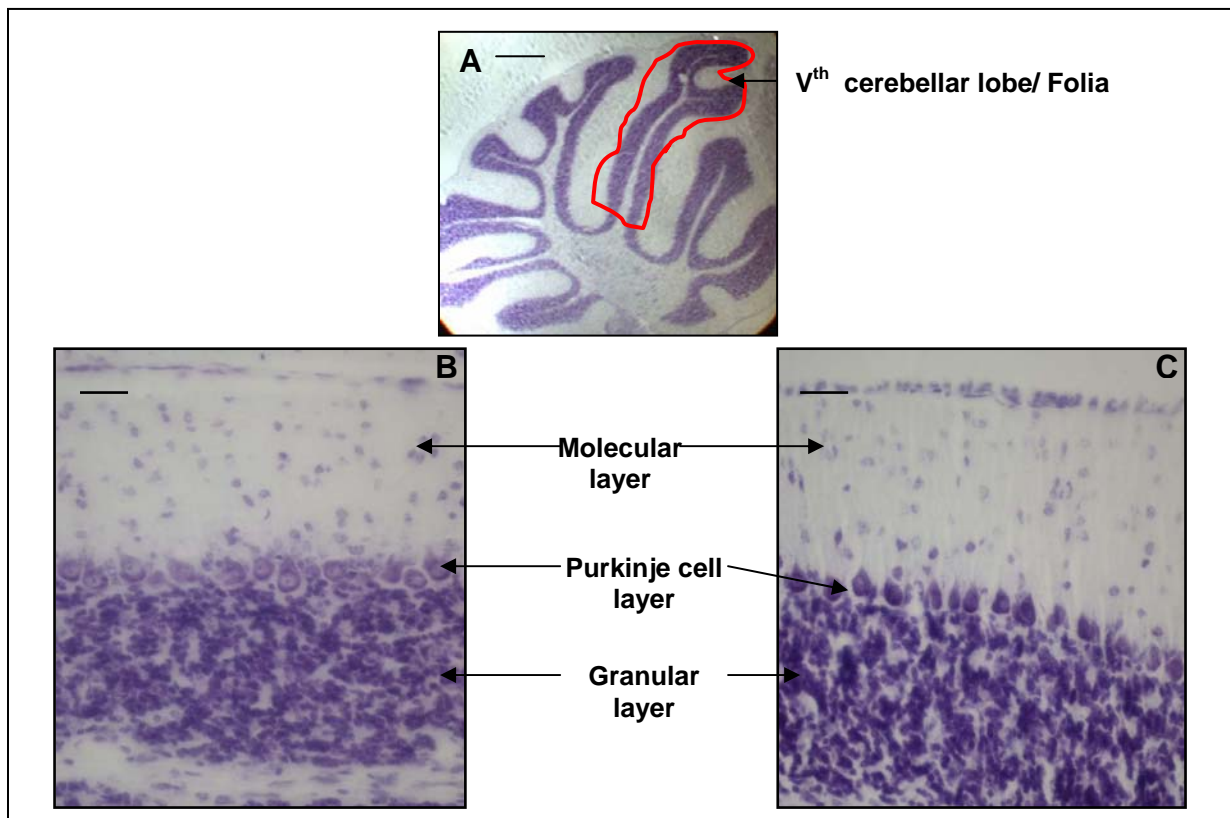
Figure 3.23 shows the histological structure of the cerebellum at vermis. Figure 3.23A shows the foliated structure of cerebellum in wild-type. Figures 3.23B and 3.23C shows the characteristic three layered structure (outer molecular layer, middle Purkinje cell layer and inner granular layer) of the cerebellum of 3 weeks old C3H and *O377* animals respectively. Careful observations revealed that the number of Purkinje cells in figure 3.23B (C3H) is **11** and that in the figure 3.23C (*O377* mutant) is **14** and also slightly smaller in size. Scale bars = 0.2mm (A) and 20µm (B, C).

3.4.6A: Stereological counting of Purkinje cells:

The number of Purkinje cells has been found to be slightly higher (11 %) [Table 3.1; figure 3.25] in the Vth lobe of cerebellum (Figure 3.24) of homozygous mutants in comparison to the wild type animals after stereological counting of Purkinje cells (from the Vth cerebellar lobe at vermis) of 9 animals of each genotype (C3H and *O377*). The Purkinje cells in the mutants also appeared to be slightly smaller in size. The difference in the number of Purkinje cells between the mutant and wild-type animals detected following stereological counting was statistically significant [**t-test**: (p-value = 0.011)]. However, no change of the gross morphology in the cerebellar lobes was observed in the mutant animals as a result of this changed number of Purkinje cells.

Specifications for the counting:

- 9 animals from each genotype [C3H and *O377* (-/-)] were analysed.
- Purkinje cells of the Vth cerebellar lobe counted for each animal, as this the best visible lobe in sagittal plane and therefore with the most prominent effect.
- Thickness of sections: 50μm
- Every 8th mounted* section was counted.

*Sections from wells 2, 6 and 10 were mounted (Refer to section 2.4.2, figure 2.2 in the materials and methods chapter).

The two most important specifications which were input in the Stereoinvestigator software at the start of counting of each brain were for the **Serial Section Set up** and **Optical Fractionator** are as follows**:**

Serial Section Set up	
Block Advance:	50μm
Mounted Section:	30μm
Section evaluation interval:	8
Starting section No.:	1
z-axis value:	0
Section Number.	XXXXXXXX

Optical Fractionator	
Scan Grid Size	250μm X 250μm
Desired Supl size:	15
Fixed distance:	3μm
Optical distance:	25μm
Mounted section:	30μm
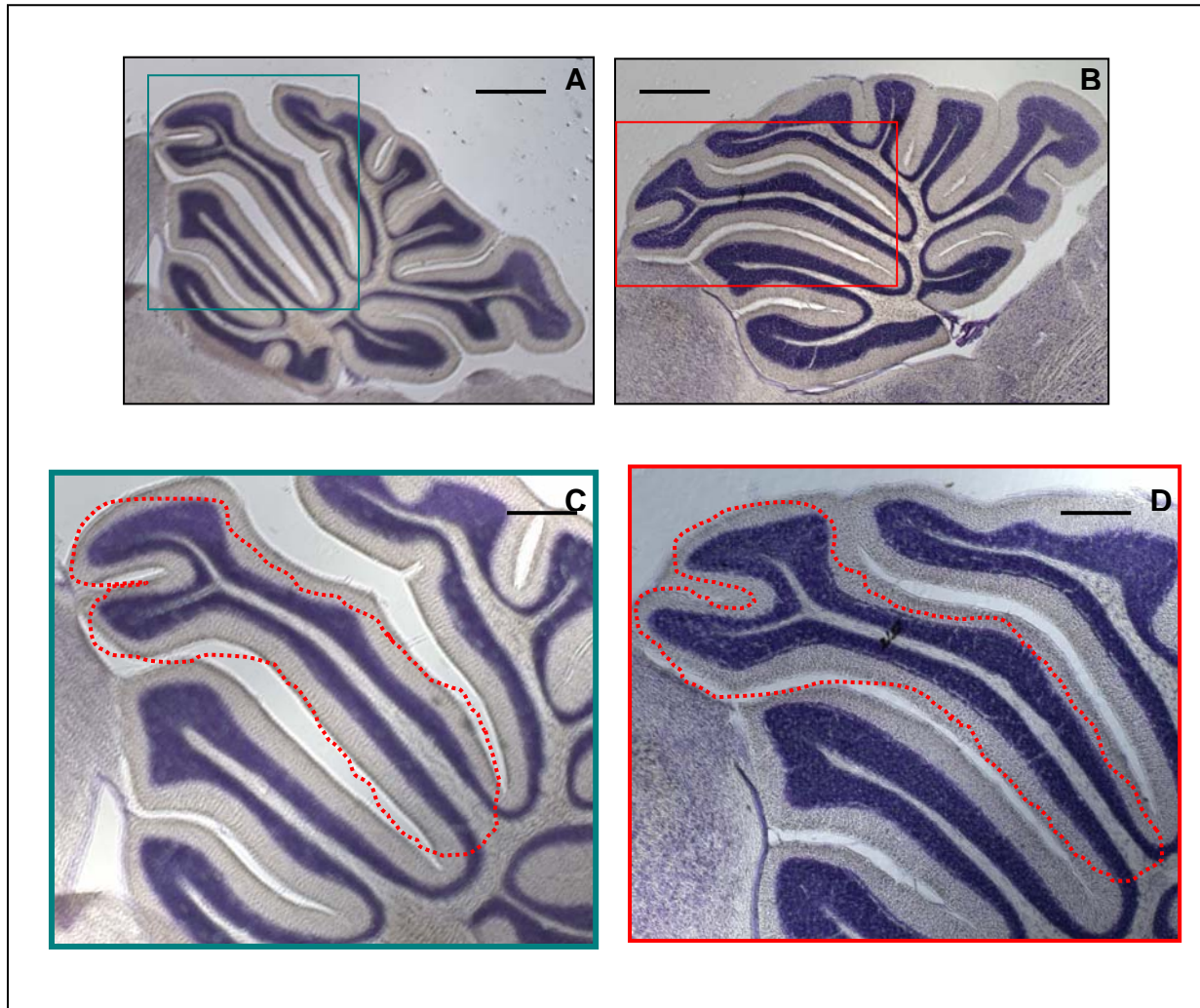
Figure 3.24: The strategy undertaken for stereological counting is explained here. Cresyl violet stained sagittal sections from identical levels (at vermis) were selected for counting for both the wild-type and mutant animals. The region of the Vth cerebellar lobe containing the Purkinje cells was pre-selected (red dotted lines in Figure C and D) using the marker (an option in the software), and the stage of the microscope moved automatically according to the specifications provided in the serial sections manager. Purkinje cells within the green axis of the software under various microscopic fields were counted by computer mouse clicking. Figures A and C represents the cerebellar lobes (at vermis) of the wild-type brain and figures B and D represents the same in the homozygous mutants. Scale bars= 0.2mm (A, B) and 100µm (C, D).

Table 3.1: Results of stereological counting of the Purkinje cells.

Animal No.	Estimated total No. of Cells counted by Optical Fractionator	Total markers* counted	Coefficient of error CE (Gundersen)
C3H			
A1	12240.00	204	m=0; 0.14 m=1; 0.07
A2	15960.00	266	m=0; 0.12 m=1; 0.07
A3	11880.00	198	m=0; 0.16 m=1; 0.08
A4	12180.00	203	m=0; 0.12 m=1; 0.07
A5	11880.00	198	m=0; 0.13 m=1; 0.08
A6	12360.00	206	m=0; 0.15 m=1; 0.08
A7	11640.00	194	m=0; 0.18 m=1; 0.07
A8	11700.00	195	m=0; 0.14 m=1; 0.08
A9	13320.00	222	m=0; 0.13 m=1; 0.07
Total No. of Cells: **Mean:**	**113260.00** **12581.11**		Standard deviation (s.d): 1361 Standard error mean (s.e.m.): 609
_O377_			
A1'	13620.00	227	m=0; 0.12 m=1; 0.07
A2'	13500.00	225	m=0; 0.15 m=1; 0.07
A3'	15060.00	251	m=0; 0.13 m=1; 0.07
A4'	13560.00	226	m=0; 0.12 m=1; 0.07
A5'	13320.00	222	m=0; 0.13 m=1; 0.07
A6'	14220.00	237	m=0; 0.11 m=1; 0.07
A7'	14340.00	239	m=0; 0.15 m=1; 0.07
A8'	14280.00	238	m=0; 0.11 m=1; 0.07
A9'	14040.00	234	m=0; 0.15 m=1; 0.08
Total No. of Cells: **Mean:**	**125940.00** **13993.33**		Standard deviation (s.d): 550 Standard error mean (s.e.m.): 246

*Markers represent the cells counted under a particular microscopic stereological field on the basis of which the Optical Fractionator of the software estimates the total number of cells.
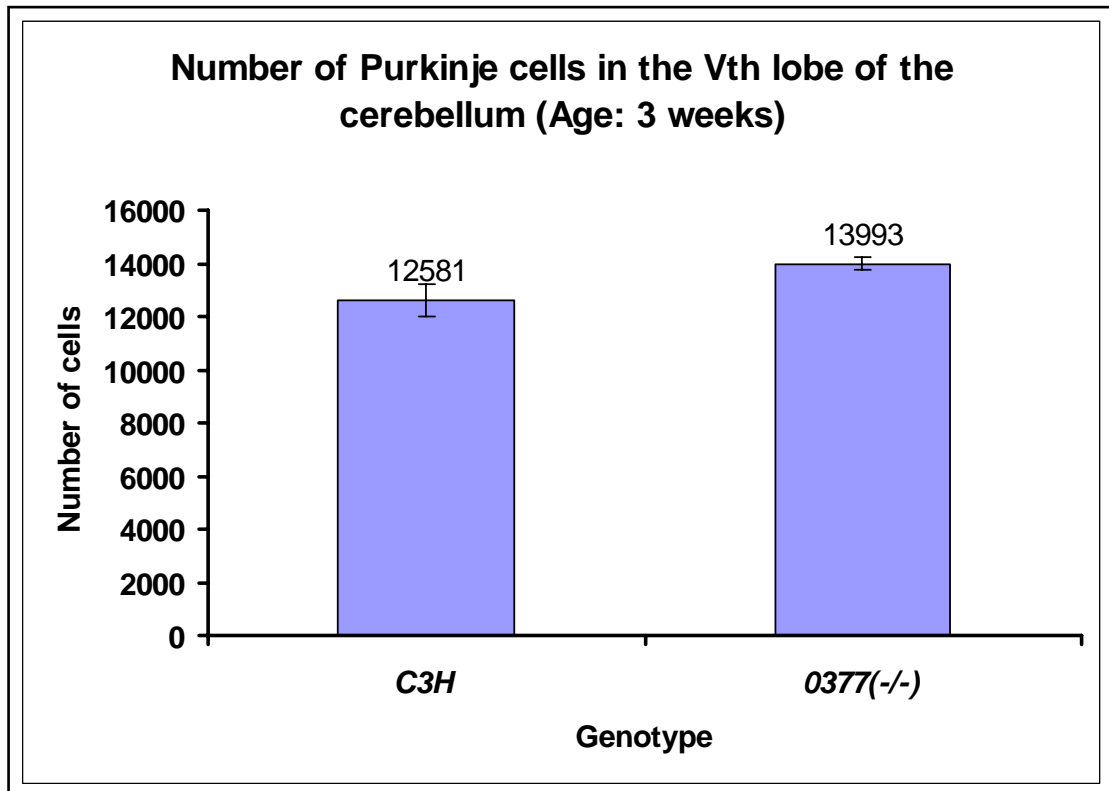
Figure 3.25: Graphical representation of the results of stereological counting of Purkinje cells of the Vth lobe in sagittal sections of C3H and *O377* brains at vermis. The Number of Purkinje cells in the *O377* mutants is 11% higher than the wild-type (C3H). [**t-test**: (p-value = 0.011)]

3.4.6B: <u>Myelin staining (cerebellum):</u>

Since expression of βB2-crystallin was observed in the axons of Purkinje cells of the cerebellum in one animal of each genotype. Myelin staining was performed on free floating sagittal cryosections to study the distribution of fibres and that in the cerebellum was observed with special emphasis. However, as expected, the orientation and distribution of the fibres are exactly the same in both the wild-type and mutant animals as can be observed from the golden brown and black/gray tracing of the fibres in figure 3.26. The quality of staining in this experiment was not optimum, so the photographs should not be interpreted based on the intensity of staining.
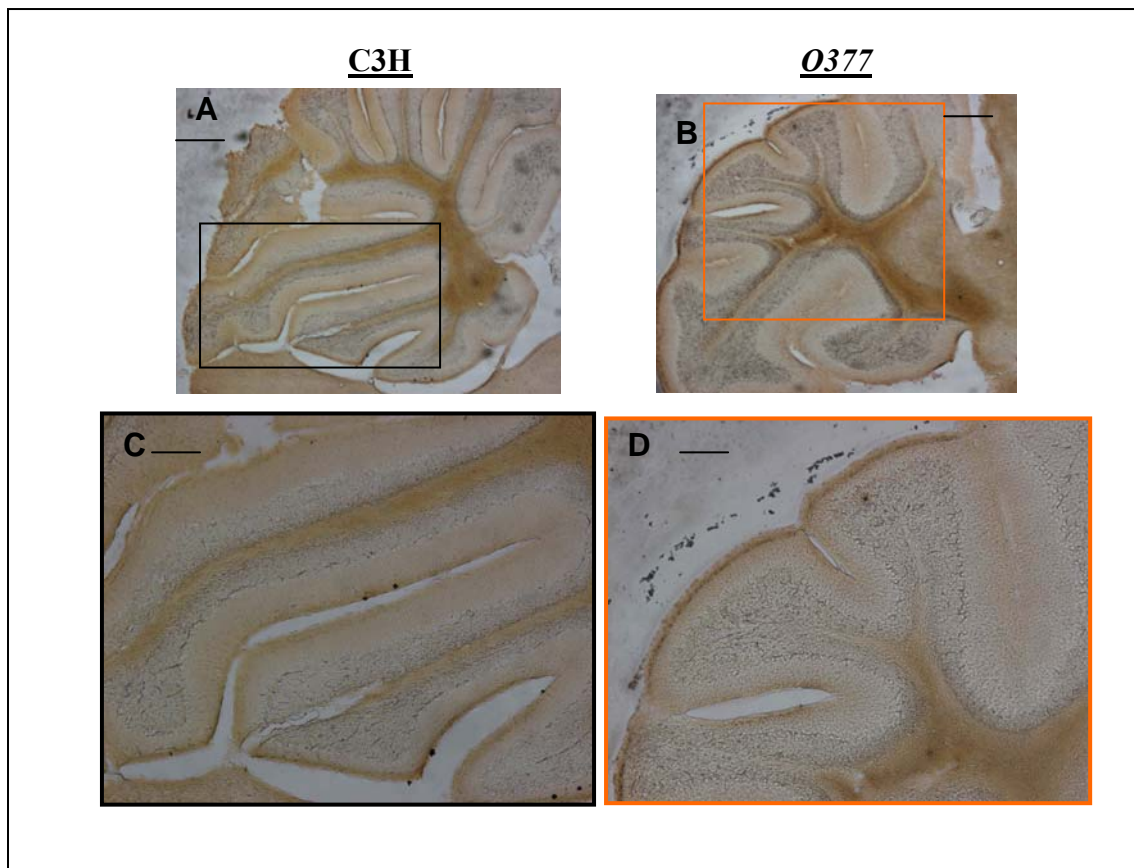
Figure 3.26: Myelin staining of the cerebellar fibers of both wild-type (3.26A, C) and mutant (3.26B, D). Scale bars= 0.2mm (A, B) and 100µm (C, D)

3.5: <u>Determination of primary antibody specificity (Preabsorption studies):</u>

Specificity of the antibody against βB2-crystallin used for immunohistochemical studies in brain have been established by immunoblottings (Western blot experiments works optimally with this antibody) and immunohistochemical studies in lens; the known tissue expression (positive control). Observation of no staining in the negative control experiments (i.e. primary antibody omitted) was actually another good reason to consider the antibody to be specific as this proves that the other reagents used during the experiment are not involved in the development of any unspecific staining. Preabsorption study is another method to verify antibody specificity which was carried out in the sagittal sections of 3 weeks old wild-type brain. Figures 3.27A (Purkinje and stellate cells; cerebellum); 3.27C (hippocampus entire); 3.27E (Dentate gyrus of the hippocampus); 3.27F (CAIII region of the hippocampus proper); and 3.27I (axons of Purkinje cells and Purkinje cell bodies)* shows the control experiments where immunostainings (indicated by red arrows) are observed. No staining or significantly reduced staining was observed in

the samples shown in Figures 3.27B (focussing on Purkinje and stellate cells, cerebellum), 3.27D (focussing on entire hippocampus), 3.27G (CAIII region of the hippocampus proper), 3.27H (Dentate gyrus of the hippocampus) and 3.27J (focussing on the axons of Purkinje cells and Purkinje cell bodies)* where the primary antibody was preabsorbed in pure β_H crystallin (StressGen) over night for immunohistochemical studies. Complete abolition of staining is not possible due to the protein interaction.

*Samples for this experiment were taken from the same set in which animals showed βB2-crystallin expression in the axonal fibres of the Purkinje cells of the cerebellum.
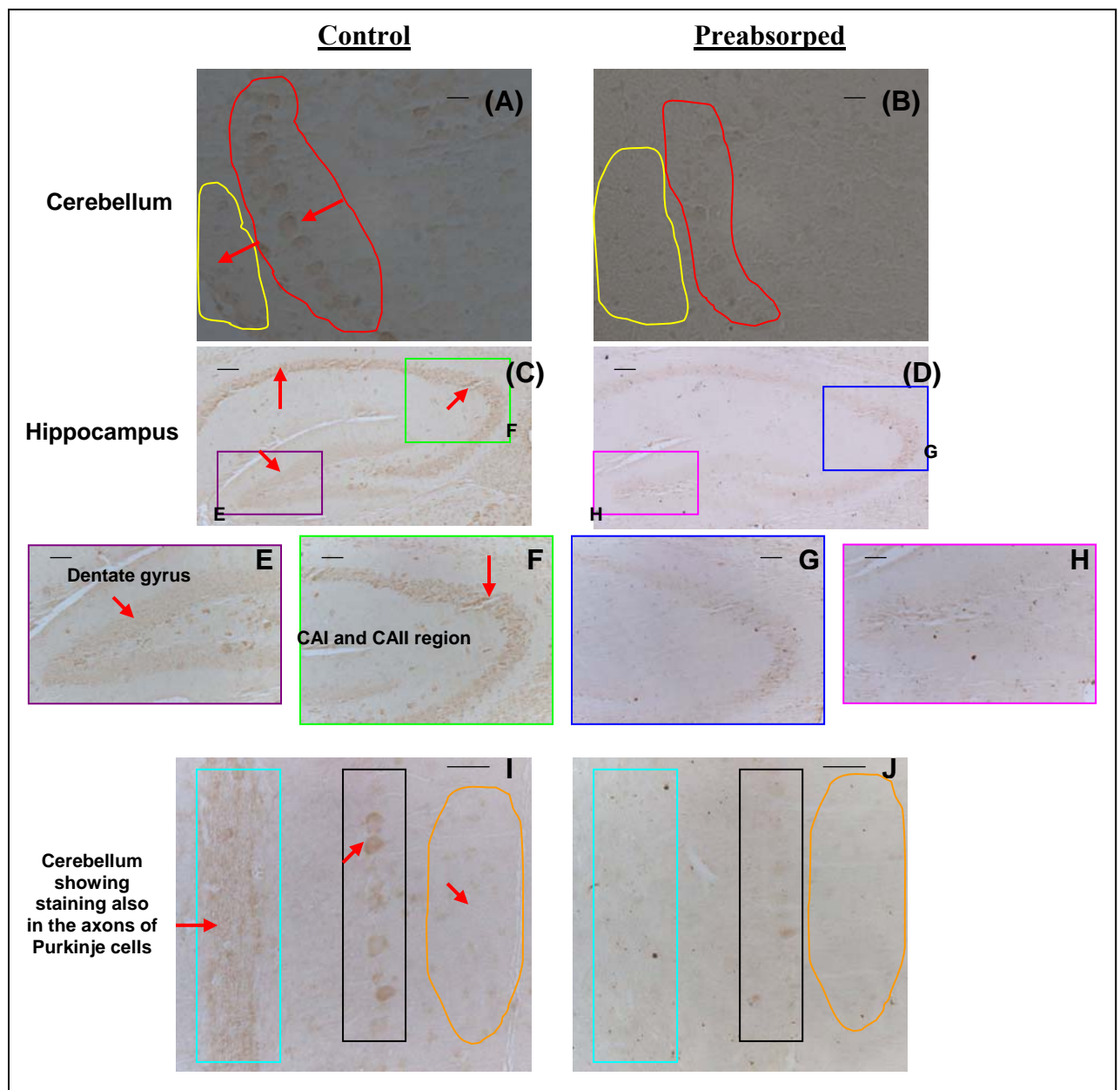
Figure 3.27: Preabsorption study to verify antibody specificity was carried out in the sagittal sections of 3 weeks old wild-type brain. Follow colour codes to view enlarged images. Expressions indicated by red arrows. Scale bars = 20μm (A, B, I, J); 0.1mm (C, D); 20μm (E-H);

3.6: <u>Expression profiling studies:</u>

Expression profiling studies were carried out using DNA microarray technique for homozygous lens; and both heterozygous and homozygous brain, to reveal the complex genetic cascade in which *Crybb2* is involved in these tissues. The genes which are up-regulated or down regulated in the mutants in the respective tissues are considered to be differentially expressed as a result of the changes at the molecular level that occurred following the mutation in the *Crybb2* gene. Hence, these differentially expressed genes are considered to be the part of the complex signalling cascade along with *Crybb2*. This is a fast screening method to choose the candidate genes for further studies. The results of expression profiling studies (for some selected genes only) were verified by an independent method, like. Real Time PCR. *In-situ* hybridisation is the other method to verify these results that can reveal not only the differential expression in a semi-quantitative manner but also the spatial expression of the gene which can provide more insight to the gene expression in a co-localized manner (Please refer to notes at the end of chapter IV). Following expression profiling experiments, a list of differentially expressed genes are obtained which were intensely studied in the databases to know about their functionalities, roles in different biochemical pathways etc. so as to use the information as a hint (semi-direct) to predict and/ find out the unknown role of *Crybb2* in brain with combination with other experimental data and to explore more about its genetic cascade in the lens.

Lenses were collected from male animals of 3 weeks of age because this is the age when cataract sets in among all the *O377* mutant animals (both heterozygotes and homozygotes) as observed by expert screeners in the animal facility (Dr. J. Favor, Dr. A. Neuhaüser-Klaus). So, the age of 2 weeks might be an earlier age or the age of 4 weeks might be little late for expression profiling of the lens tissue; at least for the first attempt. 10-16 lenses (i.e. 5-8 animals) were necessary from each genotype to extract enough RNA for carrying out DNA microarray experiments (5 hybridization experiments). The lens tissue had to be pooled for RNA extraction for both the wild-type and mutant to obtain sufficient RNA. Because of the requirement of so many animals with the mentioned specifications at the same time, expression profiling studies in lens were restricted only to the homozygous mutant animals as this is expected to show the more severe consequences at the genetic (and also phenotypic) level than the heterozygous mutant.

Brains were collected from 4-5 male animals (4 weeks old) of each genotype (+/+, +/-, -/-); tissues were dissected out from all the animals at the same time of the day; animals were from

the same mouse room; iso-genic background; kept in separate cages for 1 week before sacrifice. These procedures are known to reduce biological noise (Seltmann *et al.,* 2005)

It was important to choose the optimum age of the animals from which tissues were collected for expression profiling. The age of 4 weeks was chosen to collect the brains because of the following reasons:

i. The expression of βB2-crystallin is best between the age of 3-4 weeks both at the transcript and protein levels in the brains of the wild-type, homozygous and heterozygous mutants.

ii. It was important to keep the animals in separate cages for 1 week. This helps to reduce biological noise. However, it is not possible to separate the pups from their mother before 3 weeks of age.

3.6.1: Tissue type: *O377* (-/-) Lens

The RNA samples extracted from of the lens of 8 homozygous male animals were pooled and chip hybridisation experiments were performed from a pooled reference RNA sample of 5 wild-type (male) lens. 5 chip hybridisation experiments (of which 2 were colour flip) was possible with the available amount of pooled RNA and all the experiments were technically correct and the data obtained from all of these experiments were used for analysis. The scatter plots (Figures 3.28) for these hybridisation reactions were always moved away from the diagonals because the labelling reaction in wild-type sample was more efficient than the mutant sample. All the reactions were performed simultaneously and this was a general feature for all the experiments. There were **809** genes [Average number of genes detected in each experiment = 2509] detected in all 5 experiments. That is, the number of overlapping genes is almost one third of the total number of genes detected per experiment, which is considered as a good percentage as per the standard operation protocol (SOP) used [Expression profiling group; IEG; GSF]. **116** differentially expressed genes were identified in the homozygous mutant lens; of these **70** genes were **up-regulated** and **46** genes were **down regulated [Cut off ratio (Border of significance) = 2 i.e. two fold differential expression (up or down)]**. Functional annotations of each of these genes were then studied intensely in the available databases to ascertain their significance. Out of these 116 genes; 24 are involved in regulatory functions, 25 in transport and binding, 12 in energy metabolism, **9** are **crystallins (**structural proteins of the lens), 15 are involved in other functions, 15 of them represents ESTs and/ RIKEN cDNA etc. and the remaining 17 are of unknown identity and function (Figure 3.29) **[Last screened: 20.03.2005]**. One of the most significant information

that came out from studying the functional annotations of the known differentially expressed genes is the down regulation of the crystallins (Annexure: 3, down regulated]. A list of these differentially expressed genes involved in various functions is provided in annexure 3.
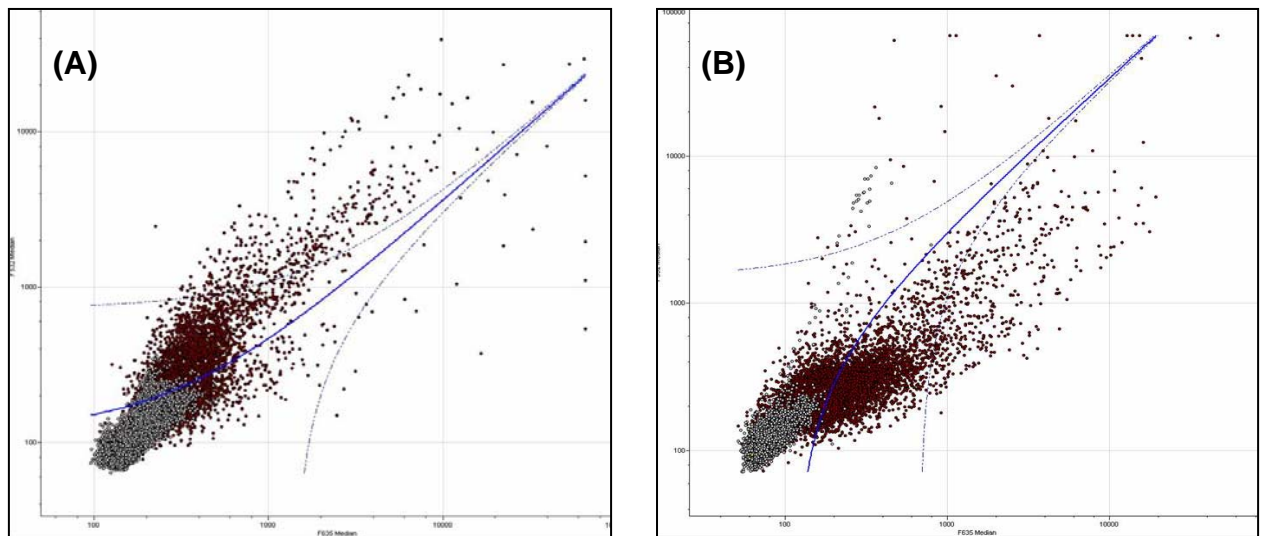
Figure 3.28: Scatter plots of *O377* (-/-) Lens hybridisation reactions. **3.28A** shows a scatter plot of a normal hybridization reaction and **3.28B** shows a scatter plot of a colour flip reaction. In both cases it can be observed that the scatter plots are moved away from the diagonals [to the right in case of normal (3.28B) and to the left in case of colour flip (3.28A) hybridisation reaction] which is because of the fact that one of the samples (in this case wild-type) has stronger signals than the other sample (mutant) because the labelling reaction was more efficient in the wild-type samples than the mutant. Since all the experiments were performed simultaneously and this was a generalized feature; the quality of data obtained following these experiments was technically good. The **X-axis** denotes the **F635 median** and the **Y-axis** denotes the **F532** median (not prominent in the figure as they are screen shots of the computer screen).
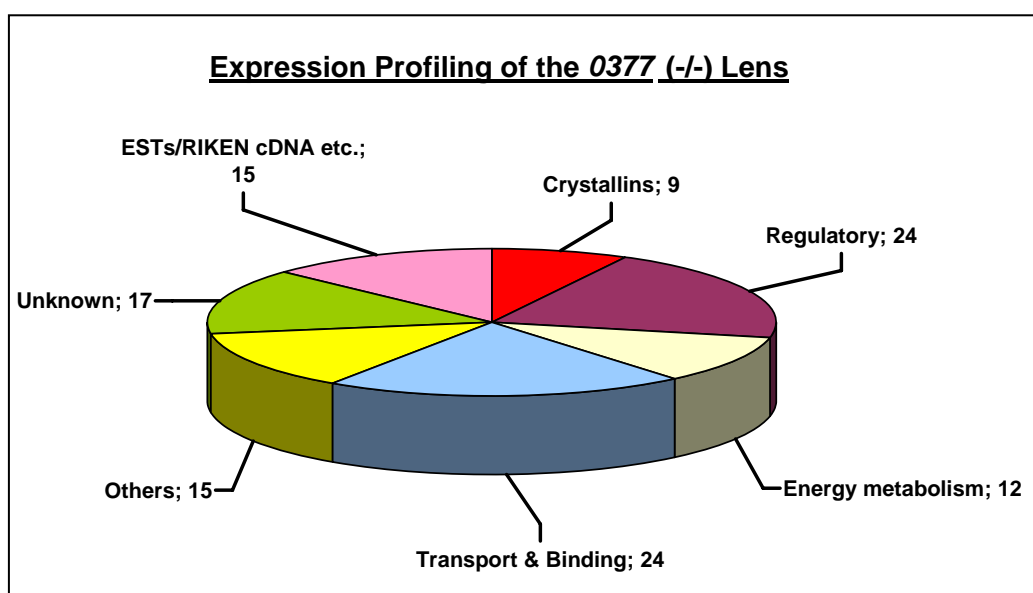
Figure 3.29: Classification of the differentially expressed genes in the *O377* (-/-) lens according to their functional classes.

Since the expression level of *Crybb2* has been found to be opposite (down regulated) in the homozygote mutant at the age of P21 following DNA microarray studies to that in the homozygote mutant lens at the age of P1 following *in-situ* hybridization experiments, the expression level of *Crybb2* in P21 lens was verified using real time-qPCR analysis; and *Crybb2* was indeed found to be down regulated at this age as can be observed from the normalized ratio in table 3.2. *Crybb2*_L7/R1 primer pair used for *Crybb2* RT-PCR was also used for this reaction. A melting curve analysis is shown in figure 3.30.

Table 3.2: Report sheet for data analysis for the ***Crybb2*** gene generated by the Relquant software (1.0) [Roche] following the Real Time-qPCR experiment.

Sample	CP (Crossing Point)	CP median	Delta CP median	Ratio Conc.	Normalized ratio
Wt_*Crybb2*	18.35	18.29	-3.13	8.75	**1.00**
Repli of Wt_ *Crybb2*	18.22				
Wt_Hprt	21.12	21.41			
Repli. of Wt_*Hprt*	21.71				
Mut_ *Crybb2*	18.79	18.62	-2.00	4.01	**0.46**
Repli of Mut_*Crybb2*	18.44				
Mut_Hprt	20.34	20.62			
Repli. of Mut_*Hprt*	20.90				

*Results analysis mono colour, duplicate values without efficiency correction.
***Correction factor:**   1.000000
***Multiplication factor:** 1.000000
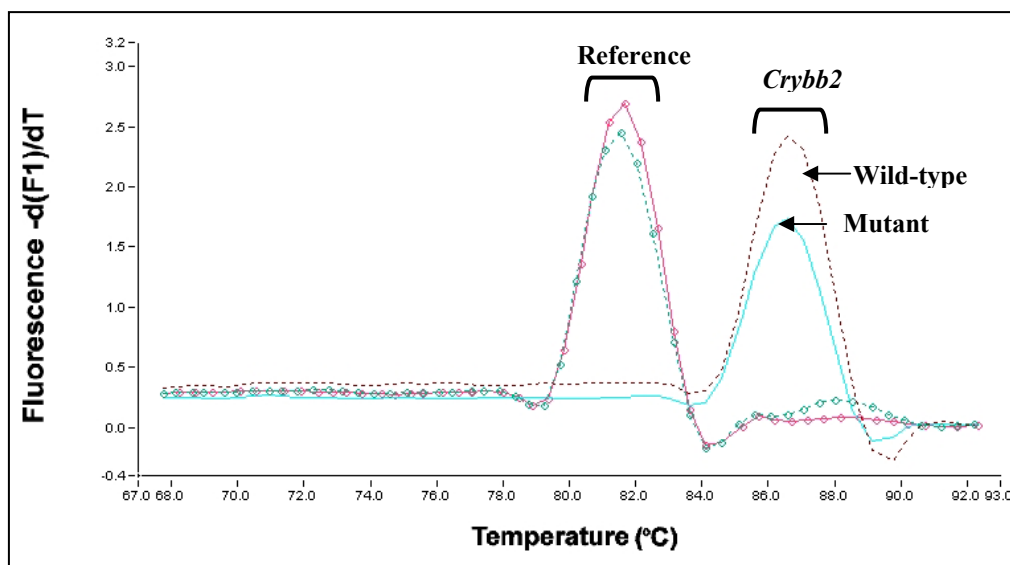
Figure: 3.30: The lightCycler Melting Peaks Report generated by the RelQuant (1.0) software for the ***Crybb2*** gene of **P21 lens** showing it's down regulation in the mutant. In this case data of one sample from each of reference and the ***Crybb2*** (target gene) of wild-type and mutant P21 lens has been shown.

The different expression profiles of *Crybb2* in the mutant lens at ages P1 (detected by *in-situ* hybridisation experiments) and P21 (detected by microarray and Real Time-PCR experiments) is discussed in section 4.2.

3.6.2: <u>Tissue type: *O377* Brain</u>

4 chip hybridisations were performed with RNA of each mutant (homozygote and heterozygote) animal. Each of these chip hybridisation experiment was performed against wild-type brain reference RNA pool of the respective litters. For each animal the chip experiments included two normal and two colour flip experiments.

3.6.2A. Homozygote (Brain):

16 chip hybridisation experiments were performed for the 4 (-/-) mutant animal brains of which 15 were technically correct (Figure: 3.31A) and the data obtained from these were analyzed. There were 2527 genes detected in all 20 experiments i.e. overlapping genes [Average number of genes detected in each experiment = 7402]. Inspection of expression profiling data from individual mice revealed a strong correlation of differentially expressed genes between all these 4 mutant animals. This revealed 14 differentially expressed genes in the homozygote mutant brain; of these 7 genes were up-regulated and 7 genes down regulated **[Cut off ratio (Border of significance) = 1.6]**. Functional annotations of each of these genes were then studied intensely in the available databases to ascertain their significance. Out of these 14 genes, **2** are involved in **regulatory functions**, **5** in **transport and binding**, **1** in **energy metabolism**, **4** are **ESTs/RIKEN cDNA** and the remaining **2** are of **unknown** identity and function (Figure 3.31B)**[Last screened: 20.03.2005]**. The most important information that came out from studying the functional annotations of the known differentially expressed genes is that many of them are somehow involved in phosphate pathways. A list of these genes is provided in table 3.3.

Table 3.3: List of the differentially expressed genes in the 4 weeks old homozygous mutant brain. * *Genes are arranged in ascending order of their P% (Chance) values.*

[Date of last screening: 20.03.2005]

No.	Gene symbol (MGI)	Name	Comments (UniGene)	LION Clone ID	NCBI Locus ID	Ratio	P, %
Up-regulated:							
1	-		No significant matches found	2,61 MG-16-176k15		3.41	0.00
2	*Serpina12*	Serine (or cysteine) proteinase inhibitor, clade A (alpha-1 antiproteinase, antitrypsin), member 12	**Transport and binding** Endopeptidase inhibitor activity	1,89 MG-13-47i12	68054	2.30	0.00
3			Tentative functional alignment with 4092-45 mouse E14.5 retina lambda ZAP II Library *M. musculus*	1,78 MG-15-70b2		2.42	0.00
4	*Tmsb4x*	Thymosin, beta 4, X chromosome	**Energy Metabolism** Actin binding; cytoplasm; cytoskeleton	1,68 MG-6-3c22	19241	1.95	0.00
5			RIKEN cDNA 5930418K15	1,51 MG-14-78g12		1.67	0.00
6	*Rab9*	RAB9, member RAS oncogene family	**Regulatory** GTP binding; GTPase activity	1,46 MG-13-61g11	56382	1.76	0.00
7	*Atp6v0a1*	ATPase, H+ transporting, lysosomal V0 subunit a isoform 1	**Transport and binding** ATPase activity; H^+ ion transporter activity	1,38 MG-6-55e7	11975	2.21	0.00

Down regulated

No.	Gene symbol (MGI)	Name	Comments (UniGene)	LION Clone ID	NCBI Locus ID	Ratio	P, %
1			Similar to nuclear localization signals binding protein 1 of *M. musculus* [ProtEST]	2,05 MG-3-19k2		2.33	0.00
2			Similar to RIKEN cDNA 2510049I19 of *M. musculus.* /CGI-144 protein	1,72 MG-6-2a13		1.95	0.00
3	-		No significant matches found	1,56 rda-F07		1.92	0.00
4	*ERG2 protein*		**Transport and binding** Cell envelope; phosphate transport	1,56 MG-16-10o9	52668	1.74	0.00
5	*Lpl*	Lipoprotein lipase	**Transport and binding** Cell envelope	1,48 MG-14-82j17	16956	1.83	0.00
6	*Sgne1*	Secretory granule neuroendocrine protein 1, 7B2 protein	**Transport and binding** Protein binding	1,46 MG-14-40o13	20394	1.96	0.00
7	*Supt16h*	Suppressor of Ty 16 homolog (S. cerevisiae)	**Regulatory** Hydrolase activity	1,40 MG-3-96d9	114741	1.73	0.00

3.6.2B. Heterozygote (Brain):

All 20 chip hybridisation experiments were technically correct (Figure: 3.32A) and the data obtained from all these experiments were used for analysis. There were 5618 genes detected in all 20 experiments i.e. overlapping genes [Average number of genes detected in each experiment = 8502]. However; there was no gene that was differentially expressed in all the 20 experiments (i.e. 5 animals). Inspection of expression profiling data from individual mice revealed a strong correlation of differentially expressed genes (especially down regulated genes) between 3 mutant animals. The expression profiling data of the remaining 2 animals were also very different among themselves. This is often encountered in expression profiling

studies. The expression data of the 3 animals showing correlation was taken only for further analysis. This revealed 26 differentially expressed genes in the heterozygous mutant brain; of these 9 genes were up-regulated and 17 genes down regulated **[Cut off ratio (Border of significance) = 1.15]**; however it must be mentioned that the *criteria for selecting these genes was rather stringent*. Functional annotations of each of these genes were then studied intensely in the available databases to ascertain their significance. Out of these 26 genes; 12 are involved in regulatory functions, 4 in transport and binding, 3 in other functions, 5 ESTs/RIKEN cDNA etc. and the rest 2 are of unknown identity and function (Figure 3.32B) **[Last screened: 20.03.2005]**. The most important information that came out from studying the functional annotations of the known differentially expressed genes (though the extent of differential expression is rather low) is that most of them are somehow involved in calcium and phosphate pathways. A list of these genes is provided in table 3.4.

Table 3.4: List of the differentially expressed genes in the 4 weeks old heterozygous mutant brain. * *Genes are arranged in ascending order of their P% (Chance) values.*

[Date of last screening: 20.03.2005]

	Gene symbol (MGI)	Name	Comments (UniGene)	LION Clone ID	NCBI ID	Ratio	P, %
Up-regulated							
1	*Ank*	Progressive ankylosis	**Regulatory** Phosphate transport; integral to membrane	1,14 MG-6-53c17	11732	1.17	0.00
2	*Camk2a*	Calcium/calmodulin-dependent protein kinase II alpha	**Regulatory** Calcium/calmodulin dependent protein kinase activity; cell communication	1,13 MG-15-167a1	12322	1.35	0.01
3	-		No significant matches found	1,11 MG-3-137p21		1.20	0.05
4	*Hpcal4*	Hippocalcin-like 4	**Regulatory** Calcium ion binding	1,10 MG-6-56n10	170638	1.17	0.11
5	*Nrgn*	Neurogranin	**Regulatory** Calmodulin binding	1,09 MG-6-41o10	64011	1.15	0.28
6	*Palm*	Paralemmin	**Others** Cytoskeletal regulatory activity; regulation of cell shape	1,09 MG-12-273h17	18483	1.17	0.28

	Gene symbol (MGI)	Name	Role/Functionality Other comments	LION Clone ID	NCBI ID	Ratio	P, %
7	*Cdh13*	Cadherin 13	**Transport and binding** Calcium ion binding; cell adhesion molecule activity	1,09 MG-6-39b7	12554	1.28	0.28
8	*Stk32c*	Serine/threonine kinase 32C	**Regulatory**	1,09 MG-6-15g7	57740	1.25	0.28
9	*Cx3cl1*	Chemokine (C-X3-C motif) ligand 1	**Others** Cytokine activity	1,08 MG-6-3h9	20312	1.15	0.67

Down regulated:

	Gene symbol (MGI)	Name	Role/Functionality Other comments	LION Clone ID	NCBI ID	Ratio	P, %
1	*Pcp2*	Purkinje cell protein 2 (L7)	Regulatory GTPase activator activity	1,28 MG-6-92b19	18545	2.15	0.00
2	*Chn2*	Chimerin (chimaerin) 2	Regulatory GTPase activator activity	1,21 MG-3-30o15	69993	1.67	0.00
3	-		No significant matches found	1,20 MG-6-14e12		1.42	0.00
4			ESTs	1,19 MG-6-43b23		1.36	0.00
5	*Zic1*	Zinc finger protein of the cerebellum 1	Regulatory Nucleic acid binding	1,16 MG-6-13e3	22771	1.67	0.00
6	*Son*	Son cell proliferation protein	Regulatory Nucleic acid binding	1,15 MG-15-193f24	20658	1.42	0.00
7			Similar to RIKEN cDNA0610038D11 of M. *musculus.*/ protein required for cell viability Ynr046wp in yeast[ProtEST],	1,14 MG-14-82n11		1.36	0.00

134

	Gene symbol (MGI)	Name	Role/Functionality Other comments	LION Clone ID	NCBI ID	Ratio	P, %
8	*Itpr1*	Inositol 1,4,5-triphosphate receptor 1	Transport and binding Calcium channel activity	1,12 MG-6-52n4	16438	1.67	0.01
9			ESTs	1,12 MG-12-259k17		1.42	0.01
10	*Zic5*	Zinc finger protein of the cerebellum 5	Regulatory Transcription regulation	1,11 MG-3-4h14	65100	1.39	0.01
11	*Slc1a6*	Solute carrier family 1 (high affinity aspartate/gluta mate transporter), member 6	Transport and binding Sodium di/tri carboxylate symporter activity	1,11 MG-6-15m21	20513	1.53	0.01
12	*Zfp265*	Zinc finger protein 265	Regulatory ATP binding	1,10 MG-6-47h7	53861	1.19	0.04
13			RIKEN cDNA 6530413N01 Similar to Zinc finger protein SLUG (Neural crest transcription factor slug)	1,10 MG-6-47h20		1.17	0.04
14			EST234479 PC12 cells, untreated, pT7T3Pac	1,08 MG-8-12a21		1.22	0.23
15	*Pcp4*	Purkinje cell protein 4	Transport and binding Calcium ion binding	1,08 MG-6-48j13	18546	1.15	0.23
16	Not given	Osmotic stress protein 94 (Heat shock 70-related protein APG	Regulatory ATP binding	1,07 MG-3-272k4	-	1.17	0.57
17	Not given	Phosphatidylin ositol 3-kinase regulatory gamma subunit (PI3-b)	Others	1,07 MG-3-218h7	-	1.17	0.57
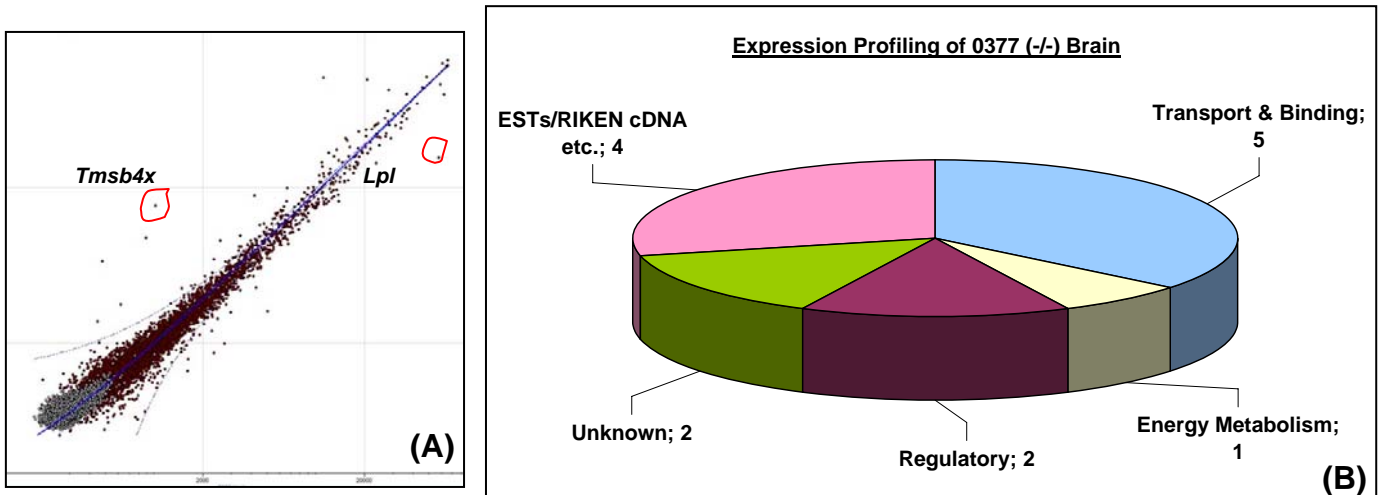
Figure 3.31: Expression profiling results of *O377* (-/-) brain. Figure 3.31A shows the scatter plots of a hybridization experiment which was used for expression data analysis. Figure 3.31B shows a classification of the differentially expressed genes according to their functional annotations. The **X-axis** denotes the **F635 median** and the **Y-axis** denotes the **F532** median (not prominent in the figure as they are screen shots of the computer screen).
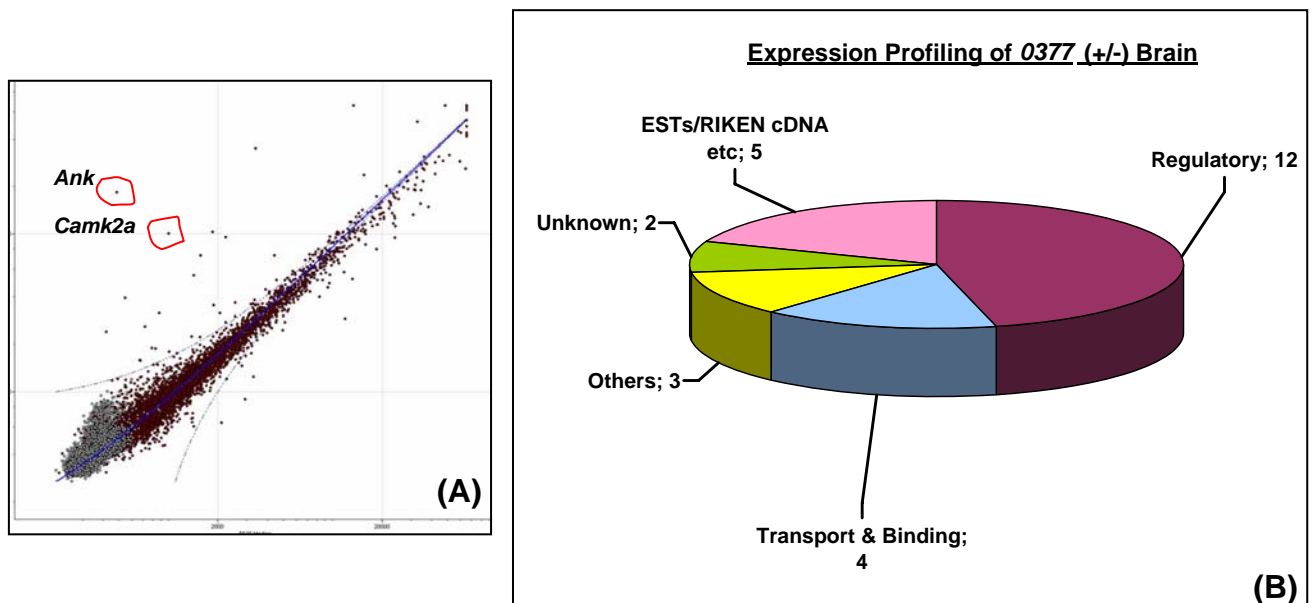
Figure 3.32: Expression profiling results of *O377* (+/-) brain. Figure 3.32A shows the scatter plots of a hybridization experiment which was used for expression data analysis. Figure 3.32B shows a classification of the differentially expressed genes according to their functional annotations. The **X-axis** denotes the **F635 median** and the **Y-axis** denotes the **F532** median (not prominent in the figure as they are screen shots of the computer screen).

3.6.3: <u>Some technical points to be considered for the microarray experiments performed:</u>

i. **Different cut off ratios for analysis of differential expression for (-/-) lens, (-/-) brain and (+/-) brain:** Apparently this may present that different criteria were used to select the differentially expressed genes in different tissues. But it has to be considered that not all tissues/ organs (brain and lens in this case) are affected equally by the mutation in all the genotypes. Thus, the criterion to select the differentially expressed genes had to be optimized according to the degree by which a particular tissue/organ is affected. In this case the mutation (*O377*) affects the lens to a much greater extent than the brain. Thus for the lens with a higher cut off ratio many differentially expressed genes are obtained whereas for the brain a lower cut off ratio had to be considered to choose the differentially expressed genes. The genes screened by this method were analyzed for their significance and were chosen for further analysis. Moreover as these experiments were performed at different time points, the software used for analysis was also upgraded during those time.

ii. **Difference in the number of overlapping genes between the (-/-) brain and (+/-) brain:** The number of overlapping genes in the (-/-) brain sample is lower than that in the (+/-) brain sample. This can be attributed to the difference in the labelling reactions. However, the percentage of overlapping genes in the (-/-) brain samples is good enough ($\sim 1/3^{rd}$ of the average number of total genes detected in each experiment). That in case of the (+/-) brain sample was exceptionally good (>1/2 of the average number of total genes detected in each experiment). The difference in labelling reactions is due to the fact that the experiments were performed at different time points (because of the availability of the animals in specific combinations and maintained conditions). At different time points, the set of dyes are different, the batches of DNA microarray chips (slides) are also different along with different sets of regaents that contribute to the different labelling reaction; but all the experiments were technically good and up to the standard.

iii. **Detection of no overlapping differentially expressed genes between the heterozygote and homozygote brain.** This is a surprising result as one would expect at least some genes to overlap between these two samples. Expression levels of the differentially expressed genes in each sample was cross checked in the other samples. Most of them showed no differential expression in the other sample and six differentially expressed genes of the heterozygote sample were even undetected in the

homozygote sample. This un-detection can be attributed to the lower number of overlapping genes in the homozygote sample compared to the heterozygote sample.

3.6.4: <u>The differentially expressed genes and βB2-crystallin are expressed in similar brain regions:</u>

The expression domains of all the 40 differentially expressed genes in both the homozygote and heterozygote brains as obtained from the databases, shows that they are also expressed in the regions of brain where βB2-crystallin is expressed [i.e. in olfactory bulb, hippocampus, cortex and the cerebellum]. Many of these differentially expressed genes were also expressed in other regions of brain than the ones mentioned. This observation is a hint to consider that βB2-crystallin has a localized function (tissue region or cell specific) in the brain.

3.6.5: <u>Real Time-qPCR of the differentially expressed genes in the (-/-) and (+/-) mutant brain :</u>

Real Time-PCR was also used to verify the expression profiling results of some selected genes. The primers used for this reaction are listed in table 2.15. Analysis of the results was performed using the RelQuant 1.0; [Roche Molecular Biochemicals]. The normalized ratio obtained from the result sheet generated by the software is the actual measure of the differential expression in this method. The differentially expressed genes selected for analyses by this method are mentioned in the following tables 3.5, 3.6 and figure 3.33. Details of each experimental data are mentioned in annexure 5 and 6.

Table 3.5: List of the differentially expressed genes in both heterozygous and homozygous *O377* mutant brains which were selected for Real-Time PCR analysis to verify the expression profiling data-

Mutant Genotype	Target Gene		Expression profiling result
+/-	*Ank* :	Progressive ankylosis	Up-regulated
	Camk2a:	Calcium/calmodulin dependent Protein kinase II alpha	Up-regulated
	Hpcal4 :	Hippocalcin-like 4	Up-regulated
	Nrgn :	Neurogranin	Up-regulated
-/-	*Tmsb4x*:	Thymosin, beta 4, X chromosome	Up-regulated
	Atpv0a1:	ATPase, H^+ transporting lysosomal V0 subunit A isoform 1	Up-regulated
	Lpl:	Lipoprotein Lipase	Down regulated

Table 3.6: Normalized ratios of the target genes following Real Time-qPCR analysis. The data is generated by the RelQuant (1.0) [Roche] software.

Target Gene	Genotype	Normalized ratio	Expression profiling ratio
Homozygote			
Tmsb4x	Wildtype	1.00	1.95 (Up)
	Mutant	1.87	
Atpv0a1	Wildtype	1.00	2.21 (Up)
	Mutant	2.66	
Lpl	Wildtype	1.00	1.83 (Down)
	Mutant	0.55	
Heterozygote:			
Ank	Wildtype:	1.00	1.17 (Up)
	Mutant	1.30	
Camk2a	Wildtype	1.00	1.35 (Up)
	Mutant	1.52	
Hpcal4	Wildtype	1.00	1.17 (Up)
	Mutant	1.12	
Nrgn	Wildtype	1.00	1.15 (Up)
	Mutant	1.12	
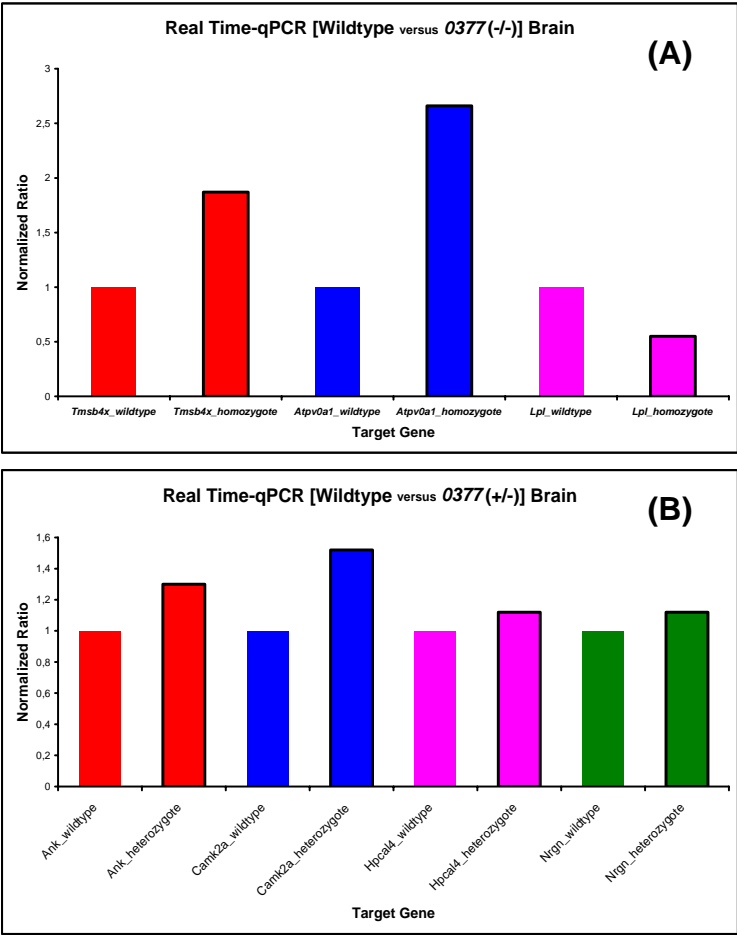
Figure 3.33: Graphical representation of the real time-qPCR results for the Homozygote (Figure A) and heterozygote (Figure B) mutant brain.

3.7: <u>Expression of calcium binding proteins:</u>

The expression profiling results revealed most of the differentially expressed genes in the brain of mutant animals are involved in calcium and phosphate pathways. It was of interest to know about the expression of some major calcium binding proteins because of the reported calcium binding properties [section 1.2.3B-C] (and indications from microarray data, table 3.4) of βB2-crystallin, in the mutant brains, as primary antibodies for them are readily available. Immunohistochemical studies were carried out for calretinin and calbindin (both members of troponin C superfamily) on sagittal sections of brain from both heterozygous and homozygous mutants in comparison to the wild-type. However, no difference in expression was observed in the mutants when compared to the wild-type (also when compared to the Mouse Brain Atlas) for calretinin (Figure: 3.34) and calbindin (Figure: 3.35).

Calretinin has been found to be expressed in the peripheral cells of the dentate gyrus of the hippocampus; in all the 6 layers (1: Superficial layer 2: Optic collicular layer 3: Intermediate gray layer 4: Intermediate white layer 5: Deep gray layer 6: Deep white layer) of the superior colliculi and in the inferior colliculi of the mid brain; and in the granular layer of the cerebellum in both the wild-type and mutants.

Calbindin is found to be expressed in the pyramidal layer of the hippocampus proper and dentate gyrus of the hippocampus, in the intermediate gray layer, intermediate white layer, Deep white layer of the superior colliculi of the mid brain; in the vestibular nuclei and inferior olive of the hind brain and in the Purkinje cells of the cerebellum in all of the wild-type, heterozygote and homozygote animals.

The size of Purkinje cells in the homozygote mutants again looks slightly smaller than the wild-type following calbindin immunostaining, a specific staining for the Purkinje cells, thereby again reconfirming the earlier qualitative observation. Slight differences that appear between corresponding figures are due to different planes of sectioning.

Unaltered expressions of the calretinin and calbindin proteins suggest that the mutation has not affected at least the major calcium binding proteins of the brain.

Calretinin expression:
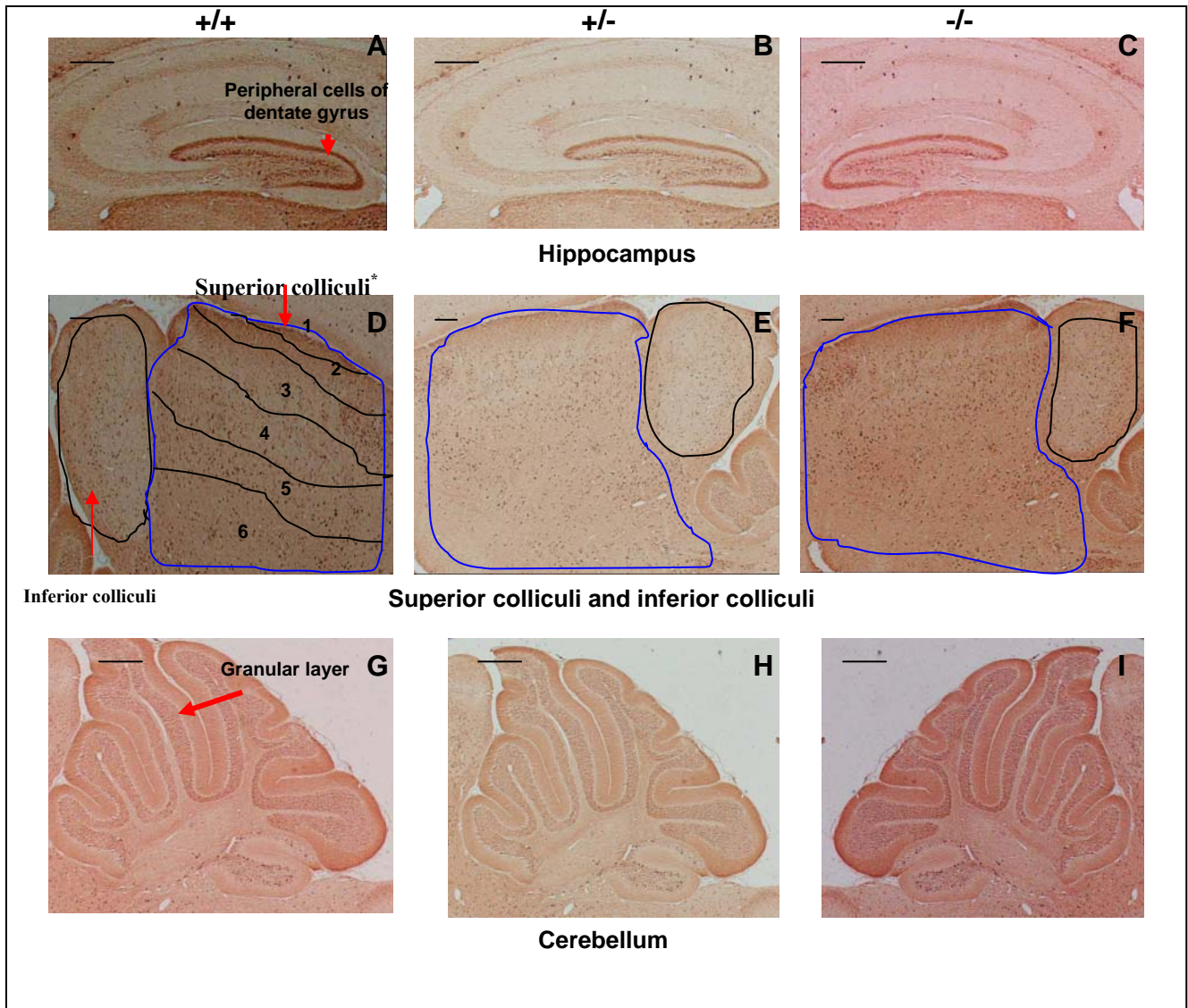
Figure 3.34: Expression of calretinin in the hippocampus (A, B and C); superior and inferior colliculi (D, E, F) and in the granular layer of the cerebellum (G, H, and I) in the wild-type, heterozygote and homozygote brain. Scale bars = 0.1mm (A-C); 0.2mm (D-I)

*Superior Colliculi

1: Superficial layer **2:** Optic collicular layer **3:** Intermediate gray layer

4: Intermediate white layer **5:** Deep gray layer **6:** Deep white layer

Calbindin expression:
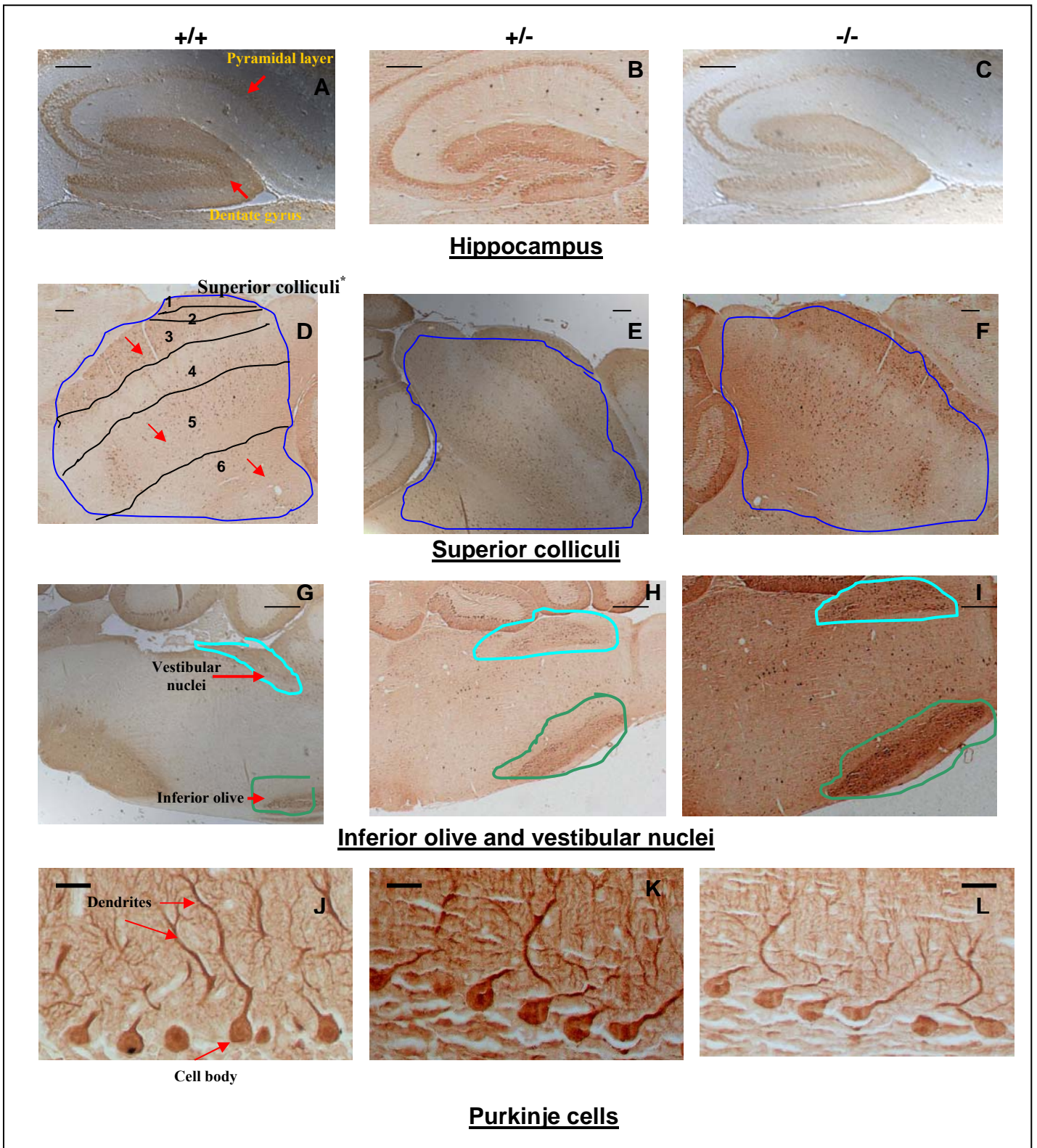
Figure 3.35: Expression of calretinin in the hippocampus (A, B and C), superior colliculi (D, E, F), inferior olive and vestibular nuclei (G, H, and I) and Purkinje cells of the cerebellum (J, K and L) in the wild-type, heterozygote and homozygote brain. Expressions indicated by red arrows. Scale bars = 0.1mm (A-C); 0.2mm (D-I); 5µm (J-L). *Superior Colliculi

1: Superficial layer 2: Optic collicular layer 3: Intermediate gray layer
4: Intermediate white layer 5: Deep gray layer 6: Deep white layer

Chapter 4

Discussion

Identification and characterization of mutant *O377* at the phenotypic and molecular level has helped us to know more about the causes, mechanism, progression, development and consequences of dominant progressive cataracts due to mutation of the *Crybb2* gene in a new murine model (After *Philly* mouse and *Aey2*). The other interesting and novel aspect that came out from this work is the knowledge about the temporal and spatial expression of βB2-crystallin in the brain. Molecular phenotyping coupled with traditional phenotyping studies (histology etc.) have shed some light on the potential non-refractive (catalytic!) function played by βB2-crystallin in the brain, which can also be considered as an essential hint about its role in non-lenticular (retina) and other non-ocular (testis) tissue where it is expressed apart from its major structural role in bringing out lens transparency.

4.1. Molecular basis of the *O377* mutation:

The **A→T** bp substitution in the first position of an acceptor splice site of intron V of the *Crybb2* gene among the offsprings of the paternally 3 Gy X-irradiated mouse has lead to the activation of a cryptic splice site, that have resulted in the incorrect splicing and the corresponding mRNA has an insertion of 57 bp at the beginning of exon VI (**Favor, J., unpublished**). As a result, the βB2-crystallin^{O377} protein is 1.9 kDa heavier than its wild-type counterpart due to the inclusion of 19 amino acids, as predicted. In case of both *Philly* mouse (Chambers *et al*., 1991) and *Aey2* (Graw *et al*., 2001) the βB2-crystallin protein is truncated as a result of the respective mutations (Refer to sections 1.3.2A-B for details). However, in all these three cases (including mutant *O377*) the IVth motif of the protein is disturbed. Predictive structural modelling of the βB2-crystallin^{O377} protein has shown that the βB2-crystallin protein is misfolded near the carboxy terminus (Figure 3.8) which probably leads to its aggregation in a similar fashion as observed in case of some γ-crystallin mutations (Sandilands *et al*., 2002). It must be mentioned here that, though the *O377* mutation was detected following irradiation experiments, yet such **A→T** bp substitutions are uncommon due to irradiation (Wijker *et al*., 1998). Thus, it might well be a spontaneous mutation but coincidentally detected in X-irradiation experiments.

4.2. <u>Disease development (cataractogenesis) in the *O377* mutant eye:</u>

All the heterozygous and the homozygous mutant animals start developing lens opacity as early as by the 3rd week of age (as observed by Dr. J. Favor, Dr. A. Neuhäuser-Klaus following slit lamp screening). At ages earlier than this, the onset of the cataractous phenotype is unpredictable (i.e. a particular age cannot be referred when onset of cataractous phenotype definitely takes place) and this can de attributed to the animal wise variation, a natural phenomenon for a biological system. In few cases, the cataract formation sets in by the 2nd week but this is not usual. The phenotype and histological alterations are very severe even among the heterozygous mutant animals along with the homozygous animals (Figure 1.10 and 3.10). Because of the expression of lens opacity among the heterozygous animals and development and increasing severity of the cataractogenesis with age, it can be referred to as a **dominant progressive cataract**.

The mechanism of the development of lens opacity for all the affected animals is due to the disorganization of the fiber cell anatomy because of the presence of the misfolded βB2-crystallin^{O377} protein in the entire cortical regions of the lens of the mutant (in wild-type βB2-crystallin protein is present only in the lateral cortical regions; Figures 3.12, 3.13) leading to the disturbance in the clarity and refractive index of the lens. High vacuolation of the lens tissues takes place due to the presence of this misfolded βB2-crystallin^{O777} protein, which as a result fails to organize the compact highly refractive and transparent lens structure especially in the two lateral cortical regions (evident from the patchy appearances in these regions in the mutant; Figures, 1.10, 3.10). Disorganization of the lens fiber cells also disturbs the adjacent tissue structures and as visible from the histological studies (Figures 1.10, 3.10) the entire lens tissue gets highly vacuolated and disorganized due to the change of cytosolic viscosity. In the *Aey2* mutants (Graw *et al*., 2001), another *Crybb2* mutant (where also the IVth motif of the βB2-crystallin protein is affected), a striking abnormality of the anterior suture, occurrence of a layer of dust like particles in the anterior cortex and intercellular cleft in the lens nucleus was observed. These are caused by disturbed denucleation process in those fibers, which are completely degraded in the normal inner lens fiber. This abnormality is attributed to impaired chromatin degradation. Central anterior region of the lens has irregular fiber cells in outer cortex with a distinct zone of discontinuity between the outer and inner fiber cells. The cellular structures of the inner fiber cells are markedly destroyed and the epithelial cells remained unaffected. The remnants of the fiber cell nuclei remains in the lens bow of the *Aey2* lens. Partially degraded nuclei are present behind the zone of discontinuity from the outer

cortex to the cataractous inner cortex (Graw *et al.*, 2001) These histological observations in the *Aey2* are very similar to that observed in the *Philly* mouse, the first *Crybb2* mutant cataract mouse model. Similar histological changes in the eyes of *O377* mutants can be explained by the fact that the same motif (IVth) is affected also in this case.

The misfolding of the protein probably leads to altered aggregation properties of βB2-crystallin as observed in case of γ-crystallin mutants causing inherited cataracts (Sandilands *et al.*, 2002). In three different inherited murine cataracts involving γ-crystallin mutations, large inclusions containing the altered γ-crystallin were found in the nuclei of primary lens fiber cells. Their formation preceded not only the first gross morphological changes in the lens but also the first signs of cataract. The inclusion contained filamentous material that could be stained with Congo red, an amyloid detecting dye. The mechanism involved in these types of cataractogenesis is therefore by nuclear targeting and deposition of amyloid-like inclusions. The mutant γ-crystallins initially disrupt nuclear function but then it progresses to a full cataract phenotype (Sandilands *et al.*, 2002). The up-regulation of ***Aplp1*** coding for amyloid beta (A4) precursor like protein in the P21, *O377* (-/-) lens, detected following expression profiling studies is a clear hint that mechanisms like amyloidosis are involved in cataractogenesis also in this case similar to that of γ-crystallin mutants.

The variation in the etiology of the disease among different *O377* mutant animals of the same age and time can be attributed to the different biochemical profile of each animal and their intrinsic property to resist disease, a natural biological phenomenon. Up-regulation of the βB2-crystallin in 1 day old mutant animals at both transcript and protein levels, as detected by *in-situ* hybridisation and immunohistochemical studies (Figures 3.11-3.13) suggests a loop mechanism for the control of *Crybb2* regulation. The cells and tissues probably perceives from its disorganized state that the βB2-crystallin^{O377} protein produced is not functioning optimally and therefore overproduces it (also in anterior and posterior cortical regions) to overcome the defect. Since the change is at the genetic level, all the proteins produced are misfolded and adds up to the collapse of the lens structure (Figure 1.10, 3.10). Lowered expression of *Crybb2*^{O377} at the 3rd week of age as detected by microarray experiments and Real Time-PCR is due to the collapsing lens structure. A technical difficulty during the dissection of the mutant lens (which becomes highly fragile at the age of P21 because of the cataract) acts as a hindrance against maximum tissue recovery. Since the degree of cataract formation is also variable among the animals the fragility of the tissues also vary. Thus the recovery of the lens tissue for the mutants of age P21 is always lower than that of wild-type. This could possibly add up to the detection of lowered expression of *Crybb2* and other

crystallins in the *O377* mutants at this age. Microarray experiments were performed with RNA extracted from pooled lens tissues from the eyes of eight *O377* (-/-) animals (P21) whereas the Real-Time PCR experiment for *Crybb2* was performed with two lenses from the eyes of one *O377* animal (P21), which explains the difference in the ratios of down regulation of this gene obtained from these two different methods; though both the procedures revealed *Crybb2* in *O377*(-/-), P21 lens is significantly down regulated.

At an age of 3 weeks, when the cataract sets in among all the mutant (heterozygote and homozygote) animals; the lens tissue recognizes the irreversible disruption of its structure at molecular, biochemical and histological level which is evident from the differential expression of a huge number (70 up-regulated and 46 down regulated; annexure 3) of genes involved in diverse biochemical processes (Regulatory, transport and binding, energy metabolism, structural proteins). Since, the suggested self repairing mechanism of the lens tissue (evident from the up-regulation of *Crybb2* at both transcript and protein level in 1 day old mutant eye) failed to prevent the disruption process, the lens structure starts collapsing and simultaneously expression of all crystallin genes (annexure 3) which are essential for lens structure (high refractive index and clarity) are found to be highly reduced at this age. Differential expression of such a large number of genes (116) at this age is a clear reflection of how severely the lens tissue is affected. However, it is not clear, which of these genes are differentially expressed prior to or after the disturbance of the tissue structure has set in (To address this biological issue, an age gradient expression profiling study is necessary; please refer to the note at the end of this chapter). The differential expression of so many genes (annexure 3) involved in diverse biochemical processes in the *O377* (-/-) mutant lens in a way can be regarded as a reflection of the major biochemical changes which can be observed in the *Philly* mouse lens associated with a variety of osmotic changes [refer to section 1.3.2A]. At 20 days of age, in *Philly* mouse there is an increase in lens water along with an alteration in electrolyte levels. Lenticular sodium rapidly increases and potassium level decreases. Concomitant with the cataract formation is an increase in total lenticular calcium and a decrease in lens dry weight, in reduced glutathione and ATP (Kador *et al.*, 1980). Changed patterns of membrane glycoproteins (Garadi *et al.*, 1983) and membrane lipids (Andrews *et al.,* 1984) are also observed. The process of cataractogenessis in these three murine models (*Philly* mouse, *Aey2* and *O377*) is caused by similar alterations in the histological and biochemical levels as in all the three cases the IVth motif of the βB2-crystallin protein is affected.

One good approach to reveal more on the molecular changes during the pathogenesis would be to perform expression profiling studies (Please refer to the note at the end of this chapter) on the lens tissue in an age gradient manner (P1, P7, P14 etc.). This would help to define exactly how the genetic cascade is altered with the disease progression. But the hindrance in such studies is the huge amount of tissue required for the extraction of sufficient RNA to perform DNA microarray experiments maintaining the strict specifications required to reduce biological noise. This would obviously demand lot of time flexibility. Because of the altered expression levels of *Crybb2* at P1 and P21, it would be of interest to make such an age gradient *in-situ* hybridisation to know more about its regulation. As the lens tissue hardens in post natal stages, paraffin sections of it cannot be prepared (except for P1 or earlier) which possess a technical draw back in performing such a study.

4.3. *Crybb2* in the retina:

Detection of the expression of *Crybb2* in the inner limiting membrane of the retina near the iris following *in-situ* hybridisation experiments leaves some open questions regarding the specificity of the detected expression. Firstly, there remains a chance of overflow of the stain from the nearby lens which has high expression (i.e. highly stained) of *Crybb2*, resulting in back ground staining; secondly, there was no detection of *Crybb2* or βB2-crystallin by other independent methods like RT-PCR or immunohistochemistry.

The probability of background staining can be excluded since these *in-situ* hybridisation results are reproducible; and observed in at least 3 different experiments with 5 different animal samples involving two different wild-type control sets (*C3H* and *C57BL6/J*). The fact that *Crybb2* is upregulated in the mutant lens although the retina of the mutant animal does not show any staining strongly emphasises that the detected expression is not due to an overflow, which would be expected more in this case. Thus the *in-situ* hybridisation staining are specific.

Reports from Head *et al*. (1995) showed the expression of βB2-crystallin in mouse and cat neural and pigmented retinas and in cat iris. This is particularly interesting in respect to the findings of *Crybb2* expression in the internal limiting membrane of the retina near the iris in both C3H and *C57BL6/J* mice. *Crybb2* transcript could not be detected in the retina following RT-PCR, though there are reports of its detection following RT-PCR (Magabo *et al*., 2000; Dirks *et al*., 1997).

One probable reason that *Crybb2* remained un-detected by RT-PCR analysis could be due to the particular region of the retinal tissue (internal limiting membrane near the iris) which was

missed out while dissection, or this tissue region was possibly required in much more quantity, taking into account the low expression level of *Crybb2* transcript as observed following *in-situ* hybridisation experiments. Xi *et al*. (2003) reported the expression of β-crystallins in general in the ganglionic cell layer, inner photo receptor layer and outer nuclear layer of the retina (10-20 days old animals) but their study was not specific to βB2-crystallin. It appears that other β-crystallins are expressed in these layers but may be not the βB2-crystallin particular. There remains also the possibility that the spatial expression of βB2-crystallin is variable depending on the metabolic status of the cells and tissues. Moreover, the *in-situ* hybridisation experiments were performed with eyes of 1 day old animals; it would be interesting to know if βB2-crystallin is also expressed in the other retinal layers at later ages. Use of immunohistochemistry to detect the expression of βB2-crystallin in the retina posed some technical problem. For the antigen retrieval step of immunohistochemical studies, the tissue is required to be boiled in microwave, and this step needs to be optimized for each tissue type. Retina and lens being two different tissues in the eye, their antigen retrieval varies accordingly. For lens it is 30- 45 seconds (with more than 1 minute the lens collapses and spills), whereas for the retinal tissue it is more. If the lens gets separated from the rest of the eye, the retinal tissue structure does not remain intact, especially considering the region of interest being near the iris [the internal limiting membrane of the retina near the iris]; so this experiment is not possible to perform.

4.4. βB2-crystallin in the brain:

Expression of βB2-crystallin in non-lenticular (retina, near iris region) and non-ocular tissues like brain (olfactory bulb, hippocampus, cortex and cerebellum) and testis (Magabo *et al.,* 2000) indicates a non-structural and non-refractive function in these tissues. The expression of βB2-crystallin from the different regions [B1-B5, Figure 3.5A] of the brain; and later its detection in some specific neuronal cell types of the brain [glomerular and mitral cell of the olfactory bulb; CAI, CAII, CAIII (CA stands for *Cornu ammonis*) and dentate gyrus of the hippocampus; Purkinje cells and stellate cells of the cerebellum and in the pyramidal cells of the cortex] by immunohistochemical studies reassigns the indication of its non-refractive role which is most probably prominent in the age between 3-4 weeks (i.e. when βB2-crystallin is best expressed). Detection of βB2-crystallin expression in the axonal fibres of the Purkinje cells of the cerebellum (Figure 3.22) in one animal out of the five tested for both of wild-type and mutant provides a good example of animal wise variation.

Detection of the entire *Crybb2* transcript in the wild-type and *O377* brain suggests that the detection of only the 3'-end of *Crybb2* in *Aey2* mutant brain (Graw *et al.*, 2001) was probably not due to alternative splice variants, instead the PCR conditions had to be optimized differently to detect *Crybb2* in the brain. As discussed in section 3.1B, the PCR conditions were optimized differently to detect *Crybb2* in brain than that in lens because of its low expression in brain.

Higher number (11%) of Purkinje cells (stereologically counted) and their smaller size (only a qualitative observation) in the homozygous *O377* mutants coupled with the information about the functionalities of the differentially expressed genes in the mutant brain (i.e. involvement in phosphate pathways in the homozygous animals and in calcium and phosphate pathways in the heterozygous animals, tables 3.3 and 3.4) and the expression of these differentially expressed genes (based on annotations in the databases) also in the domains where βB2-crystallin is expressed in the brain (i.e. olfactory bulb, hippocampus, cerebellum and brain cortex); animal wise variation (in some cases at least) in expression levels (different Western blot experiments showed the intensity of bands developed for βB2-crystallin to be variable for different animals in spite of using similar concentrations of protein; refer to section 3.2.2) and the general low expression of βB2-crystallin in brain [revealed from RT-PCR (section 3.1B) and Western blot studies] leads to hypothesize that βB2-crystallin has a secondary or tertiary role in the complex biochemical pathways in brain and retina (may be also in the testis) in a tissue region/cell specific manner. The role of βB2-crystallin in brain is referred to as secondary or tertiary as the *O377* mutant mice does not exhibit any obvious or major defect in the brain in terms of morphology, histology and physiology that may posses a challenge to its normal life/survival. It is always debatable if a 11% increase in cell number (Purkinje cells) observed in the Vth cerebellar lobe in the *O377* (-/-) mutant is physiologically or pathologically significant. This slight but statistically significant alteration in the cell number (11% higher) is possibly due to some metabolic changes at the cellular level and to compensate that the cell size is reduced (a qualitative observation only) or *vice versa* in the homozygote mutants. To identify such changes at the metabolic level very specific functional analysis like measurement of calcium (Calcium imaging using the dual fluorescence dye Fura-2, AM; A. Stampfl, Institute of Toxicology, GSF) and phosphate levels based on evidences from other experiments are necessary. Differential expression of genes involved in phosphate and calcium pathways in the mutant brain are interesting observations especially in the light of Purkinje cell frequency and size, as both these pathways and their homeostasis are well known to influence the process of cell cycle (Baran, 1996; Neef and Kladde, 2003; Gilles

et al., 1981). Since, no change in the gross morphology (larger or more expanded etc.) of the Vth cerebellar lobe is observed in spite of the 11% increase in the number of Purkinje cells and the qualitative observation of slightly reduced size of the Purkinje cells looks like an automated mechanism to maintain the normal morphology and physiology.

To mention, the heterozygote mice were screened for behavioural phenotypes as a functional analysis [Modified Hole Board (MHB) test] [Ohl *et al.*, 2001] at the German Mouse Clinic (GMC), GSF. These tests were carried out by Dr. S.M. Hölter and Dr. V. Pedersen. MHB tests revealed the male heterozyous mutants to be tendentially less anxious. However, the behavioural analysis of the homozygote animals were postponed due to unavoidable circumstances (please refer to the note at the end of this chapter) as at least 60 animals in litter mates are required for these tests (15 mutant and 15 wild-type of each sex, 6 weeks old). Nevertheless, expression of βB2-crystallin in the hippocampus, which has important inputs to the amygdala (centre of emotional and anxiety related behaviour), may provide some explanation for the less anxious behaviour in heterozygous male mutant mice. But it is important to know the behavioural pattern of the homozygous mutant mice and to verify this phenotype, if this is a sex specific effect at all. It would be interesting to know the level of stress hormones (Following forced swim tests etc.) and sex hormone (speculating any effect of this mutation on the cells (leydig cells!) of testis thereby influencing the production of testosterone, as *Crybb2* is also reported to be expressed in testis by Magabo *et al.*, 2000) of these so called less anxious male mutant mice. The question of the effect of cataract on behavioural phenotyping can be nullified based on the fact that the wild-type (C3H) mice are blind by the 3rd week of age due to the retinal degeneration (rd) caused due to a non-sense ochre mutation (C→A transversion in codon 347) in the rod photoreceptor cGMP phosphodiesterase (PDE) beta-subunit gene that truncates the normal gene product by more than half including the putative catalytic domain (Pittler *et al.*, 1991). The mutant *O377* is also on the C3H background, therefore the cataract as such does not influence their vision at this age onwards.

Detection of no overlapping differentially expressed gene (cross checked in the microarray slides of the +/- and -/- samples, refer to section 3.6.3) between the homozygote and heterozygote brain is surprising but can be explained by the gene dosage effect, animal wise variation in expression levels of βB2-crystallin (as observed from Western blot experiments) and influence of environmental factors (speculated to be stress related as β-crystallins share structural similarities with some stress related proteins, refer to section 1.2.3B). The heterozygous and homozygous animals were collected at different time points and prior to the

collection of the homozygote animals there was a long breeding stoppage (4-5 months; please refer to note at the end of this chapter) due to unavoidable circumstances, which may have contributed to this surprising result. Up-regulation of *Atp6v0a1* (ATPase, H+ transporting lysosomal V0 subunit A isoform 1) in homozygote brain and *Atp6v0c* (ATPase, H+ transporting V0 subunit C) in homozygote lens definitely suggest the role of *Crybb2* in phosphate homeostasis in both these tissues. The differentially expressed (very low level of differential expression; border of significance = 1.15) genes in the heterozygous mutant brain are mostly involved in calcium and phosphate pathways. Thus, it appears that βB2-crystallin influences phosphate and calcium homeostasis in some specific neuronal cell types of some brain regions (Localized effect). It would be interesting to know if there is also a tissue specific promoter for the βB2-crystallin like that of αB-crystallins in cardiac muscles (αBE-4 element) [Gopal-Srivastava *et al.*, 1995].

During the course of expression profiling experiments the entire brain was used to extract RNA which is obviously the first route of approach. Since, most of the differentially expressed genes have multiple domains of expression in the brain; it might be worthy to perform expression profiling studies taking separately the hippocampus, cerebellum and other brain regions of interest. As both hippocampus and cerebellum cannot be dissected out from the same mouse brain, one would require huge number of tissues to extract enough RNA from animals maintained under specified conditions and combinations, which for sure would consume lot of time. But in that case it might be necessary to pool samples from different mutant animals and this may interfere with the accuracy of the obtained results specially in this case when the difference is so subtle. On the other hand, if there is any gene that is differentially expressed specifically in a particular brain region but not in others probably can be detected in this approach which might have escaped the significance level in the method practised. Advances in protein microarray techniques might reveal some more unknown happenings at the proteomics and metabolomics level.

4.5. <u>Non-structural role βB2-crystallin?</u>

'Non-crystallin functions of crystallins' are defined as cellular physiological activities other than the structural-physical functions such as transparency, optics and refraction, historically associated with the crystallins (Bhat, 2004). Crystallins by definition are proteins that are present in the ocular lens at high concentrations to generate transparency (Bhat, 2003).

Because high concentrations of proteins are not thought to be necessary for catalytic or regulatory functions, the role of crystallins in general have been perceived as only structural proteins of the lens fiber mass engaged in maintaining the refractive index (Lubsen *et al.*, 1988; Horwitz, 2003; Wistow and Piatigorsky, 1988). There are no evolutionary constraints apparent in the physico-chemical properties of crystallins that seem to predispose a protein to provide transparency. It is well accepted that crystallins come up with a myriad of stabilities and structures [α-crystallins are polydisperse multimeric proteins (molecular mass 300,000-1,000,000); γ-crystallins are monomeric (molecular mass 20.000) while β-crystallins are oligomeric with molecular masses intermediate between α-and γ-crystallins]. There is no single structure, fold or characteristic domain or a sequence motif that makes a protein a 'crystallin'. α-crystallins and β/γ-crystallins are largely composed of beta sheets (Bax *et al.*, 1990); infact γ-crystallins are almost entirely made up of antiparallel beta sheet (Greek key motifs) which makes them highly compact proteins (Blundell *et al.*, 1981). On the other hand δ-crystallins (a taxon specific crystallin) of bird lens is predominantly α-helical (Simpson *et al.*, 1994).

Transparency is a physical phenomenon that must be dictated by universal physico-chemical principles. Phenotypes (normal or pathological) derived from or associated with such an universal physico-chemical manifestation should be identical or at least similar. Thus, if crystallins only participate merely as inanimate structural building blocks to create transparency, a mutation in a structural protein (affecting the same region of the protein) that is present in high concentrations is expected to create more or less similar phenotype. But a tremendous heterogeneity in the cataract phenotype-temporal, spatial and morphological can be found out (Francis *et al.*, 2000; Harding, 2002; Spector 1984).

A classic example of such heterogeneity comes from the phenotype of a *CRYBB2* mutation (Q155X) affecting three geographically and genetically disparate pedigrees who exhibit morphologically distinct cataract phenotypes. This mutation in the βB2-crystallin in human brings about: a Coppock-like cataract (CCL) involving the embryonic and foetal nucleus in a Swiss family (Gill *et al.*, 2000), a Cerulean cataract with opafication in concentric layers in an American family (Litt *et al.*, 1997) and a 'sutural cataract with punctuate and cerulean opacities' in an Indian family (Vanita *et al.*, 2001) [Refer to section 1.3.1A-C for details]. It is obvious from this hereogeneity that βB2-crystallin is not merely a structural protein but also an active polypeptide with non-refractive functions modulated by local anatomy, physiology and genetics of the lens fiber cells (Straatsma *et al.*, 1984).

Bhat (2004) presented a hypothetical schematic diagram (Figure 4.1) depicting the possible molecular links between crystallins and lens homeostasis. It is probable that that the initiating events that lead to age related cataractogenesis reside in such molecular relationships than in the inanimate structural (refractive) crystallin function.
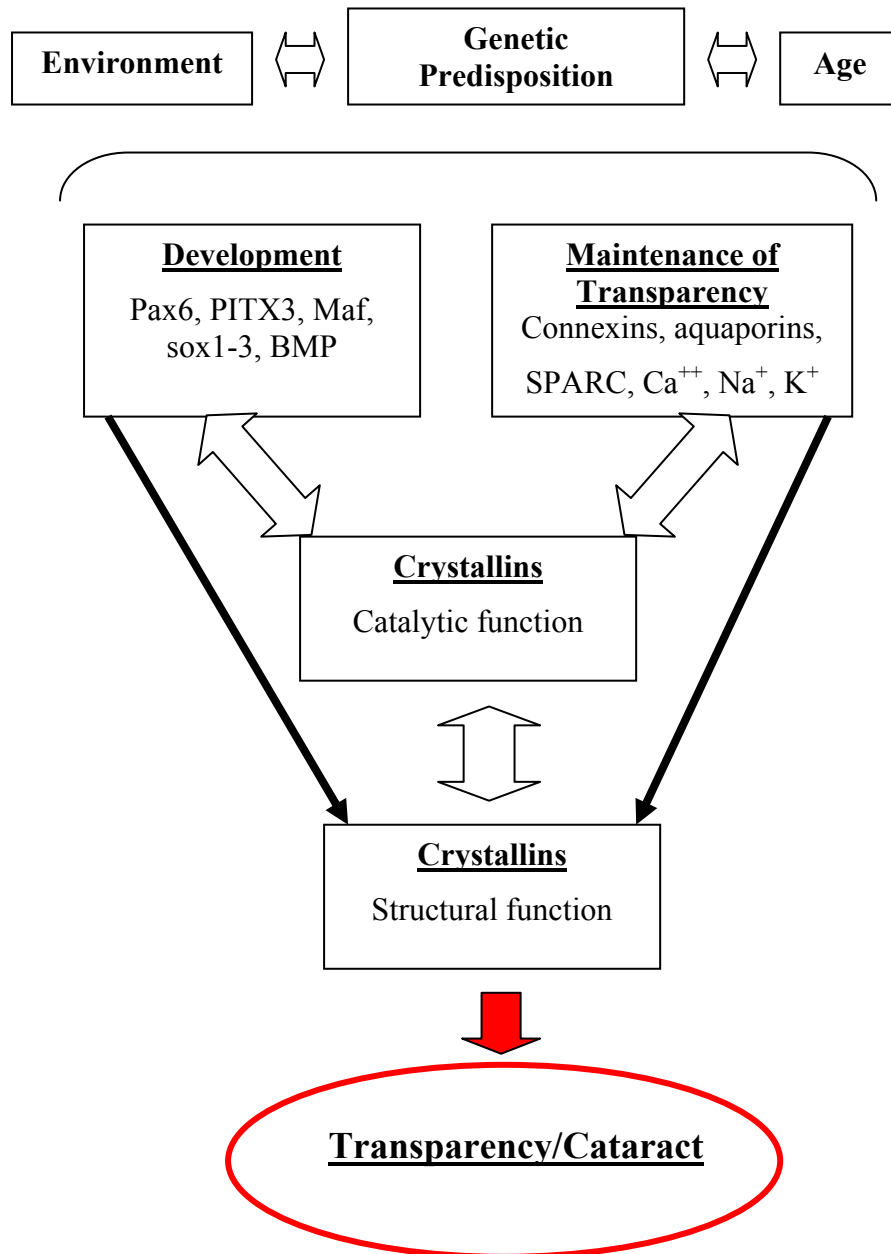
Figure 4.1: This hypothetical schematic diagram represents the central role of non-crystallin functions of crystallins, which impacts lens development, physiology as well as crystalline function and therefore transparency. All the rectangular boxes representing discrete physiological compartments are connected by double headed arrows indicating interactions, influences and modulations. The phenotype of the ocular lens muts be considered as a sum total of environmental influences and aging and their interactions with genetic factors (indicated at the top of the schematic). Presentation of crystallins at the centre does not mean the exclusion of the important contributions of the non-crystallin proteins, which may also affect the structural functions of the crystallins as shown by pointed arrows at Crystallins, SPARC, secreted protein, acidic and rich in cysteine. (Bhat, 2003). This schematic is reproduced from Bhat, 2004.

Detection of the expression of βB2-crystallin in the inner limiting membrane of the retina of C3H and *C57BL6/J* mice and in some specific neuronal cell types of the olfactory bulb (Glomerular and mitral cells); cortex (Pyramidal cells of layers three and five); hippocampus [CAI, CAII and CAII (CA= *Cornu ammonis*) region cells and dentate gyrus]; and the cerebellum (Purkinje cells and stellate cells) [Refer to sections 3.4.2-3.4.5] in both C3H and *O377* mutant along with the reported expression of βB2-crystallin in testis (Magabo *et al.*, 2000) further established the thought about its non-structural and non-refractive function. Expression of βB2-crystallin in such specific neuronal cell types of the brain and differential expression of some genes in the mutant brain is definitely a hint of its involvement in other cellular processes. Since the expression of βB2-crystallin in brain is approximately 16 fold low (as detected by Western blot experiments with gradient of protein concentration; Figure 3.7B, Section 3.2.2) compared to lens, it is unlikely that it plays any structural function in those cell types where it is expressed. Usually proteins having catalytic functions are required in such lower amounts. Moreover, the increase (11%) in the number and reduction in size (qualitative observation) of Purkinje cells in the Vth cerebellar lobe (at vermis) of the homozygous *O377* mutant mice at the age of 3 weeks indeed suggest its role in other cellular processes. It is a matter of speculation if the non-structural role of βB2-crystallin becomes more prominent under special conditions (like cellular stress etc.) as this *O377* mutation does not bring out any major alterations in the brain morphology, histology and physiology in the mutant animals under normal condition. Correspondingly the differential expressions of some genes (14 in the homozygote and 26 heterozygote) which are mostly involved in phosphate and calcium pathways do indicate its role in the complex molecular cascade of the cells where it is expressed.

β/γ-crystallins, as already mentioned, are characterized by Greek key motifs (a structure that is composed of 40 residues that fold into anti-parallel β strands). This characteristic is also shared by epidermis-specific differentiation proteins like AIM1 (absent in melanomas 1); stress related proteins of microorganisms like protein S, sperulin 3a etc. and some more (refer to section 1.2.3B). This Greek key motif is involved in binding calcium (Rajini *et al.*, 2003). It is possible that the calcium binding property of γ-crystallins (Rajini *et al.*, 2001) is more important than their crystallin function so long as the emergence of transparent phenotype is concerned. Evidences of the presence of protein-kinase C phosphorylation site immediately in front of the Greek key motif among all basic crystallins (βB2-crystallin being one such) [Zarbalis *et al.*, 1996], and *in-vivo* phosphorylation of the Ser[230] in the βB2-crystallin (Kleiman *et al.,* 1988) are important clues to its possible role also in phosphate homeostasis.

Structural patterns like the high β sheet content of the βB2-crystallin protein along with the reported Greek key fold as novel calcium binding motifs (similar to that of the helix loop helix structures of typical calcium binding proteins) leads to the speculation of its possible role in conferring stability to other cytoplasmic proteins and/ in ensuring the maintenance of storage levels of cytoplasmic calcium (Norledge *et al.*, 1997). The non-refractive functions of crystallins in the retina in general are attributed to be in cell survival and genomic stability (Xi *et al.*, 2003).

Based on the mentioned facts and experimental data it can be hypothesized that βB2-crystallin is possibly involved in calcium and phosphate homeostasis (in non-lenticular and non-ocular tissues) in a tissue region and/cell type specific manner apart from its well established refractive and structural function in maintaining (and probably also in bringing about) the transparency and clarity of the lens necessary for vision. The exact homeostatic function of βB2-crystallin might be elucidated under special cellular/tissue conditions (like stress etc.) considering that the other Greek key motif containing proteins are also stress related. But the exact nature of this cellular or physiological stress, if true, remains to be identified. Experimental approaches by over-expressing βB2-crystallin^{O377} in cell culture system could prove to be useful in identifying the changes in response to particular stress related stimuli.

To conclude, this study describes the third allele of mouse *Crybb2* gene, providing a further excellent animal model for the homologous disease in humans. Moreover together with the reports in the literature concerning mutations affecting βB2-crystallin in human and mouse along with other crystallins, this work demonstrates their importance in the functional integrity of ocular lens. The essence of this work is the description of the expression of βB2-crystallin in the brain and the consequences of the mutated βB2-crystallin in the brain at histological and molecular level. Studying the role of βB2-crystallin outside the lens is of particular significance because the non-structural role of βB2-crystallin always get masked by its major structural and refractive function in the lens. Our knowledge about the molecular mechanisms involved in the initiation and progression of cataractogenesis is therefore enhanced together with the first insight about the non-structural function of βB2-crystallin in brain. In the long run, these information should provide important inputs for the development of anti-cataract agents considering hereditary and senile cataracts as the major cause of blindness world-wide [By the year 2020, the number of blind people in the world will rise to 45 million (Foster 1999), the vast majority due to untreated cataracts, signifying the huge socio-economic impact of the disease and a growing medical problem]. The study has also

shown specifically the temporal and spatial expression of βB2-crystallin in the brain together with the effect of mutation, at histological and molecular level in the brain thereby establishing its importance in the brain and possibly in other non-lens tissues where it is reported to be expressed. This work has also opened ideas for more basic research concerning molecular mechanism of cataract and the role of βB2-crystallin in other tissues.

Note:

There were some experiments which were planned [In-situ hybridisation experiments of some of the differentially expressed genes in brain; Age gradient expression profiling of the lens] but could not be executed due to time constrains. Between the time period [March 2004-June/July 2004] it was not possible to avail any mice from the mouse room (from where I received mutant O377 mice) of the animal facility of GSF, Neuherberg because of breeding stoppage for some important and unavoidable circumstances related with maintenance of the animals. This time lag proved to be crucial later due to the time limitations for this project. During this time, wild-type (C3H) mice from other mouse rooms (not under the mentioned regulation at that point of time to my knowledge) were availed to standardize the experiments of calcium imaging (Collaboration with A. Stampfl, Institute of Toxicology, GSF) of the neurons from primary hippocampal cultures, but these experiments unfortunately were unsuccessful as a base line to measure calcium levels in these cells could not be achieved. In order to utilize this time optimally experiments with previously stored materials (pending Western blots, and PCRs and imunohistochemistry of calcium binding proteins) were performed.

5.1. <u>Summary:</u>

Mutant *O377* represents a new murine dominant progressive cataract model due to mutation in the βB2-crystallin (*Crybb2*) encoding gene. The mRNA contains a 57 bp insertion at the beginning of exon VI resulted due to incorrect splicing because of an A→T bp substitution in the acceptor splice site of intron V, detected among offsprings of paternally irradiated (3 Gy-X) mice. As a result, the βB2-crystallin^{O377} protein contains 19 amino acids more and therefore is 1.9 kDa heavier than the wild-type form (23 kDa). It is misfolded near the C-terminus due to this 19 amino acids insertion and is deposited around the entire cortical region of the mutant lens resulting in opacity. Both the wild-type and mutant form of βB2-crystallin has also been detected in the wild-type and mutant brain respectively at the transcript and protein level.

The mutant lens develops high vacuolation and patchy appearances in the region of lens fiber cells and cortex and develops cataract as early as by the 3rd week of age. At this age 116 genes, involved in various biochemical activities are found to be differentially expressed in the homozygous mutant lens suggesting severe disturbance at the molecular level. Expression of βB2-crystallin in the internal limiting membrane of the retina (not-detected in *O377* mutants); glomerular and mitral cells of the olfactory bulb; CAI, CAII and CAIII region (CA= *Cornu ammonis*) cells and dentate gyrus of the hippocampus; pyramidal cells of the cortex and in the Purkinje cells and stellate cells of the cerebellum in both wild-type and mutant suggests strongly towards its non-structural function.

Higher number (11%) of Purkinje cells in the Vth lobe of the cerebellum (at vermis) in the homozygous mutants further suggest that βB2-crystallin indeed has some non-structural function. Detection of differentially expressed genes (with expression domains similar to βB2-crystallin) involved in phosphate and calcium pathways in the homozygote and heterozygote brain at the age of 4 weeks are hints to consider the role of βB2-crystallin in phosphate and calcium homeostasis in a localized manner coupled with the already known information regarding the calcium binding properties, possible phosphorylation and structural similarities of the β/γ-crystallins with some Greek key motif containing proteins of lower organisms and differentiating tissues.

This work would therefore further enhance our knowledge on the mechanism and progression of cataractogenesis and for the first time has shed light on the temporal and spatial expression of βB2-crystallin in the brain along with some direct insight on its possible non-refractive role.

5.2. **Zusammenfassung**

Die Mutante *O377* trägt eine Mutation im βB2-Kristallin Gen (*Crybb2*); sie ist ein neues Maus-Modell für eine dominante, fortschreitende Katarakt. Die mRNA enthält eine 57 bp Insertion im Exon VI, die durch fehlerhaftes Splicen aufgrund einer A->T Basensubstitution in der *acceptor splicesite* des Intron V entsteht. Diese Mutante wurde unter den Nachkommen eines bestrahlten (3 Gy Röntgenstrahlen) Männchens entdeckt. Durch diese Mutation enthält das βB2-Krystallin^{O377} Protein 19 Aminosäuren mehr und ist 1,9 kDa schwerer als das Wildtyp-Protein (23 kDa). Durch diese Insertion wird das Protein fehlerhaft gefaltet und in der gesamten kortikalen Region der Mutanten-Linse eingelagert, wodurch eine Trübung der Linse bewirkt wird. In den Gehirnen von Wildtypen und *O377* Mutanten wurden die jeweiligen *Crybb2* Transkripte bzw. die βB2-Kristalline gefunden.

Die Linse der Mutante entwickelt eine starke Vakuolisierung und eine fleckige Erscheinung im Bereich der Linsenfaserzellen und des Kortex, was schon im Alter von 3 Wochen zur Kataraktentwicklung führt. In diesem Alter werden in der Linse von homozygoten Mutanten 116 Gene differentiell exprimiert, die an verschiedenen biochemischen Aktivitäten beteiligt sind. Die Expression von βB2-Kristallin außerhalb der Linse weist auf eine bisher unbekannte Funktion hin. In Wildtypen und in *O377* Mutanten wurde *Crybb2*-Expression in der *Membrana limitans interna* der Retina (nicht in der *O377* Mutante), in den glomerulären und Mitralzellen des Riechkolbens, in den Zellen der CAI, CAII und CAIII (CA = *Cornu ammonis*) Bereiche und des *Gyrus dentatus* des Hippocampus, in den Pyramidalzellen des Kortex und in den Purkinje-Zellen und Sternzellen des Cerebellums gefunden.

Die höhere Anzahl an Purkinje-Zellen (11%) im Lappen des Cerebellums (Schnittebene auf der Höhe der Vermis) der homozygoten Mutanten unterstützt die Hypothese, dass βB2-Kristallin über seine Eigenschaften als Strukturprotein hinaus weitere Funktionen besitzt. In Gehirnen von 4 Wochen alten homozygoten und heterozygoten Mutanten wurden differentiell exprimierte Gene (mit ähnlichen Expressionsdomänen wie βB2-Kristallin) detektiert, die an Phosphat- und Calcium-Signalwegen beteiligt sind. Dies führt, zusammen mit bereits bekannten Informationen bezüglich der Calciumbindung, der möglichen Phosphorylierung und den strukturellen Übereinstimmungen der β-/γ-Kristalline mit einigen Proteinen niederer Organismen, zu der Annahme, dass die βB2-Kristalline in einigen Geweben an der Phosphat- und Calcium-Homeostase beteiligt sind.

Diese Arbeit erweitert unser Wissen über die Mechanismen und das Fortschreiten der Kataraktentwicklung und hat zum ersten Mal Aufschluss über die zeitliche und regionale Expression des βB2-Kristallins im Gehirn gegeben.

6.0 Annexure:

Annexure 1:

Preparation of the standard curve and calculation of the protein concentrations of the C3H lens, *O377* lens, C3H brain and *O377* brain protein samples.
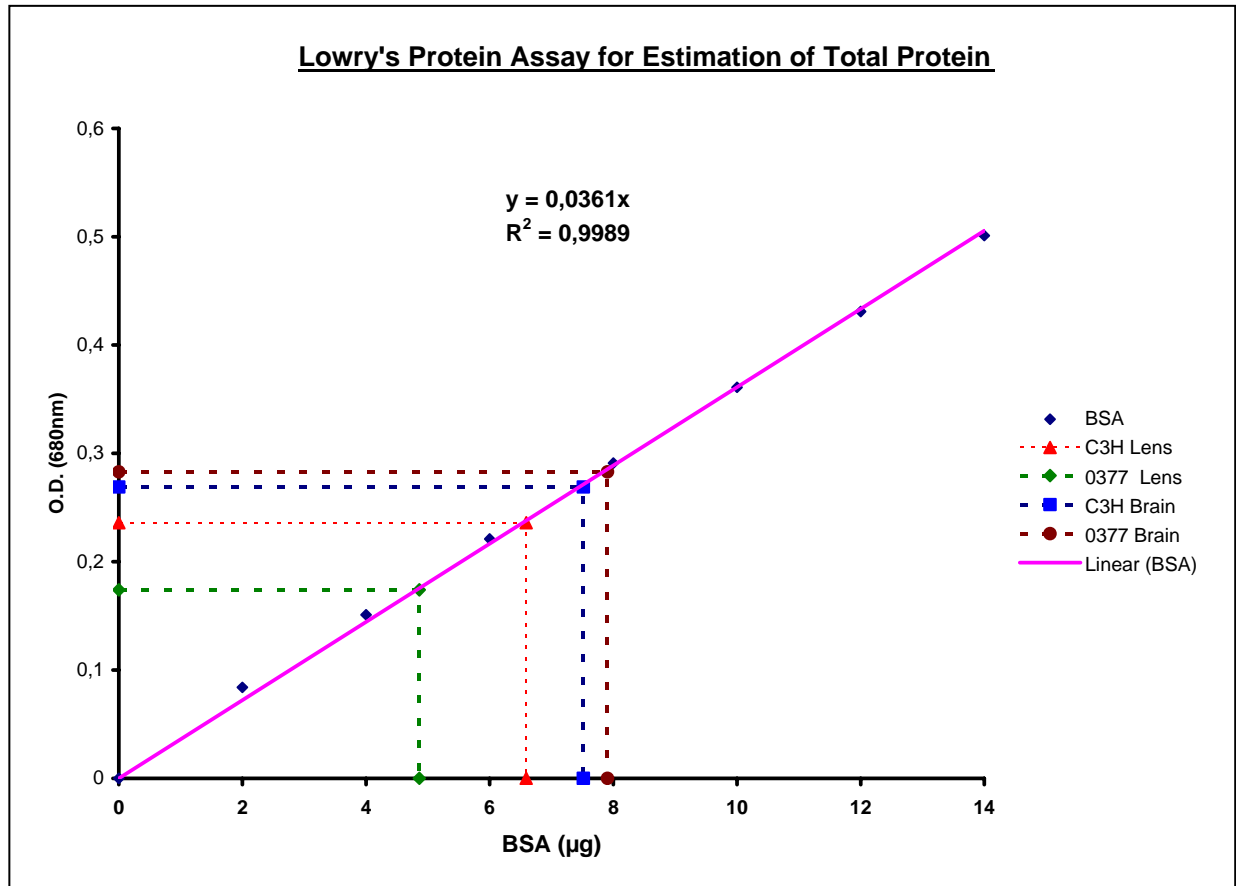
The graph shows the Standard curve obtained following the Lowry's protein assay for the standard B.S.A (**B**ovine **S**erum **A**lbumin) and the corresponding calculation of the protein concentrations in various samples after plotting the respective $O.D_{680nm}$. R is the correlation factor; [y=0.0361x] is the slope of the straight line curve.

Table: The O.Ds measured to calculate the amounts of protein in (1:10) diluted protein samples of wild-type and mutant lens and brain following Lowry's protein assay.

Protein sample	$O.D_{680nm}$ [y]	Concentration* x=y/ 0.0361 (as obtained from the curve)	Concentration in the undiluted sample 10x μg
C3H Lens	0.236	6.54μg/μl	65.4 μg/μl
O377 Lens	0.174	4.82μg/μl	48.2 μg/μl
C3H Brain	0.269	7.45μg/μl	74.5 μg/μl
O377 Brain	0.283	7.84μg/μl	78.4 μg/μl

* This is the concentration of the 1:10 diluted protein samples

Annexure 2:

Crybb2 sequence as obtained from the Genbank[*]; Location of the primers used for RT-PCR are also indicated in the sequence.

[*](http://www.ncbi.nlm.nih.gov/entrez/viewer.fcgi?db=nucleotide&val=6681034)

Organism: *Mus musculus*
ACCESSION: NM_007773
VERSION: NM_007773.1 GI:6681034

```
  1 ctcgacgcca gagagtccac c**atg**gcctca gaccaccaga cacaggcggg caagccccag
                                      Crybb2_L3

 61 ccccttaacc ccaagatcat catcttcgaa caggagaact tccagggcca ttcccacgag

121 ctcagcgggc cctgccccaa cctgaaggag actggtatgg agaaggcggg ctccgtcctg
                                                  Crybb2_L4

181 gtgcaggctg gaccctgggt gggctacgag caggctaatt gcaagggcga gcagtttgtg

241 tttgaaaagg gcgagtaccc acgttgggac tcctggacca gcagccggag gacagactcc
                  Crybb2_L5

301 ctcagctctc tgaggcccat caaagtggac agccaagagc acaagatcat cttatatgag

361 aaccccaact ttactggcaa gaagatggag attgtagacg acgatgtgcc cagcttccat
              Crybb2_L6

421 gcccatggat accaggaaaa ggtgtcttcc gtgcgtgtgc agagcggcac gtgggtgggg
              Crybb2_L7

481 taccagtacc ctggctaccg tgggctgcag tacctgctgg agaagggggga ttacaaggac

541 aacagcgact tcggggcccc tcaccccag gtgcagtctg tgcgtcgcat ccgtgacatg

601 cagtggcacc agcgaggtgc cttccacccc tccagc**tag**a gccctgaccc tcccccttccc

661 cagggtccag gcccgccacc tcggagcctc ctgacaccca gagtgaagaa taaagtgtgg
                                                    Crybb2_R1

721 ctcgtgcc
```

Annexure 3:

List of differentially expressed genes as obtained from expression profiling studies of (-/-) _O377_ Lens (Age: 3 weeks): [Date of last screening: 20.03.05.]

Genes are arranged in ascending order of their P% (Chance) values.

Up-regulated:

No.	Gene Symbol (MGI)	Name	Comments (UniGene)	LION clone ID	NCBI locus link	Ratio	P, %
1	_Sip1_	Survivor of motor neuron protein interacting protein 1 Cytoplasm, mRNA processing	Regulatory	4,23 MG-12-162c10	66603	4.62	0.00
2	**Not given**	NADH-ubiquinone oxidoreductase chain 4	Energy metabolism	3,68 MG-6-3g14		4.02	0.02
3	-		Hypothetical sequence	3,39 MG-6-82h12		3.6	0.08
4	**Not given**	NADH-ubiquinone oxidoreductase chain 1 (EC 1.6.5.3)	Energy metabolism	3,32 MG-8-117g19		3.58	0.12
5	-		No significant matches found	3,22 MG-3-247m12		6.28	0.19
6	_Camta1_	Calmodulin binding transcription activator 1	Others	3,10 MG-6-34n19	100072	3.84	0.31
7	**Not given**	Kinesin-like protein (klp4)		3,06 MG-8-17n2		3.74	0.38
8	-		No significant matches found	2,99 MG-6-56p23		3.76	0.56
9	**Not given**	Cytochrome B.	Energy metabolism	2,84 MG-6-55a1		3.2	1.09
10	-		No significant matches found	2,81 MG-6-82b9		4.22	1.23
11	_Rtn4_	Reticulon 4 Angiogenesis, cell projection	Transport and binding	2,81 MG-15-207j15	68585	4.08	1.23
12	-		No significant matches found	2,80 s0-Apaf1		3.24	1.31
13	_Arl6ip1_	ADP-ribosylation factor-like 6 interacting protein 1 Co-translational protein-membrane targeting	Transport and binding	2,74 MG-3-48b22	54208	4.1	1.63

No.	Gene Symbol (MGI)	Name	Comments	LION clone ID	NCBI locus link	Ratio	P, %
14	*Siat7f*	Sialytransferase 7 ((alpha-N-acetylneuraminyl 2,3-betagalactosyl-1,3)-N-acetyl galactosaminide alpha-2,6-sialytransferase) F Golgi apparatus	Others	2,72 MG-6-61b9	50935	3.3	1.76
15	**Not given**	Cytochrome c oxidase polypeptide II (EC 1.9.3.1)	Energy Metabolism	2,71 MG-3-49e2		3.06	1.84
16	*Cyfip2*	Cytoplasmic FMR1 interacting protein 2	others	2,71 MG-14-62p24	76884	3.2	1.84
17	*Plekhb1*	Pleckstrin homology domain containing, family B (evectins) member 1 Golgi membrane	Transport and binding	2,68 MG-6-55b22	27276	3.5	2.03
18	*Nagk*	N-acetylglucosamine kinase ATP binding	Energy metabolism	2,67 MG-6-82c1	56174	3.72	2.10
19	-		RIKEN cDNA1600013L13 gene; similar to Human Neurofilament triplet H protein, NF-H (ProtEST)	2,66 MG-6-39l2		3.38	2.15
20	-		No significant matches found	2,66 MG-6-55b1		3.3	2.15
21	*Ckb*	Creatine kinase, brain	Regulatory	2,66 MG-6-3e12	12709	3.04	2.15
22	*Slc12a5*	Solute carrier family 12, member 5	Transport and binding Amino acid transport	2,64 MG-6-71a6	57138	4.76	2.39
23	**Not given**	Plasma membrane calcium-transporting ATPase 1 (EC 3.6.3.8)	Others	2,63 MG-15-252g2		3.3	2.54

No.	Gene Symbol (MGI)	Name	Comments	LION clone ID	NCBI locus link	Ratio	P, %
24	-		*M. musculus* clone MGC 7427 IMAGE 3489024 mRNA complete cds	2,61 MG-6-86k24		4.22	2.78
25	*Rap1gds1*	RAP1, GTP-GDP dissociation stimulator 1	Others	2,60 MG-16-56j18	229877	3.26	2.93
26	*Angptl2:*	Angiopoietin-like 2	Regulatory Extracellular space	2,55 MG-14-100n16	26360	3.3	3.37
27	*Calm2*	Calmodulin 2	Transport and binding Calcium ion binding	2,55 MG-6-69i15	12314	3.86	3.37
28	*Stmn3*	Stathmin-like 3	Regulatory Intracellular signalling cascade	2,53 MG-6-3f1	20262	3.12	3.79
29	*Dbp*	D site albumin promoter binding protein	Regulatory DNA binding	2,51 MG-6-82c15	13170	3.84	4.11
30	-		RIKEN cDNA2300002D11 gene	2,47 MG-6-69d19		3.32	4.70
31	-		No significant matches found	2,46 s0-Hoxb1		2.94	4.84
32	*Atp6v0c*	ATPase, H+ transporting, V0 subunit C	Energy metabolism ATP biosynthesis;H^+ transport	2,45 MG-3-76i21	11984	2.68	4.99
33	*Car2*	Carbonic anhydrase 2	Regulatory	2,43 MG-15-1m11	12349	3.76	5.52
34	*Apoe*	Apolipoprotein E	Transport and binding Lipid binding	2,40 MG-3-27f11	11816	3.62	6.22
35	*Psip1*	PC4 and SFRS1 interacting protein 1	Others	2,39 MG-6-11l4	101739	2.98	6.61
36	-		RIKEN cDNA 6430559E15; similar to human hyothetical rotein HT036	2,33 MG-14-107l16		2.92	8.67

No.	Gene Symbol (MGI)	Name	Comments	LION clone ID	NCBI locus link	Ratio	P, %
37	*Aplp1*	Amyloid beta (A4) precursor-like protein 1	Transport and binding Apoptosis	2,33 MG-6-2g18	11803	2.52	8.67
38	*Mrpl49*	Mitochondrial ribosomal protein L49	Regulatory Protein biosynthesis	2,33 MG-16-183n19	18120	3.12	8.67
39	-		No significant matches found	2,31 MG-6-64n13		2.74	9.66
40	*Abhd4*	Abhydrolase domain containing 4	Regulatory Amino peptidase activity	2,30 MG-6-82j16	105501	3.12	10.20
41	*Vdac1*	Voltage-dependent anion channel 1	Transport and binding Anion transport	2,30 MG-14-4g12	22333	3.2	10.20
42	-		ESTs highly similar to S12207 hypothetical protein B2 element of *M. musculus*.	2,29 MG-6-19i12		3.08	10.81
43	-		No significant matches found	2,28 MG-3-43c11		3.08	11.25
44	*Diras2*	DIRAS family, GTP-binding RAS-like 2	Others	2,26 MG-6-24p12		2.72	12.55
45	-		RIKEN cDNA2810043G13 gene; similar to *H. sapiens* hypothetical protein FLJ14050	2,25 MG-4-4h13		3.26	13.38
46	*Stxbp1:*	Syntaxin binding protein 1	Transport and binding	2,23 MG-6-74f10	20910	3.66	14.26
47	-		Expressed sequence AI449753	2,20 MG-3-67m20		3.38	16.39
48	*Sh3gl2*	SH3-domain GRB2-like 2	Transport and binding	2,19 MG-14-116b2	20404	2.44	17.01
49	*Slc25a5*	Solute carrier family 25 (mitochondrial carrier, adenine nucleotide translocator), member 5	Transport and binding	2,19 MG-6-3k23	11740	2.48	17.01

No.	Gene Symbol (MGI)	Name	Comments	LION clone ID	NCBI locus link	Ratio	P, %
50	-		No significant matches found	2,17 MG-14-39j9		2.82	17.91
51	*Scn1b*	Sodium channel, voltage-gated, type I, beta polypeptide	Transport and binding	2,16 MG-6-82h17	20266	3.56	19.02
52	*Sv2a*	Synaptic vesicle glycoprotein 2 a	Transport and binding; Calcium ion homeostasis	2,16 MG-6-73i8	64051	3.06	19.02
53	*Atp6v1a1*	ATPase, H+ transporting, V1 subunit A, isoform 1	Energy metabolism ATP binding	2,15 MG-6-69b6	11964	3.3	19.76
54	-		No significant matches found	2,15 MG-6-52f3		3.84	19.76
55	-		4092-45 Mouse E14.5 retina lambda ZAP II library M. *musculus*	2,14 MG-15-70b2		5.2	20.59
56	-		RIKEN cDNA 4921506j03; protein disulphide isomerase A4 precursor	2,14 MG-3-107c15		2.2	20.59
57	*Arl6ip1*	ADP-ribosylation factor-like 6 interacting protein 1	Regulatory	2,13 MG-6-89i20	54208	4.84	22.15
58	*Ndufv1*	NADH dehydrogenase (ubiquinone) flavoprotein 1	Energy metabolism	2,12 MG-14-114a21	17995	2.2	23.25
59	-		Similar to hypothetical protein IMPACT of *H. sapiens.*; YCU9_Yeast hypothetical 29.0kDa protein, probable membrane protein	2,12 MG-6-14d13		2.26	23.25
60	*Zfp36*	Zinc finger protein 36	Regulatory DNA binding	2,12 MG-16-88k12	22695	2.58	23.25

No.	Gene Symbol (MGI)	Name	Comments	LION clone ID	NCBI locus link	Ratio	P, %
61	*Iap*	Intracisternal A particles	Others	2,10 MG-3-171n1	15598	2.72	25.31
62	-		No significant matches found	2,07 MG-3-85p15		2.4	28.68
63	*Tm4sf2*	Transmembrane 4 superfamily member 2	Transport and binding	2,06 MG-6-24a15	21912	3.1	29.95
64	*Aldoa*	Aldolase 1, A isoform	Energy metabolism	2,06 MG-15-273o1	11674	2.56	29.95
65	*Aamp*	Angio-associated migratory protein	Others	2,06 MG-6-43c16	227290	2.14	29.95
66	*Ywhaq*	yrosine 3-monooxygenase/tryptophan 5-monooxygenase activation protein, theta polypeptide	Regulatory	2,05 MG-15-254h17	22630	2.64	31.32
67	*Sept5*	Septin 5	Energy metabolism GTP binding	2,05 MG-6-55l19	18951	3.04	31.32
68	*Lman1l*	Lectin, mannose-binding, 1 like	Others	2,04 MG-6-55b12	235415	2.7	31.94
69	*Ndfip1*	Nedd4 family interacting protein 1	Transport and binding	2,03 MG-16-2i13	65113	2.72	32.39
70	*Dnmt3a*	DNA methyltransferase 3A	Regulatory	2,00 MG-6-34p21	13435	3.34	35.71

Down regulated:

No.	Gene	Name	Comments	LION clone ID	NCBI locus ID	Ratio	P, %
1	*Crygb*	Crystallin, gamma B	Lens structure	83,35 MG-8-22h22	12965	137.78	0.00
2	**Not given**	lens epithelial protein	others	45,89 MG-12-273a18		70.16	0.00
3	*Crygs*	Crystallin, gamma S	Lens structure	39,46 MG-60-1c21	12970	72.12	0.00
4	-	Gamma crystallin B (1-2).	Lens structure	37,37 MG-16-2i17		93.5	0.00
5	*Crygc*	Crystallin, gamma C	Lens structure	28,35 MG-60-1c4	12966	67.42	0.00
6	*Cryba1*	Crystallin, beta A1	Lens structure	16,75 MG-60-1e21	12957	38.98	0.00
7	*Cryaa*	Crystallin, alpha A	Lens structure	13,16 MG-60-1j5	12954	19.98	0.00
8	**Not given**	Heat-shock 20 kDa like-protein	others	11,76 MG-14-138p23			0.00
9	*Cryba2*	Crystallin, beta A2	Lens structure	11,21 MG-60-1p11	12958	22.26	0.00
10	*Cryab*	Crystallin, alpha B	Lens structure	10,46 MG-6-57j12	12955	17.02	0.00
11	**Not given**		Similarity with eye lens protein involved in phoshorylation, acetylation	9,27 MG-13-5n3		16.9	0.00
12	*Ndufs5*	NADH dehydrogenase (ubiquinone) Fe-S protein 5	Energy metabolism	6,42 MG-14-140p21	170658	7.82	0.00
13	-		No significant matches found	5,91 MG-3-174j14		8.82	0.00

No.	Gene Symbol (MGI)	Name	Comments	LION clone ID	NCBI locus link	Ratio	P, %
14	*Fabp5*	Fatty acid binding protein 5, epidermal	Transport and binding	5,78 MG-8-19b7	16592	8.4	0.00
15	-		No significant matches found	5,47 MG-8-101d21		7.0	0.00
16	-		RIKEN cDNA 4931406C07 gene similar To PTD012 protein of *H. sapiens*.	5,32 MG-12-278g10		6.3	0.00
17	-		No significant matches found	5,03 MG-3-239m24		6.06	0.00
18	*ORF9*	Open reading frame 9	Regulatory	4,73 MG-3-85f5	52793	5.42	0.01
19	*Hmgn3*	High mobility group nucleosomal binding domain 3	Regulatory	4,61 MG-15-272m19	94353	6.5	0.01
20	*Cd24a*	CD24a antigen	Transport and binding	3,87 MG-4-3l13	12484	6.72	0.02
21	*Crybb2*	Crystallin, beta B2	Lens structure	3,80 MG-60-1c10	12961	6.12	0.02
22	-		RIKEN cDNA 5730434I03 gene; similar to transcription factor BTF3	3,69 MG-3-14i7		4.92	0.02
23	*Pgam2*	Phosphoglycerate mutase 2	Energy metabolism	3,56 MG-15-2l12	56012	5.92	0.03
24	*Dbi*	Diazepam binding inhibitor	Transport and binding	3,53 MG-6-3o12	13167	5.0	0.03
25	-		No significant matches found	3,48 MG-3-28h13		4.66	0.04

No.	Gene Symbol (MGI)	Name	Comments	LION clone ID	NCBI locus link	Ratio	P, %
26	*Sorbs1*	Sorbin and SH3 domain containing 1	Transport and binding	3,41 MG-14-107a12	20411	4.04	0.04
27	*Pdlim1*	PDZ and LIM domain 1 (elfin	Regulatory	3,34 MG-3-28b13	54132	5.2	0.05
28	*Sin3b*	Transcriptional regulator, SIN3B (yeast)	Regulatory	3,30 MG-3-79d2	20467	4.64	0.05
29	-		No significant matches found	3,28 MG-3-91d9		4.84	0.06
30	*Synpo*	Synaptopodin	Others	3,26 MG-3-113b16	104027	5.72	0.06
31	*Cpt2*	Carnitine palmitoyltransferase 2	Regulatory	3,24 MG-14-3m20	12896	5.58	0.06
32	*S100a4*	S100 calcium binding protein A4	Transport and binding	2,93 MG-13-1k15	20198	5.12	0.10
33	**Not given**	Hemoglobin alpha chain.	Regulatory	2,91 MG-8-40d4		4.02	0.11
34	*Deb1*	Differentially expressed in B16F10 1	Others	2,84 MG-16-10j24	26901		0.12
35	*Glul*	Glutamate-ammonia ligase (glutamine synthase)	Regulatory	2,73 MG-8-117d11	14645	3.64	0.17
36	-		RIKEN cDNA 2810442O16; similar to probable membrane protein YFL027c-Yeast	2,72 MG-3-85h5		3.46	0.18
37	*Lgals1*	Lectin, galactose binding, soluble 1	Regulatory	2,64 MG-6-3i14	16852	3.2	0.22

No.	Gene Symbol (MGI)	Name	Comments	LION clone ID	NCBI locus link	Ratio	P, %
38	*P4ha1*	Procollagen-proline, 2-oxoglutarate 4-dioxygenase (proline 4-hydroxylase), alpha 1 polypeptide	Regulatory	2,40 MG-15-95f24	18451	4.22	0.41
39	*Casq1*	Calsequestrin 1	Transport and binding	2,38 MG-15-216f17	12372	2.9	0.44
40	*Ndrg1*	N-myc downstream regulated gene 1	Others	2,28 MG-8-86l10	17988	3.4	0.60
41	**Not given**	Cytochrome P450 monooxygenase	Others	2,27 MG-8-13f7		2.82	0.63
42	*Gsn*	Gelsolin	Regulatory	2,21 MG-3-45k24	227753	3.1	0.82
43	*S100a6*	S100 calcium binding protein A6 (calcyclin)	Transport and binding	2,21 MG-6-30n6	20200	4.46	0.82
44	**Not given**	Desert hedgehog protein precursor (DHH) (HHG-3).	Regulatory	2,17 MG-3-174p1		2.84	1.04
45	*Dhx8*	DEAH (Asp-Glu-Ala-His) box polypeptide 8	Transport and binding	2,12 MG-12-286g18	217207	4.18	1.18
46	*Tnfrsf1b*	Tumor necrosis factor receptor superfamily, member 1b	Transport and binding	2,05 MG-15-254j8	21938	2.38	1.69

Genes with higher P-values are included because they are differentially expressed in all the samples.

Annexure 4:

Informations contained in the report sheet for data analysis generated by the Light Cycler Relative quantification software (Version 1.0) following Real Time-qPCR experiment:

Experiment:	User name, run by and run date
File name(target):	Opened target file name (exported *.txt file)
File name (reference)	Opened reference file name (exported *.txt file)
File name (cof.):	Opened coefficient file name
Correction factor:	Value of the correction factor
Multiplication factor:	Value of the multiplication factor
Nr.	Number of the sample position in the rotor
Sample Information:	Description of the sample
Crossing Point:	Cp-value of the sample
Cp median:	median of the Cp-values of replicates
Delta Cp median:	median(target)-median(reference)
Ratio Conc.:	median(target)/median(reference)
Normalized ratio: (samples)	$\dfrac{\text{median(target)/median(reference)}}{\{\text{median(target}_{cal})/\text{median(reference}_{cal})\} \times \text{Correction factor}} \times \text{Multiplication factor}$
Result file name:	Name of the saved result file

Annexure 5:

Real Time PCR data; *O377* **(-/-) Brain:**

Target gene: *Tbxb4* **[Primer pair:** *TB4_For/TB4_Rev***]**

Report sheet for data analysis for the ***Tbxb4*** gene generated by the Relquant software (1.0) following the Real Time-qPCR experiment.

Sample	CP	CP median	Delta CP median	Ratio Conc.	Normalized ratio
Wt_*Tbxb4*	17.57				
Repli of Wt_ *Tbxb4*	17.17	17.37	-3.13	8.75	**1.00**
Wt_Hprt	20.58				
Repli. of Wt_*Hprt*	20.42	20.50			
Mut_ *Tbxb4*	16.72	16.63			
Repli of Mut_*Tbxb4*	16.55		-4.03	16.33	**1.87**
Mut_Hprt	20.69				
Repli. of Mut_*Hprt*	21.65	20.66			

*Results analysis mono colour, duplicate values without efficiency correction.
Correction factor: 1.000000
Multiplication factor: 1.000000

The light Cycler Melting Peaks Report generated by the RelQuant (1.0) software for the ***Tbxb4*** gene showing up-regulation of ***Tbxb4*** in the mutant.

Target gene: *Atpv0a1* [**Primer pair:** *Atpv0_For/Atpv0_Rev*]

Report sheet for data analysis for the *Atpv0a1* gene generated by the Relquant software (1.0) following the Real Time-PCR experiment. In this case samples were taken only in single instead of duplicate.

Sample	CP	CP median	Delta CP median	Ratio Conc.	Normalized ratio
Wt_*Atpv0a1*	19.81	19.81	-0.67	1.00	1.00
Wt_Hprt	20.48	20.48			
Mut_ *Atpv0a1*	18.66	18.66	-2.08	2.66	2.66
Mut_Hprt	20.74	20.74			

*Results analysis mono colour, single value without efficiency correction.
***Correction factor:**   1.000000
***Multiplication factor:** 1.000000

The light Cycler Melting Peaks Report generated by the RelQuant (1.0) software for the *Atpv0a1* gene showing up-regulation of *Atpv0a1* in the mutant.

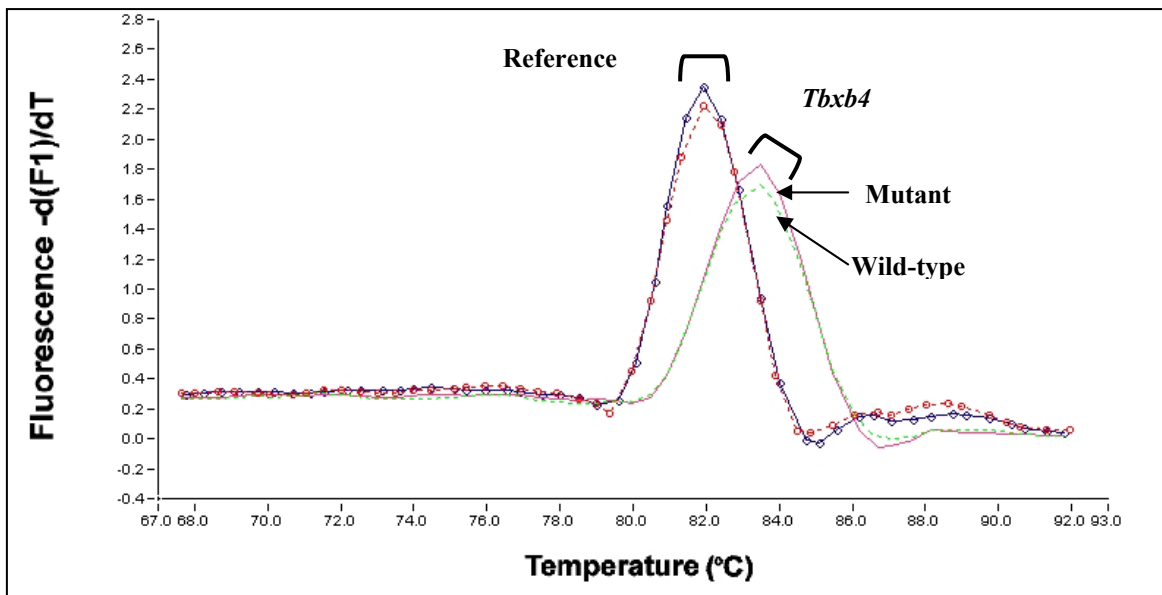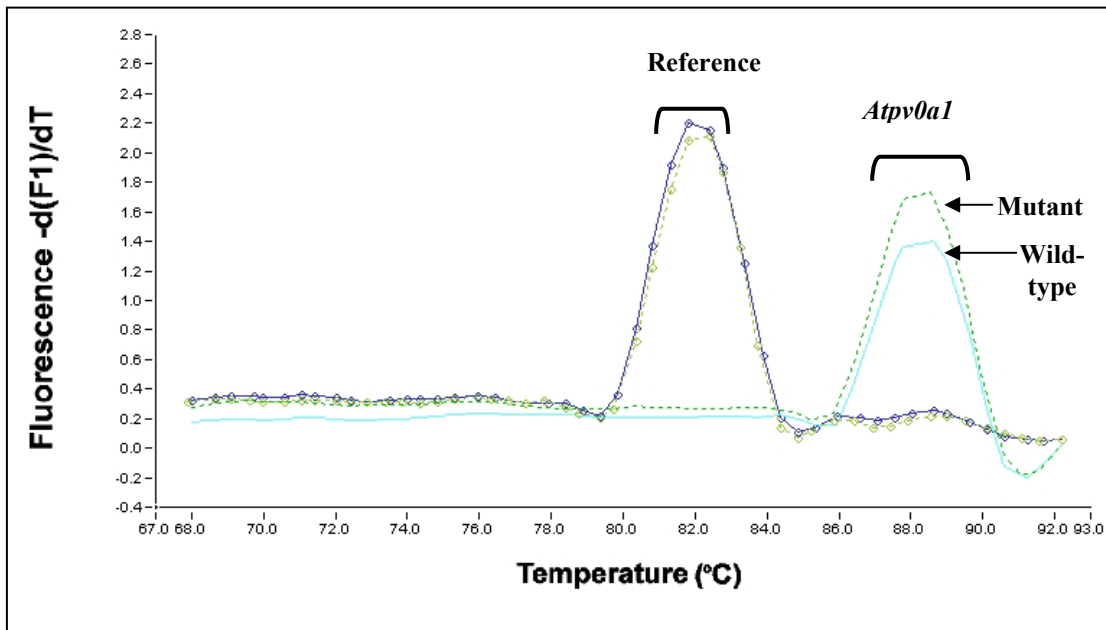**Target gene:** *Lpl* [Primer pair: *Lpl_For/Lpl_Rev*]

Report sheet for data analysis for the *Lpl* gene generated by the Relquant software (1.0) following the Real Time-PCR experiment.

Sample	CP	CP median	Delta CP median	Ratio Conc.	Normalized ratio
Wt_*Lpl*	22.83				
Repli of Wt_ *Lpl*	23.10	22.97	1.86	0.28	**1.00**
Wt_Hprt	20.89				
Repli. of Wt_*Hprt*	21.32	21.11			
Mut_ *Lpl*	23.44	23.29			
Repli of Mut_ *Lpl*	23.14		2.73	0.15	
Mut_Hprt	20.47				**0.55**
Repli. of Mut_*Hprt*	20.64	20.56			

*Results analysis mono colour, duplicate values without efficiency correction.
*Correction factor: 1.000000
*Multiplication factor: 1.000000

The light Cycler Melting Peaks Report generated by the RelQuant (1.0) software for the *Lpl* gene showing down regulation of *Lpl* in the mutant.

Annexure 6:

Real Time PCR data; *O377* (+/-) Brain:

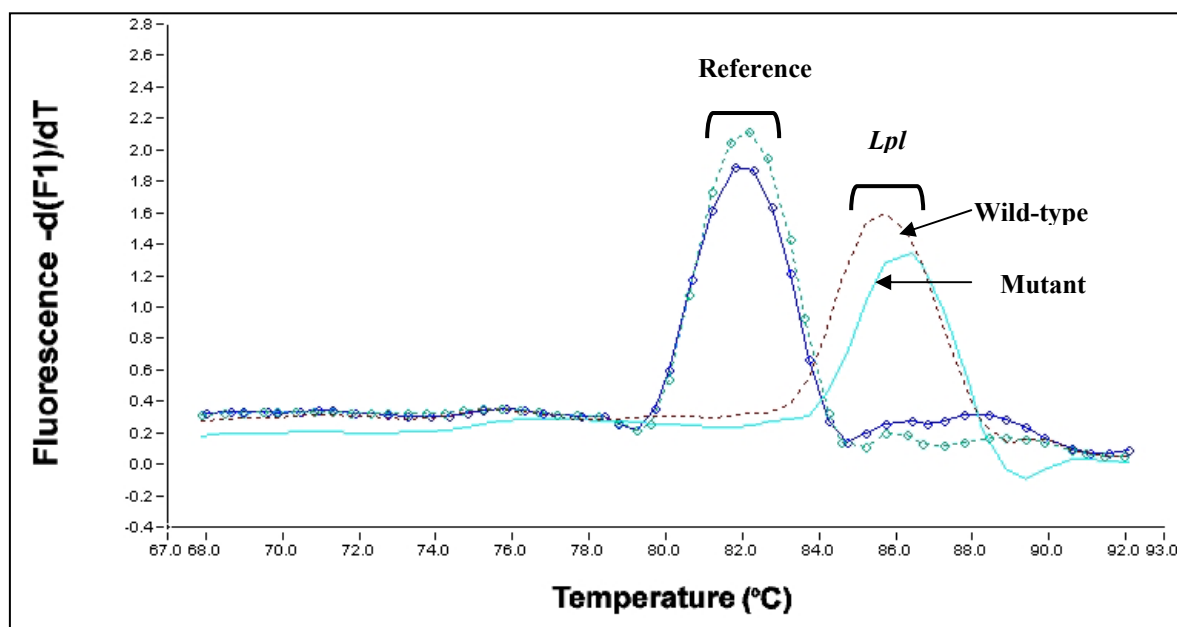**Target gene:** *Ank*: **[Primer pair: *Ank_For/Ank_Rev*]**

Report sheet for data analysis for the ***Ank*** gene generated by the RelQuant (1.0) software following the Real Time-PCR experiment.

Sample	CP	CP median	Delta CP median	Ratio Conc.	Normalized ratio
Wt_*Ank*	20.69	20.66	-0.04	1.03	**1.00**
Repli of Wt_*Ank*	20.63				
Wt_Hprt	20.67	20.70			
Repli. of Wt_*Hprt*	20.74				
Mut_*Ank*	21.32	21.13	-0.43	1.34	**1.30**
Repli of Mut_*Ank*	20.93				
Mut_Hprt	21.64	21.55			
Repli. of Mut_*Hprt*	21.46				

*Results analysis mono colour, duplicate values without efficiency correction.
Correction factor: 1.000000
Multiplication factor: 1.000000

The light Cycler Melting Peaks Report generated by the RelQuant (1.00) software for the ***Ank*** gene showing up-regulation of ***Ank*** in the mutant.

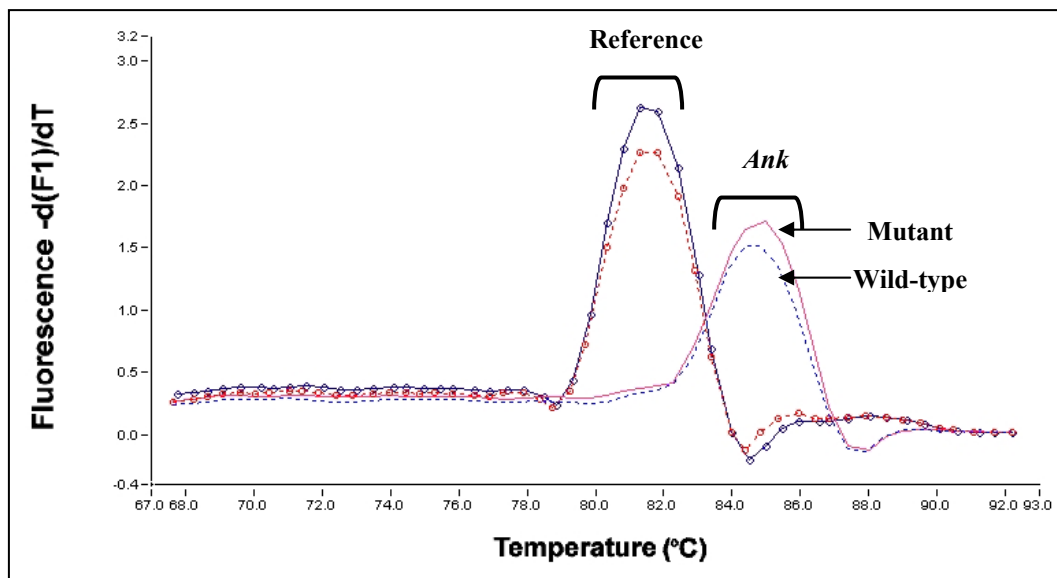**Target gene :** *Camk2a* **[Primer pair:** *Camk_For/Camk_Rev***]**

Report sheet for data analysis for the ***Camk2a*** gene generated by the Relquant (1.0) software following the Real Time-PCR experiment.

Sample	CP	CP median	Delta CP median	Ratio Conc.	Normalized ratio
Wt_*Camk2a*	18.82				
Repli of Wt_ *Camk2a*	19.13	18.98	-2.02	4.07	**1.00**
Wt_Hprt	21.24				
Repli. of Wt_*Hprt*	20.76	21.00			
Mut_ *Camk2a*	17.76	17.52			
Repli of Mut_*Camk2a*	17.29		-2.63	6.17	**1.52**
Mut_Hprt	19.63				
Repli. of Mut_*Hprt*	20.67	20.15			

*Results analysis mono colour, duplicate values without efficiency correction.
Correction factor: 1.000000
Multiplication factor: 1.000000

The light Cycler Melting Peaks Report generated by the RelQuant (1.0) software for the ***Camk2a*** gene showing up-regulation of ***Camk2a*** in the mutant.

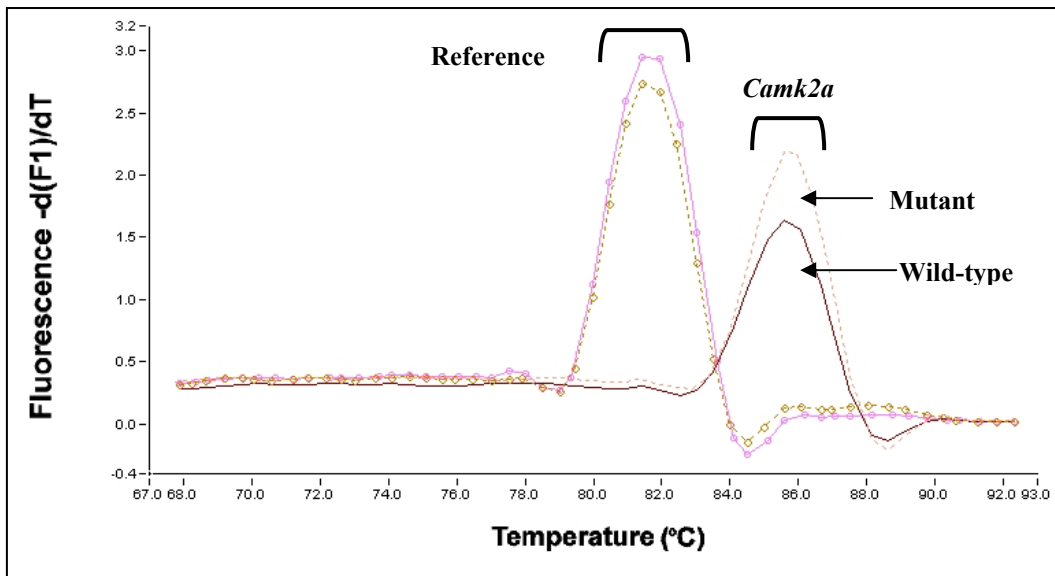**Target gene:** *Hpcal4* [**Primer pair:** *Hlp_For/Hlp_Rev*]

Report sheet for data analysis for the *Hpcal4* gene generated by the Relquant (1.0) software following the Real Time-PCR experiment.

Sample	CP	CP median	Delta CP median	Ratio Conc.	Normalized ratio
Wt_Hpcal4	18.28				
Repli of Wt_ *Hpcal4*	18.74	18.51	-2.50	5.66	**1.00**
Wt_Hprt	21.15				
Repli. of Wt_*Hprt*	20.87	21.01			
Mut_ *Hpcal4*	18.50	18.59			
Repli of Mut_*Hpcal4*	18.68		-2.66	6.32	
Mut_Hprt	21.24				**1.12**
Repli. of Mut_*Hprt*	21.26	21.25			

*Results analysis mono colour, duplicate values without efficiency correction.
Correction factor: 1.000000
Multiplication factor: 1.000000

The light Cycler Melting Peaks Report generated by the RelQuant (1.0) software for the *Hpcal4* gene showing up-regulation of *Hpcal4* in the mutant.

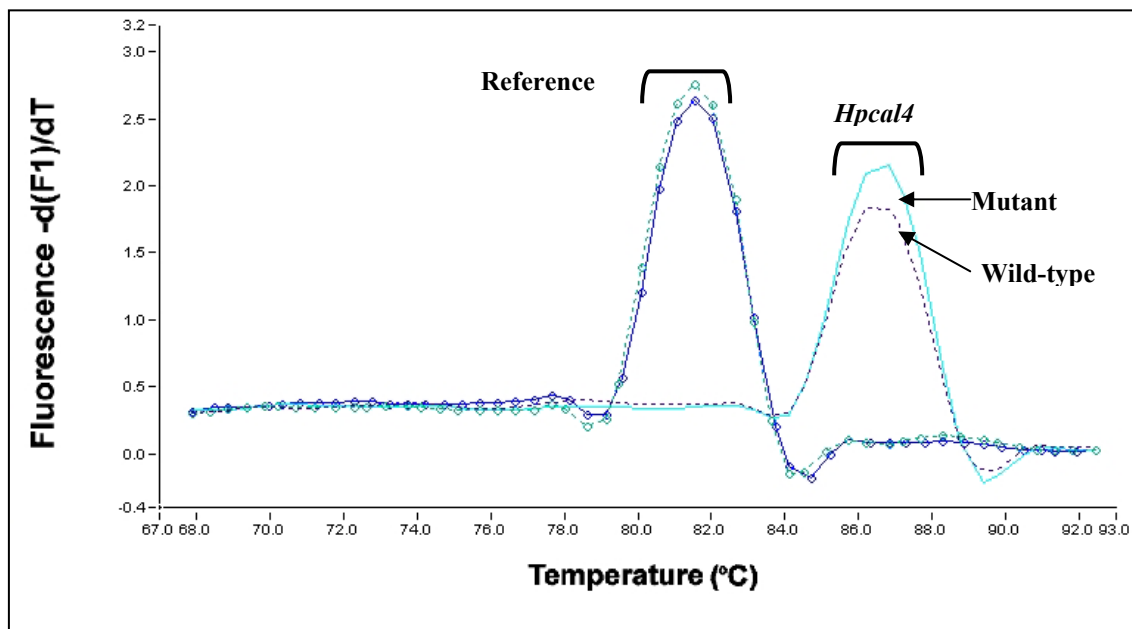**Target gene:** *Nrgn* **[Primer pair:** *Nrgn_For/Nrgn_Rev***]**

Report sheet for data analysis for the *Nrgn* gene generated by the Relquant (1.0) software following the Real Time-PCR experiment.

Sample	CP	CP median	Delta CP median	Ratio Conc.	Normalized ratio
Wt_*Nrgn*	23.29				
Repli of Wt_ *Nrgn*	23.67	23.48	-2.55	0.17	**1.00**
Wt_Hprt	20.97				
Repli. of Wt_*Hprt*	20.89	20.93			
Mut_ *Nrgn*	24.05	23.98			
Repli of Mut_*Nrgn*	23.90		-2.39	0.19	
Mut_Hprt	21.53				**1.12**
Repli. of Mut_*Hprt*	21.65	21.59			

*Results analysis mono colour, duplicate values without efficiency correction.
***Correction factor:**   1.000000
***Multiplication factor:** 1.000000
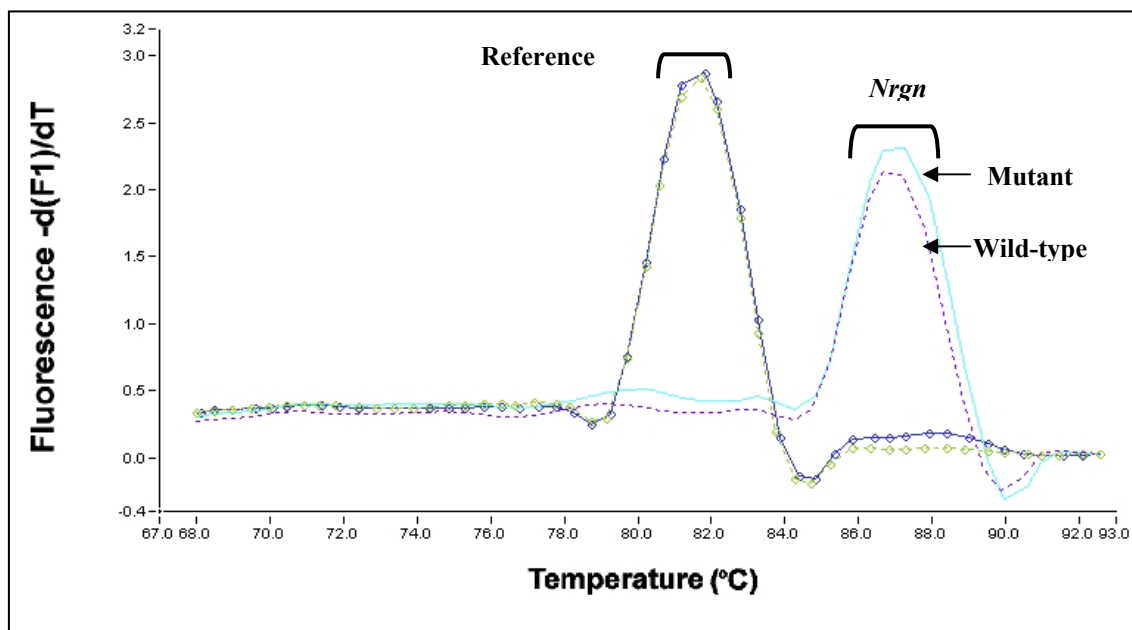
The LightCycler Melting Peaks Report generated by the RelQuant (1.00) software for the *Nrgn* gene showing up-regulation of *Nrgn* in the mutant.

7.0. <u>References:</u>

Aarts HJ, Lubsen NH, Schoenmakers JG; Crystallin gene expression during rat lens development.; Eur J Biochem. 1989 Jul 15;183(1):31-6.

Andrews JS, Leonard-Martin T, Kador PF.; Membrane lipid biosynthesis in the Philly mouse lens. I. The major phospholipid classes.; Curr Eye Res. 1984 Feb;3(2):279-85.

Antuch W, Guntert P, Wuthrich K.; Ancestral beta gamma-crystallin precursor structure in a yeast killer toxin.; Nat Struct Biol. 1996 Aug;3(8):662-5.

Bagby S, Harvey TS, Eagle SG, Inouye S, Ikura M.; Structural similarity of a developmentally regulated bacterial spore coat protein to beta gamma-crystallins of the vertebrate eye lens.; Proc Natl Acad Sci U S A. 1994 May 10;91(10):4308-12.

Baran I.; Calcium and cell cycle progression: possible effects of external perturbations on cell proliferation.; Biophys J. 1996 Mar;70(3):1198-213.

Barbato R, Menabo R, Dainese P, Carafoli E, Schiaffino S, Di Lisa F.; Binding of cytosolic proteins to myofibrils in ischemic rat hearts.; Circ Res. 1996 May;78(5):821-8

Bateman JB, Geyer DD, Flodman P, Johannes M, Sikela J, Walter N, Moreira AT, Clancy K, Spence MA.; A new betaA1-crystallin splice junction mutation in autosomal dominant cataract.; Invest Ophthalmol Vis Sci. 2000 Oct;41(11):3278-85.

Bax B, Lapatto R, Nalini V, Driessen H, Lindley PF, Mahadevan D, Blundell TL, Slingsby C.; X-ray analysis of beta B2-crystallin and evolution of oligomeric lens proteins.; Nature. 1990 Oct 25;347(6295):776-80.

Berry V, Francis P, Reddy MA, Collyer D, Vithana E, MacKay I, Dawson G, Carey AH, Moore A, Bhattacharya SS, Quinlan RA.; Alpha-B crystallin gene (CRYAB) mutation causes dominant congenital posterior polar cataract in humans.; Am J Hum Genet. 2001 Nov;69(5):1141-5. Epub 2001 Sep 27.

Bhat SP.; Crystallins, genes and cataract.; Prog Drug Res. 2003;60:205-62.

Bhat SP.; Transparency and non-refractive functions of crystallins--a proposal.; Exp Eye Res. 2004 Dec;79(6):809-16.

Blundell T, Lindley P, Miller L, Moss D, Slingsby C, Tickle I, Turnell B, Wistow G.; The molecular structure and stability of the eye lens: x-ray analysis of gamma-crystallin II.; Nature. 1981 Feb 26;289(5800):771-7.

Borras T, Persson B, Jornvall H.; Eye lens zeta-crystallin relationships to the family of "long-chain" alcohol/polyol dehydrogenases. Protein trimming and conservation of stable parts.; Biochemistry. 1989 Jul 25;28(15):6133-9.

Brady JP, Garland D, Duglas-Tabor Y, Robison WG Jr, Groome A, Wawrousek EF.; Targeted disruption of the mouse alpha A-crystallin gene induces cataract and cytoplasmic inclusion bodies containing the small heat shock protein alpha B-crystallin.; Proc Natl Acad Sci U S A. 1997 Feb 4;94(3):884-9.

Brady JP, Garland DL, Green DE, Tamm ER, Giblin FJ, Wawrousek EF.; AlphaB-crystallin in lens development and muscle integrity: a gene knockout approach.; Invest Ophthalmol Vis Sci. 2001 Nov;42(12):2924-34.

Brakenhoff RH, Aarts HJ, Reek FH, Lubsen NH, Schoenmakers JG.; Human gamma-crystallin genes. A gene family on its way to extinction.; J Mol Biol. 1990 Dec 5;216(3):519-32

Brakenhoff RH, Aarts HJ, Schuren F, Lubsen NH, Schoenmakers JG.; The second human beta B2-crystallin gene is a pseudogene.; Exp Eye Res. 1992 May;54(5):803-6.

Brown PO, Botstein D.; Exploring the new world of the genome with DNA microarrays.; Nat Genet. 1999 Jan;21(1 Suppl):33-7.

Bu L, Yan S, Jin M, Jin Y, Yu C, Xiao S, Xie Q, Hu L, Xie Y, Solitang Y, Liu J, Zhao G, Kong X.; The gamma S-crystallin gene is mutated in autosomal recessive cataract in mouse.; Genomics. 2002 Jul;80(1):38-44.

Burry RW.; Specificity controls for immunocytochemical methods.; J Histochem Cytochem. 2000 Feb;48(2):163-6.

Carper D.; Deficiency of functional messenger RNA for a developmentally regulated beta-crystallin polypeptide in a hereditary cataract.; Science. 1982 Jul 30;217(4558):463-4.

Chambers C, Cvekl A, Sax CM, Russell P.; Sequence, initial functional analysis and protein-DNA binding sites of the mouse beta B2-crystallin-encoding gene.; Gene. 1995 Dec 12;166(2):287-92.

Chambers C, Russell P.; Deletion mutation in an eye lens beta-crystallin. An animal model for inherited cataracts.; J Biol Chem. 1991 Apr 15;266(11):6742-6.

Chan CW, Saimi Y, Kung C.; A new multigene family encoding calcium-dependent calmodulin-binding membrane proteins of Paramecium tetraurelia.; Chan CW, Saimi Y, Kung C..

Chang B, Hawes NL, Roderick TH, Smith RS, Heckenlively JR, Horwitz J, Davisson MT.; Identification of a missense mutation in the alphaA-crystallin gene of the lop18 mouse.; Mol Vis. 1999 Sep 10;5:21

Chiesi M, Bennardini F.; Determination of alpha B crystallin aggregation: a new alternative method to assess ischemic damage of the heart.; Basic Res Cardiol. 1992 Jan-Feb;87(1):38-46.

Das KP, Surewicz WK.; On the substrate specificity of alpha-crystallin as a molecular chaperone.; Biochem J. 1995 Oct 15;311 (Pt 2):367-70.

Dirks RP, Kraft HJ, Van Genesen ST, Klok EJ, Pfundt R, Schoenmakers JG, Lubsen NH.; The cooperation between two silencers creates an enhancer element that controls both the lens-preferred and the differentiation stage-specific expression of the rat beta B2-crystallin gene.; Eur J Biochem. 1996 Jul 1;239(1):23-32.

Dirks RP, Van Genesen ST, KrUse JJ, Jorissen L, Lubsen NH.; Extralenticular expression of the rodent betaB2-crystallin gene.; Exp Eye Res. 1998 Feb;66(2):267-9.

Doerwald L, Nijveen H, Civil A, van Genesen ST, Lubsen NH.; Regulatory elements in the rat betaB2-crystallin promoter.; Exp Eye Res. 2001 Nov;73(5):703-10.

Drobyshev AL, Machka C, Horsch M, Seltmann M, Liebscher V, Hrabe de Angelis M, Beckers J.; Specificity assessment from fractionation experiments (SAFE): a novel method to evaluate microarray probe specificity based on hybridisation stringencies.; Nucleic Acids Res. 2003 Jan 15;31(2):E1-1.

Duguid JR, Rohwer RG, Seed B.; Isolation of cDNAs of scrapie-modulated RNAs by subtractive hybridization of a cDNA library.; Proc Natl Acad Sci U S A. 1988 Aug;85(15):5738-42.

Duncan MK, Haynes JI 2nd, Piatigorsky J.; The chicken beta A4- and beta B1-crystallin-encoding genes are tightly linked.; Gene. 1995 Sep 11;162(2):189-96.

Duncan MK, Roth HJ, Thompson M, Kantorow M, Piatigorsky J.; Chicken beta B1 crystallin: gene sequence and evidence for functional conservation of promoter activity between chicken and mouse.; Biochim Biophys Acta. 1995 Mar 14;1261(1):68-76.

Everett CA, Glenister PH, Taylor DM, Lyon MF, Kratochvilova-Loester J, Favor J.; Mapping of six dominant cataract genes in the mouse.; Genomics. 1994 Apr;20(3):429-34.

Foster A.; Cataract--a global perspective: output, outcome and outlay.; Eye. 1999 Jun;13 (Pt 3b):449-53.

Frachman , S. *et al*.., Betaine and DMSO: Enhancing agents for PCR; Promega notes Number 65, 1998, p27.

Francis PJ, Berry V, Bhattacharya SS, Moore AT.; The genetics of childhood
cataract.; J Med Genet. 2000 Jul;37(7):481-8.

Gallyas F.; Silver staining of myelin by means of physical development.; Neurol Res. 1979;1(2):203-9.

Garadi R, Reddy VN, Kador PF, Kinoshita JH; Membrane glycoproteins of Philly mouse lens.; Invest Ophthalmol Vis Sci. 1983 Sep;24(9):1321-4.

Garland D, Rao PV, Del Corso A, Mura U, Zigler JS Jr.; zeta-Crystallin is a major protein in the lens of Camelus dromedarius.; Arch Biochem Biophys. 1991 Feb 15;285(1):134-6.

Gill D, Klose R, Munier FL, McFadden M, Priston M, Billingsley G, Ducrey N, Schorderet DF, Heon E.; Genetic heterogeneity of the Coppock-like cataract: a mutation in CRYBB2 on chromosome 22q11.2.; Invest Ophthalmol Vis Sci. 2000 Jan;41(1):159-65.

Gillies RJ, Ugurbil K, den Hollander JA, Shulman RG.; 31P NMR studies of intracellular pH and phosphate metabolism during cell division cycle of Saccharomyces cerevisiae.; Proc Natl Acad Sci U S A. 1981 Apr;78(4):2125-9.

Goenka S, Rao CM.; Inability of chaperones to fold mutant zeta crystallin, an aggregation-prone eye lens protein.; Mol Vis. 2000 Nov 8;6:232-6.

Gonzalez P, Rao PV, Nunez SB, Zigler JS Jr.; Evidence for independent recruitment of zeta-crystallin/quinone reductase (CRYZ) as a crystallin in camelids and hystricomorph rodents.; Mol Biol Evol. 1995 Sep;12(5):773-81.

Gopal-Srivastava R, Haynes JI 2nd, Piatigorsky J.; Regulation of the murine alpha B-crystallin/small heat shock protein gene in cardiac muscle.; Mol Cell Biol. 1995 Dec;15(12):7081-90.

Goring DR, Breitman ML, Tsui LC.; Temporal regulation of six crystallin transcripts during mouse lens development.; Exp Eye Res. 1992 May;54(5):785-95.

Graw J, Jung M, Loster J, Klopp N, Soewarto D, Fella C, Fuchs H, Reis A, Wolf E, Balling R, Hrabe de Angelis M.; Mutation in the betaA3/A1-crystallin encoding gene Cryba1 causes a dominant cataract in the mouse.; Genomics. 1999 Nov 15;62(1):67-73

Graw J, Loster J, Soewarto D, Fuchs H, Meyer B, Reis A, Wolf E, Balling R, Hrabe de Angelis M.; Characterization of a new, dominant V124E mutation in the mouse alphaA-crystallin-encoding gene.; Invest Ophthalmol Vis Sci. 2001a Nov;42(12):2909-15.

Graw J, Loster J, Soewarto D, Fuchs H, Reis A, Wolf E, Balling R, Hrabe de Angelis M.; Aey2, a new mutation in the betaB2-crystallin-encoding gene of the mouse.; Invest Ophthalmol Vis Sci. 2001b Jun;42(7):1574-80.

Graw J, Loster J.; Developmental genetics in ophthalmology.; Ophthalmic Genet. 2003 Mar;24(1):1-33.

Graw J, Neuhauser-Klaus A, Klopp N, Selby PB, Loster J, Favor J.; Genetic and allelic heterogeneity of Cryg mutations in eight distinct forms of dominant cataract in the mouse.; Invest Ophthalmol Vis Sci. 2004 Apr;45(4):1202-13.

Graw J.; Congenital hereditary cataracts.; Int J Dev Biol. 2004;48(8-9):1031-44.

Graw J.; The crystallins: genes, proteins and diseases.; Biol Chem. 1997 Nov;378(11):1331-48.

Graw J.; The genetic and molecular basis of congenital eye defects.; Nat Rev Genet. 2003 Nov;4(11):876-88.

Grimm C, Sporle R, Schmid TE, Adler ID, Adamski J, Schughart K, Graw J.; Isolation and embryonic expression of the novel mouse gene Hic1, the homologue of HIC1, a candidate gene for the Miller-Dieker syndrome.; Hum Mol Genet. 1999 Apr;8(4):697-710.

Harding JJ.; Viewing molecular mechanisms of ageing through a lens.; Ageing Res Rev. 2002 Jun;1(3):465-79.

Head MW, Sedowofia K, Clayton RM.; Beta B2-crystallin in the mammalian retina.; Exp Eye Res. 1995 Oct;61(4):423-8.

Heinzmann C, Kojis TL, Gonzalez P, Rao PV, Zigler JS Jr, Polymeropoulos MH, Klisak I, Sparkes RS, Mohandas T, Bateman JB.; Assignment of the zeta-crystallin gene (CRYZ) to human chromosome 1p22-p31 and identification of restriction fragment length polymorphisms.; Genomics. 1994 Sep 15;23(2):403-7.

Héon E, Priston M, Schorderet DF, Billingsley GD, Girard PO, Lubsen N, Munier FL.; The gamma-crystallins and human cataracts: a puzzle made clearer.; Am J Hum Genet. 1999 Nov;65(5):1261-7.

Higuchi Y, Iwaki T, Tateishi J.; Neurodegeneration in the limbic and paralimbic system in progressive supranuclear palsy.; Neuropathol Appl Neurobiol. 1995 Jun;21(3):246-54.

Hitotsumatsu T, Iwaki T, Fukui M, Tateishi J.; Distinctive immunohistochemical profiles of small heat shock proteins (heat shock protein 27 and alpha B-crystallin) in human brain tumors.; Cancer. 1996 Jan 15;77(2):352-61.

Horwitz J.; Alpha-crystallin can function as a molecular chaperone.; Proc Natl Acad Sci U S A. 1992 Nov 1;89(21):10449-53

Horwitz J.; Alpha-crystallin.; Exp Eye Res. 2003 Feb;76(2):145-53.

Huang QL, Russell P, Stone SH, Zigler JS Jr.; Zeta-crystallin, a novel lens protein from the guinea pig.; Curr Eye Res. 1987 May;6(5):725-32.

Inana G, Piatigorsky J, Norman B, Slingsby C, Blundell T.; Gene and protein structure of a beta-crystallin polypeptide in murine lens: relationship of exons and structural motifs.; Nature. 1983 Mar 24-30;302(5906):310-5.

Iwaki T, Kume-Iwaki A, Liem RK, Goldman JE.; Alpha B-crystallin is expressed in non-lenticular tissues and accumulates in Alexander's disease brain.; Cell. 1989 Apr 7;57(1):71-8.

Jones SE, Jomary C, Grist J, Makwana J, Neal MJ.; Retinal expression of gamma-crystallins in the mouse.; Invest Ophthalmol Vis Sci. 1999 Nov;40(12):3017-20.

Kador PF, Fukui HN, Fukushi S, Jernigan HM Jr, Kinoshita JH.; Philly mouse: a new model of hereditary cataract.; Exp Eye Res. 1980 Jan;30(1):59-68.

Kim RY, Gasser R, Wistow GJ.; mu-crystallin is a mammalian homologue of Agrobacterium ornithine cyclodeaminase and is expressed in human retina.; Proc Natl Acad Sci U S A. 1992 Oct 1;89(19):9292-6.

Kannabiran C, Rogan PK, Olmos L, Basti S, Rao GN, Kaiser-Kupfer M, Hejtmancik JF.; Autosomal dominant zonular cataract with sutural opacities is associated with a splice mutation in the betaA3/A1-crystallin gene.; Mol Vis. 1998 Oct 23;4:21.

Kantorow M, Piatigorsky J.; Alpha-crystallin/small heat shock protein has autokinase activity.; Proc Natl Acad Sci U S A. 1994 Apr 12;91(8):3112-6.

Kerscher S, Church RL, Boyd Y, Lyon MF.; Mapping of four mouse genes encoding eye lens-specific structural, gap junction, and integral membrane proteins: *Cryba1* (crystallin beta A3/A1), *Crybb2* (crystallin beta B2), *Gja8* (MP70), and Lim2 (MP19).; Genomics. 1995 Sep 20;29(2):445-50.

Kerscher S, Glenister PH, Favor J, Lyon MF.; Two new cataract loci, Ccw and To3, and further mapping of the Npp and Opj cataracts in the mouse.; Genomics. 1996 Aug 15;36(1):17-21.

Kilby GW, Carver JA, Zhu JL, Sheil MM, Truscott RJ.; Loss of the C-terminal serine residue from bovine beta B2-crystallin.; Exp Eye Res. 1995 May;60(5):465-9.

Kleiman NJ, Chiesa R, Kolks MA, Spector A.; Phosphorylation of beta-crystallin B2 (beta Bp) in the bovine lens.; J Biol Chem. 1988 Oct 15;263(29):14978-83.

Kramer P, Yount J, Mitchell T, LaMorticella D, Carrero-Valenzuela R, Lovrien E, Maumenee I, Litt M.; A second gene for cerulean cataracts maps to the beta crystallin region on chromosome 22.; Genomics. 1996 Aug 1;35(3):539-42.

Krausz E, Augusteyn RC, Quinlan RA, Reddan JR, Russell P, Sax CM, Graw J.; Expression of Crystallins, Pax6, Filensin, CP49, MIP, and MP20 in lens-derived cell lines.; Invest Ophthalmol Vis Sci. 1996 Sep;37(10):2120-8.

Kretschmar M, Jaenicke R.; Stability of a homo-dimeric Ca(2+)-binding member of the beta gamma-crystallin superfamily: DSC measurements on spherulin 3a from Physarum polycephalum.; J Mol Biol. 1999 Sep 3;291(5):1147-53.

Kretschmar M, Mayr EM, Jaenicke R.; Homo-dimeric spherulin 3a: a single-domain member of the beta gamma-crystallin superfamily.; Biol Chem. 1999 Jan;380(1):89-94.

Kretschmar M, Mayr EM, Jaenicke R.; Kinetic and thermodynamic stabilization of the betagamma-crystallin homolog spherulin 3a from Physarum polycephalum by calcium binding.; J Mol Biol. 1999 Jun 18;289(4):701-5.

Krumpaszky HG, Klauss V.; Epidemiology of blindness and eye disease.; Ophthalmologica. 1996;210(1):1-84.

Lampi KJ, Ma Z, Shih M, Shearer TR, Smith JB, Smith DL, David LL.; Sequence analysis of betaA3, betaB3, and betaA4 crystallins completes the identification of the major proteins in young human lens.; J Biol Chem. 1997 Jan 24;272(4):2268-75.

Lens crystallins: gene recruitment and evolutionary dynamism; Wistow G.; Trends Biochem Sci. 1993 Aug;18(8):301-6.

Litt M, Carrero-Valenzuela R, LaMorticella DM, Schultz DW, Mitchell TN, Kramer P, Maumenee IH.; Autosomal dominant cerulean cataract is associated with a chain termination mutation in the human beta-crystallin gene CRYBB2.; Hum Mol Genet. 1997 May;6(5):665-8.

Litt M, Kramer P, LaMorticella DM, Murphey W, Lovrien EW, Weleber RG.; Autosomal dominant congenital cataract associated with a missense mutation in the human alpha crystallin gene CRYAA.; Hum Mol Genet. 1998 Mar;7(3):471-4.

Lowe J, Landon M, Pike I, Spendlove I, McDermott H, Mayer RJ.; Dementia with beta-amyloid deposition: involvement of alpha B-crystallin supports two main diseases.; Lancet. 1990 Aug 25;336(8713):515-6.

Lubsen NH, Aarts HJ, Schoenmakers JG.; The evolution of lenticular proteins: the beta- and gamma-crystallin super gene family.; Prog Biophys Mol Biol. 1988;51(1):47-76

Mackay DS, Boskovska OB, Knopf HL, Lampi KJ, Shiels A.; A nonsense mutation in CRYBB1 associated with autosomal dominant cataract linked to human chromosome 22q.; Am J Hum Genet. 2002 Nov;71(5):1216-21. Epub 2002 Oct 1.

Magabo KS, Horwitz J, Piatigorsky J, Kantorow M.; Expression of betaB(2)-crystallin mRNA and protein in retina, brain, and testis.; Invest Ophthalmol Vis Sci. 2000 Sep;41(10):3056-60.

Morner,C.T.; Untersuchungen de Proteinsubstanzen in den lichtbrechenden Medien des Auges; Z. Physiol. Chem. 18, 1893, 61-106.

Nakamura M, Russell P, Carper DA, Inana G, Kinoshita JH.; Alteration of a developmentally regulated, heat-stable polypeptide in the lens of the Philly mouse. Implications for cataract formation.; J Biol Chem. 1988 Dec 15;263(35):19218-21.

Norledge BV, Trinkl S, Jaenicke R, Slingsby C.; The X-ray structure of a mutant eye lens beta B2-crystallin with truncated sequence extensions.; Protein Sci. 1997 Aug;6(8):1612-20.

Ohki SY, Kariya E, Hiraga K, Wakamiya A, Isobe T, Oda K, Kainosho M.; NMR structure of Streptomyces killer toxin-like protein, SKLP: further evidence for the wide distribution of single-domain betagamma-crystallin superfamily proteins.; J Mol Biol. 2001 Jan 5;305(1):109-20

Ohl F, Holsboer F, Landgraf R.; The modified hole board as a differential screen; Behav Res Methods Instrum Comput. 2001 Aug;33(3):392-7.

Peterson CA, Piatigorsky J.; Preferential conservation of the globular domains of the beta A3/A1-crystallin polypeptide of the chicken eye lens.; Gene. 1986;45(2):139-47.

Pittler SJ, Baehr W.; Identification of a nonsense mutation in the rod photoreceptor cGMP phosphodiesterase beta-subunit gene of the rd mouse.; Proc Natl Acad Sci U S A. 1991 Oct 1;88(19):8322-6.

Polyphosphate loss promotes SNF/SWI- and Gcn5-dependent mitotic induction of PHO5.; Neef DW, Kladde MP.; Mol Cell Biol. 2003 Jun;23(11):3788-97.

Pras E, Frydman M, Levy-Nissenbaum E, Bakhan T, Raz J, Assia EI, Goldman B, Pras E.; A nonsense mutation (W9X) in CRYAA causes autosomal recessive cataract in an inbred Jewish Persian family.; Invest Ophthalmol Vis Sci. 2000 Oct;41(11):3511-5.

Rajeevan MS, Ranamukhaarachchi DG, Vernon SD, Unger ER.; Use of real-time quantitative PCR to validate the results of cDNA array and differential display PCR technologies.; Methods. 2001 Dec;25(4):443-51.

Rajeevan MS, Vernon SD, Taysavang N, Unger ER.; Validation of array-based gene expression profiles by real-time (kinetic) RT-PCR.; J Mol Diagn. 2001 Feb;3(1):26-31.

Rajini B, Graham C, Wistow G, Sharma Y.; Stability, homodimerization, and calcium-binding properties of a single, variant betagamma-crystallin domain of the protein absent in melanoma 1 (AIM1).; Biochemistry. 2003 Apr 22;42(15):4552-9.

Rajini B, Shridas P, Sundari CS, Muralidhar D, Chandani S, Thomas F, Sharma Y.; Calcium binding properties of gamma-crystallin: calcium ion binds at the Greek key beta gamma-crystallin fold.; J Biol Chem. 2001 Oct 19;276(42):38464-71. Epub 2001 Aug 13.

Rao PV, Gonzalez P, Persson B, Jornvall H, Garland D, Zigler JS Jr.; Guinea pig and bovine zeta-crystallins have distinct functional characteristics highlighting replacements in otherwise similar structures.; Biochemistry. 1997 May 6;36(18):5353-62.

Rao PV, Krishna CM, Zigler JS Jr.; Identification and characterization of the enzymatic activity of zeta-crystallin from guinea pig lens. A novel NADPH:quinone oxidoreductase.; J Biol Chem. 1992 Jan 5;267(1):96-102.

Rao PV, Zigler JS Jr.; Mutant zeta-crystallin from guinea-pig hereditary cataracts has altered structural and enzymatic properties.; Exp Eye Res. 1992 Apr;54(4):627-30.

Ray ME, Wistow G, Su YA, Meltzer PS, Trent JM; AIM1, a novel non-lens member of the betagamma-crystallin superfamily, is associated with the control of tumorigenicity in human malignant melanoma.; Proc Natl Acad Sci U S A. 1997 Apr 1;94(7):3229-34.

Reddy MA, Bateman OA, Chakarova C, Ferris J, Berry V, Lomas E, Sarra R, Smith MA, Moore AT, Bhattacharya SS, Slingsby C.; Characterization of the G91del CRYBA1/3-crystallin protein: a cause of human inherited cataract.; Hum Mol Genet. 2004 May 1;13(9):945-53. Epub 2004 Mar 11.

Renkawek K, de Jong WW, Merck KB, Frenken CW, van Workum FP, Bosman GJ.; alpha B-crystallin is present in reactive glia in Creutzfeldt-Jakob disease.; Acta Neuropathol (Berl). 1992;83(3):324-7.

Richardson J, Cvekl A, Wistow G.; Pax-6 is essential for lens-specific expression of zeta-crystallin.; Proc Natl Acad Sci U S A. 1995 May 9;92(10):4676-80.

Robinson ML, Overbeek PA; Differential expression of alpha A- and alpha B-crystallin during murine ocular development.; Invest Ophthalmol Vis Sci. 1996 Oct;37(11):2276-84.

Rodriguez IR, Gonzalez P, Zigler JS Jr, Borras T.; A guinea-pig hereditary cataract contains a splice-site deletion in a crystallin gene.; Biochim Biophys Acta. 1992 Oct 13;1180(1):44-52.

Rosinke B, Renner C, Mayr EM, Jaenicke R, Holak TA; Ca2+-loaded spherulin 3a from Physarum polycephalum adopts the prototype gamma-crystallin fold in aqueous solution.; J Mol Biol. 1997 Aug 29;271(4):645-55.

Russell P, Chambers C.; Interaction of an altered beta-crystallin with other proteins in the Philly mouse lens.; Exp Eye Res. 1990 Jun;50(6):683-7

Sandilands A, Hutcheson AM, Long HA, Prescott AR, Vrensen G, Loster J, Klopp N, Lutz RB, Graw J, Masaki S, Dobson CM, MacPhee CE, Quinlan RA.; Altered aggregation properties of mutant gamma-crystallins cause inherited cataract.; EMBO J. 2002 Nov 15;21(22):6005-14.

Santhiya ST, Abd-alla SM, Loster J, Graw J.; Reduced levels of gamma-crystallin transcripts during embryonic development of murine Cat2nop mutant lenses.; Graefes Arch Clin Exp Ophthalmol. 1995 Dec;233(12):795-800.

Santhiya ST, Manisastry SM, Rawlley D, Malathi R, Anishetty S, Gopinath PM, Vijayalakshmi P, Namperumalsamy P, Adamski J, Graw J.; Mutation analysis of congenital cataracts in Indian families: identification of SNPS and a new causative allele in CRYBB2 gene.; Invest Ophthalmol Vis Sci. 2004 Oct;45(10):3599-607.

Seltmann M, Horsch M, Drobyshev A, Chen Y, de Angelis MH, Beckers J.; Assessment of a systematic expression profiling approach in ENU-induced mouse mutant lines.; Mamm Genome. 2005 Jan;16(1):1-10.

Sergeev YV, David LL, Chen HC, Hope JN, Hejtmancik JF.; Local microdomain structure in the terminal extensions of betaA3- and betaB2-crystallins.; Mol Vis. 1998 Jun 18;4:9.

Sharma Y, Balasubramanian D.; Calcium binding properties of beta-crystallins.; Ophthalmic Res. 1996;28 Suppl 1:44-7.

Sharma Y, Rao CM, Narasu ML, Rao SC, Somasundaram T, Gopalakrishna A, Balasubramanian D.; Calcium ion binding to delta- and to beta-crystallins. The presence of the "EF-hand" motif in delta-crystallin that aids in calcium ion binding.; J Biol Chem. 1989 Aug 5;264(22):12794-9.

Shastry BS.; Immunological studies on gamma crystallins from Xenopus: localization, tissue specificity and developmental expression of proteins.; Exp Eye Res. 1989 Sep;49(3):361-9.

Simpson A, Bateman O, Driessen H, Lindley P, Moss D, Mylvaganam S, Narebor E, Slingsby C.; The structure of avian eye lens delta-crystallin reveals a new fold for a superfamily of oligomeric enzymes.; Nat Struct Biol. 1994 Oct;1(10):724-34.

Sinha D, Esumi N, Jaworski C, Kozak CA, Pierce E, Wistow G.; Cloning and mapping the mouse Crygs gene and non-lens expression of [gamma]S-crystallin.; Mol Vis. 1998 Apr 30;4:8.

Southern E, Mir K, Shchepinov M.; Molecular interactions on microarrays.; Nat Genet. 1999 Jan;21(1 Suppl):5-9.

Spector A.; The search for a solution to senile cataracts. Proctor lecture.; Invest Ophthalmol Vis Sci. 1984 Feb;25(2):130-46.

Srivastava OP, Srivastava K.; BetaB2-crystallin undergoes extensive truncation during aging in human lenses.; Biochem Biophys Res Commun. 2003 Jan 31;301(1):44-9.

Sterrenburg E, Turk R, Boer JM, van Ommen GB, den Dunnen JT.; A common reference for cDNA microarray hybridizations.; Nucleic Acids Res. 2002 Nov 1;30(21):e116.

Straatsma BR, Horwitz J, Takemoto LJ, Lightfoot DO, Ding LL.; Clinicobiochemical correlations in aging-related human cataract. The Pan American Association and American Journal of Ophthalmology lecture.; Am J Ophthalmol. 1984 Apr;97(4):457-69.

Teintze M, Inouye M, Inouye S.; Characterization of calcium-binding sites in development-specific protein S of Myxococcus xanthus using site-specific mutagenesis.; J Biol Chem. 1988 Jan 25;263(3):1199-203

Treton JA, Jacquemin E, Courtois Y, Jeanny JC.; Differential localization by in situ hybridization of specific crystallin transcripts during mouse lens development.; Differentiation. 1991 Aug;47(3):143-7.

Uga S, Kador PF, Kuwabara T.; Cytological study of Philly mouse cataract.; Exp Eye Res. 1980 Jan;30(1):79-92.
Van Leen RW, Breuer ML, Lubsen NH, Schoenmakers JG.; Developmental expression of crystallin genes: in situ hybridization reveals a differential localization of specific mRNAs.; Dev Biol. 1987 Oct;123(2):338-45.

van Rens GL, Raats JM, Driessen HP, Oldenburg M, Wijnen JT, Khan PM, de Jong WW, Bloemendal H.; Structure of the bovine eye lens gamma s-crystallin gene (formerly beta s).; Gene. 1989 May 30;78(2):225-33.

Vanita, Sarhadi V, Reis A, Jung M, Singh D, Sperling K, Singh JR, Burger J.; A unique form of autosomal dominant cataract explained by gene conversion between beta-crystallin B2 and its pseudogene.; J Med Genet. 2001 Jun;38(6):392-6.

Vogt Weisenhorn DM, Celio MR, Rickmann M.; The onset of parvalbumin-expression in interneurons of the rat parietal cortex depends upon extrinsic factor(s).; Eur J Neurosci. 1998 Mar;10(3):1027-36.

Wenk M, Mayr EM.; Myxococcus xanthus spore coat protein S, a stress-induced member of the betagamma-crystallin superfamily, gains stability from binding of calcium ions.; Eur J Biochem. 1998 Aug 1;255(3):604-10.

Wijker CA, Wientjes NM, Lafleur VM.; Mutation spectrum in the lacI gene, induced by gamma-radiation in aqueous solution under oxic conditions.; Mutat Res. 1998 Jul 17;403(1-2):137-47.

Wistow G, Jaworski C, Rao PV.; A non-lens member of the beta gamma-crystallin superfamily in a vertebrate, the amphibian Cynops.; Exp Eye Res. 1995 Nov;61(5):637-9.

Wistow G, Summers L, Blundell T.; Myxococcus xanthus spore coat protein S may have a similar structure to vertebrate lens beta gamma-crystallins.; Nature. 1985 Jun 27-Jul 3;315(6022):771-3.

Wistow G.; Evolution of a protein superfamily: relationships between vertebrate lens crystallins and microorganism dormancy proteins.; J Mol Evol. 1990 Feb;30(2):140-5.

Wistow GJ, Piatigorsky J.; Lens crystallins: the evolution and expression of proteins for a highly specialized tissue.; Annu Rev Biochem. 1988;57:479-504.

Wride MA, Mansergh FC, Adams S, Everitt R, Minnema SE, Rancourt DE, Evans MJ.; Expression profiling and gene discovery in the mouse lens.; Mol Vis. 2003 Aug 22;9:360-96.

Xi J, Farjo R, Yoshida S, Kern TS, Swaroop A, Andley UP.; A comprehensive analysis of the expression of crystallins in mouse retina.; Mol Vis. 2003 Aug 28;9:410-9.

Zarbalis K, Chatterjee B, Loster J, Werner T, Graw J.; Sequence analysis of the beta B2-crystallin cDNA of hamster containing a domain conserved among vertebrates.; Gene. 1996 Sep 26;174(1):181-4.

Zarina S, Slingsby C, Jaenicke R, Zaidi ZH, Driessen H, Srinivasan N.; Three-dimensional model and quaternary structure of the human eye lens protein gamma S-crystallin based on beta- and gamma-crystallin X-ray coordinates and ultracentrifugation.; Protein Sci. 1994 Oct;3(10):1840-6.

Zhang Z, Smith DL, Smith JB.; Human beta-crystallins modified by backbone cleavage, deamidation and oxidation are prone to associate.; Exp Eye Res. 2003 Sep;77(3):259-72.

8.0: <u>Abbreviations:</u>

°C	Degree celcius	NTP	Nucleosidetriphosphate
A	Adenine	L	Litre
A	Ampere	LB	Luria-Broth
aa	Amino acid	kDa	Kilo dalton
Ac	Acetate	m	milli
AMP	Adenosine mono phosphate	μm	Micron meter
Amp	Ampere	μ	micron
AP	Alkaline phosphate	M	Mole
ATP	Adenosine tri phosphate	min	minutes
bp	Base pair	mRNA	Messenger RNA
C	Cytosine	O.N.	Over night
cDNA	Complementary DNA	p	pico
CTP	Cytosine tri phosphate	P	Postnatal day
Da	Dalton	PBS	Phosphate buffer saline
DAB	Diaminobenzidine	PCR	Polymerase chain reaction
dATP	Deoxy adenosine tri phosphate	PFA	Paraformaldehyde
dCTP	Deoxy cytosine tri phosphate	pmol	picomol
DEPC	Diethylpyrocarbonate	RNA	Ribose nucleic acid
dGTP	Deoxyguanine tri phosphate	RNase	Ribonuclease
Dig	Digoxigenin	rpm	Rotations per minute
DNA	Deoxyribonucleic acid	RT	Room temperature
DNase	Deoxyribonuclease	RT-PCR	Reverse transcriptase polymerase chain reaction
dNTP	Deoxynucleosidetriphosphate	SDS	Sodiumdodecylsulphate
E	Embryonic stage	secs	seconds
EDTA	Ethyldiaminetetraacetate	SSC	Sodium chloride-sodium citrate
EST	Expression sequence tags	T	Thymine
et al.	*et alteres*	TAE	Tris-Acetate-EDTA buffer
FA	Formamide	TBE	Tris-Borate-EDTA buffer
g	gramm	TBS	Tris buffer saline
G	Guanine	TE	Tris-EDTA
GTP	Guanosine tri phosphate	UTP	Uraciltriphosphate
ISH	*In-situ* hybridization	V	Volts
k	kilo		
Kb	Kilo base		

Symbols for amino acids:

A	Ala	Alanine	**M**	Met	Methionine
C	Cys	Cysteine	**N**	Asn	Asparagine
D	Asp	Aspartic acid	**P**	Ro	Proline
E	Glu	Glutamic acid	**Q**	Gln	Glutamine
F	Phe	Phenyl alanine	**R**	Arg	Arginine
G	Gly	Glycine	**S**	Ser	Serine
H	His	Histidine	**T**	Thr	Threonine
I	Ile	Isoleucine	**V**	Val	Valine
K	Lys	Lysine	**W**	Trp	Tryptophan
L	Leu	leucine	**Y**	Tyr	Tyrosine